MEASUREMENT AND MODELLING OF ESTUARINE CHEMISTRY

A. G. PUNT

Ph. D. 2000

Measurement and Modelling of Estuarine Chemistry

By

Adrian Gavin Punt M.Sc., B.Sc. (Hons)

A thesis submitted to the University of Plymouth in partial fulfilment for the degree of

Doctor of Philosophy

Department of Environmental Sciences
Faculty of Science

In Collaboration with:

Centre for Coastal Marine Science
Plymouth Marine Laboratory

Measurement and Modelling of Estuarine Chemistry

Adrian Gavin Punt M.Sc., B.Sc. (Hons)

Abstract

A 1-D tidally resolving hydrodynamic model of the Tweed Estuary has been encoded using the Estuarine Contaminant Simulator, ECoS. The model results of axial and time series variations in water elevation, salinity and turbidity are compared to field data recorded during the LOIS survey programme.

The organic and inorganic controls on estuarine pH have also been investigated by encoding a new template to predict the effect of changing salinity and temperature on the pH of estuarine water. The template has been coupled to the hydrodynamic model to predict pH variations in the estuary. The model results have shown conservative behaviour of the inorganic carbon system through out the majority of the estuary, but also identified an area of potentially high photosynthetic activity near the limit of saline intrusion during periods of low summer flows. Low (< 2 $\mu g\ l^{-1}$) concentrations of chlorophyll *a* in the water column and increases in pH correlated with tidal inundation of the river estuary banks imply that benthic photosynthetic process are important water chemistry in the upper estuary.

The effects of salinity, turbidity and pH on K_d(Cd) and K_d(Zn) has been investigated using radiotracer incubation experiments and analytically determined measurements. The results show a reduction in K_d with increased salinity, but that the K_ds determined analytically are an order of magnitude higher than those measured when radiotracers are used. Analytically determined K_ds are reduced with increasing SPM concentration and increased at higher pH. Although no photosynthetically mediated control of radiotracer uptake was identified partitioning was significantly reduced (> 90 %) when a metabolic inhibitor was added.

The K_d has been encoded as an exchange transfer and used to predict axial distributions and the flux of these metals from the riverine catchment to the sea. Model results indicate that the partition coefficients determined from the radiotracer studies can not fully account for the analytically determined distribution between phases. It is hypothesised that colloids and Fe-Mn oxides precipitates play a significant role in trace metal transport in low turbidity, high pH conditions. The results have implications for the measurement and modelling of chemical fluxes in low turbidity systems.

Acknowledgements

- The author wishes to thank all those who assisted in the completion of this study. I wish to thank Professor Geoff Millward (Director of Studies) for his never ending support, encouragement and interest in all aspects of the project and my well being.

- Dr John Harris (Supervisor) of CCMS Plymouth Marine Laboratories for his enthusiasm in the project and guidance on the novel application of ECoS to estuarine systems.

- Dr Alan Tappin for his advise and assistance and for generously allowing use of his data in the modelling work.

- The 'Tweed Team' including Robin Howland for numerous discussions on the Tweed, Nick Bloomer for his patient assistance during the field work and also Dr Pete Shaw, Dr Helen Jarvie, Dr Tonia Sands and Dr Manuela Martino for their help during the Tweed field work.

- The technical staff of the Department of Environmental Science, University of Plymouth for their help with both field and laboratory work and giving instruction on analytical techniques and instrumentation.

- Sarah Watts and Mark Williams for their support and friendship during the project.

- Reverend Geoff Flather Shihan and the members of Banyu Hatten Aikido to who I am indebted for their support and guidance.

- Finally I wish to thank my partner, Karen for her tolerance and encouragement throughout the study.

Declaration

At no time during the registration for the degree of Doctor of Philosophy has the author been registered for any other University Award.

The study was financed with the aid of a CASE award from the Natural Environment Research Council in collaboration with CCMS Plymouth Marine Laboratory. This thesis is a holistic treatment of the large scale multi-disciplinary LOIS study of the Tweed Estuary and the assistance of all those involved is duly and gratefully acknowledged (see acknowledgement section). The thesis however, remains the sole work of the author.

A programme of advanced study was undertaken that included:

- Guided reading in estuarine physical and biogeochemical processes.
- Development of proficiency in the use of the Estuarine Contaminant Simulator, ECoS.
- Instruction in estuarine survey techniques including the successful completion of the RYA Level 4 Power Boating Certificate, RYA Emergency Fist Aid and HSE First Aid in the Workplace.
- Training in the use of flame atomic adsorption spectrometry and gamma spectrometry analysis.

Relevant scientific seminars and conferences were regularly attended at which work was often presented; external institutions were visited for consultation purposes, and annual reports produced for the University of Plymouth, CASE collaborator and NERC.

Meetings, Courses and external visits

- RYA Level 4 power boat handling, University of Plymouth, UK, November 1996.
- Environmental Agency ECoS Training Seminar, Lichfield, UK, November 1996.
- HSE First Aid, University of Plymouth, UK, February 1997.
- NERC Graduate School, University of Sheffield, UK, September 1998.
- Modelling Environmental Systems, University of Cranfield, UK, April 1999.
- Microsoft Access database management, CCMS PML, UK, June 1999.

Data Available

The original data collected during this study is available as spreadsheets created using Microsoft Excel 97 and stored on the CD ROM contained in an appendix to copies of this thesis held by the University of Plymouth Library.

Conferences and Presentations

- Oral presentation and demonstration: "*An incipient ECoS model of the Tweed*" at the **ECoS Work Shop**, University of Hull, UK, March 1997.
- Poster presentation: "*An incipient ECoS model of the Tweed*" at the **2nd Annual LOIS Conference**, University of Hull, UK, March 1997.
- Oral presentation: "*Trace metal behaviour in the Tweed Estuary*" at the **Department of Environmental Science Research Seminar**, University of Plymouth, June 1997.
- Oral presentation: "*Using ECoS to model the transport of Cd & Zn in the Tweed Estuary*" at the **2nd Progress in Chemical Oceanography Conference**, University of Southampton, October 1997.
- Poster presentation: "*Modelling Trace Metal Behaviour Using ECoS in the Tweed Estuary*" at the **3rd Annual LOIS Conference**, University of East Anglia, March 1997.
- Oral presentation: "*ECoS, a coupled hydrodynamic-geochemical model*" **Department of Environmental Science Research Seminar**, University of Plymouth, April 1998.
- Oral presentation: "*Modelling trace metal behaviour using ECoS in the Tweed Estuary*" **UK Oceanography**, University of Southampton, UK, September 1998.
- Oral presentation and model display: "*Using ECoS to Predict Trace Metal Behaviour*" at **The Cornish Coast 98**, University of Exeter, Falmouth, UK, October 1998.
- Oral presentation: *"A hydrodynamic model of water and sediment transport in the Tweed Estuary"* **Department of Environmental Science Research Seminar**, University of Plymouth, February 1999.
- Oral presentation: *"Modelling the carbonate system and pH in the Tweed Estuary, UK"* at the **3rd Progress in Chemical Oceanography Conference**, University of Plymouth, September 1999.
- Weekly attendance of Environmental Science Research Seminars.

Signed.....

Date..... 20th Oct 2000

Contents

Chapter 1

Introduction

1 Introduction

This work describes the investigation of hydrodynamic and biogeochemical process in the Tweed River Estuary and the development of a simulation model that has been used to help understand these. The model has been encoded as a series of modules using the Estuarine Contaminant Simulator (ECoS). The development of the hydrodynamic (water and sediment transport), water quality (pH) and trace metal components are presented separately in this thesis to underline the different approaches developed within each model component.

1.1 Estuarine Management

There is growing public awareness of pollution in rivers, estuaries and coastal systems (Brown, 1992) and the evaluation of anthropogenic disturbance to estuarine environments is now a major issue in coastal zone studies (Regnier *et al.*, 1997). Europe has a relatively long coastline (89,000 km) compared to its land area (European Commission, 1999a). At present more than 50 % of the world's population lives within 50 km of the sea and the majority of the largest cities are located along estuarine systems (Saliot *et al.*, 1997). Disturbance to the environment arises from the wastes produced as a by-product of industrial and domestic activities (Environment Agency, 1999). Estuaries are therefore not only sites of high population density and associated industry but also suffer the consequences of industrial, agricultural and urban activities throughout the riverine catchment and adjacent coastline (Real *et al.*, 1993). A wide range of leisure activities take place in the coastal zone and the expected growth in tourism with its strong seasonal variation will increase the pressure on these areas. Coastal ecosystems are biologically productive and diverse. A third of the European Union's wetlands are located on the coast in addition to more than thirty per cent of conservation areas for wild birds, and twenty per cent of habitats listed in the Natural Habitats Directive. A significant proportion of the fish and shellfish industry relies on the breeding and nursery grounds of the coastal zone and almost half of the jobs in the fisheries sector are support by the catch from this area (European Commission, 1999a). Although the ecological, economic and social importance of natural coastal resources has long been acknowledged the inevitable consequence of human impact is a reduction in estuarine water quality with significant socio-economic implications (Edwards *et al.*, 1997).

From the 1970's, the European Union has been developing common rules to protect the aquatic environment and prevent pollution. The two approaches adopted are i) Water Quality Objectives (WQO) and ii) Emission Limit Values (ELV) (European Commission, 1999b). However lack of co-ordination between policies and actions carried out at various levels from local to European government has meant that, despite a considerable body of legislation, deterioration of the environment has continued (European Commission, 1999a). Implementation of recent integrated coastal zone management legislation uses a combined approach employing both WQO and ELV directives and includes the Integrated Pollution Prevention and Control (IPPC) Directive (European Commission, 1999b). In October 1999 all member states must have implemented the IPPC Directive. Its overall objective is a higher level of protection for the environment that is much broader ranging than previous Directives. It also places much greater emphasis on the prevention of accidents and the limitation of their environmental consequences and environmental recovery of a site after operations have ceased (Environment Agency, 1999).

Financial penalties and adverse public opinion are strong incentives for industries to manage and reduce the environmental impact of their activities and it is an offence to contravene these directives by causing or knowingly permitting polluting matter or effluent to enter controlled waters in England and Wales. Controlled waters include virtually all freshwater, groundwaters, tidal and coastal waters to a distance of three nautical miles from the shore (Environment Agency, 1999). Regulatory authorities may prosecute under such circumstances and the Environment Agency made a total of 744 prosecutions resulting in fines of over £2 million in 1998. The biggest offender was ICI with fines totalling £382,500. Water companies also feature heavily in the Environment Agency 'Hall of Shame' (Environment Agency, 1999). With increasingly stringent controls on pollution discharge through out Europe, industry and the regulatory authorities require more than ever, strategies for the effective monitoring and sustainable management of river-estuary systems. There is also a demand for more sophisticated understanding from industry who fear their activities will be unnecessarily restricted by crude legislation. These strategies must include forecasting techniques that will allow industrial or environmental managers to assess the risk of short or long-term changes to ecosystem and man. Computer based tools for predicting contaminant behaviour and impacts are increasingly being developed and provide important decision support for coastal zone management. There were fewer examples of coupled numerical models involving hydrodynamics and contaminant

geochemistry reported in the literature prior to the 1990's, but simulation models are becoming increasingly important for regulatory authorities, industry and research.

Compared to riverine or coastal processes the steep and often rapidly changing physico-chemical gradients that occur in estuarine waters (Morris *et al.*, 1982) mean these systems are more complex and that biogeochemical processes are more difficult to predict. The hydrodynamic regime of the estuary will govern the salinity distribution and sediment transport, two critical factors influencing the transport and transformation of pollutants through these systems. The temperature, pH and dissolved oxygen concentrations will be influenced by atmospheric and biological processes in addition to the hydrodynamic conditions, and may also play a role in pollutant transformations. In addition to the inherent complexity of estuaries, other factors are coming into play through environmental change induced by climatic modification. For instance it has been proposed that "extreme" precipitation events are becoming more frequent (Tsonis, 1996). Since the major fluxes of solutes and particles through estuaries occurs during brief spates of high flow (GESAMP, 1987) it is important to consider these events. Coastal zone managers therefore require decision support tools that are not only capable of predicting complex pollution dispersion under existing environmental conditions, but can provide indication of the consequences of future climatic change. If meaningful results are to be gained from these models there must be sufficient and appropriate data available for model development, and the answers gained must be adequately quantified with realistic confidence limits (IAEA, 1991).

1.2 Physical processes in estuaries

1.2.1 Estuarine hydrodynamics

An estuary is a semi-enclosed body of water which has free connection with the seawater and within which seawater is measurably diluted by freshwater from land drainage (Dyer, 1997). The potentially large chemical and physical differences between river and seawater means that estuaries are the sites of strong hydrodynamic and physico-chemical gradients in salinity, temperature, suspended particulate matter (SPM), pH and dissolved oxygen. These water quality constituents may change by an order of magnitude through the estuary (Morris *et al.*, 1982) and these changes have important consequences for the distribution of trace elements between dissolved and particulate fractions (Oakley *et al.*, 1981; Turner *et al.*, 1991; Martin *et al.*, 1993; Paucot & Wollast, 1997; Zwolsman *et al.*, 1997). The time,

magnitude and location of any biological productivity maximum may also control concentrations of biochemically reactive elements (Church, 1986).

The mixing of these different water masses produces a salinity gradient which can vary between freshwater, by definition zero salinity to marine values, typically 34 to 34.5 units for English coastal waters (Lee, 1980). Salinity is an essential variable in determining the biogeochemistry of an estuary and saline intrusion into the estuary is determined by the complex and site specific interactions of tidal and atmospheric forcing and local topography. The volume of saline water entering the estuary during the flood tide changes according to the tidal range and salt intrusion becomes more intense under spring tides (Uncles & Stephens 1996b; Sylaios & Boxall, 1998). Estuarine cross-sectional area tends to decrease with increasing distance from the mouth (Ibanez *et al.*, 1997), and the effect of freshwater flow on preventing tidal propagation becomes more significant as channel cross-sectional area decreases (Unnikrishnan *et al.*, 1997). During periods of high river discharge strong fluvial advection reduces the effect of the flood tide in the upper estuary and pushes the tidal limit down stream (Wolanski *et al*, 1996; Grabemann *et al.*, 1997; Unnikrishnan *et al.*, 1997). River discharge is the main factor controlling the hydrologic dynamics of the Ebre and Rhone Estuaries (Ibanez *et al.*, 1997) in contrast to Southampton Water where tidal effects are more important then freshwater flow (Sylaios & Boxall, 1998). Local rainfall draining through tributaries may also reduce salinity (Niu *et al.*, 1998), although the effect may only be noticeable during times of heavy rain fall (Morris *et al.*, 1982). Trade winds are important in determining the salinity distribution in the Fly estuary (Wolanski *et al.*, 1997) and strong winds can modify water movement obscuring tidal effect when the tidal range is small (Niu *et al.*, 1998). Channel topography is also important and sills and troughs can reduce saline intrusion into the estuary (Ibanez *et al.*, 1997; Sylaios & Boxall, 1998). It has not been possible to provide a definitive prediction of estuarine structure based on a few parameters (MacCready, 1999), although multiple regression models relating salinity to a range of environmental models are available, they are site specific (Niu *et al.*, 1998). The mixing of seawater and freshwater in the estuary can however be divided into a range of broad types. The three main types typical of estuaries are shown in Figure 1.1.

These different mixing processes are critical in controlling, not only the physical transport of material, but also the extent and time available for chemical reactivity within the estuary. Salt wedge estuaries (Figure 1.1a), are often shallow with a small width to depth

ratio and are dominated by high and variable volumes of river discharge relative to tidal movement (Dyer, 1991). The lower density freshwater flows out of the estuary over the surface of the seawater, penetrating as a salt wedge along the bottom of the estuary. The stratification results in a sharp halocline between the two water masses with limited entrainment of salt water up into the upper freshwater flow (Dyer, 1997). Reduced vertical mixing means that the mixing zone may be restricted so that there is a rapid increase in salinity and a distinct fresh-seawater interface (Dyer, 1994). The isohaline of salinity 1 has been proposed as the approximate location of the freshwater-saline water interface, FSI (Bourg, 1988). This divides two chemical zones; i) the mixing zone at salinity < 1 and ii) the dilution zone at salinity > 1. The mixing zone is characterised by a high degree of chemical and biological reactivity (Ackroyd *et al.*, 1986; Morris *et al.*, 1986) while the dilution zone is more controlled by physical mixing processes (Bourg, 1988).

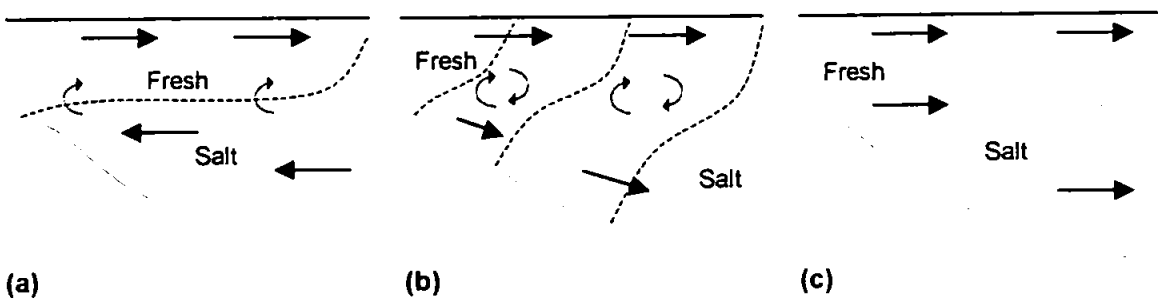

Figure 1.1 Estuarine oceanography showing different degrees of mixing between fresh and salt water. Adapted from Dyer (1997): (a) salt-wedge estuary; (b) partially mixed estuary and (c) well mixed estuary.

In a partially mixed estuary (Figure 1.1b), the tidal range is normally between 2 to 4 m (Dyer, 1994) and the whole mass of water moves up and down the length of the estuary in response to the tidal oscillation. Friction between tidal currents and the bed causes turbulence that results in much greater degree of mixing between the river water and seawater, consequently the vertical gradient is much shallower than in a salt wedge estuary. The axial distribution of salinity in a partially mixed estuary displays an S-shaped profile consisting of freshwater and seawater salinities separated by a zone of mixing. (Dyer, 1997). Partially mixed estuaries often exhibit different great variation in structure between neap and spring tides. The stronger tidal currents associated with spring conditions can cause vertically homogeneous conditions, but stratification can develop at neap tides (Dyer, 1991; Peters, 1997) when the tidal range is general less than 2 m (Dyer, 1994). Under greater tidal range conditions (Figure 1.1c), the resulting turbulence is large enough to break down the vertical salinity stratification so that the water column becomes

vertically homogenous resulting in a well mixed estuary (Dyer, 1997). Well mixed estuaries tend to be restricted to conditions when the tidal range is large (> 4 m) (Dyer, 1994). The stratification and relative degree of mixing in the estuary will determine how the solute, in this case salinity, will dispersion with distance. This is measured by the water dispersion coefficient, K_H, that may vary with distance, freshwater flow and tidal state. Reduced stratification due to increased mixing will increase the solute dispersion and reduce the limit of saline intrusion (Dyer, 1997).

Stratification is important when the net fluxes across the mouth of an estuary are measured. Many studies concentrate on measurements in the deep channel with limited vertical resolution of the water velocity and concentration gradient. The error associated with cross-sectional averaged fluxes, based on limited measurements are likely to increase as the vertical and horizontal stratification in the estuary increases (Dyer, 1997).

Hydrodynamic adjustment times of shallow estuaries to changes in river flow and tidal state can be rapid (MacCready, 1999) and a key control on chemical reactivity in an estuary is the flushing time, τ given by:

$$\tau = \frac{V}{Q} \qquad (1.1)$$

where V is the volume of freshwater accumulated in the whole or section of the estuary (m^3) and Q is the river flow in $m^3\ s^{-1}$ (Dyer, 1997). The volume of water in the estuary and hence residence time is also determined by tidal state (Uncles & Stephens, 1996b). Flushing time will also increase logarithmically down-estuary because of the exponential increase of the total volume of water (Uncles *et al.*, 1985). The flushing time of the upper estuary can vary from minutes to hours increasing to days or years in the high salinity zone (Uncles *et al.* 1983). If the residence time is less than the tidal period, the estuary is likely to be flushed on each ebb tide (Uncles & Stephens, 1996b). The mean freshwater flow rate, tidal range and other physical characteristics of a range of North Sea estuaries are shown in Table 1.1.

Flushing time is an important factor when determining if there is sufficient time for thermodynamic equilibria to exist within the mixing zone of an estuary. For ~99 % of the conversion of a reactant or pollutant the first order reaction half-life ($t_{1/2}$) must be less than

10 % of the flushing time (Morris, 1990). Therefore the shorter the flushing time the more likely it is that chemical reactions have insufficient time to reach equilibrium.

Table 1.1 Physical features of a range of North Sea estuaries.

	Catchment area, A (km^2)	Sediment flux (10^5 T yr^{-1})	Mean river flow Q (range) (m^3 s^{-1})	Tidal range	Estuarine mixing	Flushing time (days)
Elbe	148,500	6.5	726 (145-3620)	2.5/3.3	WM	4-7
Weser	44,304	2.5	326 (120-1181)	3.4	WM	2-50
Humber	27,000	1.7	246 (60-450)	3.5/6.2	WM	<40
Scheldt	21,580	1.4	100 (40-350)	4.0	WM	~60
Thames	9,900	0.9	82 (9-210)	3.3/5.1	WM	20-75
Tay	6000	0.5	198 (39-1465)	2.4/4.7	PM-WM	2-11
Tweed	4,900	0.5	78 (8-1500)	2.5/4.1	PM-SW	0.5-2.8
Forth	1036	0.1	60 (10-300)	2.5/5.0	PM-WM	7-48

Sediment flux calculated according to Wilmot & Collins (1981). Estuarine stratification; well mixed, WM; partly mixed, PM and salt-wedge, SW. Turner *et al.*, 1991; Balls, 1992; Balls, 1994; Millward *et al.*, 1990; Laslett & Balls, 1995; Uncles & Stephens, 1996b; Ferrier & Anderson, 1997).

1.2.2 Flux and fate of estuarine particles

Natural particulate matter is a complex assemblage of different chemical phases that varies in space and time, the physical and chemical properties of which are critical to understanding and predicting trace metal behaviour (Ackroyd *et al.*, 1986; Turner *et al.*, 1992b; Garnier *et al.*, 1993; Wood *et al.*, 1995; Lofts & Tipping, 1998; Tipping *et al.*, 1998). Particulate matter in an estuary will ultimately have originated from material transported in to the estuary by fluvial and/or marine inputs such as mineral phases including clays, quartz, feldspars, and carbonates derived from catchment and coastal erosion. Biological or chemical production and *in situ* flocculation can produce further particulate matter in the estuary while atmospheric deposition is a minor contribution (Millward & Turner, 1995). With the exception of areas undergoing significant coastal erosion, river-borne material is the main input of particulate matter to an estuary. The material supplied to the estuary through riverine inputs, y (T yr^{-1}) is in part controlled by the size of the catchment area and can be calculated for temperate estuaries according to the equation devised by Wilmot & Collins (1981):

$$y = 60A^{0.78} \quad (1.2)$$

where A is the catchment area, km^2. In most rivers there is considerable annual variability in sediment discharge. The erosional power of a stream rises rapidly with flow rate and most of the sediment discharge will occur during occasional storm events (Dyer, 1994). For example in the Tweed, SPM concentrations are strongly correlated to flow and can increase from 0.1 to 10 mg l^{-1} (Uncles & Stephens, 1997) to 500 mg l^{-1} during spate conditions (Neal *et al.*, 1997). A similar relationship is reported for the Tamar and concentrations can increase from 10 to100 mg l^{-1} at the beginning of spate conditions (Grabemann *et al.*, 1997). In the Tamar and Weser Rivers a hysteresis in the relationship of flow and SPM concentration occurs and during prolonged periods of high flow the catchment may become depleted of material that can be mobilised and the turbidity may decrease (Dyer, 1986; Grabemann *et al.*, 1997). The combination of a high concentration of SPM coupled with a much greater flow rate means that in many examples, 90 % of sediment discharge can occur in only 5 % of the time and for 80 % of the time virtually no sediment discharge occurs (Dyer, 1994).

Particle size distribution of the riverine SPM may be small, for example in the Mekong River SPM is composed of mainly of silt (2.5 to 3.9 μm) and the clay fraction (<2 μm) accounts for 15 to 20 % of the riverine SPM load (Wolanski *et al.*, 1996). The transport of temporarily suspended clay, silt and sand may however increases with flow (Uncles & Stephens, 1997) and in the Rhine plume Naudin *et al.* (1997) found that the percentage of temporarily suspended material increased from 30 to 60 % during flood periods. When suspended sediment concentrations are low (< 10 mg l^{-1}), and are invariant, or display a linear relationship with salinity there is little interaction with the bed sediment (Turner, 1999). For instance fine grained material such as silt and clay solids and low-density organic material and phytoplankton that may remain permanently suspended will be transported with the residual water flow (Uncles & Stephens, 1997). In stratified estuaries the river-borne particulate matter can be transported rapidly seaward in the upper waters and has limited opportunity to interact with either bed sediment or dissolved fractions in the lower water column. A fraction of the SPM (~5 % in the Mekong Estuary) can however be returned to the estuary on the flood tide and may then become involved in estuarine geochemical cycling (Wolanksi *et al.*, 1996).

Tidal resuspension of bed sediment is a regular feature of the low salinity zone significantly increasing the overall turbidity and particle sorption processes (Turner *et al.*, 1991). West European estuaries tend to have marked SPM maxima in the low salinity region where the concentrations of SPM are much higher than that in the riverine or marine end members (Muller *et al.*, 1994). The turbidity maximum zone (TMZ) is usually associated with the FSI, but occasionally occurs further up estuary (Uncles & Stephens, 1989; Wolanski *et al.*, 1996). The TMZ is generated by the tidal resuspension of fined grained coastal and riverine sediment that have accumulated in the mid and upper reaches of the estuary through the action of asymmetrical tides (Ackroyd *et al.*, 1986; Uncles & Stephens, 1989; Dyer, 1994). In macrotidal estuaries the duration of the flood tide tends to be shorter than that of the ebb. The greater current velocity and resulting erosion during the flood tide compared to the ebb that 'pumps' particulate matter into the upper reaches of the estuary, particularly during low flow conditions (Uncles *et al.*, 1985; Uncles & Stephens, 1989). Further upstream particle transport is prevented when the fluvial flow balances tidal pumping (null point). Fluvial flow can be highly variable and explains about 80 % of the variation of the position of the TMZ during spring tides in the Tamar Estuary (Uncles & Stephens, 1989). During periods of high flow bed sediment is scoured from the upper estuary and the TMZ is shifted down estuary (Uncles *et al.*, 1994). Increased river flow normally implies greater sediment discharge from the catchment, so that the mass of sediment in the TMZ also increases (Dyer, 1994). Tidal velocities are obviously important and the spring-neap tidal cycle was found to significantly effect tidal pumping in the Ribble Estuary (Lyons, 1997). The tidal pumping of suspended sediment up a macrotidal estuary and the generation of a TMZ is shown in Figure 1.2. During low flow conditions (Fig. 1.2a) the TMZ is situated further up the estuary and overall SPM concentrations are lower. During high winter flows (Fig. 1.2b) the null point and location of the TMZ shifts down estuary. This is not the case for all estuaries and in the Forth higher concentration of SPM in the TMZ occur during low riverine flows (445 mg l^{-1}) compared to high riverine flows (38 mg l^{-1}). Wind generated wave resuspension of bed sediments may also generate regions of elevated turbidity and this has been observed at the mouth of the Tweed Estuary (Uncles & Stephens, 1997).

The axial distribution of particle sizes changes with fluvial flow and fine grained material may be winnowed out and transport down estuary during high flow (Bale, 1987). Significant variations in size structure of suspended particles can also occur over a tidal cycle. In the Tamar Estuary the slack water population of predominantly large (~100 μm)

low density aggregates is replaced by higher concentrations of smaller (~10 to 30 μm), denser and discrete particles during peak water velocity. The change in particle type is interpreted as the mobilisation of discrete particles from the bed and the dissagregation of fragile flocs (Bale *et al.*, 1989). These smaller particles, with greater surface areas and associated binding sites may then adsorb significantly more dissolved contaminants compared to the larger aggregates (Millward *et al.*, 1990).

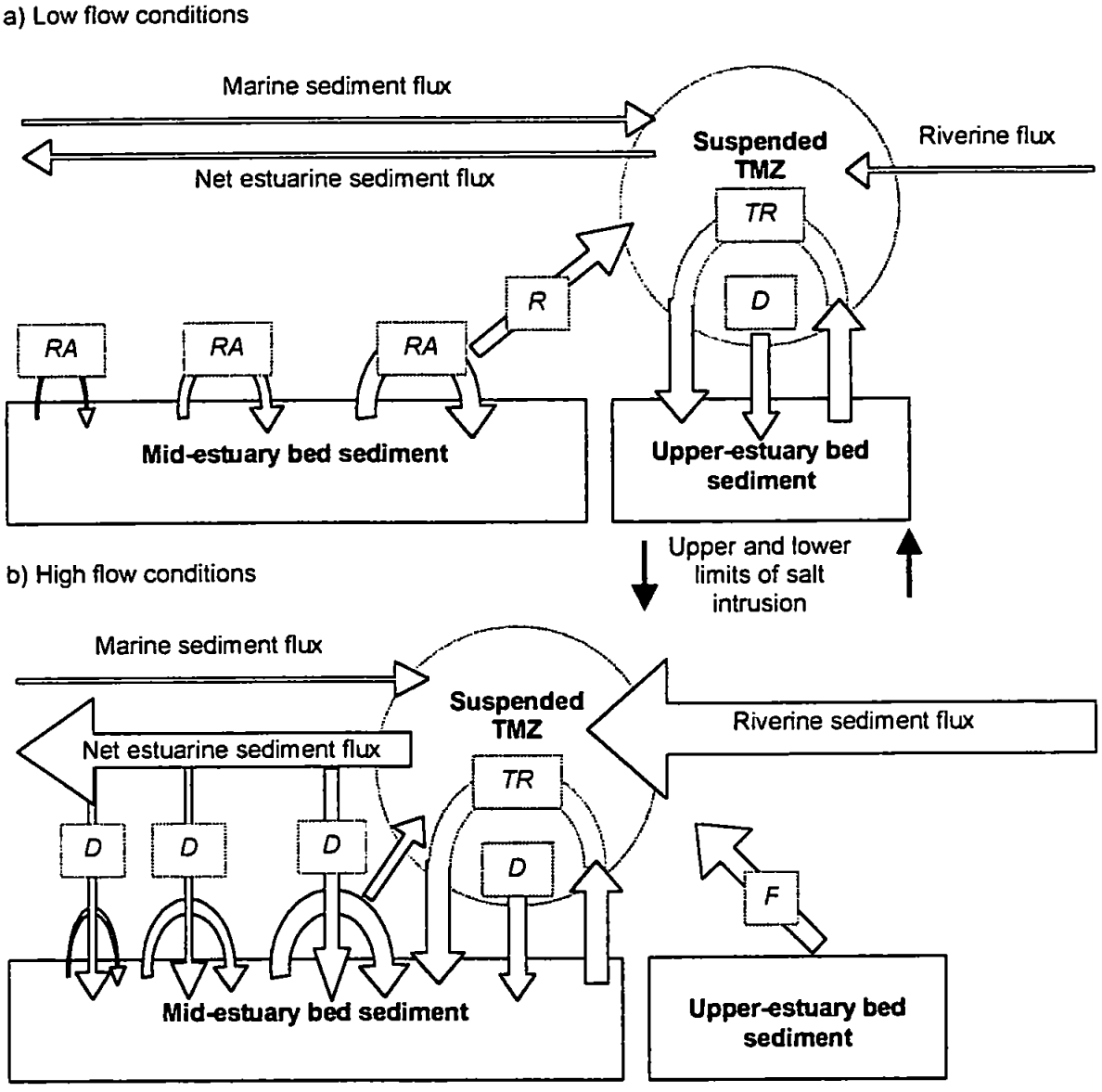

Figure 1.2 Schematic representation of resuspended sediment transport in the Tamar Estuary during a) low and b) high flow conditions. Processes represented are: Bed sediment resuspension, *R* and asymmetrical tidal pumping, *RA*. Tidal resuspension with no net transport at the null point, *TR*; net deposition, *D* and high flow remobilization, *F*. Adapted from Morris *et al.*, (1986).

An important consequence of periodic resuspension and tidal pumping is a much greater residence time of particles compared to the flushing time of the water. Table 1.2 compares

the estuarine flushing time with the particle residence time for the Humber, Mersey and Tamar estuaries.

Table 1.2 Comparison of the estimated flushing time and particle residence time for three macrotidal estuaries.

Estuary	Water flushing time, days	Particle residence time, years	Reference
Tamar	7-14	1.4	Uncles *et al.*, 1985; Bale *et al.*, 1985
Mersey	20-50	40	Nation Rivers Authority, 1995; Watts *pers. comm.* 1999
Humber	40	18	Turner, 1990

1.3 Dissolved oxygen, carbon dioxide, pH and alkalinity

1.3.1 Dissolved oxygen and carbon dioxide in estuarine waters

Dissolved oxygen and carbon dioxide saturation in an estuary will be determined by the marine and riverine values and localised physical, chemical and biological processes in the estuary. Both O_2 and CO_2 co-vary in the Clyde as a result of end member mixing and do not reach equilibrium with the atmosphere except during high winds (Muller *et al.*, 1994). The physical process of water – air flux of a gas will increase as the concentration in the water differs from the equilibrium value. The rate of gas transfer will also be determined by wind speed and mixing conditions (Cai & Wang, 1998; Frankignoulle *et al.*, 1996) an increase in which will that promote gas exchange (Muller *et al.*, 1994). Physical processes therefore tend to maintain equilibrium between the water and atmosphere. However, the net effect of diurnal variation in algal and microbial respiration and photosynthesis on the oxygen-carbon dioxide balance may completely exceed other processes influencing not just the gas partial pressures, but also the pH and metal speciation. The oxidation of organic matter by aerobic respiration is formalised as:

$$CH_2O + O_2 \rightarrow HCO_3^- + H^+ \qquad (1.3)$$

and has the effect of reducing oxygen and acidifying the system. Photosynthesis which drives Equation 1.3 from the right to the left using light energy has the reverse effect. The partial pressures of oxygen and pH will rise and partial pressures of carbon dioxide will decrease as photosynthetic activity increases (Regnier *et al.*, 1997). However, primary productivity and associated elevated partial pressures of oxygen and elevated pH is limited to day light periods and during the night oxygen saturation and pH may sag.

Seasonal variations in dissolved oxygen profiles in the Tamar show near equilibrium conditions with respect to the atmosphere in winter with the progressive development of mid-estuarine sags through the spring to summer (Morris *et al.*, 1982). Sags in dissolved oxygen have also been recorded in the Forth Estuary (Balls, 1994) and Weser Estuary (Turner *et al.*, 1992b) as a consequence of the high biological oxygen demand (BOD) of suspended particles in the TMZ (Balls, 1994). The oxidation of organic matter is mediated by hetertrophic respiration and the numbers of attached bacteria increased from 2 x 10^6 cells ml^{-1} to 135 x 10^6 cells ml^{-1} in the region of the Weser TMZ and then decreased with increasing salinity (Turner *et al.*, 1992b). In the Forth, the occurrence of the highest SPM concentrations in the summer is coincident with warm water temperatures and the resulting bacterial respiration reduces the dissolved oxygen saturation to approximately 40 % (Laslett & Balls, 1995). High concentrations of SPM are introduced into the Scheldt River and two-thirds of the load can be attributed to domestic and agricultural activities. The high rates of bacterial respiration and nitrification result in undersatuartion in the winter and partial or complete anoxia in the summer (Paucot & Wollast, 1997; Regnier *et al.*, 1997). Anoxic conditions may alter the iron and manganese hydrous-oxide and organic coatings of particles changing their surface properties (Garnier *et al.*, 1993). The dissolved oxygen saturation in the Scheldt Estuary then increases rapidly with salinity. This has a significant effect on the reoxidation of trace metal sulfides generated in the anoxic river releasing metals back to the dissolved phase (Zwolsman *et al.*, 1997; Zwolsman & van Eck, 1999). Organic pollution is also responsible for low oxygen saturation in the Westerschelde (Kromkamp *et al.*, 1995) Delaware Estuary (Sarin & Church, 1994) and Clyde Estuary (Turner, 1999).

Oxygen supersatuaration in estuaries is attributed to photosynthetic production and is typically higher in the summer and absent in the winter (Balls, 1994). The temperature, in addition to light, may have significant effects on the photosynthetic capacity of phytoplankton, introducing additional seasonal variability (Blanchard *et al.*, 1997). High dissolved oxygen saturation (125 %) in the Tamar has been attributed to localized concentrations of phytoplankton (Morris, 1978). Algal and macrophyte growth also exerts significant controls on dissolved oxygen saturation in the Tweed River (Robson *et al.*, 1996; Clayton, 1997) and estuary (Howland *et al.*, 2000). At the estuarine mouth, supersaturation may however arise due to breaking waves introducing air bubbles beneath the surface (Balls, 1994). In situations where oxygen supersaturation is mediated by

photosynthetic activity diurnal cycles may be apparent characterised by oxygen sags during the night (Bourg & Bertin, 1996).

1.3.2 Estuarine pH

The pH is a commonly measured variable during estuarine studies and a critical component of water quality monitoring (Davison *et al.*, 1994). Yet, the dynamic and often steep physico-chemical gradient that occurs during the mixing of fresh and seawater in macrotidal systems means the abiotic and biotic controls on pH in estuaries can be difficult to assess.

1.3.2.1 Abiotic controls on estuarine pH

The pH of estuarine water is buffered by the inorganic carbon (C_T) system; CO_2, HCO_3^- and CO_3^{2-} where the distribution of dissolved carbon species is governed by the temperature and salinity dependent dissociation of carbonic acid (Regnier *et al.*, 1997). Hydroxide constituents such as boron and organic anions will also buffer the system to various degrees (Whitfield & Turner, 1986) and this is discussed more full in the next section. The increase in the first and second dissociation constants of carbonic acid with salinity controls a chemical rearrangement between HCO_3^- and CO_3^{2-} species that may result in a pH minimum at a specific salinity, see Figure 1.3 (Mook & Koene, 1975). This characteristic estuarine pH minimum has been observed in the Clyde (Muller *et al.*, 1994), Fraser (de Mora, 1983), Scheldt (Frankignoulle *et al.*, 1996; Paucot & Wollast, 1997; Zwolsman & van Eck, 1999) and Tamar (Morris *et al.*, 1978) Estuaries. A pH minimum in the low salinity region of the Delaware is however attributed to pollution input (Sarin & Church, 1994). The resulting change in pH with salinity is strongly dependent upon the freshwater pH and also the alkalinity of the fresh and seawater (Morris, 1978). Low freshwater pH will result in a rapid increase in pH with salinity as observed in the Satilla and Altamaha Estuaries (Cai & Wang, 1998; Cai *et al.*, 1998). The pH is however invariant in the acidic Tinto Estuary, but increases with salinity in the less extensively mined, but still relatively low pH Odiel Estuary (Elbaz-Poulichet *et al.*, 1999). The pH distribution through an estuary can be complicated by the varying response of the system to changing tidal state, freshwater flow input and climatic conditions.

1.3.2.2 Biotic controls on estuarine pH

Biotic, in addition to abiotic, processes may effect the pH (Morris, 1978, Robson *et al.*, 1996; Clayton, 1997; Zwolsman *et al.*, 1997; Howland *et al.*, 1999). Seasonal differences in the pH distribution in the Scheldt show a rapid increase of pH with salinity in the winter, but the presence of a pH minimum at salinity of approximately 5 during spring and summer (Zwolsman *et al.*, 1997). No pH minima in the Tamar was observed during the summer (Morris, 1978) and a pH maximum in the high salinity region coincided with localised increases in dissolved oxygen and chlorophyll *a* concentration (Morris *et al.*, 1982). A pH maximum has also been reported in the Fraser Estuary (de Mora, 1983) and Tweed Estuary (Howland *et al.*, 2000) coincident with high oxygen saturation. Diurnal changes with the gradual development of a low salinity maximum in pH between mid-day and late afternoon has been observed in the Tamar and is attributed to the effects of photosynthesis on the inorganic carbon balance (Morris, 1978). Carbon uptake during bright sunshine of 0.6 to 1.8 mg l^{-1} with corresponding increase of 0.5 pH units in 2 h have been recorded in some very productive lake systems (Maberly, 1996). As CO_2 is removed from the inorganic store of carbon in the water, there is an increase of pH and CO_3^{2-}, a decrease in HCO_3^- and a buffered decrease in CO_2. The increase in CO_3^{2-} balances the HCO_3^- removal so that total alkalinity is relatively unaffected (Crawford & Purdie, 1997). Conversely when high dissolved organic carbon (DOC) concentrations occur, bacterial respiration will increase CO_2 saturation and the pH will decrease (Morris *et al.*, 1978).

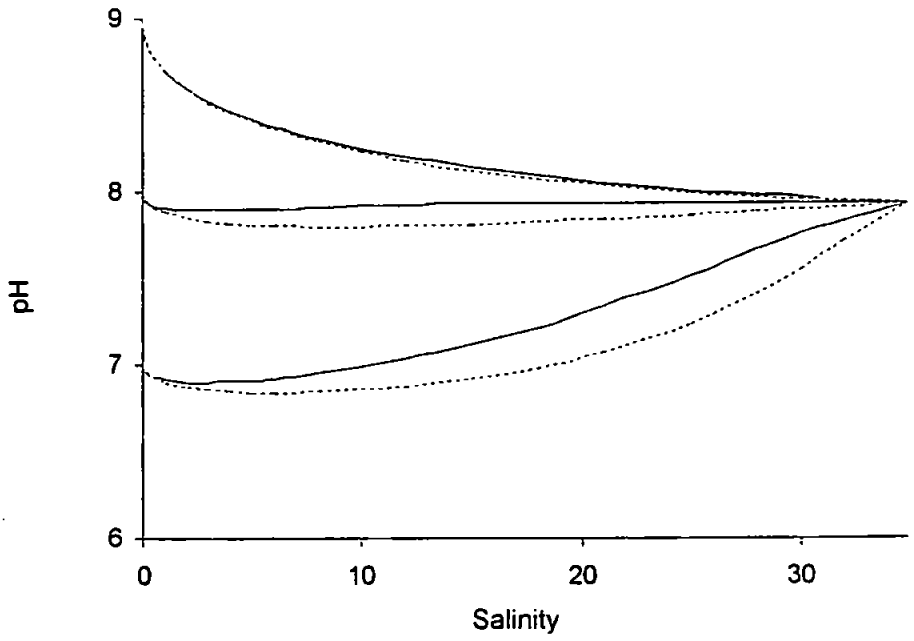

Figure 1.3 Calculated pH as a function of salinity (15°C). Alkalinity ratios of river water to sea water are 1.0 (—) and 2.0 (—). Calculations based on Mook & Koene (1975).

Muller *et al.* (1994) has successfully modelled conservative behaviour of total inorganic carbon while comparison of observed profiles with those predicted for carbonate equilibrium in Tamar shows summer profiles to be below those predicted (Morris *et al.*, 1982) and this may be due to non-conservative behaviour of alkalinity or DOC mineralization. Accurate interpretation of pH distribution in an estuary must therefore take account the chemical, biological and physical perturbations to the inorganic carbon system (Whitfield & Turner, 1986). The variation in alkalinity and pH values for a range of freshwater and estuarine systems is shown in Table 1.3. This review primarily concentrates on medium to high pH situations, but does included some examples of low pH systems for comparison.

1.3.3 Control of estuarine alkalinity

The alkalinity in an estuary will depend on the alkalinity of the river and seawater and biological and chemical processes within the estuary. Alkalinity of river water is strongly controlled by catchment geology and fluvial flow rate. The calcium carbonate content of the catchment geology is important as it acts a source of HCO_3^- ions through weathering (Rebsdorf *et al.*, 1991). Depending on catchment geology during low flow conditions a higher proportion of alkaline deep water that has been associated with the underlying geology, opposed to the soil profile may enter the watercourses in the catchment (Reynolds *et al.*, 1986) and higher HCO_3^- concentrations can occur (Neal & Hill, 1994). During storm flow rain water enters water courses through a greater variety of routes being exposed to a different range of organic or mineral components than those under base flow conditions with generally reduced contact with the bed rock (Reynolds *et al.*, 1986). As flow increase lower alkalinity water from surface and subsurface flow reduces the total river water alkalinity (Sutcliffe & Carrick, 1988; Rebsdorf *et al.*, 1991; Maberly, 1996).

Alkalinity of seawater is much less variable and values of 2.4 mequiv. l^{-1} have been reported for North Atlantic surface waters (Wong, 1979), 2.0 to 2.2 mequ. l^{-1} in the Straits of Georga (de Mora, 1983), 2.0 to 3.0 mequ. l^{-1} in the Gulf of Mexico (Benoit *et al.*, 1994), ~2.25 in San Francisco Bay (Cifuentes *et al.*, 1990) and 2.0 to 3.0 in British coastal waters (Muller *et al.*, 1994; Howland *et al.*, 2000).

Total alkalinity, A_T of an estuarine sample is defined as:

$$A_T = [Z^-] - [H^+] \quad (1.4)$$

where Z^- represents:

$$Z^- = HCO_3^- + 2CO_3^{2-} + OH^- + X^- \quad (1.5)$$

carbonate alkalinity (HCO_3^- and CO_3^{2-}), hydroxide and X^-, non-carbonate and non hydroxide constituents such as $SiO(OH)_3^-$, $B(OH)_4^-$ and organic anions.

Effluent enriched in boron such as boron containing materials used in washing powders may also influence river water concentrations (Neal *et al.*, 1998a). Conservative behaviour of boron in the Tamar has been reported by Liddicoat *et al.* (1983) and the contribution of boron to alkalinity in low salinity water will be minimal (Cai *et al.*, 1998). In marine water boron contributes ~2 % of the total alkalinity (Liddicoat *et al.*, 1983), but the greater carbonate buffering capacity ensures that the pH shift due to boric acid ionisation is small despite the increased concentrations (Whitfield & Turner, 1986). Mine drainage waters may also significantly effect the total alkalinity and pH. Drainage waters from large sulphide deposits such as the Iberian Pyrite Belt introduce sulfuric acid to water courses producing pH values as low as 2.5 (Elbaz-Poulichet *et al.*, 1999). At pH of 5 hydroxy-aluminium may also contribute to A_T when hydrogen ions are consumed to form dissolved aluminium; $Al(OH)^{2+} + H^+ = Al^{3+} + H_2O$ (Sutcliffe & Carrick, 1988). Humic acids from salt marshes or river water may effect the alkalinity of estuarine waters (Cai *et al.*, 1998) if the C_T concentration and pH are also low compared to dissolved organic carbon (Herczeg & Hesslein, 1984; Neal & Hill, 1994).

The estuarine distribution of alkalinity will depend upon the range of processes occurring in the estuary. Conservative behaviour of alkalinity has been reported in a range of estuaries (Wong, 1979; Cai & Wang, 1998). Non-conservative behaviour of alkalinity is however reported for the Scheldt Estuary (Frankignoulle *et al.*, 1996; Regnier *et al.*, 1997); Satilla River and to a lesser extent the Altamaha River (Cai & Wang, 1998) and is also noted in the Fraser Elbe, Weser and Ems River estuaries (de Mora, 1983). Non-conservative behaviour occurs when sediments act as a proton source and alkalinity is reduced through bacterial mediated nitrification (Frankignoulle *et al.*, 1996; Regnier *et al.*, 1997) and SO_4^{2-}, Fe^{3+} or Mn^{4+} reduction (Lerman & Stumm, 1989). Photosynthetic removal of CO_2 will elevate the pH and under extreme carbon depletion and high pH HCO_3^- may decrease by conversion to CO_3^{2-} (Maberly, 1996). Direct photosynthetic assimilation of HCO_3^- may also occur if CO_2 is limiting (Crawford & Purdie, 1997). The biological production of calcium carbonate shells will also reduce the alkalinity (Whitfield

Table 1.3 Alkalinity and pH values for lake, river and estuarine systems.

	pH	Alkalinity	Reference
Lakes & reservoirs			
Esthwaite Water	<10.5	320-450	Talling, 1976
Esthwaite Water	7.1-10.3	328-572	Maberly, 1996
Kis-Balaton	8.1-8.3	- -	Istvanovics, 1994
Various tarns	5.3-4.2	7-1227	Sutcliffe & Carrick, 1988
Windermere	<9.6	~240	Talling, 1976
Rivers			
Don	7.7-8.3	- -	Warren & Zimmerman, 1994
Falling Spring Run	7.1-8.2	352-313*	Hoffer-French & Herman, 1989
Humber rivers	7.5-8.0	80-210*	Jarvie *et al.*, 1997
King	4.6-4.8	- -	Featherstone & O'Grady, 1997
La Solana	8.2-8.3	3580-4480	Guasch *et al.*, 1998
LOIS UK	6.6-10.4	65-4425	Neal *et al.*, 1998d
Lot	8.0-8.7	1.3-1.6	Bourg & Bertin, 1996
Milwaukee	7.6-8.7	- -	Shafer *et al.*, 1997
Riera Major	7.8-8.5	1110-1850	Guasch *et al.*, 1998
Thames	7.8-9.4	- -	Neal *et al.*, 1998b
Tinto	2.4-3.1	- -	Elbaz-Poulichet *et al.*, 1999
Tweed	6.7-10.4	64-3220	Neal *et al.*, 1998c
Vaal River	~8.10	~180	Roos & Pieterse, 1995
Wisconsin Rivers	6.8-8.4	- -	Shafer *et al.*, 1999
Wolf	7.3-8.7	- -	Shafer *et al.*, 1997
Estuaries & coastal lagoons (freshwater & low salinity)			
Altamaha	6.6-6.8	0.3-0.4† (c/n)	Cai *et al.*, 1998
Clyde	7.3-7.4	960-1500 (c)	Muller *et al.*, 1994
Danube	8.0-8.3	- -	Guieu *et al.*, 1998
Delaware	7.6-6.8	0.85-0.98† (n)	Sarin & Church, 1994
Fraser	7.6-8.2	810-1310 (n)	de Mora, 1983
Humber	6.5-7.9	- -	Turner *et al.*, 1991
James River	7.5-7.7	~700 (n)	Wong, 1979
Maeklong	6.6-7.7	- -	Windom *et al.*, 1991
Odiel	2.8-8.3	- -	Braungardt *et al.*, 1998; Elbaz-Poulichet *et al.*, 1999
Ogeechee	6.4-6.5	- -	Cai & Wang, 1998
Rhine Delta	7.1-8.4	- -	Admiraal *et al.*, 1995
San Francisco Bay	- -	1050-1650 (c)	Cifuentes *et al.*, 1990
Satilla	5.5-6.2	0.1† (n)	Cai *et al.*, 1998
Savannah	5.5-7.0	0.5 † (c)	Windom *et al.*, 1991, Cai *et al.*, 1998
Scheldt	7.1-8.8	~5000 (n)	Turner *et al.*, 1991; Frankignoulle *et al.*, 1996; Paucot & Wollast, 1997; Zwolsman *et al.*, 1997, Zwolsman & van Eck, 1999
Tamar	6.9-8.7	- -	Morris, 1978; Morris *et al.*, 1978; 1982
Terminos lagoon	6.3-8.5	- -	Vazquez *et al.*, 1999
Texas estuaries	- -	400-4800 (c/n)	Benoit *et al.*, 1994
Tweed	7.5-10.4	800-1900 (c)	Howland *et al.*, 2000

Alkalinity reported as μequiv. l^{-1} with the exception of * mg l^{-1} HCO_3 and † mM l^{-1} HCO_3^-. Estuarine behaviour of alkalinity is detailed as conservative, c or non-conservative behaviour, n.

& Turner, 1986; Lerman & Stumm, 1989). Removal of HCO_3^- reduces alkalinity, the corresponding increase of H^+ driven through the K_1 dissociation reaction is countered by a H^+ decrease through the K_2 dissociation reaction so that the pH is relatively unaffected (Crawford & Purdie, 1997). Alternatively, alkalinity can be increased by bicarbonate release from sediments during chemical dissolution of $CaCO_3$ (Whitfield & Turner, 1986) or NO_3^- or SO_4^{2-} reduction (Lerman & Stumm, 1989). Non-conservative behaviour of A_C is controlled by anaerobic and benthic processes such as reduction while C_T is also controlled by respiratory and photosynthetic processes and air-water exchange (Cai & Wang, 1998). C_T therefore exhibits much greater spatial and temporal variability, with no clear relationship between C_T and alkalinity in rivers of North East England (Neal *et al.*, 1998d).

1.4 Estuarine reactivity of cadmium and zinc

This work concentrates on the estuarine behaviour of the trace metals; Cd and Zn. Zinc is regarded as essential micronutrient for the growth of phytoplankton (Morel *et al.*, 1991), but above certain concentrations is toxic to many aquatic organisms (Bryan *et al.*, 1987; Florence *et al.*, 1994). Filter feeding bivalves accumulate Cd (Pollet & Bendell-Young, 1999) and Zn (Bilos *et al.*, 1998) from SPM and are routes of exposure to man. The potential danger that elevated concentrations of these elements pose to habitat and human health is in part controlled by how they are transported through environmental systems and each exhibit a different estuarine geochemistry.

Measurements of dissolved metal concentrations can be divided into a range of species and soluble and colloidal material (Sung, 1995). The size range of ions, humates, oxides, mineral particles and biogenic particles are shown in Figure 1.4. How a dissolved element behaves in an estuarine environment is normally described by comparing its concentration to that of another solute, typically salinity to generate a mixing curve (Morris, 1990), see Figure 1.5.

In a two component system where the composition of end members is constant, a linear relationship between the constituent and salinity demonstrates conservative behaviour. A concave, convex or variable relationship may indicate non-conservative behaviour or variability in the end member composition. Either factor may be significant when considering the flux and fate of pollutants in the coastal zone (Oakley *et al.*, 1981; Pankow & McKenzie, 1991; Kraepiel *et al.*, 1997; Turner, 1999).

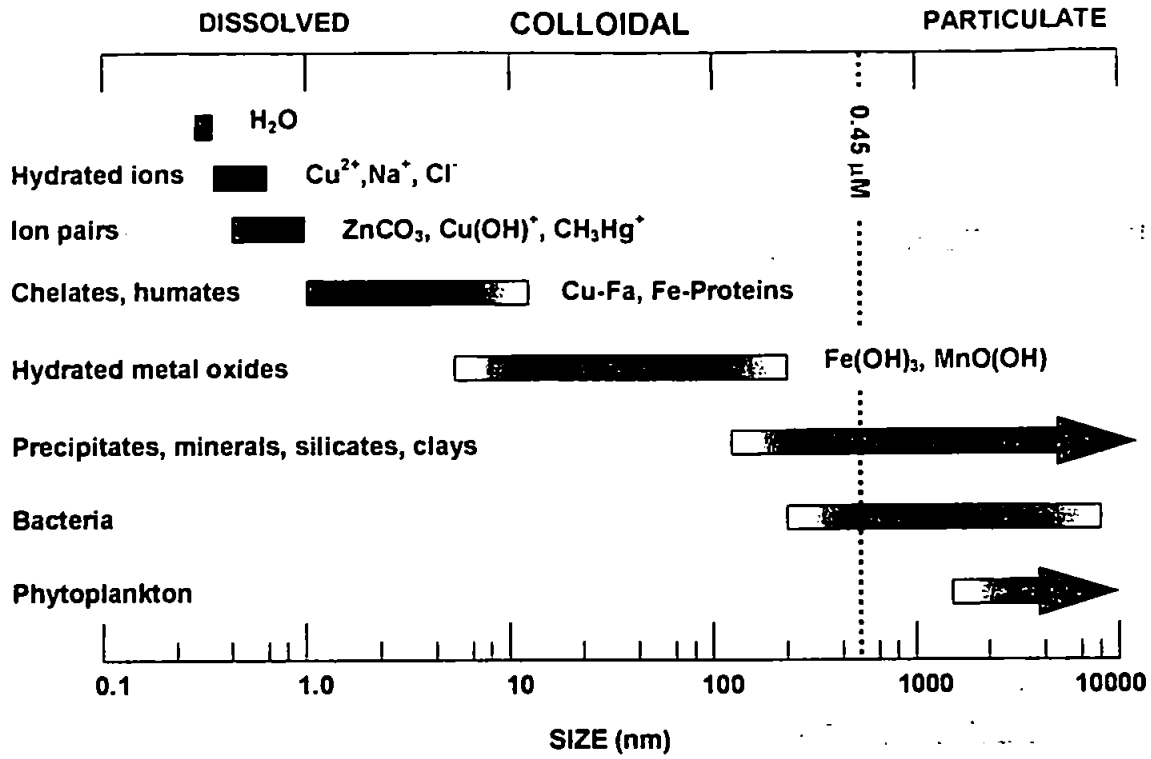

Figure 1.4 The dimensions of soluble, colloidal, and particulate matter in estuaries. The operational distinction between dissolved and particulate fractions is typically 0.45 µm. Adapted from Mantoura & Morris (1983).

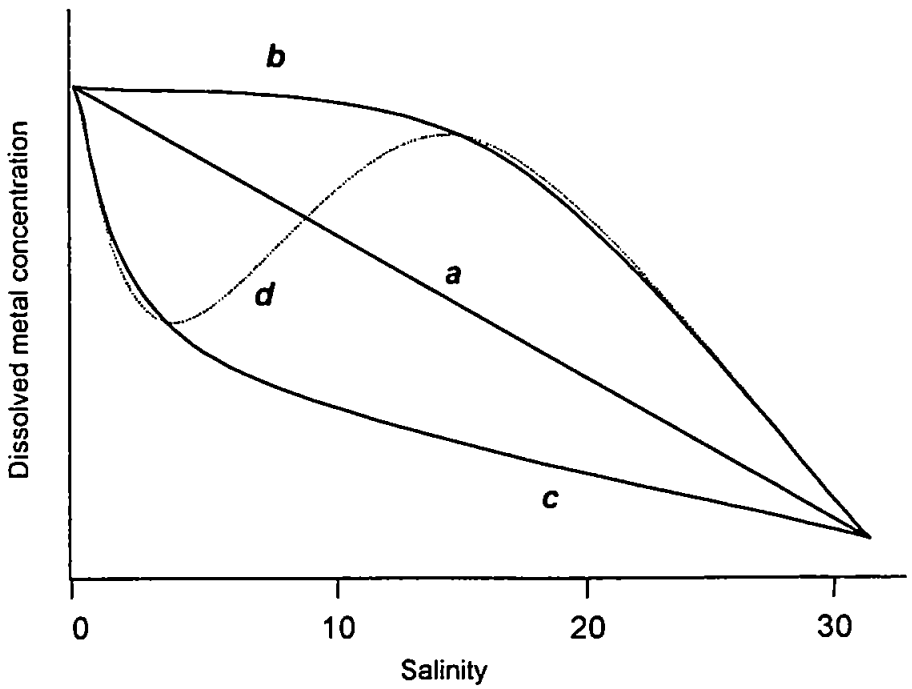

Figure 1.5 Schematic representation of the estuarine distribution of a dissolved constituent under steady state conditions of fixed end members; conservative, *a*; addition, *b*; removal, *c* and variable, *d* behaviour. Adapted from Mantoura & Morris (1983).

The geochemical behaviour of Cd and Zn are illustrated in Table 1.4. This shows that each metal exhibits considerable inter-estuarine variability in response to the unique biogeochemical and hydrodynamic conditions of the system. A general behaviour for each

metal does however become apparent. Zinc is characterised by removal from the dissolved phase at low salinities and subsequent release as the salinity increases. Cadmium shows less removal and is more commonly released from particles at higher salinity.

Non-conservative behaviour occurs when metals are removed from or released to the dissolved phase. This will depend on particle adsorption and desorption processes and discharges of dissolved metal or water into the estuary. The transfer of a metal from dissolved to particulate phases depends critically on speciation, colloidal interaction, redox sensitivity, microbial mediation, existing metal loading and particle composition (Oakley *et al.*, 1981; Glegg *et al.*, 1988; Turner *et al.*, 1992b; Hamilton-Taylor *et al.*, 1993; Tipping *et al.*, 1998). These are all processes that can vary between sites and respond to seasonally variable conditions (Church, 1986; Morris, 1986; Sarin & Church, 1994; Wood *et al.*, 1995; Koelmans & Radovanovic, 1998).

Table 1.4 Field observations of dissolved concentrations of Cd and Zn illustrating removal from, and release to the dissolved phases and conservative behaviour between dissolved and particulate phases.

Estuary	Trace metal	Reference
Release		
Danube (low salinity)	Cd	Guieu *et al.*, 1998
Forth (mid estuary)	Zn	Balls *et al.*, 1994; Laslett & Balls, 1995
Gironde & Rhone (low salinity)	Cd	Elbaz-Poulichet *et al.*, 1987
Gironde (mid salinity)	Cd, Zn	Kraepiel *et al.*, 1997; Pham *et al.*, 1997
Hudson	Cd	Yang & Sanudo-Wilhelmy, 1998
Humber	Cd	Comber *et al.*, 1995
Loire	Cd	Thouvenin *et al.*, 1997
Scheldt (mid salinity)	Cd, Zn	Zwolsman *et al.*, 1997; Baeyens *et al.*, 1998
Scheldt (low-mid salinity)	Cd, Zn	Paucot & Wollast, 1997
Tamar (mid estuary)	Zn	Ackroyd *et al.*, 1986, Liu, 1996
Removal		
Forth (low salinity)	Zn	Balls *et al.*, 1994; Laslett & Balls, 1995
Medway, Savannah & Maeklong	Zn	Windom *et al.*, 1991
Mersey (low-mid salinity)	Cd, Zn	Comber *et al.*, 1995
Scheldt (low salinity)	Cd, Zn	Zwolsman & van Eck, 1999
Tamar (low salinity)	Zn	Ackroyd *et al.*, 1986; Liu, 1996
Conservative		
Danube	Zn	Guieu *et al.*, 1998
Forth	Cd	Balls *et al.*, 1994
Loch Linnhe	Cd	Hall *et al.*, 1996

1.4.1 Trace metal adsorption by estuarine particle

Substantial removal of dissolved trace metals is a consistent feature of the low salinity high turbidity zone of macrotidal estuaries (Morris, 1986) and occurs through a range of processes. Iron and Mn oxides on particle surface are important in controlling the uptake of Cd and Zn in estuarine environments (Millward *et al.*, 1994; Moffett & Ho, 1996). Co-precipitation may then occur when pre-existing Mn-Fe oxide coatings on particles or microbially mediated oxidation enhance precipitation of Mn (Morris & Bale, 1979; Vojak *et al.*,1985; Ackroyd *et al.*, 1986; Turner *et al.*,1992a; Moffett & Ho, 1996). Oxidation is also dependent on seasonally variable dissolved oxygen saturation (Owens *et al.*, 1997).

Adsorption of ionic metals onto colloids and subsequent coagulation of colloids onto larger particles is a dominant process of metal removal in low suspended particle situations and is important for Fe, but less so for Cd and Zn (Li *et al.*, 1984a). The control of Zn by Fe phases has however been shown to be significant in the Tamar (Ackroyd *et al.*, 1986). Coagulation and precipitation of colloidal Fe has also been observed in the Gironde Estuary (Kraepiel *et al.*, 1997) and precipitation of Fe in the Humber leads to elevated SSA (Turner *et al.*, 1991).

Behaviour of the colloidal fraction is important as it can form a significant proportion of the total dissolved (<0.45 μm) concentration and values of 34 to 40 % of Cd, 50 to 54 % of Mn and 60 to 87 % of Fe are reported in the Danube River (Guieu *et al.*, 1998) and Venice Lagoon (Martin *et al.*, 1995). High proportions of colloidally bound Fe and Zn have also been reported in a range of other systems (Martin *et al.*, 1993; Benoit *et al.*, 1994; Morgan *et al.*, 1996; Wen *et al.*, 1997). Measurements of dissolved concentration may however be restricted to the labile fraction and fail to account for these colloidal bound metals (Camusso *et al.*, 1997).

In the Danube River pH values around 8 units lead to precipitation of hydrated oxides removing Fe and Mn from solution (Guieu *et al.*, 1998) and Admiraal *et al.* (1995) found enhance Mn precipitation during phytoplankton blooms in the River Rhine. They do not however identify to what degree this is due to increased oxygen saturation or elevated pH. Non-conservative behaviour of Fe due to precipitation of hydrated oxides and flocculation due to high pH has also been noted by Li *et al.* (1984b). In the Scheldt, spring and summer phytoplankton blooms increased the pH by up to one unit (Zwolsman *et al.*, 1997), while in the Tweed river and estuary pH ranges from less than 7 to nearly 10.5 (Howland *et al.*,

2000). There are varied reports of the effect of pH on trace metal behaviour, although there are very few data for metal behaviour in estuarine systems with pH ranges as high as the Tweed. Gagnon *et al.* (1992) showed that Cd speciation and subsequent uptake is affected by pH and Hegeman *et al.* (1992) and Zwolsman *et al.* (1997) agree that increases in pH enhanced adsorption. This maybe due to metal precipitation as oxides, hydroxides or hydrocarbonates as well as adsorption (Johnson, 1986). Despite a large degree of scatter in their data Bourg & Bertin (1996) identified diurnal changes in dissolved Zn that were inversely correlated to changes in pH mediated by photosynthetic activity. When freshwater pH is less than that of seawater the rapid increase of pH with salinity will promote adsorption (Zwolsman *et al.*, 1997), however salinity has been shown to be more significant than pH, resulting in net Cd and Zn desorption (Li *et al.*, 1984b). The influence of pH and oxygen was also minor compared to the effect of salinity and particulate concentration on Zn and Mn adsorption in the Tamar (Ackroyd *et al.*, 1986). The pH minima in an estuary may however destabilizes soluble metal-carbonate complexes leading to metal precipitation (Sarin & Church, 1994). Carbonate species are important for Cd, and hydroxy species may be important for a range of elements under high pH freshwater conditions (Mantoura *et al.*, 1978; Tipping *et al.*, 1998).

In addition to the effects of primary productivity on the oxygen saturation and pH of the water and the resulting consequences for metal uptake by lithogenic particles, metals may be adsorbed by particulate organic matter (POC). High concentrations of POC are associated elevated suspended solids originating from organic rich soil material introduced under high river flows (Neal *et al.*, 1997) or with phytoplankton blooms that lead to seasonal variation in the overall SPM composition (Balls, 1990, Zwolsman & van Eck, 1999). In comparison to the high affinity of some metals for the Fe-Mn oxides Cd tends to be more concentrated in biogenic particles (diatoms and dinoflagellates) than non-biogenic ones (Noriki *et al.*, 1985; Balls, 1990; Turner *et al.*, 1992a; Owens *et al.*, 1997). Kuwabara *et al.* (1989) and Turner *et al.* (1991) have also shown correlation of particulate Cd and Zn with particulate organic carbon associated with phytoplankton blooms. The preferential incorporation of some elements in phytoplankton may then result in seasonally variable removal of metals from the dissolved phase (Balls, 1990).

Riverine particles that are already at equilibrium with the dissolved phase will not adsorb further metal ions unless an appropriate thermodynamic drive exists (Morris, 1990). In macrotidal estuaries the tidal pumping of particles provides metal depleted material that

can subsequently adsorb metals from the dissolved phase when resuspended (Ackroyd *et al.*, 1986; Morris, 1990; Zwolsman *et al.*, 1997). These particles then be flushed down the estuary desorbing the bound metal as salinity increases. The extent of metal release is variable (Hegeman *et al.*, 1992; Paalman *et al.*, 1994) and there is evidence that particle reactivity diminishes with age (Moore & Millward, 1988). This may be particularly significant in estuaries such as the Mersey where particle residence times may be as long as ~40 years (Watts, 1999 *per. comm.*).

The processes discussed above occur over a range of time scales, although strongly binding metals tend to adsorb more rapidly compared to those that are more weakly held (Jannasch *et al.*, 1988). Generally, initial rapid adsorption is followed by much slower uptake processes as the partitioning between phases moves towards equilibrium (Comans *et al.*, 1991) and initial rapid uptake can occur less than a minute while sequentially slower sorption processes may last several days (Jannasch *et al.*, 1988; Turner *et al.*, 1992a). During the initial uptake phases metals rapidly bind to particle surface sites, the subsequently slower phase may then involve migration to more internal sites within the clay structure or mineral lattice (Moore & Millward, 1988). This type of biphasic adsorption has been reported for Zn (Glegg *et al.*, 1988; Hegeman *et al.*, 1992) and rapid uptake from freshwater accounted for the removal of 50 % of dissolved Zn in 2 hours with a total of 70 % removal after 90 hours (Millward *et al.*, 1992). Cd adsorption was also found to occur rapidly with 90 % adsorbed within a few hours (Paalman *et al.*, 1994). Higher rates of removal have been reported for Rhine River particles, removing most of the Zn from the dissolved phases in as little as 6 hours (Hegeman *et al.*, 1992). Salinity reduced adsorption and lower rates have been reported with 30 % removed after 90 hours (Millward *et al.*, 1992) and in Puget Sound seawater ^{65}Zn was found to require up to 6 days to reach 90% removal (Jannasch *et al.*, 1988).

1.4.2 Cd and Zn desorption from estuarine particles

Mid-estuarine regions of elevated dissolved metal are also a typical feature of many systems. If maxima in dissolved metal concentrations are uncorrelated with concentrations of SPM, then dissolved concentration may be influenced by processes other than desorption from re-suspended particle (Owens & Balls, 1997). Dissolved metals introduced into the mid estuary through domestic and industrial discharge, sewage treatment plants and shipping activities in the Clyde Estuary complicate the otherwise conservative metal-

salinity relationship (Muller *et al.*, 1994). The decay of marsh vegetation is a potential source of Zn in the Tay Estuary where sewage pollution is less relevant (Owens & Balls, 1997). Positive deviations from conservative behaviour of metals in the Humber could not be explained by particle sorption processes and were attributed to input from the River Trent (Comber *et al.*, 1995). Conversely the lack of a clear anthropogenic signal in the industrialised Forth Estuary may result from the high SPM concentrations which 'buffer' the effects of any point sources of metals entering the estuary (Owens *et al.*, 1997). It is therefore important to distinguish between external (pollution) and internal (sediment-water) interaction (Turner, 1999).

Addition from sediment pore waters or desorption from resuspended sediments is mainly controlled by redox state and salinity. Mn can then be reduced to a more soluble form in oxygen depleted waters or sediments and trace metals such as Zn that co-precipitated with the Mn (Owens *et al.*, 1997) are released into the pore waters (Turner, 1999). The reduced Mn (II), and Zn may then be liberated from the sediments (Laslett & Balls, 1995) through processes such as wind resuspension of bottom sediments (Owens & Balls, 1997) or high river flows flushing out anoxic bottom waters (Garnier *et al.*, 1993). Photochemically induced dissolution of particulate Mn may also release bound metals back to the dissolved phase as reported in the Humber (Millward *et al.*, 1996).

Redox conditions are also important in controlling sulfide-metal oxidation processes, but unlike Mn oxyhydroxides, sulfides precipitate under anoxic conditions. The existence of anoxic conditions in the upper part of the Scheldt Estuary is probably the main factor in controlling the behaviour of inorganic elements in this estuary. Cadmium and Zn co-precipitation with sulphites under anoxic and low pH conditions are then subsequently released back to the dissolved phase under the oxic conditions of the mid to lower estuary, resulting in estuarine maxima (Paucot & Wollast, 1997; Zwolsman *et al.*, 1997; Baeyens *et al.*, 1998).

The change in salinity within an estuary is one of the most significant processes in controlling the distribution of Cd and Zn between dissolved and particulate phases and is due to chloride complexation and cation competition. The proportion of free metal ions that bind with Cl^- and SO_4^{2-} anions increases with salinity enhancing mobilisatisation from the particle and preventing particle readsorption (Mantoura *et al.*, 1978; Elbaz-Poulichet *et al.*, 1987; Comber *et al.*, 1995; Tipping *et al.*, 1998). Cadmium has a higher chlorocomplex

stability than Zn and thermodynamic equilibrium calculations of Cd speciation show a progressive decease in free aquo ions from $CdCl^{-} \rightarrow CdCl_2 \rightarrow CdCl_3^{-}$ as salinity increases (Comber *et al.*, 1995). In addition to chlorocomplexation the occupation of sorption sites by seawater cations such as Na^{+}, K^{+}, Ca^{2+} and Mg^{2+} also prevents other cations from adsorbing on to the particle surface (Paalman *et al.*, 1994; Turner & Tyler, 1997).

1.4.3 Conservative behaviour of Cd and Zn in estuaries

If the dissolved phase appears to behave conservatively, sorption processes may be thermodynamically or kinetically limited or are below the level of detection. Physical time constraints are important in regulating the particle induced behaviour of trace metals (Ackroyd *et al.*, 1986). The dissolved metal concentrations observed will depend critically on the rate and extent of chemical or physical transformation compared to speed of transportation, all of which can be seasonally dependent (Church, 1986). The smaller or more rapidly flushed the estuary, the lower the available reaction time. If reactions involving the constituent are too slow, or only utilise a small proportion of the total concentration then no 'measurable' change may occur (Morris, 1990). For instance, the short residence time (3 to 7 days) and low SPM (2 to 10 mg l^{-1}) is responsible for the quasi-conservative behaviour of a range of metals in the Clyde Estuary (Muller *et al.*, 1994).

The flocculation of metal rich colloids does not imply that these newly formed particles will then settle out of suspension and their filterability does not necessarily equate to their tendency to be deposited in the estuary (Mayer, 1982). In these instances, the colloidal metals may continue to behave conservatively. Colloidal fractions of Cd and Zn show conservative behaviour in the Gironde Estuary (Kraepiel *et al.*, 1997) and metal binding to humic material may reduce particle uptake (Turner *et al.*, 1998), although humic acids will have less effect on metal speciation at higher pH (Mantoura *et al.*, 1978). If there are sufficient sorption sites then competition between metals will not be significant in affecting adsorption (Koelmans & Radovanovic, 1998). Under low SPM concentrations, competition between metals for adsorption sites may however become important and Ni will compete with Cd for the same adsorption sites reducing its removal from the dissolved phase (Gagnon *et al.*, 1992).

1.4.4 The partition coefficient, K_d

The transfer of a pollutant between phases can be numerical described using a range of equilibrium or kinetic expressions. The partition coefficient K_d is widely used to describe the solid-solution partitioning of not only stable isotope trace metals, but also radionuclides (Hamilton-Taylor *et al.*, 1993; Turner, 1996), PCBs and dioxins (Turner & Tyler, 1997). The K_d is defined as the ratio of the concentration of a constituent in the solid phases, C_P ($\mu g\ g^{-1}$), to that in solution, C_S ($\mu g\ l^{-1}$):

$$K_d = \frac{C_P}{C_S} \qquad (1.6)$$

Partition coefficients can be derived by several means. These means include field measurements of dissolved and particulate concentrations (Turner *et al.*, 1992b; Balls *et al.*, 1994; Millward & Turner, 1995) and radioisotopes (Jannasch *et al.*, 1998; Turner *et al.*, 1993; Millward *et al.*, 1994; Turner & Tyler, 1997) or stable isotope (Liu. 1996) controlled partitioning experiments. Analytically determined concentrations are highly dependent on the digest used. Total or partial extraction of the particulate phase may liberate metals that had been absorbed, or precipitated releasing a greater fraction than that normally available for exchange under natural conditions. Radioisotope experiments also experience several analytical limitations (Benes *et al.*, 1988) and experimental conditions cannot be varied accurately in accordance with the nature and time-scales of *in situ* processes (Turner, 1996). The partitioning of any metal may also be highly site specific and the K_d can vary by an order of magnitude with changes in the source and composition of the particles (Li *et al.*, 1984a; Turner *et al.*, 1992b; Wood *et al.*, 1995). Due to the differences in water chemistry, particle chemistry or analytical or experimental procedure, K_ds determined in one system may not be appropriate for another when trying to parameterise solid-solution reactions (Koelmans & Radovanovic, 1998).

The K_d approach also assumes that adsorption and desorption are effectively instantaneous and fully reversible (Turner, 1996). For many rapid processes this may be a valid assumption (Hoffmann, 1981). For instance abiotic processes, involving inorganic carbon are close to equilibrium compared to the time scales occurring during estuarine transport (Regnier *et al.*, 1997) and an equilibrium approach has been successfully used by Kraepiel *et al.* (1997) to model the distribution of Cd. Depending on the time scales considered steady-state assumptions may be inappropriate and lead to significant errors (Regnier *et al.* 1997). For instance, apparent K_ds may be far removed from equilibrium in rapidly flushed

estuaries (Morris, 1990; Turner *et al.*, 1992b) and models of their behaviour may need to include kinetics (van Gils *et al.*, 1993) or multiple steps (Moore & Millward, 1988; Koeppenkastrop & de Carlo, 1993) to accurately replicate the sorption process. The key issue is what approach, whether equilibrium or kinetic, or single or multiple step is appropriate for the system or metal under examination.

The K_d has, however, found less favour in freshwater systems (Tipping *et al.*, 1998). Nevertheless the change of K_d in response to changes in salinity and particle type (Turner *et al.*, 1992a; 1993; Turner, 1996; 1999) means that, despite the assumptions and limitations the K_d is a powerful tool to predict the flux and fate of pollutants in estuaries, even when there is little understood about the sorption mechanisms involved (Turner, 1996; Turner & Tyler, 1997). However, the K_d is dependent on the accurate determination of the exchangeable particulate and dissolved concentrations and the operationally defined distinction between these of 0.45 μm. The K_d may therefore be strongly biased by a range of experimental introduced factors.

1.5 Simulation modelling of estuarine systems

The first step in assessing the concentrations at which materials may be disposed of in the environment is the identification of an appropriate technique to predict the behaviour and concentration of the pollutant in the coastal zone (IAEA, 1991). A model is a 'representation of reality' that provides a simplified description of an object, process or group of processes (Hess *et al.*, 1999). Various different types of model are employed in environmental studies. Physical models such as tidal hydraulic models were common place in the 1970's. At this time, there was insufficient computing power available to predict the complex array of physical processes that occur in estuaries. Physical models however suffered from several problems, such as the large size required to reduce scaling problems, friction and the difficulties of simulating salinity density gradients (McDowell & O'Conner, 1977). The alternative to a scale replica is a mathematical model where processes can conventionally be considered to include empirical or mechanistic calculations. Empirical models use statistical fits of data determined from analysis of variance and simple or multiple linear regression to predict the response of one variable to changes in one or more other variables (IAEA, 1991). In contrast, mechanistic models employ a prior knowledge about an individual processes and are often based on conservation or thermodynamic laws (van Straten, 1998). Mechanistic models may

therefore have a wider applicability than empirical models, which tend to be very site specific. Mechanistic models are however limited by the degree of understanding of a process, while empirical models are not. Statistically derived parameters should also be regarded as a means of interpolation as they are most applicable within the range of data from which they were generated (IAEA, 1991; van Straten, 1998). Simulation modelling is a broad term describing models where multiple numerical relationships, often empirical together with mechanistic relationships are solved to provide a description of a complex system. For any physical or numerical model to have any significant value it must be based on a sound conceptual design that is able to relate a particular environmental variable to the appropriate driving force. If an essential process is omitted from the conceptual model then no matter how accurate the encoding of existing parameters the model will not provide a true representation of the natural system.

1.5.1 Simulation models

There were few examples of simulation models of estuaries reported in the literature prior to the early 1980's. The greater need to understand and predict estuarine systems has led to a marked increase in the development and application of simulation models and software tools to predict the flux of water, sediment and other constituents (Falconer & Lin, 1997). There are at present commercially available software packages such as the Estuarine Contaminant Simulator, ECoS (Harris *et al.*, 1993; Gorley & Harris, 1998; Harris & Gorley, 1998a,b), Pollution Information System for Contaminants in Estuaries and Seas, PISCES (Ng *et al.*, 1996) and the Danish Hydraulic Institute 1-D (MIKE 11) and 2-D (MIKE 21) models (Danish Hydraulic Institute, 1995, 1996). These modelling environments that can be parameterised for specific processes or systems using a graphical interface to reduce the need for detailed computer programming skills. The simulation models are useful tools for both researchers and environmental mangers. For instance it may be impossible, impractical or too costly to build a scale model (Falconer, 1992). By dividing the system into a hierarchy of components and testing the response of each component to forcing influences, a simulation model can be developed (Tyler *et al.*, 1997). The action of building the model in itself establishes a systematic framework for analysing a problem and helps to provide a greater understanding of the system, pinpointing areas of inadequate understanding (IAEA, 1991; Wood *et al.*, 1995). It can also save time and money in current studies by reducing field measurements or indicating which conditions would provide the most important information. It may also not be possible to observe a real

system under the required range of conditions or required time scale (Gillibrand & Balls, 1998). Once a model design has been developed and tested it can be encoded for other areas or run using a range of scenarios to predict the transport and fate of contaminants during accidental or authorised discharges under current or hypothetical climatic conditions (IAEA, 1991; Bewers *et al.*, 1992; Ng *et al.*, 1996; Falconer & Lin, 1997). Model can then be used to assess the environmental-economic consequences of the effects of different wastewater and pollution control schemes such as the MIKE 11 models of biological oxygen demand in the Forth Estuary (Hanley *et al.*, 1998) and Yamuna River (Kazmi & Hansen, 1997).

1.5.2 Review of modelling strategies

The choice of modelling strategy depends upon management or research questions posed and the resources available for model development and implementation. It also depends on the nature of the contaminant to be investigated, and on the spatial and temporal time scales and resolution of interest (IAEA, 1991; Bewers *et al.*, 1992).

Estuarine models can be categorised according to two types. Firstly, there are models that begin by modelling the hydrodynamic structure of the system to provide a representation of the physical processes of tidal propagation, mixing and transport of material in solution and in suspension. Secondly, there are models that are concerned with processes within the estuary (chemical, biological or physical), but do not include advection-dispersion terms, assuming that these phenomena can be adequately accommodated in other ways. Members of the first group (*e.g.*, ECoS and MIKE 11 and 21) can be classed as coupled hydrodynamic-geochemical models while those of the second are more typical of speciation models such as the Windermere Humic Aqueous Model, WHAM (Tipping *et al.*, 1998), Sediment Water Algorithm for Metal Partitioning, SWAMP (Koelmans & Radovanovic, 1998) and those of Hoffmann, (1981), Oakley *et al.* (1981) and Sung (1995). Examples of coupled hydrodynamic-geochemical models reported in the current literature for trace metal and other water quality constituents are shown in Table 1.5.

The estuarine models listed in Table 1.5 are generally aimed to simulate complex natural systems based on a small range of readily attainable data sets driving a number of key variables (Nilsson *et al.*, 1996; Abreu *et al.*, 1998). Whether a processes is essential or not may however be difficult to quantify and perhaps not at all evident at the outset of a

Table 1.5 Coupled hydrodynamic-biogeochemical simulation models for a range of water quality variables. The models are listed according to their publication date in the scientific literature to illustrate the increase in model development in the mid-late 1990's.

Area	Model / Software	A	H	S	T	O_2	pH	C_A	NP	BD	P	N		Reference
Hong Kong	DELWAQ (2-D)	C	•	•					•	•		•	FC	Postma, 1984
Tamar	FORTRAN (1-D)	E	•	•									AH, Cd	Harris *et al.*, 1984
Tamar	FORTRAN (1-D)	E	•	•									Cd	Uncles, *et al.*, 1987
San Francisco	FORTRAN (1-D)	C	•					•				•		Cifuentes *et al.*, 1990
Scheldt	D. C. I (1-D)	E	•	•		•	•	•	•	•			Cd, Cr, Cu, Zn	van Eck & de Rooji, 1990
Scheldt	SAWES (1-D)	E	•	•		•			•		•	•	Cd, Cu, Zn	van Gils *et al.*, 1993
North Sea	Policy model (3-D)	C	•	•	•								Cd, Pb	Murphy & Odd, 1993
Vilaine Bay	Box model (3-D)	C	•		•	•			•	•	•	•		Chapelle *et al.*, 1994
North Sea	P-C-B (3-D)	C	•	•	•				•		•			Skogen *et al.*, 1995
Plym	ECoS (1-D)	E	•						•					Smith, 1995
San Francisco	ELAmet (2-D)	C	•	•				•					Cd, Cu, Zn	Wood *et al.*, 1995
North Sea	NSP Model (2-D)	C	•	•									Cd, Cu, Pb, Zn, Ni	McManus & Prandle, 1996
Humber	DIVAST (2-D)	E	•	•									Cd, Zn	Ng *et al.*, 1996
Odiel	4 Phase (2-D)	E	•	•									^{226}Ra	Perianez *et al.*, 1996a, b
Scheldt	WASP (1-D)	E	•	•									PCB	Vuksanovic *et al.*, 1996
Humber	TRIVAST (3-D)	E	•	•		•				•			FC	Falconer & Lin, 1997
Yamuna	MIKE 11 (1-D)	R	•	•		•				•		•		Kazmi & Hansen, 1997
Lake Michigan	Simplified (1-D)	L	•	•									PCB	Lick *et al.*, 1997
Odiel	4 Phase (2-D)	E	•	•									Th	Perianez *et al.*, 1997

Gironde	ECoS (1-D)	E	•	•										Cd	Pham *et al.*, 1997
Scheldt	Carbon cycle (1-D)	E	•			•	•		•						Regnier, *et al.*, 1997
North Sea	NOSTRADAMUS (2-D)	C	•	•		•			•			•	•	Cd, Cu, Ni, Pb, Zn	Tappin *et al.*, 1997
Loire	SAM (1-D)	E	•	•		•								Cd	Thouvenin *et al.*, 1997
West Java Sea	PISCES (2-D)	C	•	•										Phenol	Tyler *et al.*, 1997
Forth	MIKE 11 (1-D)	E	•	•		•					•		•		Wallis & Brockie, 1997
Bedford Ouse	QUASAR (1-D)	R	•		•	•	•				•		•		Whitehead *et al.*, 1997
Ria de Aveiro	ECoS (1-D)	E	•	•										Hg	Abreu *et al.*, 1998
Lake Ijsselmeer	DIASPORA (2-D)	L	•	•										Pb	Blom & Winkels, 1998
Scheldt	WASP (1-D)	E	•	•											de Smedt *et al.*, 1998
Ythan	Salt intrusion (1-D)	E	•										•		Gillibrand & Balls, 1998
Forth	MIKE 11 (1-D)	E	•	•		•					•		•		Hanley *et al.*, 1998
Novaya Zemlya	THREETOX (3-D)	C	•	•										^{137}Cs, ^{90}Sr	Koziy *et al.*, 1998
Angara-Yenisey	AYRSSM	E	•	•										^{60}Co, ^{137}Cs, U	Krapivin *et al.*, 1998
Tamar	ECoS (1-D)	E	•	•										Zn, Ni	Liu *et al.*, 1998
Scheldt	SAWES (1-D)	E	•	•		•	•	•	•						Ouboter *et al.*, 1998
Ribble	VERSE (2-D)	E	•	•										Th, ^{137}Cs	Gleizon, 1999
Dnieper-Bug	THREETOX (3-D)	C	•	•	•									^{137}Cs, ^{90}Sr	Margvelashvily *et al.*, 1999
Scheldt	Toxic Transport	E	•	•										Cu, Zn	Mwanuzi & de Smedt, 1999

(Area A: estuarine, E; lake, L; river, R; ocean and coastal seas, C. Model parameters: hydrodynamic, H; sediment transport, S; temperature, T; alkalinity, C_A; nutrients, NP; biological oxygen demand, BD, organic nitrogen, N; primary productivity, P. Contaminants: faecal colliforms, FC; aromatic hydrocarbons, AH.

project. Single model parameters often represent a range of processes or sub-processes (van Straten, 1998) and important questions to ask are to what degree of sophistication must a process be parameterised and are there critical levels of detail or accuracy beyond which the parameterisation becomes meaningless? It is however important not to develop models that are too conditional or system dependent (Nilsson *et al.*, 1996) and no single model is appropriate for all purposes and not all processes need to be included at the same level of detail (IAEA, 1991). The prediction of the rate and direction of transport of an un-reactive *i.e.*, conservative, solute need only consider water movement (Bewers *et al.*, 1992). The complex processes of degradation, speciation and particle adsorption however may cast doubt on the usefulness of this approach and models must include both physical processes, and the partitioning between phases or addition and removal from the water to predict water quality accurately (Huthnance *et al.*, 1993).

The majority of models were initially designed as research tools and therefore tended to focus on a small number of processes such as hydrodynamics and sediment transport. Water quality management tends to be a more interdisciplinary subject requiring the consideration of a wider range of variables. Portability, the ability to rapidly adapt an existing model for a new site or new contaminant is also very desirable, both for research and management. Portability of a model will depend upon the degree of site or contaminant specific parameterisation. For instance, an existing model of ^{226}Ra distribution in the Odiel Estuary was adapted to simulate U and Th isotope transport by only adjusting those parameters that related to the particle adsorption of the isotopes (Perianez & Martinez-Aguirre, 1997). Although many estuarine processes can be considered as generic, the particular combination of processes relevant to any one site will probably not be applicable for another (IAEA, 1991). This problem can be reduced by increased modular development of models where model sub-units can be readily re-used by transporting to other systems to aid in their set up (van Straten, 1998). In this way, van Gils *et al.*, (1993) included model sub-units to determine gas solubility and respiratory / photosynthesis balance as a function of available nutrients and light in addition to the metal partitioning sub-models Equilibria and kinetics of metal sulphite oxidation for the Scheldt Estuary van Eck & de Rooij (1990) and references within present the development of a multi-component model consisting of separate transport, water quality and bioaccumulation sub-models. Their model is however limited by the assumption that micropollutants do not affect water quality constituents, *e.g.*, pH or the plankton sub-model.

The coupling of water quality models to geographical information systems (GIS) is problematic as GIS systems normal employ static data sets and not the time variable ones generated by numerical models. Coupled water quality-GIS models are available for MIKE 11 (Danish Hydraulic Institute, 1995) and are under development for PISCES (Tyler, *per. comm.*, 1998).

It is also important for estuarine models to be able to interact with, for instance, catchment source models such as the carbon flux model used within LOIS (Eatherall *et al.*, 1998), river models dealing with dissolved oxygen and pH (Whitehead *et al.*, 1997) or the Cd dispersal model of Kern *et al.* (1998). An ECoS model of ammonium concentrations in a harbour is suggested by Smith (1995) where processes within a harbour embayment could act upon the variation in water quality from the estuary. Estuarine models can then be used to provide flux estimates for estuarine plume models (Morris *et al.*, 1995; Millward *et al.*, 1996), water quality models such as that of the Hong Kong coastal waters (Postman, 1984), and transport (Murphy & Odd, 1993; Tappin *et al.*, 1997) and eutrophication models such as those of the North and Irish Sea (Danish Hydraulic Institute, 1995).

If the concentration of a pollutant is in equilibrium between different phases or components a kinetic description may not be required and a simple concentration ratio between different compartments can be used (Bewers *et al.*, 1992). The empirically-derived partition coefficient has been widely used in modelling water-sediment partitioning processes (Uncles *et al.*, 1987; Wood *et al.*, 1995; Ng *et al.*, 1996; Pham *et al.*, 1997; Abreu *et al.*, 1998; Liu *et al.*, 1998). However, some believe that due to the short time-steps often used in simulation models the K_d is not an appropriate method to describe solute-solid partitioning and rate constants from kinetics are more applicable (Perianez *et al.*, 1996a,b; Perianez & Martinez-Aguirre, 1997). The modelling of non-conservative behaviour of trace metals in estuaries still requires further investigation due to the complexity of coupling-hydrodynamics with chemical dynamics (Liu *et al.*, 1998) and more mechanistic model of adsorption are less widely used. Complexation reactions at the particle surface such as co-adsorption are not considered in single anion adsorption models, which can not account for the effects of competition and altered overall charge (Nilsson *et al.*, 1996). Harris *et al.* (1984) includes the stability complexes of cadmium with major seawater anions and competition due to humic acids and major cations to estimate metal binding. A complexation model solving the thermodynamic equations governing the balance between free ion Cd^{2+} and chloride, sulfate and hydroxide ions is

also presented by Thouvenin *et al.* (1997). The effect of microbial respiration on the kinetic rates of solute profiles in the Scheldt has been illustrated by Regnier *et al.* (1997).

Modellers may however be limited in the scope of their activities by the complexity of their model or the availability of kinetic information and may be restricted to using K_d values reported in the literature. The distribution of sediment and how this is transported in relation to the hydrodynamic regime of a system will govern the distribution of substances that adsorb onto particles. If there is net removal of a contaminant through sediment burial, sediment deposition will act as a sink for the contaminant (Bewers *et al.*, 1992). The effects of sediment transport on contaminant dispersal in the Tamar Estuary has been used to predict dissolved Cd concentrations under various scenarios by Uncles *et al.* (1987) and desorption from seaward advecting particles was included in the model of Liu *et al.* (1998). Sediment transport models tend to employ particles of uniform properties. Liu *et al.* (1998) showed that permanently and temporarily suspended material exhibited different chemical reactivates. The model included these two broad categories of particle type where the permanently material was characterised by higher absorption rates than the temporarily suspended material. Separate particle populations of <62.5 μm and >62.5 μm bed material and <62.5 μm suspended material are also used by Perianez *et al.* (1996a,b) and Perianez & Martinez-Aguirre (1997). Sorption processes are also important when modelling the estuarine transport of other pollutants such as PCBs (Vuksanovic *et al.*, 1996). In addition to non-solute transport processes particle scavenging by ice may play an important part in pollutant dispersal through Arctic systems and a dynamic-thermodynamic ice submodel is included in the model of Koziy *et al.* (1998). Additional processes of degradation may result in higher toxicity compounds (O'Neill, 1993), e.g., parent and daughter radioactive decay chains may need to be considered and the methylation of inorganic mercury in seabed sediments also represents a significant change of form (Bewers *et al.*, 1992).

The majority of water quality models are 1-D, predicting distributions and processes along the longitudinal axis of the estuary where variables are averaged over the width and depth of the channel (Pham *et al.*, 1997; Abreu *et al.*, 1998). If an estuary is well mixed and the lateral gradients are small compared to the longitudinal gradients a 1-D approached can be used (van Eck & de Rooji, 1990). In the Ribble Estuary depth average 1-D models have failed to replicate estuarine dynamics and contaminant dispersal because of their inability to take into account the vertical gradients and fluxes of suspended matter (Burton, 1994) in these instances a vertically resolving model may provide more accurate representation of

the system (Gleizon, 1999). Three dimensional models are important when the distribution of a pollutant needs to be determined both in solution, suspended sediments and bottom sediments. Although 2-D and 3-D models are available to simulate estuarine hydrodynamics and sediment transport (Kraepiel *et al.*, 1997; Edinger *et al.*, 1998; Kurup *et al.*, 1998), there is still a need to couple these models with chemical sub-models to improve our ability to forecast the flux and fate of pollutants in the coastal zone (Pham *et al.*, 1997). Reconstruction of radionuclide release from Chernobyl and scuttled reactors and resulting contamination of bottom sediments have been conducted with a 3-D model (Koziy *et al.*, 1998; Margvelashvily *et al.*, 1999). Falconer & Lin, (1997) also present a model capable of simulation 3-D estuarine hydrodynamics, salinity, faecal coliforms concentrations, BOD and sediment transport. The increased computational time required for multi-dimensional models however means that costs are incurred in the rate at which the model can be run and this tends to be off set by a reduction in the model complexity for other water quality constituents. The problem of excessive computational time is clearly illustrated by Rajar *et al.* (1995). They describe a three-dimensional model for simulating oil slick transport in the Gulf of Trieste in the Adriatic. The model required up to 10 hours to predict where an oil slick would reach the coast following a discharge in the Gulf. The Gulf of Trieste is relatively small (25 x 25 km) and oil would be likely to reach the coast in a similar time span. The model therefore had to be simplified to reduce computational time before it was of practical use in the determining where pollution prevention and cleaning operations were best located. The question therefore arises where should the effort be put to improve prediction and understanding? The more detail include in a model the greater the number of degrees of freedom and the more difficult it is to calibrate and validate.

1.6 Aims of present study

The objectives of this project are to investigate and model the temporal and spatial variability in estuarine water chemistry and estuarine particle concentration. Variation in the K_d partition coefficient will be understood in relation to changing estuarine physico-chemical parameters and used to develop a coupled hydrodynamic-chemical model that can be used to predict the variation in flux and fate of trace metal in the coastal zone under seasonal scenarios. The specific objectives are as follows:

- To identify seasonal variability and environmental driving forces in estuarine physico-chemical parameters using the LOIS core programme surveys of the Tweed Estuary, Scottish Environment Protection Agency data and additional field studies.

- To develop a hydrodynamic model of the Tweed Estuary using the Estuarine Contaminant Simulator, ECoS. The model will use the tidal and fluvial flow variable hydrodynamic regime of the estuary to predict the distribution of salinity and turbidity.

- To encode the Mook and Koene (1975) conceptual model of estuarine pH distribution as an ECoS module to identify conservative or non-conservative behaviour of alkalinity and total inorganic carbon in the Tweed Estuary.

- To carry out radionuclide incubation studies to assess the variability in Cd and Zn partition coefficients as a function of water and particle chemistry. The empirically derived K_d will then be used to develop an ECoS sub-model to predict seasonally variable trace metal behaviour and the flux of Cd and Zn to the North Sea.

Chapter 2

Estuarine hydrodynamic modelling using ECoS

2 Estuarine hydrodynamic modelling using ECoS

In the past, modelling was largely in the domain of specialists. However, interactive computing and modern graphical modelling tools have made it easier for environmental managers and scientists with less mathematical expertise to design, build and run their own models (Hess *et al.*, 1999). Nonetheless, these modelling packages may produce results that are open to possibly misinterpretation (Dyke, 1996). It is therefore essential that a logical and structured approach be taken when constructing a model and that the results at each stage be critically evaluated. The development of a simulation model can be divided into three main stages; i) Design of a conceptual framework around the management questions under investigation. ii) Identifying and encoding of a model to include all the processes that are relevant and significant. iii) Evaluation through verification, sensitivity analysis, calibration and validation against an independent data set (Hess *et al.*, 1999). Each stage can be highly iterative and this is illustrated in Figure 2.1.

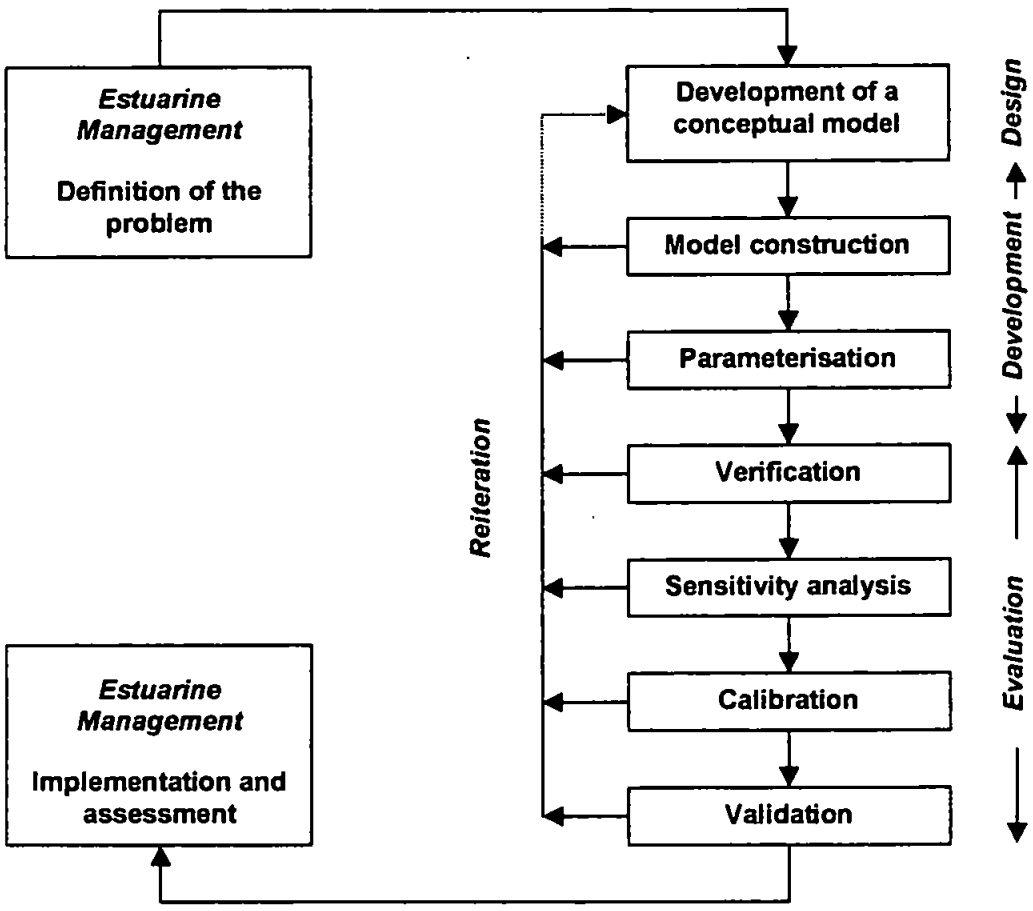

Figure 2.1 Stages in modelling process. (Adapted from Hess *et al.*, 1999).

2.1 ECoS

The ECoS modelling shell has formed the basis for the modelling work undertaken in this study. ECoS is a commercially available software package that has been developed to provide a modelling environment for the one and two dimensional modelling of tidal or tidally averaged physical, chemical and biological processes in estuarine systems. ECoS has been encoded with varying degrees of complexity for the Gironde Estuary (Pham *et al.*, 1997), Plym Estuary (Smith, 1995), Ria de Aveiro (Abreu *et al.*, 1998) and Tamar Estuary (Liu, 1996; Liu *et al.*, 1998).

All of these examples were developed using the ECoS V2 or earlier and used 1D cubature calculations. The models of Smith (1995), Liu (1996), Pham *et al.* (1997) and Liu *et al.* (1998) are also based on tidally averaged simulations. Estuarine surveying typically involves sampling along the axis of the estuary and this is commonly performed around high water. Tidally averaged models do not include the semi-diurnal variability in model constituents such as salinity and turbidity and this was noted as a limitation in the model of Pham *et al.* (1997). Comparisons of tidally averaged model results with axial measurements collected during a small percentage of the tidal cycle may therefore be meaningless in small tidally dominated estuaries. For instance, the location of the turbidity maximum zone predicted by Liu *et al.* (1998) in the Tamar Estuary in error by about 5 km compared to observed results. The predicted concentrations were also over estimated by a factor of three to four. Without the availability of time series data the performance of a tidally averaged model cannot be assessed and the results cannot therefore be used to estimate the flux of dissolved and suspended material through an estuary.

ECoS3 was released in 1998 (Gorley & Harris, 1998; Harris & Gorley, 1998a,b). Although ECoS3 is generally applicable to a wide range of spatially extended systems, the application of earlier versions to questions of estuarine environmental quality has been improved by the provision of a series of water quality constituent and estuarine templates. These templates that have evolved from the examples presented in previous versions are specifically designed to be inter-compatible and allow the user to rapidly establish a simulation model by importing the appropriate templates to a foundation structure. Due to the historical development of the ECoS software the default parameters within the model templates are based on the Tamar Estuary. However, these default

values can be readily altered to simulate any real or hypothetical estuary. The range of templates currently supplied with ECoS3 are shown in Table 2.1.

Table 2.1 Templates provided with ECoS3 (Harris & Gorley, 1998b).

ECoS3 template	Alternative approaches where available
• Foundation structure	
• Estuarine cross-sectional area	Fixed / depth variable
• Estuarine dynamics	Hydrodynamic / cubature
• Tides	Tidally averaged / tidal (2 or 6 component)
• River Flows	
• Salinity	Fixed dispersion / variable dispersion
• Heat	
• Light	
• Gas exchange	
• Sediment	Tidally averaged / tidal
• Trace metal	
• Organic contaminant	
• Nutrients & primary productivity	

The application of the hydrodynamic and tidally variable templates of ECoS3 have not been reviewed in the literature. However, Pham *et al.* (1997) described a tidally averaged ECoS model where the estuarine cross-section had been represented as a rectangle. This chapter describes and tests the hydrodynamic and tidal templates as presented by Harris & Gorley (1998a,b) and Gorley & Harris (1998) and identifies the benefits and also problems associated with this approach. The default parameters of the Tamar Estuary, south-west England, see Figure 2.2 have been used. This allows these new approaches to be investigated using existing data that has already been applied to ECoS modelling of an estuary. Once a thorough understanding of the supplied model structures has been gained they will be used as a basis for models of the Tweed Estuary.

2.2 Model structure

ECoS allows the user to model transfers in space, such as along the axis of an estuary and transfers between discrete constituents such as exchange between particulate and dissolved constituents. An ECoS model consists of a hierarchy of components, which allows the model structure to reflect the natural hierarchy of the system you are modelling. The top component represents the system itself, and is used to define a time co-ordinate. Within the system, one or two dimensional spaces components can be defined using X and Y co-ordinates. Within these spaces are constituents that represent the mass, volume or energy of the processes or elements that the user wishes to model.

For example a constituent within a space could be the cross-sectional area representing the volume per unit length of water in a channel. Sub-constituents within the water may include solutes such as salinity or dissolved metals that are transported with the water conservatively or particles that behave non-conservatively. These particles may themselves include further sub-constituents such as particle-bound metal. The movement of material between one constituent and another is determined by transfers, which may be uni-directional or bi-directional and can occur at a point source (*i.e.*, at a fixed locality) or be extended throughout the system. These can be set at fixed values or varied in accordance with some other environmental parameter (real or simulated). In Figure 2.3 the transfer between particulate matter on the estuarine bed and that suspended in the water column is determined by water velocity and particle nature, described by erosional and depositional constants and settling velocities. Another type of transfer is the exchange of metal ions between the dissolved phase, (D-metal) and particle bound phase, (S-metal) that is controlled by a salinity-K_d relationship.

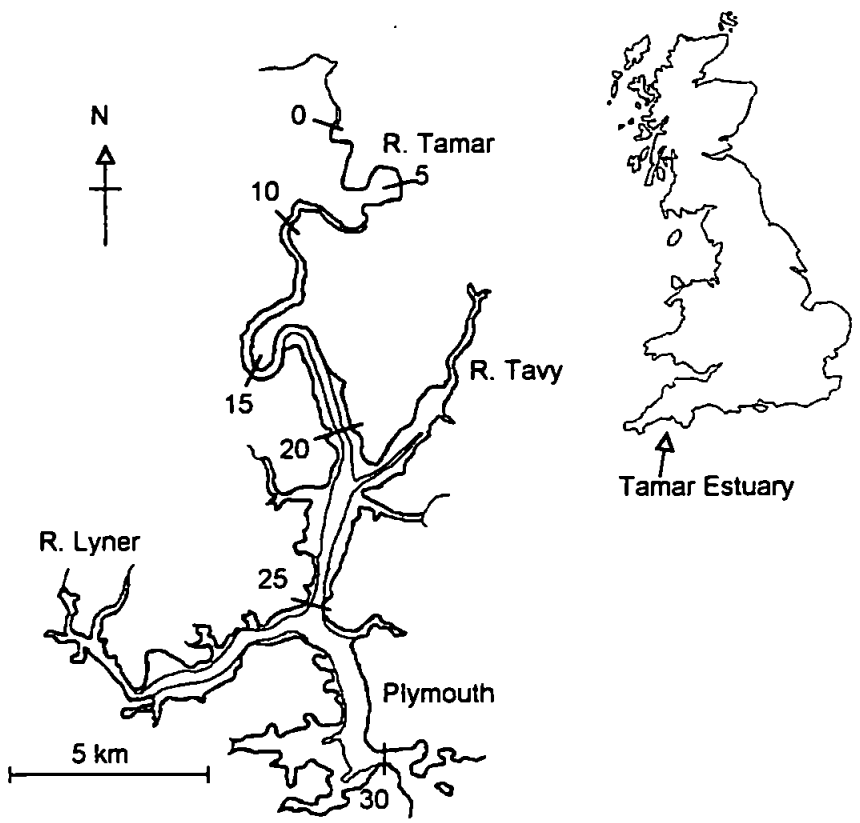

Figure 2.2 The Tamar Estuary, south-west England. The Kilometre marks along the main channel correspond to the segmentation used in the model.

The model structure will depend upon the purpose of the model and the resources available for development. The more complex the model the greater the data requirements for parameterisation and calibration and the longer the computational time required.

Model development will therefore be a balance between the required level of accuracy or detail and the resources available.

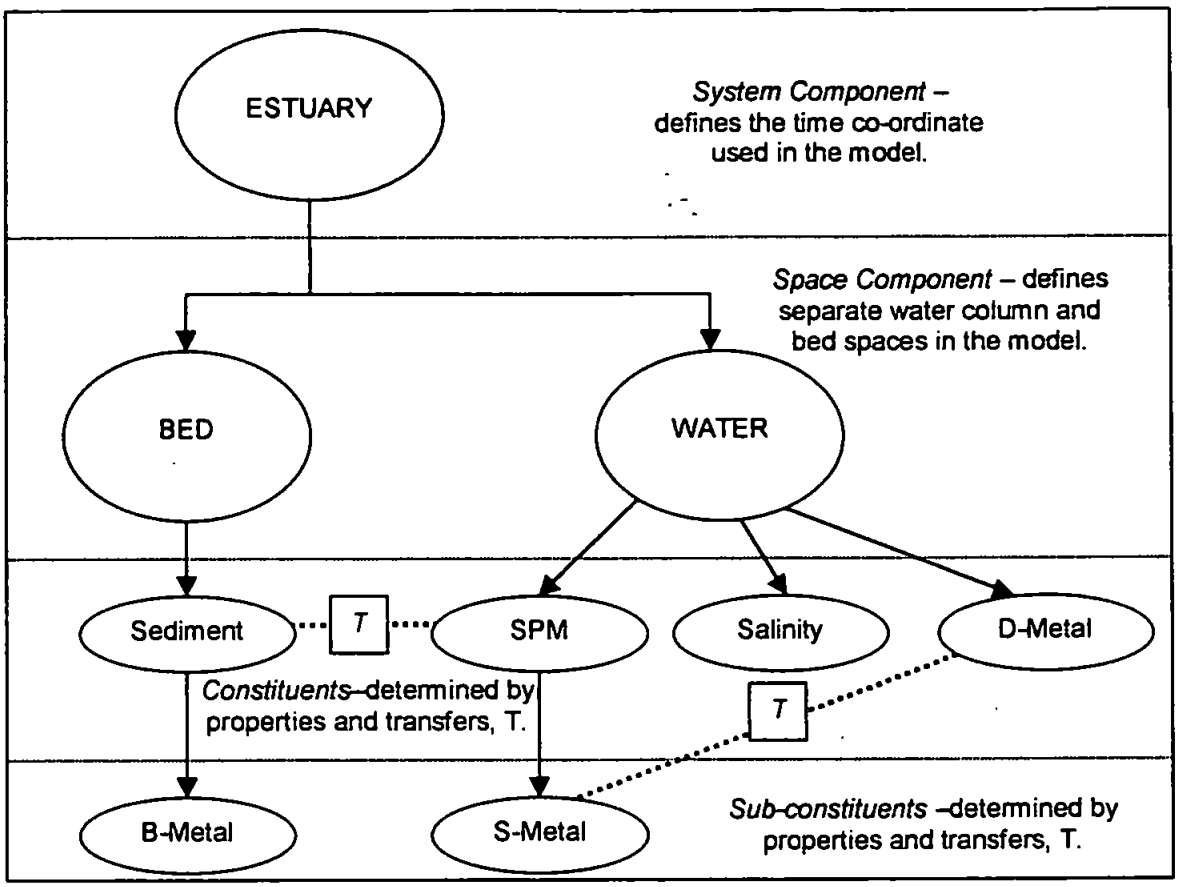

Figure 2.3 Levels of organisation within ECoS3 illustrating the transfer of sediment between the bed and water column and the transfer of a trace metal between the dissolved phase, (D-Metal) and SPM phase, (S-Metal). Accumulation of metal in the bed sediment, B-Metal occurs through settling of a fraction of the S-Metal phase.

2.3 Modelling Estuarine Hydrodynamic and Transport Processes

Estuarine processes are 4-D in nature, varying in space and time and may exhibit significant transverse variability in addition to vertical stratification along the axial gradient (Wong & Moses-Hall, 1998). In a vertically well mixed system where the principal gradients are along the longitudinal axis of the estuary 1-D models may be sufficient to simulate the features without the need for more complex 2 or 3-D models (van Eck & de Rooij, 1990; Gillibrand & Balls, 1998). This can produce significant time savings as a two-dimensional modelling may require up to a day to simulate 15 to 20 tides (Falconer & Lin, 1997). Increasingly complex models also tend to employ a larger number of estimated variable and the confidence in model reliability may be diminished by these uncertainties (Oresker *et al.*, 1994).

2.3.1 Numerical techniques in ECoS

ECoS allows the user to define how a component is transported within the water by defining advection and dispersion terms. The dispersion represents the tendency of the metal concentration to level out due to mixing processes. In one dimension the concentration modelled are averaged over the width and depth of the channel can be described mathematically by the differential equation (Harris & Gorley, 1998a):

$$\frac{\partial C}{\partial T} = -\frac{\partial (UC)}{\partial X} + \frac{\partial (K \partial C / \partial X)}{\partial X} + f(C) \qquad \textbf{(2.1)}$$

where U is the velocity in the direction of increasing distance, X, C the concentration of dissolved or particulate constituent, and K the dispersion coefficient. T is the time co-ordinate. The first term describes the changes in concentration due to net flow. The second term describes the changes in concentration due to dispersion. The third term is a function, f to represent generation and loss of concentration by means other than transport.

If there are s chemical species that are generated and lost by transfers between each other, then for the nth species:

$$\frac{\partial C_n}{\partial T} = -\frac{\partial (U_n C_n)}{\partial X} + \frac{\partial (K_n \partial C_n / \partial X)}{\partial X} + f_n(C_1, C_2, \ldots, C_S) \qquad \textbf{(2.2)}$$

where

$$f_n(C_1, C_2, \ldots, C_S) = \sum_i C_i g_{i,n}(C_1, C_2, \ldots, C_S) - C_n \sum_i g_{n,i}(C_1, C_2, \ldots, C_S) \qquad \textbf{(2.3)}$$

The $g_{i,n}$ are the transfers from species i to n and could represent the exchange of metal ions from dissolved to the particulate phase controlled by a user defined function such as the K_d-salinity relationship of Bale (1987) or Harris (1987). The set of equations for the C_i are solved implicitly (*i.e.*, using future values) in two parts. Firstly the changes due to the transfers are calculated, then the changes due to transport. To describe the transfer, if the time step is ΔT, the initial concentration of the nth species is $C_n^{\#}$, and the final concentration (before transport) is C_n^{Δ}, the following equations must be solved:

$$C_n^{\Delta} - C_n^{\#} = \sum_i C_i^{\Delta} g_{i,n}(C_1^{\#}, C_2^{\#}, \ldots, C_s^{\#}) - C_n^{\Delta} \sum_i g_{n,i}(C_1^{\#}, C_2^{\#}, \ldots, C_s^{\#}) \qquad \textbf{(2.4)}$$

For each transfer between phases that occurs ECoS solves a sequence of pairs of the above equation. The concentrations in each component (dissolved and particulate metal), $C^{\#}$ are updated continuously as each pair of equations is solved. To describe the calculation of transport terms the estuarine length is divided into equally spaced increments of length ΔX. Then, if C is the concentration of a species at the end of the next time step, ΔT and if C_X is used to donate the concentration, C at position X then $\Delta a_X = a_{X+\Delta X} - a_X$, for whatever a, in which the X increment, ΔX is defined to have the opposite sign to the velocity, U. Then for $\frac{\partial(UC)}{\partial X}$ we use: $\frac{\Delta(UC)}{\Delta X}$ and for $\frac{\partial(K\partial C/\partial X)}{\partial X}$ we use: $\frac{\Delta(K_X \Delta C_X/\Delta_X)}{\Delta X}$ using this we have for each species:

$$C - C^{\Delta} = \left(-\frac{\Delta(UC)_X}{\Delta X} + \frac{\Delta(K_X \Delta C_X/\Delta_X)}{\Delta X} \right) \Delta T \qquad \textbf{(2.5)}$$

which is solved to provide the final concentration C. These then provide the initial concentrations, $C^{\#}$ for the next time step. Time step, ΔT, and computational segment length, ΔX, are user defined parameters and may have a significant effect on the speed and accuracy of the calculation of transport processes under certain simulation types. The change in computational time with different time step and segment length is illustrated in Figure 2.4. this shows that although the 10 seconds time step allowed a greater reduction in segment size it incurred a large increase in computation time. However, the spatial and temporal numerical scheme used has little effect on the computational speed.

ECoS divides the estuary into a number of equal-length segments along its length and in a 1-D simulation assumes that within the water column conditions are laterally and vertically homogeneous. Spatially variable estuaries may require a greater number of segments in the model to approximate to the conditions in the estuary, but may potentially require a larger database to set up and test the predictions. Comparison of model predictions to actual data must also consider the time step. The time step is the internal time interval between successive updates to time variable quantities. Under steady state conditions the time step should not effect the advection-dispersion equations, but a steady state assumption may not be appropriate under all conditions and can lead to model inaccuracies (Harris *et al*, 1993).

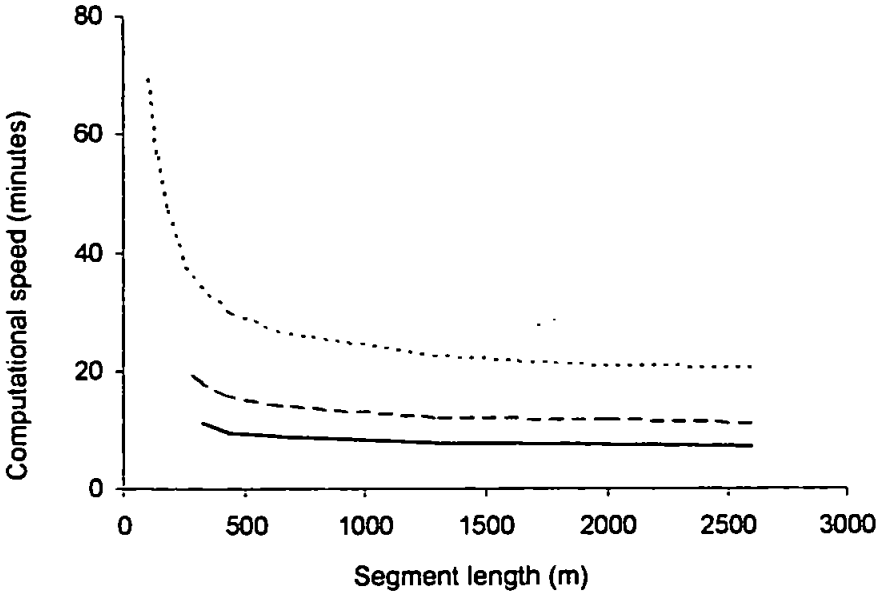

Figure 2.4 The computational time required to run a 10 day hydrodynamic simulation of the Tamar Estuary (X = 31 km) with time steps of 10 (—), 20 (– –) and 1000 (—) seconds. CPU specification = 133 MHz Pentium processor with 32 Mb RAM.

ECoS gives a choice of a numeric scheme that is either implicit or central-temporal. The implicit scheme is first order in the time step, but stable and is suitable for longer time steps of:

$$\frac{\Delta X}{\Delta T} < U_W \tag{2.6}$$

such as during long term tidally average simulations. The alternative central scheme is a second-order approximation that is more accurate for shorter time steps, but less stable:

$$\frac{\Delta X}{\Delta T} > U_W \tag{2.7}$$

where ΔX is segment length, ΔT is the time step and U_W the water velocity (Gorley & Harris, 1998). These restrictions are illustrated in Figure 2.5 which shows when either scheme is more appropriate depending on time step, segment size and water velocity.

2.3.2 Parameterisation of estuarine hydrodynamics

The direction and velocity of water moving through an estuary is critical in determining the slope and direction of estuarine physico-chemical gradients and describing water movement is the next stage in model development. The velocity, U of water calculated using hydrodynamics is determined by the transport, generation and loss of momentum.

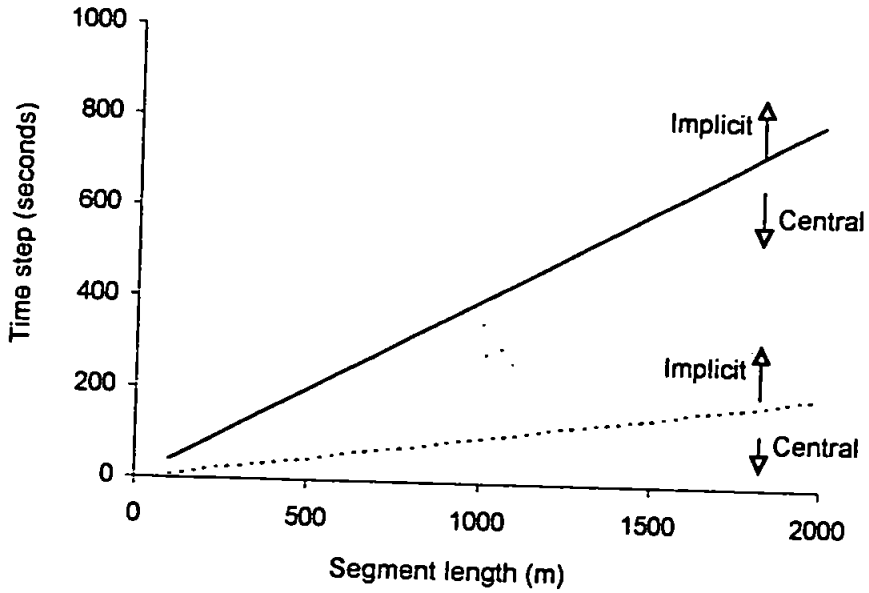

Figure 2.5 The choice of temporal numeric scheme is dependent on the ratio of $\Delta X/\Delta T$ and water velocity. The implicit scheme is generally more stable and can be used with larger time steps than the central scheme. This is illustrated at a water velocity of 2 m s^{-1} (—) and 10 m s^{-1} (—).

The hydrodynamic template can be used to model the physical dynamics of water movement allowing for gravity, pressure and friction, driven by freshwater flow and tides at the mouth. This template uses conservation of momentum to determine the water movement and tidal propagation through the estuary. Momentum is modelled as an advected constituent of water and in a similar manner to solute transport is effected by dispersion. The dispersion coefficient for momentum, K_M is the turbulent kinematic viscosity of water, V and, typically varies between 100 to 1000 m^2 s^{-1} along the axis of the estuary (Harris & Gorley, 1998b). The rate of gain of momentum due to the slope of the water is a product of the density, ρ, the acceleration due to gravity, g, the tidally variable cross-sectional area, A, and the surface slope $\partial H/\partial X$:

$$\rho * g * A * \frac{\partial H}{\partial X} \qquad (2.8)$$

where H is the height of the water surface above a defined datum. In addition to advection and dispersion momentum is lost due to bottom friction reducing water velocity and gained due to water surface slope. The bottom friction, B_F, controls how the estuary attenuates and distorts the tides defined at the mouth using a general algorithm function of depth and velocity which, following the Manning relation, can be described as (Harris & Gorley, 1998b):

$$B_F = a * U * D^b \tag{2.9}$$

where b = -1.33 and a is determined from the Manning coefficient, n, and gravity, g according to:

$$a = g * n^2 \tag{2.10}$$

Typical values of the Manning coefficient range from 0.013 to 0.026, increasing with reduced depth (McDowell & O'Connor, 1977) and width, and a value of 0.03 was used by Unnikrishnan *et al.* (1997) for channel widths less than 100 m. Bottom substrate is also important and values can range from 0.015 for muddy beds with low friction to 0.025 common for sandy estuaries (Wolanski *et al.*, 1997). The effect of changes in the Manning coefficient on model predictions of tidal elevation are shown in Figure 2.6. Increasing the Manning coefficient reduces the tidal propagation into the estuary.

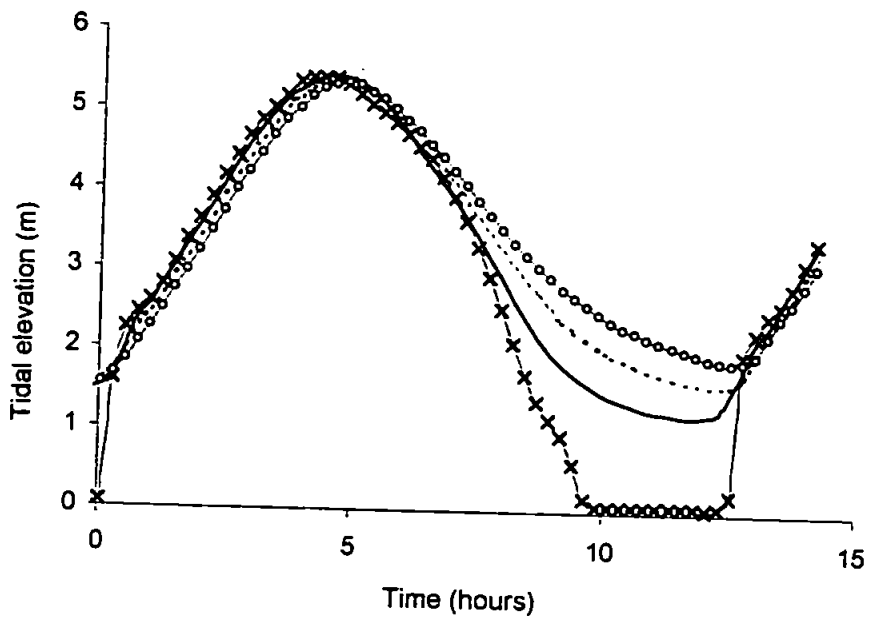

Figure 2.6 The effects of changing the Manning coefficient on mid estuarine tidal elevation in the Tamar model simulation where the Manning coefficient = 0 (-o-), 0.01 (—), 0.02 (—) and 0.03 (-x-).

2.3.3 Representing cross-section area in a tidal model

The cross-sectional area, A is therefore important in calculating the velocity of water through the estuary. Under tidal scenarios the cross-sectional area will vary not only along the length of the estuary, but will also changes in response to tidal state and river flow, see Figure 2.7.

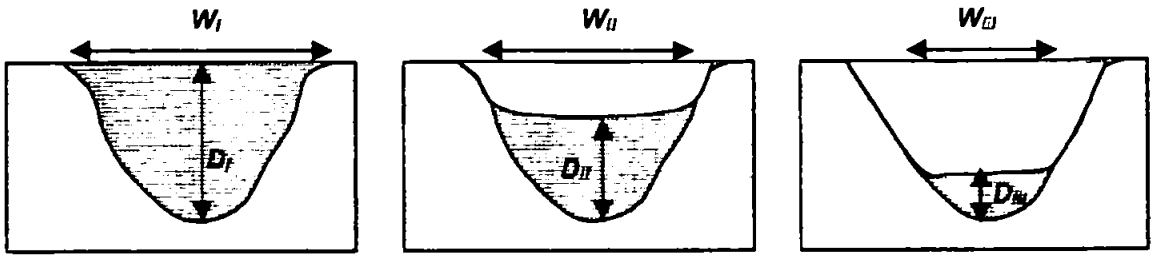

Figure 2.7 Tidally variable estuarine cross-sectional area (hatched region) and maximum water depth, *D* and width, *W*. High tide-*i*; mid tide-*ii* and low tide-*iii*.

The tidally averaged model of Liu *et al.* (1998) used fixed values of cross-sectional area. This approach is unsuitable for tidal simulations, where the cross-sectional area will change as a function of the tidally variable water depth. To model this, the tidally variable cross-sectional area can be described by a statistical function of depth determined by least-squares regression of measurements of cross-sectional area on water depth along the axis of the estuary.

If the estuarine cross-section is roughly triangular or rectangular, a simple quadratic regression forced through the origin can be used to model the variation in cross-sectional area, (A) with depth (D):

$$A = aD + bD^2 \qquad (2.11)$$

where the cross-sectional area is related to depth employing the parameters a and b that are tabulated as a function of distance (*c.f.* Figure 2.8). The number of points along the estuary that a and b are determined will depend upon the balance between the variability in channel bathymetry and the ease with which bathymetry data can be obtained. The depth of water will depend on the bathymetry below a fixed datum given by a table of observed depths and the tidal range at that point. It is therefore possible to relate cross-sectional area to tidal height in a way which reflects the actual bathymetry of the estuary. The average width, W of the water surface can also be derived from the cross-sectional area and depth according to:

$$W = 2 * a * D \qquad (2.12)$$

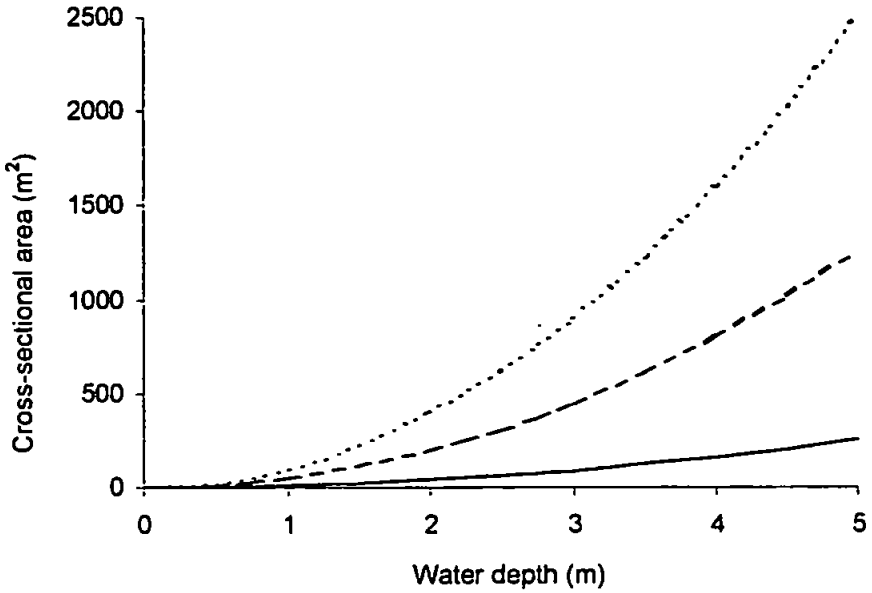

Figure 2.8 Cross-sectional area as a function of water depth as expressed in Equation 2.8 where a = 10 (—), 50 (– –) and 100 (—).

2.3.4 Tidal elevation at the mouth

Tidally-averaged models are useful to understand the net flux of material through estuaries over long periods of time. Environmental managers often, however need to be able to predict the concentration at a particular place and time that results from a discharge which in itself may be timed to coincide with a particular phase of the tide. In this case the model must be able to simulate the ebb and flow of the tide. For instance the Forth River Purification Board found that a tidally averaged model introduced too many uncertainties into their predictions (Wallis & Brockie, 1997).

In tidal models, observed water elevation data can be used to drive the seaward boundary of the model (Ng *et al.*, 1996), but this data may not be available. Alternatively, ECoS provides a two and six-component templates to model the semidiurnal ebb and flow of the tide, T_D (Harris & Gorley, 1998b). The two-component template simulates a semidiurnal tide using a sine wave with a period of 12.42 hours, whose amplitude also varies sinusoidally on the 14.76 day spring-neap cycle. A more detailed representation of the tide is achieved by defining the frequency, T_F amplitude, T_A and phase, T_P of the M_2, S_2, K_1, O_1, M_4 and M_6 harmonic tidal components.

A comparison of semi-diurnal and diurnal tides produced by the 2 and 6 component templates using values for Tamar Estuary at Devonport (Hydrographic Office, 1989a) are

shown in Figure 2.9. Either tidal prediction method is compatible with the hydrodynamic template.

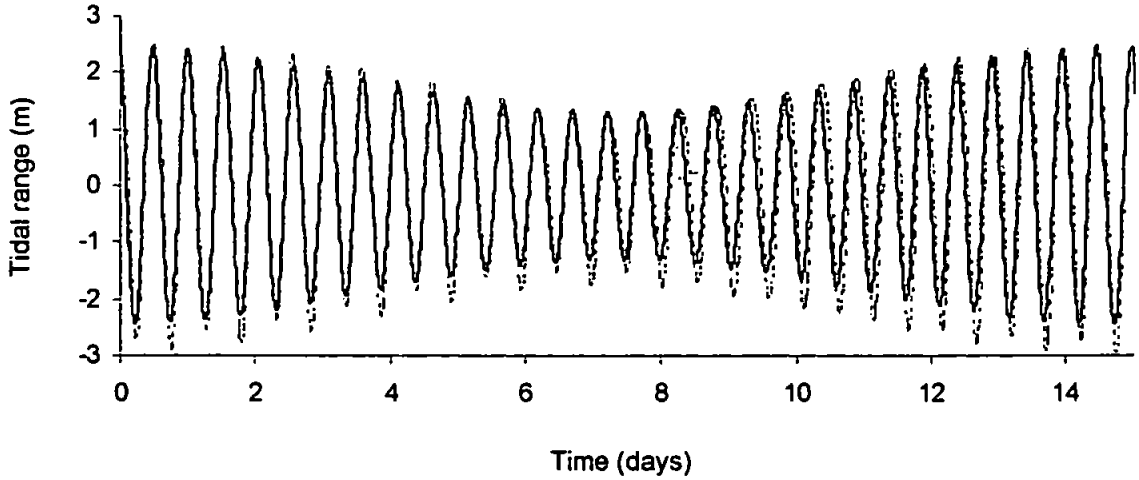

Figure 2.9 Semi-diurnal and spring neap tidal predictions using the two component (—) and six (—) component templates with values for the Tamar Estuary at Devonport (Hydrographic Office, 1989a).

2.3.5 Freshwater flow into the tidal reaches

Freshwater can also be introduced into any of the estuarine segments using a transfer function and any number of tributaries can be included if their position are specified (Harris & Gorley, 1998b). The ECoS3 river template provides flow data for the River Tamar at the head and the flows and distance (m) from the head for three tributaries. These values can be replaced by hypothetical or recorded values that are tabulated in external files as time dependent flows (*e.g.*, $m^3 s^{-1}$). ECoS then interpolates linearly between each value to give a time variant flow rate.

Abreu *et al.* (1998) did not consider high energy events such as river floods when modelling mercury contamination in the Ria de Aveiro. The majority of sediment transport in river and estuarine systems however tends to occur during spate conditions (Dyer, 1994) and may account for some of the discrepancies between modelled and observed results presented by Abreu *et al.* (1998). Annual or seasonally averaged flows may not therefore be sufficient and in fluvial dominated estuaries, daily or hourly flows may be required to adequately describe the hydrodynamic variability in the estuary.

2.3.6 Solute transport

Salinity is a fundamental parameter in estuarine studies and can be represented as a single component within the model structure. The following description is also applicable to any advected constituent the transport velocity of which is set equal to that of the water. In the case of salinity, the freshwater concentration is set by definition to zero while the concentration can be specified at the mouth of the estuary (or varied according to the freshwater input if the marine limit of the model does not extend out beyond the mouth of the estuary and the salinity is effected by high river flows).

In addition to advection processes, the transport of a solute is also determined by dispersion. The solute dispersion in an estuary reflects the mixing of the freshwater and seawater due to the action of tides and freshwater flows. This is measured by the water dispersion coefficient, K_W that is typically in the range of 100 to 300 $m^2 s^{-1}$ (Dyer, 1997). The K_W can be more variable and some reported values are shown in Table 2.2.

Table 2.2 Variation in the water dispersion coefficient, K_W.

Estuary	K_W ($m^2 s^{-1}$)	Reference
Delaware	52-277	Cifuentes *et al.*, 1990
Gironde	250-400	Pham *et al.*, 1997
San Francisco	16-812	Cifuentes *et al.*, 1990

The effect of changing the dispersion coefficient on saline intrusion in the Tamar model is shown in Figure 2.10.

2.3.7 Sediment transport

Particles, like solutes, are an advected constituent, but may have different velocities and dispersion coefficients compared to solutes. Axial gradients of particle concentration, *i.e.*, turbidity are the product of the flow and dispersion between end members, but in addition may include the flux of particulate matter between the bed and water column or biological or chemical processes in the water column. Liu (1996) and Liu *et al.* (1998) considered two types of suspended particle. Permanently suspended particles have a settling velocity that is sufficiently slow in comparison to the residence time in the estuary that they can be considered to be transported conservatively by the residual flux of water. Temporarily suspended particles on the other hand exchange with the bed sediment. Temporarily suspended particles in the water column will be transport with the water with a velocity

and dispersion equivalent to that of the water. At any time, the total turbidity in the water column will be the sum of these two particle populations. The different sediment constituents are illustrated in Figure 2.11.

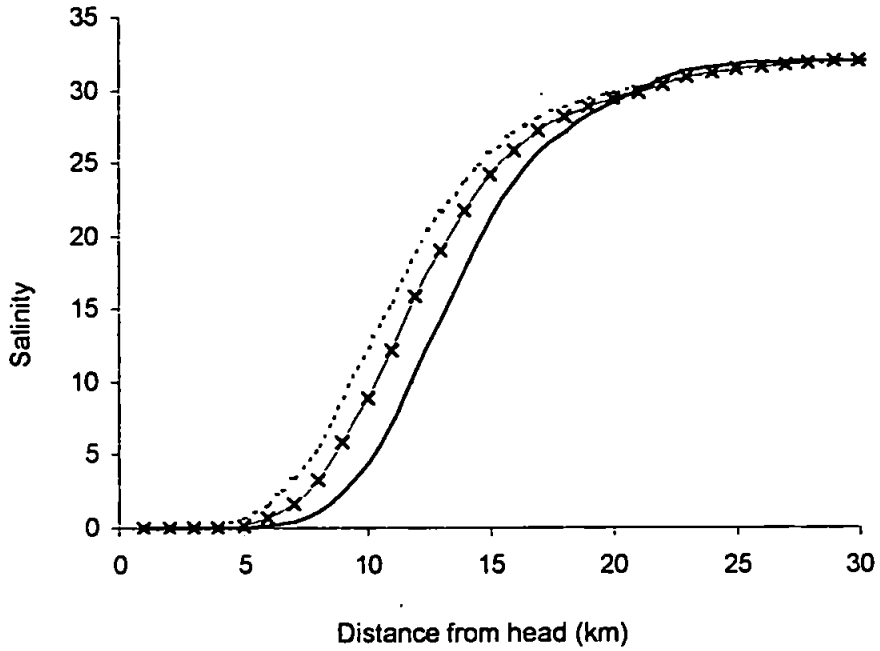

Figure 2.10 The effect of changing the dispersion coefficient on saline intrusion in the Tamar Estuary simulation, when K_S = 500 (---), K_s = 250 (-x-) and K_s = 0 (—).

The estuarine bed is modelled as a separate space component that contains the bed sediment constituent. Following Harris *et al.* (1984) and Ng *et al.* (1996) the bed sediment is assumed to be a single well mixed layer. The proportion of the total bed area that is submerged and hence the mass of deposited sediment that can be resuspended will change in response to tidal variations in depth and estuarine bathymetry. Following the method for describing water column cross-sectional area the submerged bed width can also be described as a polynomial function of water depth. The submerged area will then vary from a maximum at high water to a minimum at low water. The tidally variable exposed area of the bed will then simply be the sum of total bed area minus that submerged.

Transfers between the water column and bed sediment are determined by erosion and deposition processes. Particles that have been deposited on the bed are assumed to not move along the estuary and their velocity and dispersion is set to zero (Harris & Gorley, 1998b).

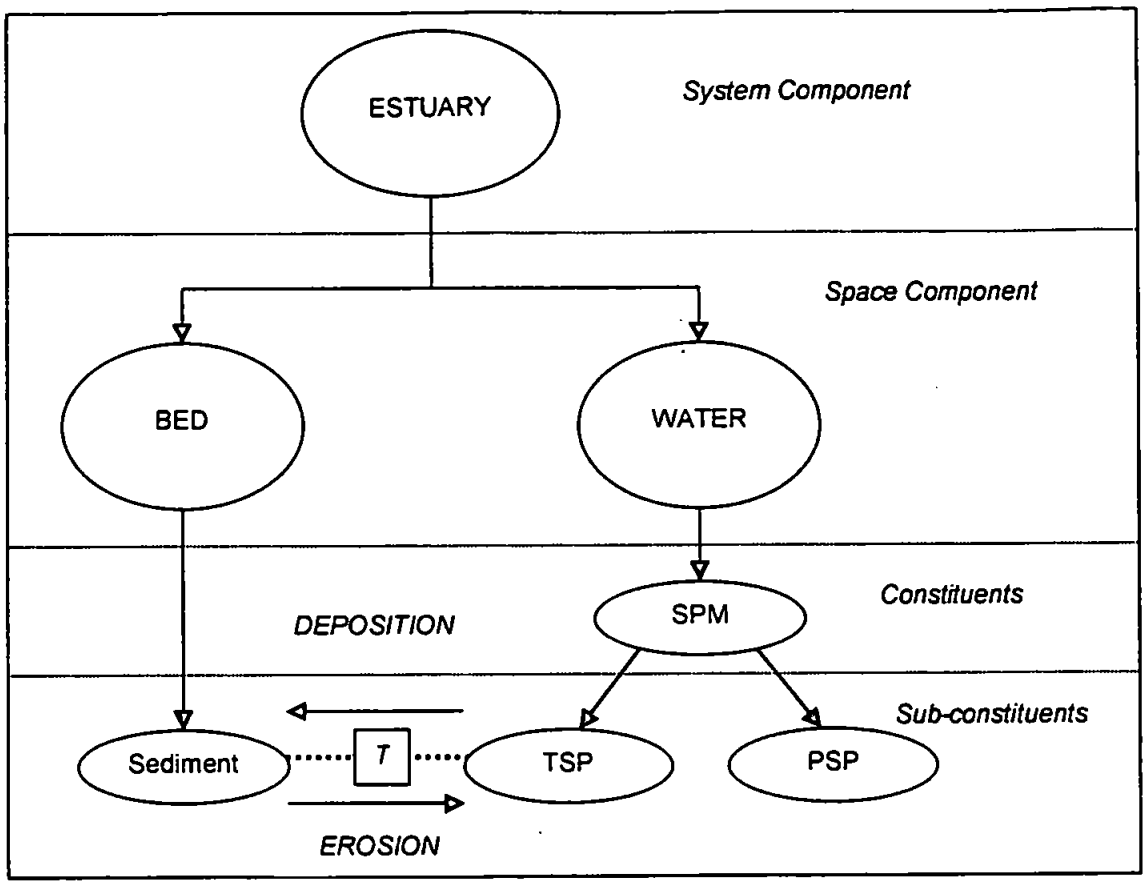

Figure 2.11 The hierarchical structure of ECoS3 illustrating the separate sediment constituents of permanently suspended particle, PSP; bed exchangeable particles, BEPS and bed sediment.

Unless settling studies have been performed, gravimetric determination of turbidity will give the total turbidity, *i.e.*, the sum of permanently and temporarily suspended particles concentrations. The relationship between flow and turbidity outlined by Harris *et al.* (1984) can be used to estimate riverine end member values for total turbidity. The ratio of permanently to temporarily suspended material can then be set as a constant or varied in response to flow rate. The transfer of sediment between the bed and water column can be related to particle characteristics *e.g.*, size, density and cohesiveness and water velocity. Following Uncles *et al.* (1985) the tidal erosion, M_E of sediment from the bed to the water column is given by:

$$M_E = M\left(\left(\frac{U}{U_E}\right)^2 - 1\right) \qquad \textbf{(2.14)}$$

while the deposition, M_D from the water column to the bed is given by:

$$M_D = V_S\left(1 - \left(\frac{U}{U_D}\right)^2\right) \qquad \textbf{(2.15)}$$

The erodability, M and particle sinking velocity, V_S can be set as constants or varied in response to seasonal or flow related changes in particle size and concentration. An erodability value of 3 x 10^{-5} kg m^2 s^{-1} has been reported by Uncles *et al.* (1988) and 5 x 10^{-5} kg m^2 s^{-1} by Clarke & Elliott (1998) while Portela & Neves (1994) used values ranging from 3 to 12 x 10^{-5} kg m^2 s^{-1} depending on water depth. Assuming spherical particles the sinking velocity can be calculated according to Stokes Law:

$$V_S = \frac{P_D^2}{18}\left(\frac{\rho_S - \rho}{V}\right)g \qquad (2.16)$$

where P_D is the particle diameter, ρ_S and ρ are the density of the particle and water respectively, V is the kinematic viscosity and g gravity (*e.g.*, Dyer, 1986). Some reported values, determined from field work are shown in Table 2.3.

Table 2.3 Comparison of maximum current velocity, threshold velocity and particle sinking velocity for the Mekong, Forth and Tamar Estuaries.

Estuary	U^* (m s^{-1})	U_E (m s^{-1})	U_D (m s^{-1})	V_S (10^{-4} m s^{-1})	Reference
Mekong	0.4/1.2	0.4-0.5	1.0-0.6	2.5-4.0	Wolanski *et al.*, 1996
Forth	1.4/1.3	0.03	0.02	1	Clarke & Elliott, 1998
Tamar	1.0/0.6	0.2-1.7	0.2-0.3	0.9*[SPM]$^{1.9}$	Uncles *et al.*, 1985; Uncles & Stephens, 1989; Uncles & Stephens, 1993; Uncles *et al.*, 1994

U* Peak tidal current velocities on the flood/ebb tides. [SPM] = sediment concentration (g l^{-1}).

The influence of flocculation on increased settling of fine particles or colloids has been included in the modelling of the Forth (Clarke & Elliott, 1998) and could be coded as a function of salinity (Harris *et al.*, 1993) or particle concentration (Uncles *et al.*, 1985), but could not be defined by Ng *et al.* (1996) and was excluded from their model. Erosion and deposition occurs when the water velocity, U either exceeds the erosion threshold, U_E or drops below the deposition threshold, U_D during the ebb and flow of the tide. These threshold values are user defined parameters and can be variable according to particle density and type (Cancino & Neves, 1995) or set as constants (Harris & Gorley, 1998b). Clarke & Elliott (1998) noted that the erosion threshold changed as a function of the spring-neap tidal cycle where consolidation of the bed sediment during lower tidal velocities occurred.

2.4 *Limitations and instability of hydrodynamic models*

2.4.1 Time step and model instability

Potential instability of hydrodynamic models places quite severe restrictions on the time step and segment size that can be used. Instability is the tendency for the solution of the model to oscillate, generating spurious short-waves rather than settling down to an acceptable value. This may or may not result in the simulation crashing. Uncles & Stephens (1990) developed a moving-element numerical scheme to overcome a similar problem in the Tamar Estuary while Gillibrand & Balls (1998) employed a first order upstream differencing scheme combined with a anti-diffusion formulation when modelling the Ythan Estuary. The finite difference approximations used by ECoS are predefined and can not be modified by the user. Model stability can therefore only be increased by reducing the time step or increasing the segment size.

Increasing the segment size, increases the amount of averaging in space so that the variations are averaged out. This dampens down the oscillation, but in doing so increases the numerical dispersion. An alternative option is to use first order upwind spatial differencing, although this also tends to increase numerical dispersion (Gillibrand & Balls, 1998).

To avoid model instability the ratio of ΔX to ΔT must be also greater than the velocity of a shallow-water wave, U_W (Gorley & Harris, 1998). This can be determined from fundamental wave theory, *e.g.*, McDowell and O'Conner (1977):

$$U_W = \sqrt{(gH)} \qquad \textbf{(2.17)}$$

where g is the acceleration due to gravity (9.81 m s^{-2}) and H is the depth of water (m) and used to define the Courant Number, C_R:

$$C_R = U_W \frac{\Delta T}{\Delta X} \qquad \textbf{(2.18)}$$

As the change in water level travels at a speed corresponding to U_W, the Courant Number expresses how many grid points the information moves in one time step. The weakness of the hydrodynamic approach is that the waves move much faster than the water. The maximum value that can be used to maintain model stability depends on the bathymetry and high numbers (> 5) should only be used when the bathymetry is very uniform (Danish

Hydraulics Institute, 1996). Using equations 2.6 and 2.17 celerity and hence maximum time step for a range of water depths can be calculated, see Figure 2.12.

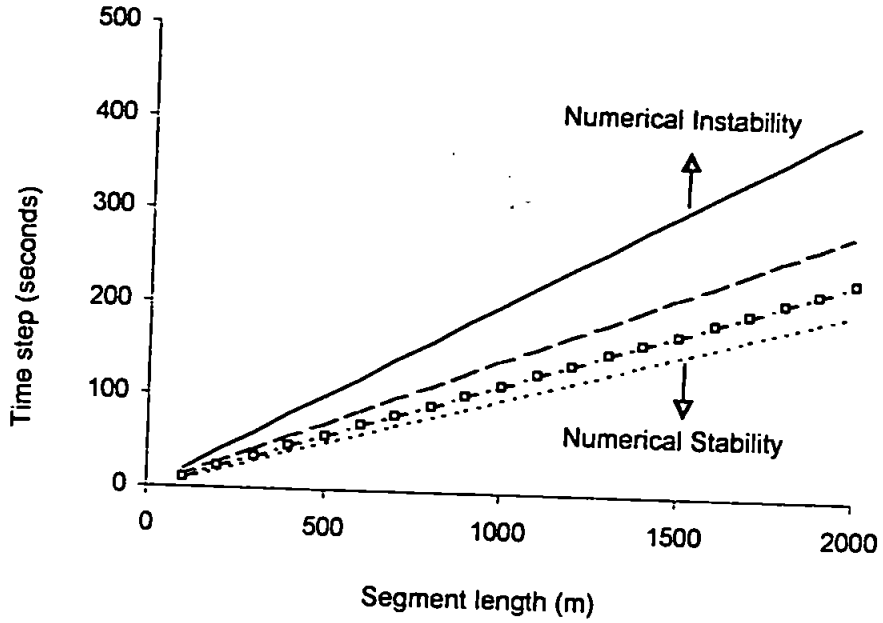

Figure 2.12 Time step limitations in hydrodynamic simulations determined by segment length at water depths of 2.5 m (—); 5 m (– –); 7.5 m (– □ –) and 10 m (——). Ratios of $\Delta X/\Delta T$ that are above the line may lead to numerical instability

The choice of segment size and time step in a range of hydrodynamic models, see Table 2.4.

Table 2.4 Typical time step and segment size reported for a range of hydrodynamic models.

System	Time step (s)	Segment Length (km)	$\Delta X/\Delta T$ ($m\ s^{-1}$)	Reference
Bristol channel	60	~4	67	Amin & Flather, 1996
Humber	60	0.3	5	Ng *et al.*, 1996
Swan	90	1	11	Kurup *et al.*, 1998
Mandovi-Zuari	110	2	18	Unnikrishnan *et al.*, 1997
Fly	120	1.4	12	Wolanski *et al.*, 1997
Scheldt	150	2	13	Regnier *et al.*, 1997

This shows that the choice of time step required for a segment length of 1 km will range between 200 and 100 seconds with water depths of 2.5 to 10 m respectively. This short time step means that the central numerical scheme is appropriate when running hydrodynamic simulations. There is therefore a balance between needing a sufficient number of segments to adequately represent the spatial continuum of the natural system and the increase in computation time incurred as the time step is reduced.

2.4.2 Numerical dispersion

The generation of numerical dispersion may also occur through the approximation or rounding off during computer calculation and is particularly problematic when dealing with the advective transport of variables with steep gradients (Gomez-Reyes & Blumberg, 1995). The numerical diffusion and dispersion (truncation error) generated can distort the model solutions and lead to significantly higher dispersion than that defined by any water dispersion coefficients (Kowalik & Murty, 1993). Numerical dispersion can be reduced by increasing the segment number, *i.e.*, reducing segment size, see Figure 2.13. This may however require a reduction in the time step to maintain model stability that may subsequently increase the computational time (Harris *et al.*, 1993). Figure 2.13 also illustrates how sensitive dispersion and hence saline intrusion is to changes in segment length as the effects seen here are greater than those for K_S values of 250 and 500 shown in Figure 2.10.

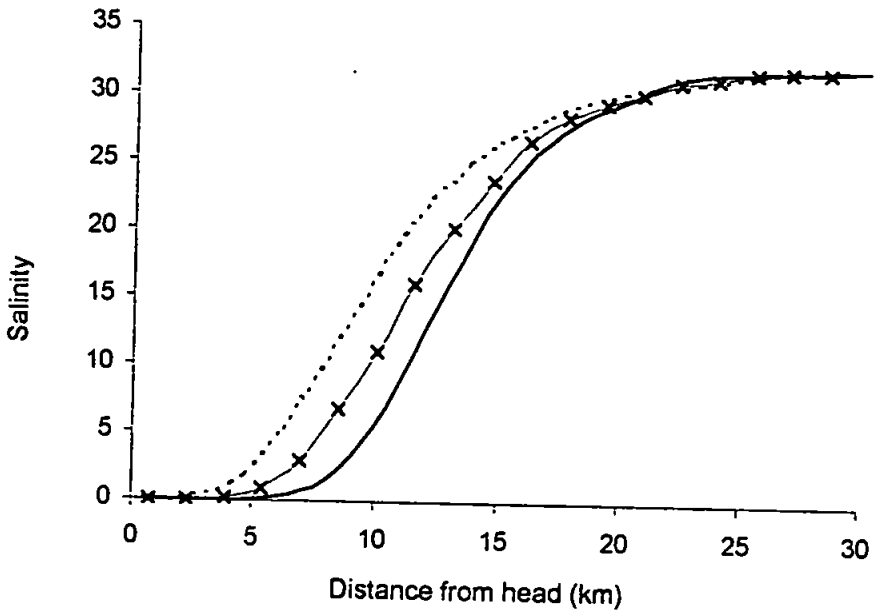

Figure 2.13 The effect of changing the segment number and hence segment length on saline intrusion in the Tamar Estuary simulation, 10 segments of 3.1 km (—), 20 segments of 1.6 km (–x–) and 30 segments of 1 km (—).

These errors will also in part depend on the numerical scheme used to solve the differential equations. ECoS uses either the UPWIND or quadratic upstream interpolation for convective kinematics (QUICK) spatial numerical schemes in addition to the choice of temporal numeric schemes. The UPWIND scheme is stable and accurate to first order in the segment size (MacCready, 1999), but can generate excessive numerical diffusion, while the QUICK scheme is accurate to the second order and generates less numerical

dispersion (Gorley & Harris, 1998). The effect of numerical scheme on saline intrusion is shown in Figure 2.14.

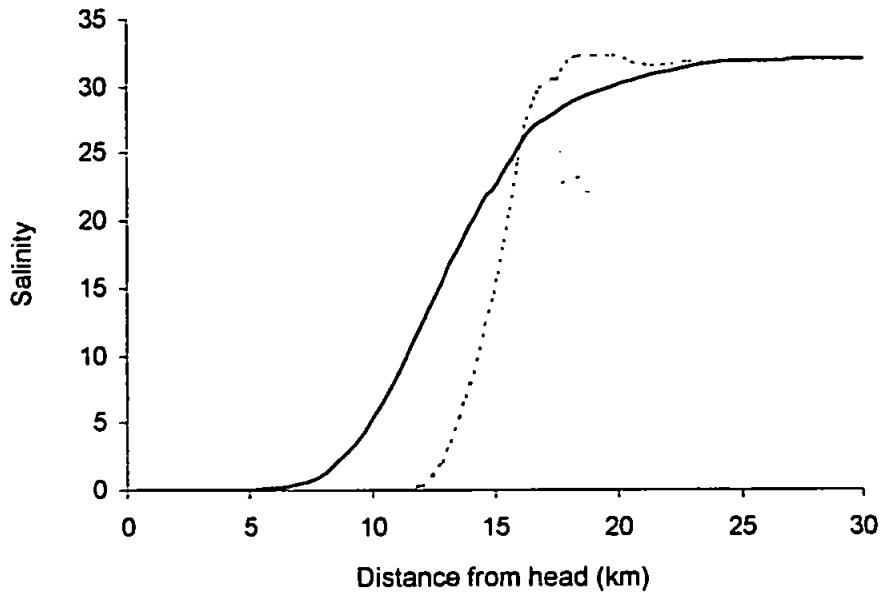

Figure 2.14 The effect of changing the spatial numeric scheme on saline intrusion in an estuary using either the UPWIND (—) or QUICK scheme (----).

Depending on model set up, the dispersion coefficient used may have to be significantly less than that determined by field observations and can be varied by trial and error to give realistic axial profiles. Due to numerical dispersion, this may require the value of K_H and hence K_S to be set to zero (Harris & Gorley, 1998b).

2.4.3 Model run-up period

Models may produce unrealistic profiles over the first few time steps that they are run and require a certain amount of time to 'settle down'. For instance, the tidal propagation model of Unnikrishnan *et al.* (1997) required approximately two days at a time step of 110 s to stabilise. This period can be reduced by providing initial conditions, that is typical concentrations for any modelled variable in external *.tab files. In the case of salinity this may consist of an axial distribution of tidally averaged values. These values are not critical, but may help to provide more realistic starting conditions for the simulation.

2.5 Data requirements for model set up

When an ECoS model is being parameterised for a new site some or all of these values may have to be changed. Values can be derived from field and laboratory studies, those

reported in the literature or through model calibration. Bathymetry which is site specific may have to be measured and the quantity and quality of the bathymetry data may play a significant role in model set up. Directly measuring all parameters may not be practical in terms of time, money or expertise and values for some parameters such as the velocity threshold for erosion and deposition may be taken from the literature. Site specific values may exist, if not those from comparable systems may have to be used. Values such as the Manning coefficient are difficult to measure and can be derived during model calibration. Calibration can also be used to provide values for parameters such as the water dispersion coefficient that may not be direct representations of field values, but instead include effects generated in the model such as numerical dispersion. Alternatively, generic values such as the period of the spring-neap tidal cycle, can be set as constants. Evaluation of individual parameters and the model as a whole is a complex and iterative process and the relative importance of each parameter has therefore been evaluated.

Chapter Two has discussed the ECoS hydrodynamic model set up. Construction and parameterisation of a hydrodynamic model that includes sediment transport for an estuary therefore requires information on:

- Estuarine bathymetry to determine the cross-sectional area and hence water velocity and how this varies with tidal state.
- Tidal elevation as the driving factor at the marine boundary.
- River and tributary flows driving the riverine boundary.

calibration and validation of the model requires information on:

- Water elevation within the estuary as a function of tidal state and river flow to assess the performance of the hydrodynamic predictions.
- Salinity or other conservative solute data that can be used to determine an appropriate water dispersion parameter.
- Suspended and bed sediment data to identify particle transport processes.

These requirements set the scene for Chapter Three which describes the collection of data that has then been used to develop and test a hydrodynamic model of the Tweed Estuary.

Chapter 3

Measurement and monitoring of master variables in the Tweed River Estuary

3 Measurement and monitoring of master variables in the Tweed River Estuary

After describing a hydrodynamic model of the Tamar Estuary in the previous chapter, this chapter deals with the data collection undertaken for the parameterisation, calibration and validation of a hydrodynamic model of the Tweed Estuary. This includes river flow, tidal elevation and propagation, estuarine bathymetry, and solute (salinity) and particle (turbidity) transport. A variety of data sources were approached, (UK Meteorological Office, Scottish Environment Protection Agency and the Land Ocean Interaction Study) in order to achieve the parameterisation process.

3.1. The Tweed Estuary

The Tweed Estuary is situated on the UK north east coast where it discharges into the North Sea (see Figure 3.1). Elevated levels of trace metals in North Sea coastal waters compared to ambient North Sea concentrations has caused concern and led to the extensive study of many of the North Sea estuarine systems (Turner *et al.*, 1992b). The Land Ocean Interaction Study (LOIS) is a collaborative project the aim of which has been to increase the understanding of how the coastal zone works as an integrated whole. This understanding can then be used to model the flux of particles, biogeochemically important elements and contaminants from the land, through estuaries to the sea (NERC, 1994). The LOIS experimental area extended from the Yare Estuary in the south to the Tweed Estuary on the English-Scottish border. The LOIS surveys focused on the east coast because of its susceptibility to rising sea level and that it provided an area including estuaries with a significant pollution problem, the Humber and a comparative reference site with much lower levels of anthropogenic disturbance, the Tweed (NERC, 1994). The Tweed Estuary is also responsible for the second highest flux of water into the North Sea from the UK. The highest flux being from the rivers entering the Humber (Fox & Johnson, 1997). The relatively pristine environment of the Tweed allows natural transport-reaction processes to be more clearly evaluated and understood in comparison to estuaries with higher levels of anthropogenic disturbance such as the more densely populated and industrialised catchment of the Humber (Turner *et al.*, 1992b; Martin *et al.*, 1993). The Tweed is also hydrodynamically simple with only one main tributary within the tidal reaches and does not suffer from the problems associated with multiple inputs in more complex systems such as the Humber. The Tweed Estuary is however a rapidly flushed dynamic system characterised by variable (10 to 1000 m^3 s^{-1}) river flow rates and

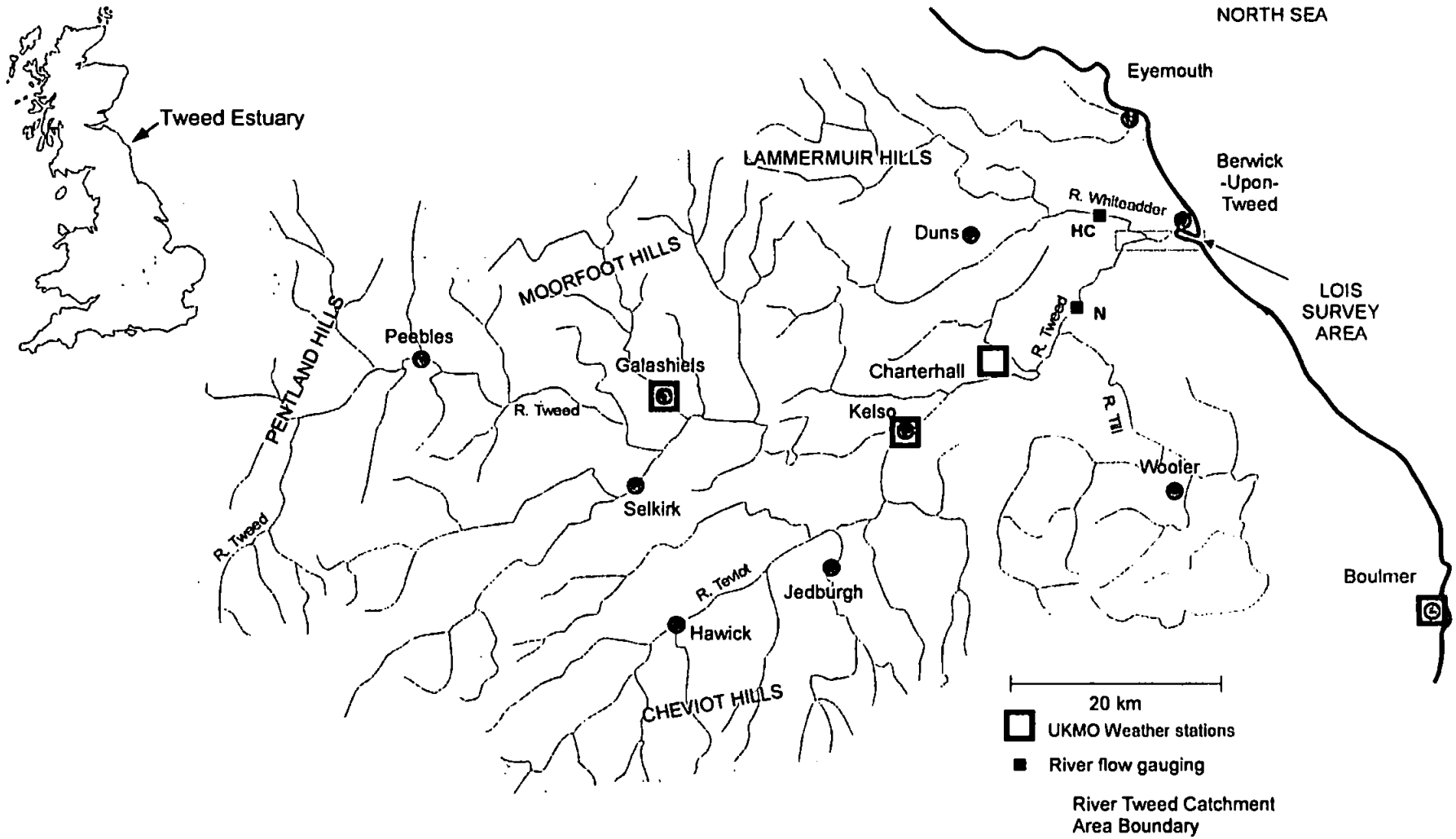

Figure 3.1 Catchment area of the Tweed Estuary showing the main rivers of the Tweed, Teviot, Till and Whiteadder. The UK Meteorological Stations and Scottish Environment Protection Agency river monitoring sites at Norham (N) on the Tweed and Hutton Castle (HC) on the Whiteadder are also shown in relation to the LOIS survey are

corresponding variability in saline intrusion (Uncles *et al.*, 2000), high (7 to 10) pH, supersaturated concentrations of dissolved oxygen (Howland *et al.*, 2000), and typically low (< 10 mg l^{-1}) turbidity (Balls, 1994) that can increase dramatically during spate conditions (Robson *et al.*, 1996; Neal *et al.*, 1997). The flushing time of the Tweed has been estimated as ranging from approximately 12 hours (Uncles & Stephens, 1996b) to just under 3 days (Balls, 1994) depending on tidal state and river flow. Compared to estuaries like the Tamar where the flushing time is 7 to 12 days (Millward, 1995) the Tweed will be more rapidly responsive to changes in tidal and flow regime.

The start of this project coincided with the 14 month LOIS investigation of the Tweed Estuary. Development of a coupled hydrodynamic-geochemical estuarine model by its very nature requires data on the physical structure, water movement, and sediment solute transport through the system. Involvement with the LOIS core programme therefore provided an opportunity to participate in a large collaborative project with access to a much broader range of data, equipment, technical support and scientific expertise than would normally be available. In addition to the importance of the Tweed as outlined by the above rationale the dynamic and variable nature of the estuary also provided a modelling challenge to expand and test the existing applications of ECoS.

3.2. *Weather data for the Tweed Area*

Variation in weather and climate are important considerations when attempting to interpret the data acquired during any major field programme. A inherent assumption often made when linking new environmental data with that acquired in the past is that average or stable climatic conditions applied during both observational periods. Data of this nature is however variable at all scales and to expect any sort of steady-state average may therefore be unrealistic. Marsh & Sanderson (1997) concluded that, for the Humber catchment, during the LOIS Programme there had been large spatial and temporal variations in rainfall and the seasonal contrasts were increasing. Consequently, deviation from normal runoff patterns and unprecedented water temperatures may have occurred. Their findings broadly agree with current global trends of "extreme" precipitation events becoming more common and intense rainfall more frequent (Tsonis, 1996). Similarly, the hydrological conditions in the Tweed during the LOIS Programme may have been different to those under previous conditions. Fox and Johnson (1997), in their analysis of the evolution of the hydrology of the River Tweed, found that the ratio of winter to summer runoff was increasing and the

"flood-rich" period was identified as the late 1980s and early 1990s. If this were the case during the LOIS Programme then the transport of contaminants from storage regions in the catchment area, river basins and the upper estuary may have been more pronounced than would have been predicted from average conditions.

Precipitation is important in controlling the freshwater flow through the Tweed Estuary and hence has an affect on the flux and fate of material in the estuary. The average annual rainfall over the Tweed Estuary catchment (1961 to 1990) shown in Figure 3.1 is 969 mm yr^{-1} (Tweed River Purification Board, 1992). A high proportion of the catchment consists of upland ground of the Moorfoot, Pentland and Lammermuir Hills with elevations exceeding 800 m (Robson *et al.*, 1996) and there is a marked rainfall gradient between about 2000 mm yr^{-1} in the uplands in the west and about 600 mm yr^{-1} in the lowlands nearer the coast (Neal *et al.*, 1997). This east-west gradient is significantly effected by winds and weather fronts in addition to the catchment topography (Fox & Johnson, 1997). Snow melt contributions to major floods are rare.

The British Atmospheric Data Centre (BADC) holds two sets of UK surface data, climate station data and synoptic station data. Climate station measurements form a long term record of daily observations. In contrast, the synoptic stations allow the analysis of current weather systems with hourly resolution.

The nearest synoptic and climatic stations to Berwick that were recording data during 1996 to 1997 are at Charterhall (26 km), Kelso (34 km), and Galashiels (54 km) within the Tweed catchment and at Boulmer (47 km) a coastal station to the south-east, see Figure 3.1. The parameters measured vary from station to station and not all parameters are available form all stations, see Table 3.1.

Table 3.1 Wind, air pressure and rainfall parameters measured by the UKMO weather stations nearest to Berwick-upon-Tweed (BADC, 1998).

	Station type	Wind speed (knots) & direction (°)	Rainfall (mm)	Sunshine (hours)	Global radiation ($W\ m^{-2}$)
Charterhall	Synoptic	Hourly mean	Hourly total	- -	Hourly total
Kelso	Climatic	- -	24 h total	- -	- -
Galashiels	Climatic	Daily mean	24 h total	Hourly total	- -
Boulmer	Climatic	Daily mean	Hourly total	Hourly total	- -

Rainfall data from Kelso and Galashiels stations (see Appendices) within the Tweed catchment was chosen as being the most likely to relate to local variations in river flow, although rainfall in the upland areas may be significantly different. Data from the two stations is quite consistent (correlation coefficient of 0.82) and the average daily rainfall during the survey periods was 1.7 mm day^{-1}. Several surveys occurred when the rainfall in the area was below detection, while rainfall in excess of 10 mm day^{-1} occurred during October, November and December 1996 and February, May and July 1997.

Wind data from the Boulmer site was however investigated as this was felt to be more representative of wind conditions especially at the mouth of the Tweed were wind induced wave resuspension of suspended sediments has been reported (Uncles & Stephens, 1997). The average wind speed and direction for the survey periods (see Appendices) was 9 knots and 175° relative to true north. Mean daily wind speeds up to 30 knots prior to the survey dates occurred, but only exceeded 10 knots during the surveys on a limited number of occasions (October and November 1996 and February, March and April, 1997). The Tweed Estuary runs predominantly along an east-west axis and the mouth of the estuary faces due east. Wind direction of 90° is therefore likely to have caused the most significant resuspension of bed sediments. On shore winds occurred during surveys in July and September 1996 and March, June and August 1997 and sampling was not conducted at the most seaward during surveys in September and November 1996 and February, June and August 1997 due to the rough sea state.

3.3. *Monitoring freshwater input to the Tweed tidal reaches*

There is one main freshwater input to the tidal reaches of the Tweed Estuary, the River Tweed at the head of the estuary. In addition, the River Whiteadder (normally < 10 % of the freshwater input) joins the estuary at approximately 6 km from the mouth. The River Tweed extends over 160 km in the rural Scottish Borders to the south of Edinburgh (Robson & Neal, 1997) before reaching the North East Coast at Berwick-Upon-Tweed, see Figure 3.1. The Tweed is the second largest river basin in Scotland and the sixth largest in mainland Britain (Clayton, 1997) and has a catchment area of 4390 km^2. The River Whiteadder has a much smaller catchment of 503 km^2 and is situated in much of the lower lying areas to the east of the region. Anthropogenic influences on the water resources of the catchment include approximately 3 % abstraction to supply the Lothians and Edinburgh, but compensation releases and freshet reservoir release may enhance the flows

in the lower reaches by as much as 50 % during dry weather flows. These typically last for 24 hours and are commonly made on a weekly basis when river flows are low and water temperatures high (Fox & Johnson, 1997).

The River Tweed catchment falls under the jurisdiction of the Scottish Environment Protection Agency (SEPA) who maintain several flow-gauging stations and undertake water quality assessment at a range of sites. The locations of flow-gauging stations are often determined by water resources, flood prevention and land drainage and are not specifically designed to measure the land to sea flows. Tidal back up and flow reversal can also make flow measurements difficult in tidal reaches (Leeks *et al.*, 1997). The two freshwater inputs into the tidal reaches, are however monitored at sites relatively near to the tidal limit at Norham (Tweed) and Hutton Castle (Whiteadder) (Tindall, *per. comm.*, 1996) and are shown in Figure 3.1. The Institute of Hydrology (IH) Rivers Data Centre was set up to collate data from the statutory river flow measurement agencies and to provide water quality and quantity data to the LOIS community for 1986 to1996 (Tindall & Moore, 1997). River flow information is normally available as mean daily flow (MDF) in units of m^3 s^{-1}. Mean daily flow data for the River Tweed at Norham and River Whiteadder at Hutton Castle was kindly supplied by the IH Data Centre for the period 1963 to 1996 and 1969 to 1996, respectively (Tindall, *per. comm.* 1996, 1997). The 1970's were characterised by low flows compared to the 1980's (Fox & Johnson, 1997) and these large data sets were felt important to establish how the flows during the LOIS period related to those of preceding years. More detailed data for the Norham and Hutton Castle gauging stations including mean quarter hourly flow (QHF) data and also MDF data for 1997 kindly was supplied directly from SEPA (McDraw, *per. comm.*1998, 1999). There will also be a time lag between changes in flow recorded at the gauging stations and those in the estuary. Due to the rapid propagation of flood waters through the catchment this is likely to be only one or two hours during spate and has therefore been assumed to be negligible.

3.3.1. Annual variability

The annual discharges for both the River Tweed (mean 2.4 km^3 yr^{-1}) and River Whiteadder (mean 0.2 km^3 yr^{-1}) are quite variable, see Figure 3.2. The Tweed discharge varied by a factor of three between a minimum of 1 km^2 yr^{-1} in 1973 to a maximum of 3 km^2 yr^{-1} in 1979. Both rivers exhibited low annual flow in 1973 and 1989. Although the annual

discharge may provide some indication of long term changes, it does not show how the flow pattern may vary though a year.

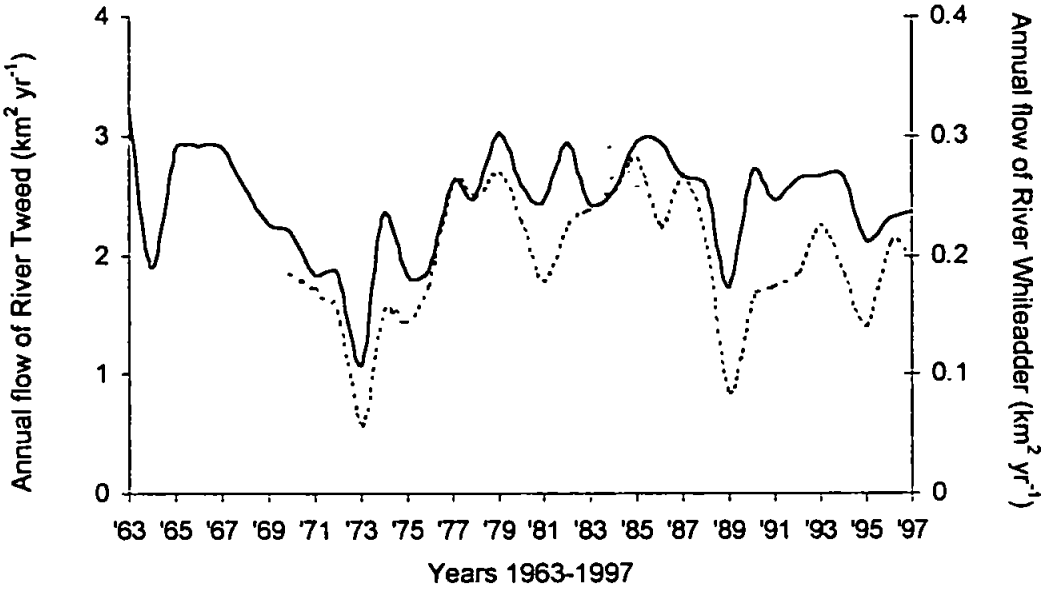

Figure 3.2 Annual flow for the Rivers Tweed (—) and Whiteadder (---). Data supplied from the IH Rivers Monitoring Centre and SEPA.

3.3.2. Seasonal variability

The averaged mean daily flow for the Tweed and Whiteadder rivers is shown in Table 3.2. The Whiteadder accounts for a mean of 8 % of the total freshwater flow into the tidal reaches of the estuary. The mean daily river flow for the Tweed and Whiteadder rivers during the LOIS survey period of 1996 to 1997 is shown in Figure 3.3.

Table 3.2 A comparison of the mean, range and relative standard deviation of daily freshwater flow for the Tweed at Norham and Whiteadder at Hutton Castle during the LOIS survey period with a long term data set.

River flow	River Tweed		River Whiteadder	
($m^3 s^{-1}$)	1963-1995	1996-1997	1963-1995	1996-1997
mean	77.8	71.1	6.2	6.0
(min-max)	(7.4-1169)	(9.4-641)	(0.4-173)	(0.9-65.6)
RSD	0.90	0.89	0.70	0.78

A log scale is used to reflect the tendency of the variation in flow to be proportional rather than additive. The flow of both rivers gradually decreased through the spring and summer then rapidly increased in the autumn and was interspersed with short periods of flood. The spring and summer of 1997 experienced a greater number of these flood events than the preceding year. The flows during the axial survey period can be compared with the monthly ranges for 1990 to 1995 using a Box-Whisker plot, see Figure 3.4.

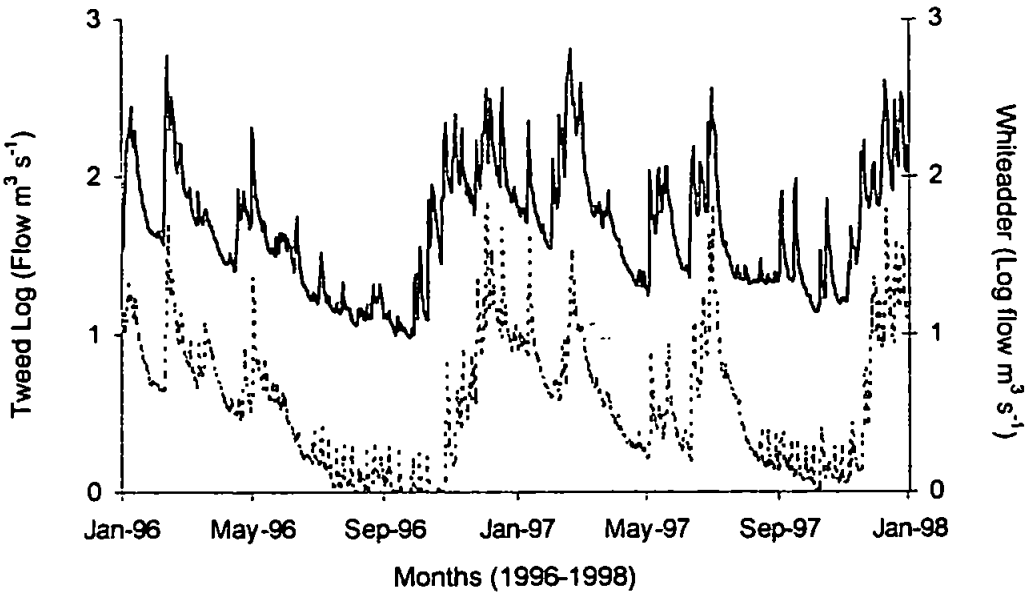

Figure 3.3 Daily flows in the Tweed at Norham (—) and Whiteadder at Hutton Castle (—).

Comparisons were limited to a recent period to avoid the possibility of long term changes in the flow regime producing ranges that are unrealistic of the current situation. Due to the low annual flow in 1989 it was decided to limit this comparison data set to 1990 to 1995. The Box-Whisker plot shown in Figure 3.4 further illustrates the seasonal variability in flow with the greatest mean flows in December (Whiteadder, 8 m^3 s^{-1}) and January (Tweed, 145 m^3 s^{-1}) with minimum mean flows in August (Tweed, 20 m^3 s^{-1} and Whiteadder, 1.5 m^3 s^{-1}). The range of flows within each month also varied and was greatest in the winter compared to the summer for both the Tweed and Whiteadder Rivers. Comparing the monthly ranges to mean daily flows recorded during the axial surveys of the estuary show that most of the surveys were conducted within the 95 % range of flows typical for those months. The obvious exception is the July 1997 survey when the River Tweed mean daily flow during the survey was 217 m^3 s^{-1} and two days previously had peaked at 361 m^3 s^{-1}. July flows in excess of 200 m^3 s^{-1} have only been exceeded on 15 occasions during 1963 to 1995 and those in excess of 300 m^3 s^{-1} only 5 times in the same period. The corresponding flow in the Whiteadder River on the day of the survey (19 m^3 s^{-1}) had also only been exceeded 5 times in the period 1969 to 1995. The peak flow two days previously of 62 m^3 s^{-1} was the highest July flow recorded since 1969 and one of the highest flows recorded in the Whiteadder between 1996 and 1997 (a maximum of 66 m^3 s^{-1} recorded in December, 1996).

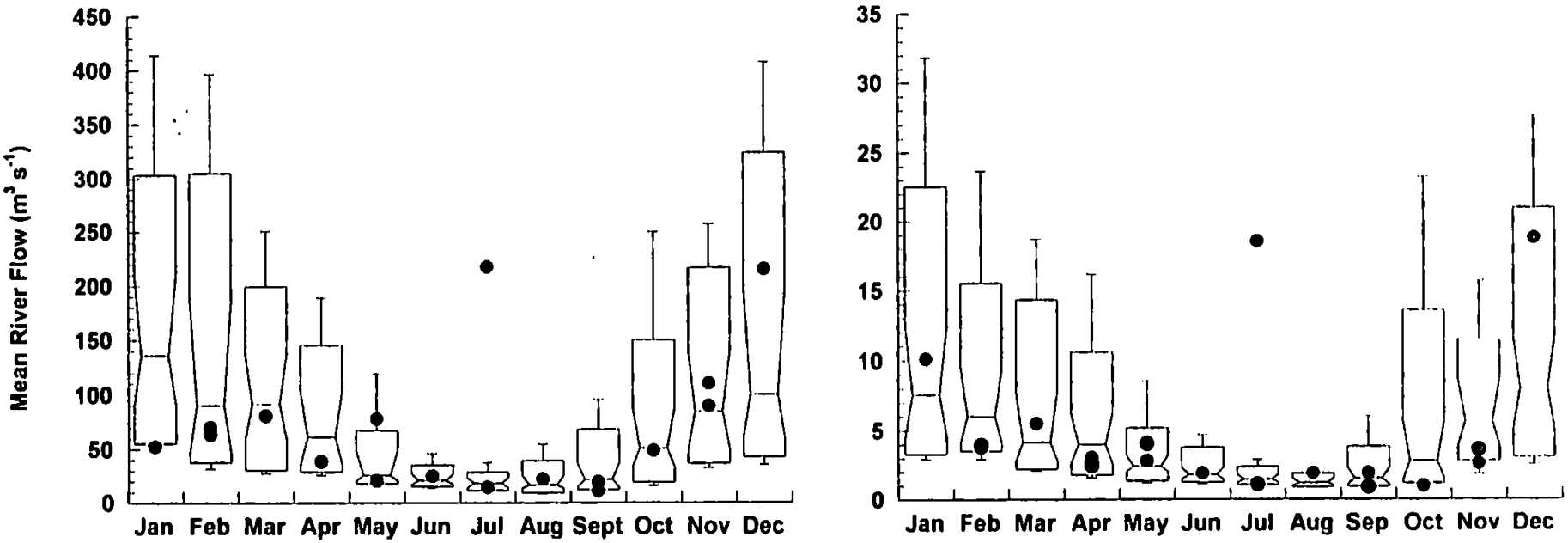

Figure 3.4 Mean river flow for a) the River Tweed and b) the River Whiteadder during the LOIS axial surveys (1996-1997) of the Tweed Estuary (•) compared to the 95 % range recorded between 1990 and 1995. Data supplied by the IH Rivers Data Centre.

3.3.3. Daily variability

Flood events originating from high precipitation in the uplands typically require 15 to 24 h to move from the headwaters to the estuary (Fox & Johnson, 1997). The flood peaks in October and November 1996 and February, May and July 1997 were preceded by high rainfall on the day before. The data from Galashiels and Kelso does not however show high rainfall preceding the December 1996 and January 1997 floods and indicates that the increased flow probably originated from the upland regions. Short flood periods mean that the flow between one day and the next can change very rapidly in the Tweed and Whiteadder rivers by up to 300 $m^3 s^{-1}$ and 40 $m^3 s^{-1}$ respectively (1996 to 1997). Hysteresis effects on the flow-turbidity relationship can be significant (Dyer, 1986; Grabemann *et al.*, 1997) and the mean daily flows for a period of 6 to 7 days prior to each survey is shown in Figure 3.5. This shows that some surveys were conducted during a constant flow regime while others occurred on either falling or apparently rising hydrographs. In these situations, the actual flow during and preceding the survey may differ sufficiently from the mean daily averaged value. Quarter hourly flow values may then be more accurate and were kindly supplied by the Scottish Environment Protection Agency (McDraw, 1998 *per. comm.*). The quarter hourly flow values showed that during the October 10 and February 9 surveys the flow did not increase until between late afternoon and early evening, *i.e.*, after the survey. During January 10 and May 4 surveys the flow did not increase until the following day so would also have not directly effected the hydrology of the estuary, see Figure 3.6. None of the axial surveys were therefore conducted on a rising hydrograph.

Due to the topographic and geographic differences between the Tweed and Whiteadder catchments, flows in the Whiteadder may not always change with those in the Tweed. Floods in the Whiteadder, however do tend to correspond to those in the Tweed, *e.g.*, December 1996, and July 1997, indicating catchment wide precipitation. Increased flow in the Tweed due to high precipitation in the west of the catchment did not however always lead to increased flow in the Whiteadder, *e.g.*, November 1996, and February 1997. Between 1996 and 1997 the Whiteadder flow varied from 1 to 27 % (mean 8 %) of the total freshwater into the tidal reaches and will have had varying effects on the flux of material through the estuary.

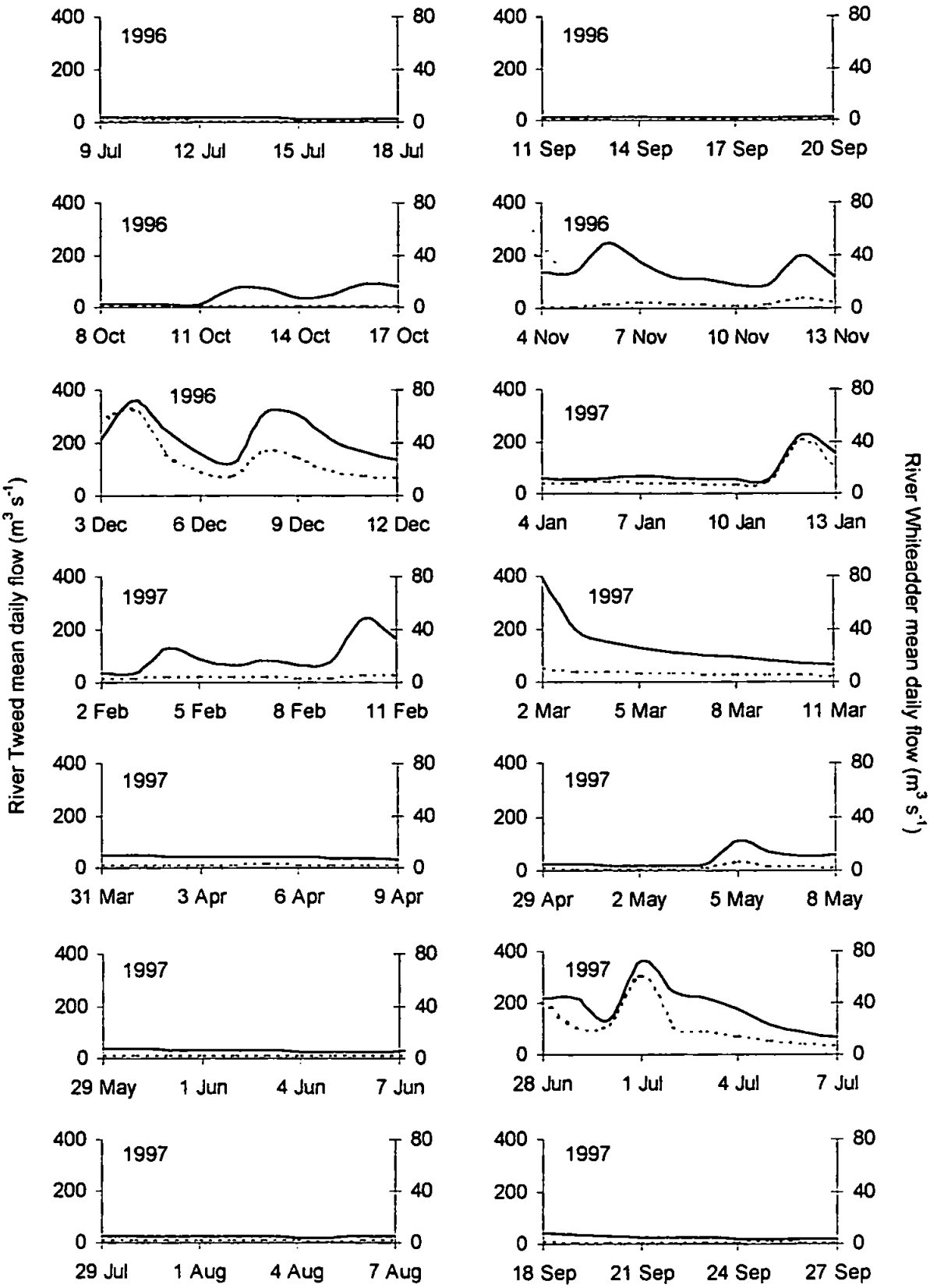

Figure 3.5 Mean daily river flow for the Tweed at Norham (—) and Whiteadder at Hutton Castle (—) illustrating the changing hydrograph during each survey period.

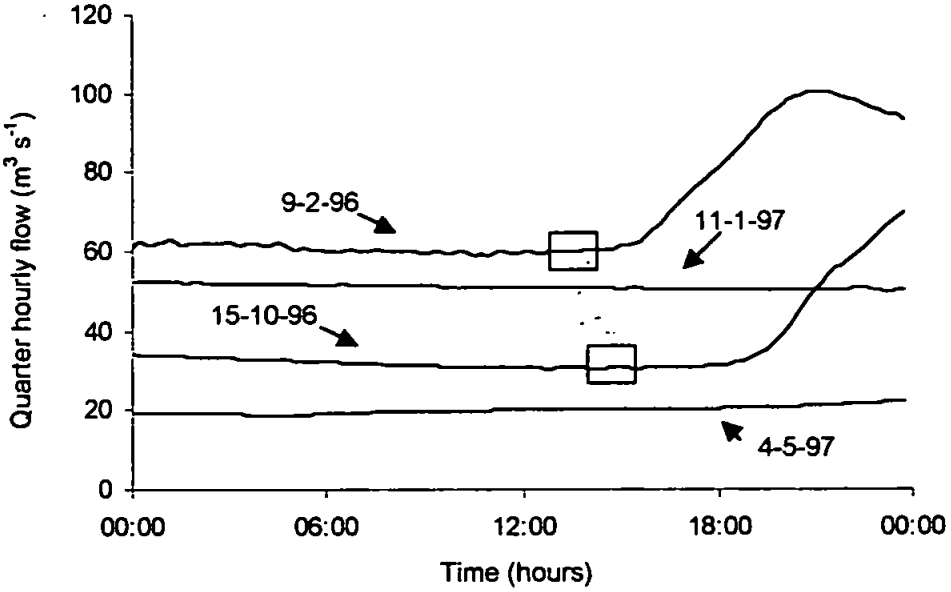

Figure 3.6 Variability in Tweed flow at Norham over 24 hours. The shaded blocks shown indicate the period over which the axial survey was conducted during the February and October surveys.

3.4. Measurement and sampling strategies in the Tweed Estuary

The LOIS core programme was established to monitor the seasonal variability of standard suite variables (salinity, temperature, turbidity, dissolved oxygen and pH), nutrients (phosphate, silicate, nitrate, nitrite and ammonia) chlorophyll *a* and carbon to nitrogen ratios. Core programme sampling and analysis was predominately conducted by personnel from CCMS PML with some assistance from the LOIS laboratory based at the University of Hull. In addition to the core programme, collaboration by special topics groups from the University of Plymouth, University of Southampton and Institute of Hydrology Wallingford led to an even wider range of variables measured.

The LOIS core programme surveys of the Tweed Estuary consisted of 13 monthly field visits between July 1996 and August 1997. An additional survey in September 1997 was also conducted as a collaborative effort between the University of Plymouth and the University of Southampton. With the exception of the September 1997 survey, survey dates were arranged to coincide with spring tides. Spring tidal conditions were required to ensure adequate water depth in the estuary for the survey vessels. Each survey period consisted of between 4 and 6 days at Berwick. The survey dates, tidal ranges and freshwater flows during each survey are shown in Table 3.3. This shows that flows during the surveys ranged from between 11 and 309 $m^3 s^{-1}$ and with the exception of September 1997 tidal ranges varied from 3.1 to 5.3 m. During each survey standard suite (Howland *et*

al., 2000; Uncles *et al.*, 2000) and other measurements were made using extended axial transects (EATs), repetitive axial transects (RATs), anchor stations (ASs) and remotely deployed instrument arrays (IAs).

Table 3.3 Survey dates with the and range and average of the mead daily freshwater flows (MDF) and tidal ranges

Survey	Dates	Tweed MDF ($m^3 s^{-1}$)	Whiteadder MDF ($m^3 s^{-1}$)	Whiteadder MDF as a % of total flow	Date of maximum tidal range	Predicted tidal range at the mouth (m)
1	Jul 96	14	1.2	7.9	18 Jul	3.4
	(15-18)	(14-15)	(1.1-1.3)			(3.2-3.6)
2	Sep 96	11	0.9	7.6	16 Sep	3.9
	(16-19)	(11-12)	(0.9-1.0)			(3.5-4.2)
3	Oct 96	65	0.9	1.4	15 Oct	4.3
	(13-17)	(36-89)	(0.9-1.0)			(4.0-4.4)
4	Nov 96	122	4.2	3.3	13 Nov	4.1
	(8-13)	(90-200)	(2.6-7.7)			(3.3-4.7)
5	Dec 96	226	22.2	8.9	12 Dec	4.0
	(8-12)	(136-309)	(14.2-33.6)			(3.1-4.6)
6	Jan 97	109	16.8	13	11 Jan	4.8
	(9-13)	(52-227)	(7.2-41.2)			(4.7-5.0)
7	Feb 97	127	4.6	3.5	10 Feb	5.0
	(7-11)	(64-248)	(3.8-5.5)			(4.7-5.2)
8	Mar 97	83	5.6	6.3	10 Mar	4.9
	(7-11)	(66-98)	(5.0-6.4)			(4.0-5.3)
9	Apr 97	37	2.5	6.3	9 Apr	4.5
	(5-9)	(33-40)	(2.3-3.0)			(3.9-5.1)
10	May 97	64	4.0	5.9	7 Apr	4.2
	(4-8)	(21-109)	(2.8-7.4)			(3.7-4.6)
11	Jun 97	26	2.0	7.1	6 Jun	4.0
	(3-7)	(25-28)	(1.8-2.4)			(3.6-4.1)
12	Jul 97	132	12.1	8.5	6 Jul	3.6
	(3-7)	(68-217)	(7.8-18.5)			(3.3-3.8)
13	Aug 97	21	1.8	7.9	6 Aug	3.7
	(3-7)	(21-22)	(1.8-1.9)			(3.4-3.9)
14	Sep 97	20	1.4	6.5	23 Sep	2.3
	(23-26)	(19-21)	(1.2-1.9)			(1.8-3.2)

3.4.1. Extended axial transects.

Between one and four extended axial transects of the Tweed Estuary were conducted using a 4.2 m semi-rigid inflatable boat during each survey period. Throughout the LOIS surveys a consistent set of sampling localities was used. The stations were selected to ensure adequate coverage of the freshwater-salt water interface (FSI) and to provide full spatial cover of the estuary. Details of the sampling stations are shown in Figure 3.7 and Table

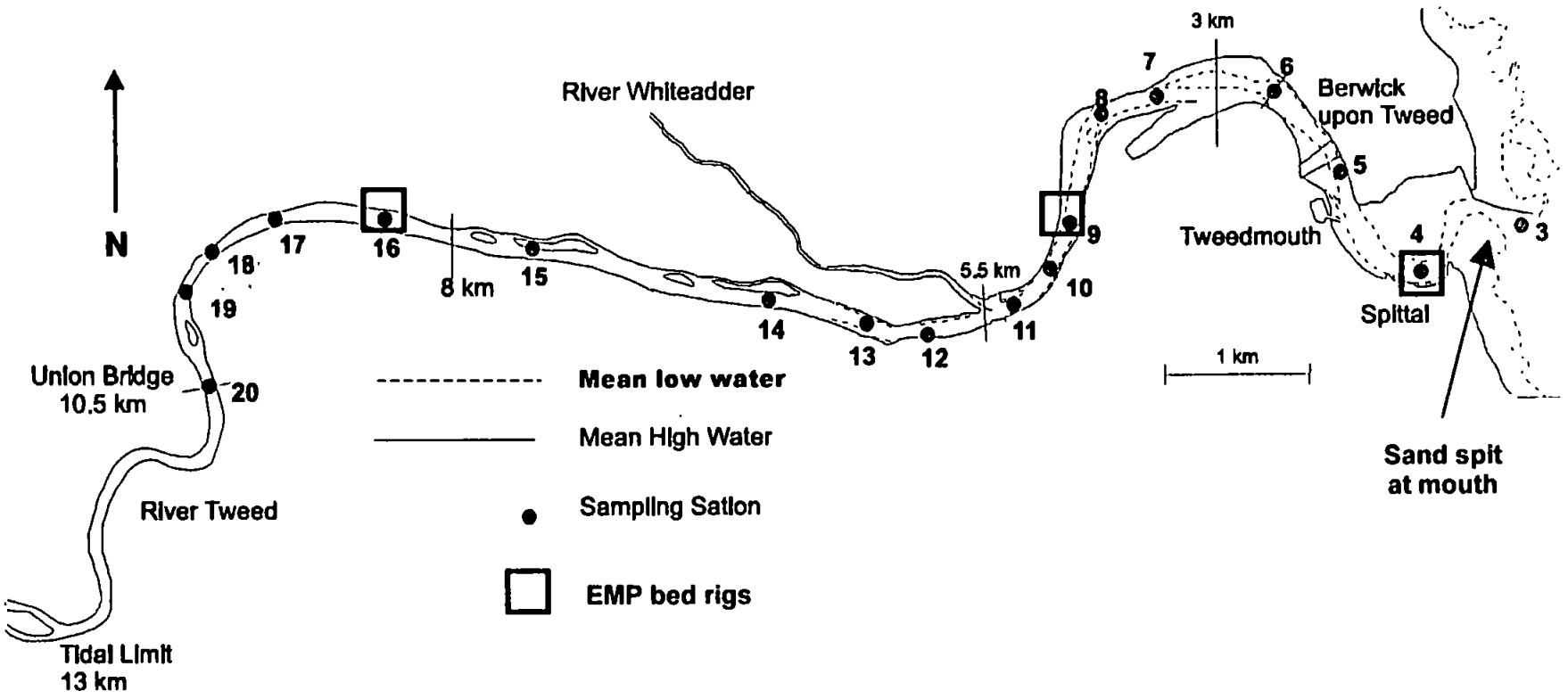

Figure 3.7 LOIS survey stations in the Tweed Estuary between station 3 at the mouth of the estuary and station 20 at Union Bridge. The distances shown are from the mouth.

3.4. Two additional stations off-shore were also planned, but not routinely visited. Due to shallow water depths, and to maintain consistency between surveys, sampling was performed as near to high tide as possible. There was some unavoidable variability in sampling time relative to predicted high water and the direction of sampling, either upstream or downstream was also not consistent. Details of the 36 EATs conducted in the Tweed Estuary are shown in Table 3.5. The Tweed Estuary is rapidly flushed (Balls, 1994; Uncles & Stephens, 1996b) and these time differences need to be considered when comparing observations *e.g.*, water depth or salinity with values predicted using a tidal model.

Table 3.4 LOIS core programme survey stations for the Tweed Estuary, shown in Figure 3.10

Station name	Station No.	Distance from mouth (km)	Position*
Off-shore	1	- -	- -
Off-shore	2	- -	- -
Lighthouse	3	0.17	009 524
Lifeboat station	4	1.17	002 520
Chandlery	5	2.02	997 527
Royal Border Bridge	6	2.71	993 532
High Pool	7	3.56	984 532
Lower Yarrow Shiel	8	3.96	981 530
Toddles Shiel	9	4.67	979 523
New Water Shiel	10	4.91	978 521
A1 road bridge	11	5.35	974 517
North Middle Ord	12	6.02	968 516
Heugh Shiel	13	6.45	964 517
West Ord	14	7.10	958 518
Coroners Meadow	15	7.91	951 519
Low House	16	8.31	946 521
Yardford Shiel	17	8.96	930 522
Paxton	18	9.38	935 520
Quarry	19	9.84	932 516
Union Bridge	20	10.48	934 510

*National grid reference, Ordnance Survey Pathfinder 438.

3.4.2. Repetitive axial transects.

The R.V. *Tamaris*, a flat-bottomed 12 m Rotork Seatruck was used to perform repetitive transects in the lower reaches of the estuary. The transects were made between stations 3 and 8 during a period 2 to 3 hours either side of high water over 1 to 3 days. At other times and due to a shallow water area beyond station 8 the estuary was not safely navigable by the vessel.

Table 3.5 Extended axial survey details of the Tweed River Estuary between stations 3 and 20.

Survey period	Date	Predicted tidal range (m)	Tweed MDF ($m^3 s^{-1}$)	Time of HW (GMT) at mouth	Start time before HW (mins)†	Finish time after HW (min)‡	Survey direction*
Jul 96	16	3.4	14	15:10	17	76	D
	17	3.6	14	15:25	25	50	D
Sep 96	17	4.1	11	17:00	81	-3	U
	18	3.8	11	17:30	111	-33	U
	19	3.5	11	06:00	49	16	U
Oct 96	14	4.4	36	15:25	103	0	U
	15	4.4	49	16:00	42	64	U
	16	4.3	89	16:40	112	-20	U
Nov 96	9	3.3	112	13:00	50	50	U
	10	3.8	90	13:45	80	25	U
	11	4.2	92	14:30	110	0	U
Dec 96	9	3.7	304	13:10	85	23	U
	10	4.0	215	14:00	86	5	U
	11	4.4	164	14:50	39	-6	U
Jan 97	10	4.8	52	15:11	85	-61	U
	11	5.0	52	15:56	95	-26	U
Feb 97	8	4.9	64	14:56	71	89	D
	9	5.2	77	15:39	106	0	U
Mar 97	7	4.0	98	13:00	-34	84	U
	8	4.0	95	13:52	32	85	U
	9	4.1	81	14:37	59	54	U
	10	4.6	73	15:21	23	26	U
Apr 97	5	3.9	40	12:45	-43	176	D
	6	3.9	39	13:33	18	112	D
	7	4.7	36	14:18	-35	137	D
May 97	4	3.7	21	12:24	-9	100	D
	6	4.4	78	13:59	-39	90	D
Jun 97	3	3.6	28	12:56	2	80	D
	5	4.1	25	14:30	28	74	D
Jul 97	3	3.3	217	13:35	15	65	D
	5	3.7	113	15:30	55	24	D
Aug 97	3	3.4	22	14:47	4	79	D
	4	3.7	21	15:22	23	57	D
	5	3.8	21	15:55	27	46	D
	6	3.9	22	16:28	13	42	D
Sep 97	25	1.9	19	09:36	14	50	D

†Negative values indicate that the surveys commenced after and ‡finished before predicted time of high water at the mouth. *Survey direction U = up estuary, D = down estuary.

3.4.3. Anchor station surveys.

One 12 to13 hour anchor station survey was conducted on each of the surveys when R.V. *Tamaris* was available. Details of these are shown in Table 3.6. During high flows, surface salinity was reduced and the salinity range observed is also shown. During this period the vessel was anchored at station 5 (or stemming the tide if anchoring was not possible) allowing sampling and standard suite measurement throughout a tidal cycle. The location of the anchor station was constrained by the requirement of a site that was also sufficiently sheltered with a minimum water depth at low water to prevent the vessel grounding. A wide salinity range during the tidal cycle had also been observed at this site during July and September 1996 surveys and choice of the site was also based on the ability to sample the entire salinity range. The anchor station was also held for additional shorter periods for instance when there was insufficient water depth for the vessel to make the repetitive axial transects. No anchor station was conducted in March due to engine problems with the R.V. *Tamaris* .

Table 3.6 Full tidal cycle anchor stations in the Tweed Estuary conducted at station 5.

Date	Tidal range (m)	Tweed MDF ($m^3 s^{-1}$)	Salinity† (min-max)
17 Oct 96	4.0	79	0-13.0
12 Nov 96	4.4	200	0-7.6
11 Dec 96	4.4	164	0-2.2
12 Jan 97	4.9	227	0-2.6
10 Feb 97	5.2	248	0-26.1
8 Apr 97	5.0	35	0.5-33.2
5 May 97	4.0	109	1.0-33.8
4 Jun 97	3.9	26	0-33.0
4 Jul 97	3.5	178	0-1.8
7 Aug 97	3.8	22	0-32.5

†Salinity range measured at 0.5 m below the surface through out the anchor station.

3.4.4. Remotely deployed instrument rigs.

Three instrument arrays logging standard suite variables were remotely deployed at stations 4, 9 and 16 during the surveys. The instrument arrays at stations 9 and 16 were attached to bed mounted rigs that were deployed at low water at the start of the survey period and then recovered at the end. The instrument at station 4 was attached to the pilings below the life boat station and each deployment last approximately a month, the instrument being replaced during each subsequent survey. Following the October deployment high river flow prevent recovery of the instrument until the January survey.

The proximity of station 9 to an area frequented by anglers prevented deployment of the EMP2000 at this point during the summer months.

3.5. *Instrumentation deployment and calibration*

During the EATs, RATs and ASs Yellow Springs Instruments (YSI) 6000 multi-parameter water quality monitors were used to measure standard suite variables. On board the R.V. *Tamaris* water was pumped from a depth of 0.5 m into a sealed flow-through cell in the laboratory, into which a YSI 6000 sensor array was located for the measurement of standard suite variables. Data was logged at 12 second intervals and periodically downloaded to computer. Data was subsequently reduced and filtered by averaging over 15 minute intervals. A second YSI instrument was manually deployed on a weighted cable from a semi-rigid inflatable boat when surveying in the upper reaches of the estuary and also from R.V. *Tamaris*. Surface readings were made at a depth of 0.5 m and on occasion readings taken through the water column to establish the degree of saline stratification. This chapter predominately deals with the data requirements of the hydrodynamic model and will discuss the measurement and modelling of those parameters relevant to this section. Other parameters that include trace metals, dissolved oxygen, pH, nutrients, chlorophyll *a* and C/N will be dealt with later.

Calibration and operation of the YSI 6000 were according to the manufactures instructions (Yellow Springs Instruments Incorporated, 1993). The depth sensor was factory calibrated and output is directly proportional to the hydrostatic pressure acting on the sensor. The instrument automatically compensates for changes in density due to variations in salinity and results were post-calibrated for changes in atmospheric pressure. The thermistor is factory calibrated and requires little or no maintenance. Readings were however periodically checked by comparison to a pair of mercury thermometers. Turbidity is measured using a light emitting diode producing near infrared radiation (830 to 890 nm) and a photodiode at 90° to the light source. The sensor measures the amount of light scattered by particles present in the water and provided readings in nephelometric turbidity units (NTUs). Turbidity signals from each instrument were calibrated against frequently collected discrete SPM samples, which were measured gravimetrically. A measured volume (1 to 2 l depending on turbidity) of sample was filtered through a pre-ashed, weighed GF/C filter. Residual salt was removed from the filter by rinsing with 1 to 2 ml of Milli-Q water and the filter stored frozen in a petri-slide until ready for analysis. Samples were then freeze dried and re-weighed. The effect of temperature and salinity on the

turbidity sensor is small, however the system is sensitive to particle size and the particle nature in addition to the concentration that passes across the optics on the probe face. To avoid unrepresentative readings in a variable medium a continuous 8 point running average facility of the software was used during manual deployment. Conductivity was post-calibrated against discrete samples analysed using an Autolab Model 601 Mk III salinometer. The YSI 6000 instrument parameters are shown in Table 3.7.

Table 3.7 YSI 6000 Instrument parameters including accuracy and resolution of depth, temperature, turbidity and conductivity measurements (Yellow Springs Instrument Incorporated, 1993).

Parameter	Sensor Type	Range	Accuracy	Resolution
Depth	Strain gauge	0-10 m	± 0.018 m	0.01 m
Temperature	Thermistor	-5-45°C	± 0.15°C	0.01°C
Turbidity	90° scatter sensor	0–1000 NTU	± 5 % of reading or 2 NTU	0.1 NTU
Conductivity	4 electrode cell	0–100 mS cm^{-1}	± 0.5 % of reading	0.01 mS cm^{-1}
Salinity	Calculated from conductivity and temperature	0-70	± 1.0 % of reading or 0.1	0.01

The second main type of sensor array was the W. S. Ocean Systems Environmental Monitoring Probe (EMP) 2000 instrument arrays (Applied Microsystems Limited, 1993) that were remotely deployed at stations 4, 9 and 16. Pressure, temperature and conductivity sensor calibration and operation was similar to that described for the YSI 6000 instrument and parameter range, accuracy and resolution is shown in Table 3.8 (Applied Microsystems Ltd., 1993).

Table 3.8 EMP 2000 Instrument parameters show the range, accuracy and resolution of depth, temperature and conductivity measurements (Applied Microsystems Ltd., 1993).

Parameter	Sensor type	Range	Accuracy	Resolution
Depth	Pressure transducer	0-300 m	± 0.3%	0.05 m
Temperature	Thermistor	-2-32°C	0.05°C	0.001°C
Conductivity	4 electrode cell	0.02-65 mS cm^{-1}	± 0.1 mS cm^{-1}	0.03 mS cm^{-1}
Salinity	Calculated from conductivity and temperature	0-40	± 0.1	0.003

3.6. *Monitoring tidal elevation*

Modelling the changing volume of the estuary both in time and space is important to accurately predict the effects of water velocity, dilution and dispersion on the transport of material through the system. The Tweed is a fairly steeply rising and shallow estuary and the tidal limit is quoted as being approximately 13 km from the mouth (Uncles & Stephens, 1996b). Tides are semi-diurnal with mean spring and neap ranges of 4.1 and 2.5 m, respectively. Mean high water and low water levels relative to chart datum are 4.7 to 0.6m and 3.8 to 1.3 m during spring and neap tides, respectively (Hydrographic Office 1989a).

The extent of tidal propagation up the estuary will depend on river flow and tidal state and during the survey periods tidal elevation was monitored at three sites by the EMP 2000 bed rigs fitted with pressure transducer sensors (stations 4, 9 and 16). Due to technical problems that occurred with the EMP rigs the data available was unfortunately spasmodic. Figure 3.8 shows tidal elevation at station 4 during periods starting in October 1996 and February and March 1997. The observed spring-neap tidal ranges were 4.3 to 1.4 m and 3.7 to 1.7 m in October and March respectively. The high flow and missing data during February means tidal values have not been established. The data also showed a difference in the semidiurnal tides with the second tide of the day being larger by up to 0.5 m during spring tides in October. Tidal elevation at the mouth was predominately controlled by tidal state, but at sites further up the estuary river flow became increasingly important. At stations 9 and 16 consecutive data over several tides was also available for limited periods. At station 20 additional measurements of tidal elevation were made on two occasions. During the February survey a tidal pole was used to measure water elevation at 15 to 30 minute intervals during one tidal cycle and in April a YSI 6000 was remotely deployed on the bed for 4 days logging data at 15 minute intervals, see Figure 3.9. This showed tidal amplitudes at station 9 of 1.6 to 2.8 m, at station 16 of 0.4 to 1.4 m and at station 20 of 0.7 to 1.3 m. Uncles and Stephens (1997) noted a considerable reduction in tidal amplitude over a distance of 2.4 km prior to station 9. The results presented here concur that the majority of the reduction in tidal amplitude occurred in the lower half of the estuary.

Although high river flow appears to have had little effect on the maximum tidal elevation it had a significant influence on water depth at low water with an increase of 1 m during the February flow of approximately 400 $m^3 s^{-1}$. Plotting the increase in low water depth against flow for both stations 9 and 16 showed a significant ($p < 0.001$) linear relationship, see Figure 3.10. It is important for the model to be able to replicate the increase in water depth

with flow so as to not over predict velocity at low water and these data can be later used to test the model output.

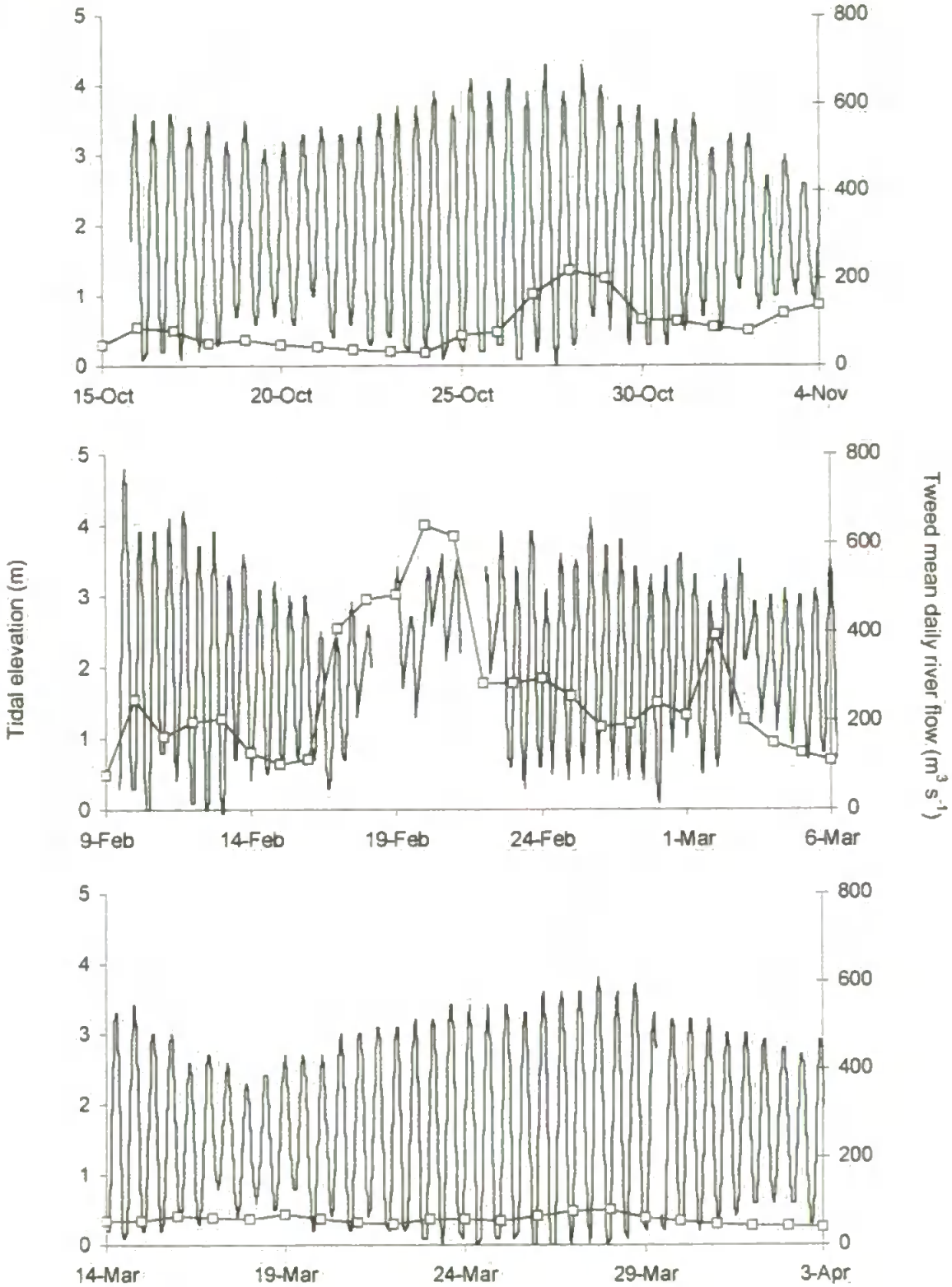

Figure 3.8 Tidal elevation at station 4 near the mouth of the Tweed (—) and mean daily river flow (-□-). The results have been normalised relative to minimum low water.

The time lag of local high water increases up the estuary relative to that at the mouth. During the relatively low flow in April the time of high water at station 20 was 30 to 45 minutes after that at the mouth while in February a delay of approximately one hour occurred. This further highlights the problems of sampling at 'high water' particularly for those surveys conducted in the up estuary direction during high flow events. For example in December 1996, surveys that were completed prior to high water at the mouth may have sampled in the upper estuary approximately 2 hours before high water. This needs to be considered when interpreting the results and comparing field data to model predictions.

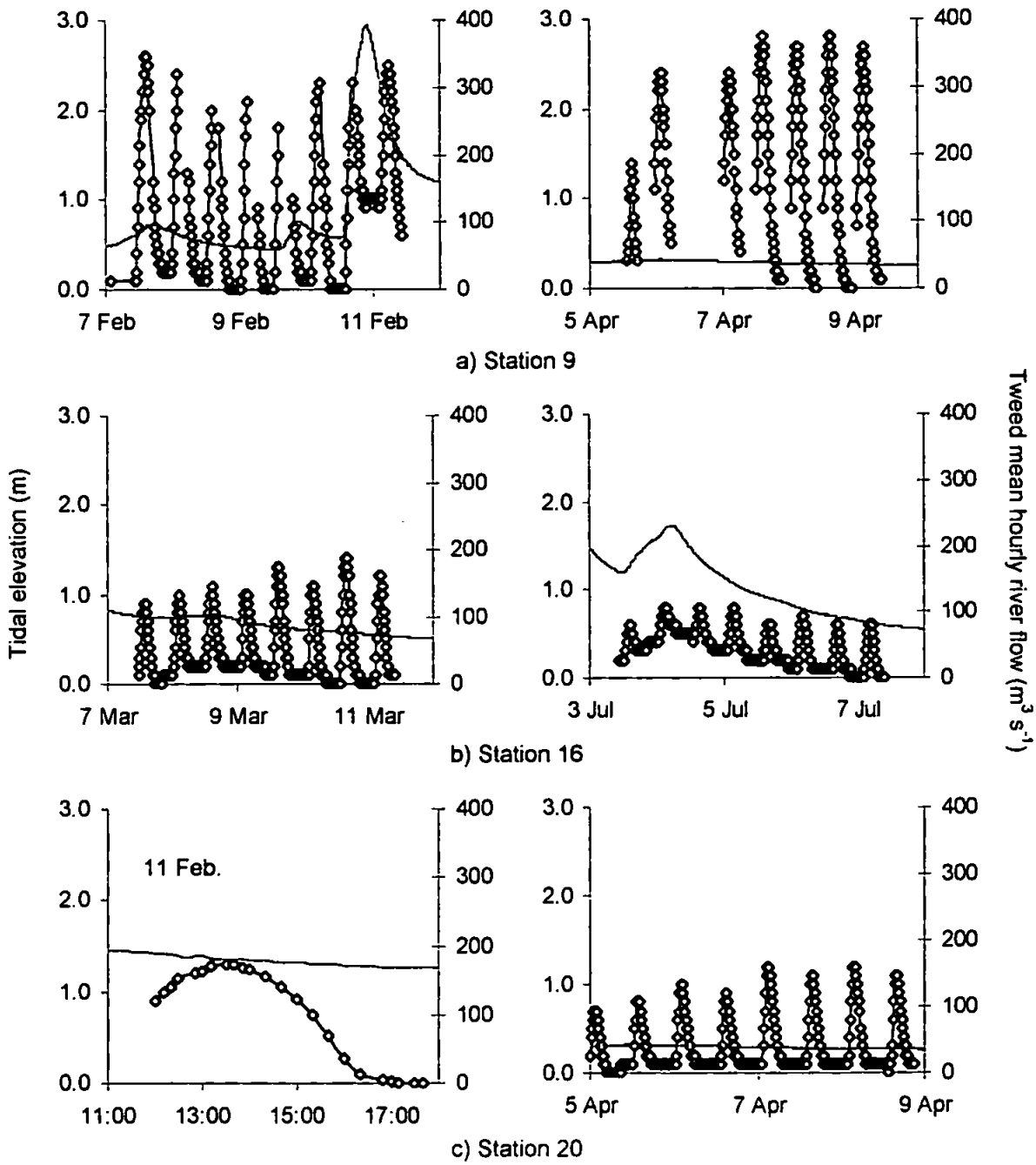

Figure 3.9 Tidal elevation at stations a) 9, b) 16 and c) 20 (—◇—) and mean hourly river flow (—). The tidal results have been normalised relative to minimum low water.

In addition to water elevation, current velocity is commonly used in the calibration of hydrodynamic models (Hsu *et al.*, 1999). Velocity was not however routinely measured during the survey campaign in the Tweed. Uncles and Stephens (1996a) however estimate maximum tidal currents at the inlet of the Tweed (between stations 3 and 4) of 0.27 m s^{-1}. Uncles and Stephens (1997) also report current velocities between stations 5 and 6 and in the region of station 9. During their study, the Tweed river flow and tidal elevations ranged from 35 to 130 m^3 s^{-1} and 3.2 to 4.6 m respectively. The root mean square current velocities recorded between stations 5 and 6 varied between 0.22 and 1.43 m s^{-1} while that in the region of station 9 varied from 0.18 to 0.3 m s^{-1} and in a similar manner to tidal elevation showed a substantial reduction in the lower reaches of the estuary.

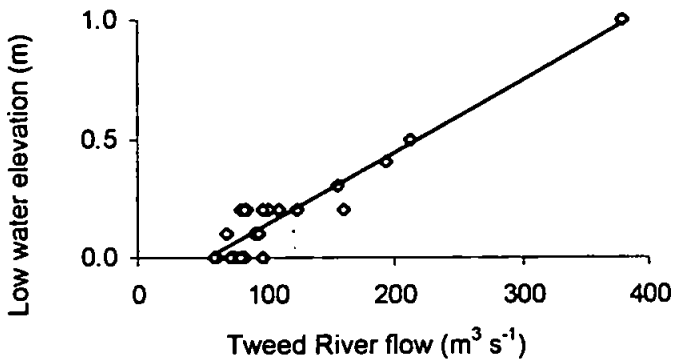

Figure 3.10 Linear regression of low water depth with river flow from stations 9 and 16. R^2 = 0.90 or 0.73 (n = 22, p = 0.001) if the data point recorded during the highest flow is omitted.

3.7. Estuarine width and cross-sectional area

How the width and hence cross-sectional area vary as water depth changes are important in determining the hydrodynamic characteristics of an estuary. The mouth of the Tweed is confined between the Pier head to the north and a sand spit to the south. The sand spit is exposed at low water and confines the inlet of the Tweed to approximately 50 m. In the vicinity of station 4 (Figure 3.7) the high water width is approximately 700 m and decreases to a width of about 80 m at the limit of tidal intrusion (Uncles & Stephens, 1996a). High and low water widths determined from Ordnance Survey maps are shown in Figure 3.11.

Some information on bathymetry was available from the Hydrographic Chart 1612 (Hydrographic Office, 1992), but this only provides information for the lower 3 km of the estuary. A longitudinal survey of deep channel depths was made by Uncles & Stephens (1996b) and the results are shown in Figure 3.12. This shows a series of deep holes in the

estuary that are immediately down estuary of bridges, but provides no indication of the cross-sectional area. No other published bathymetric data were available for the remainder of the estuary and tidal reaches of the river.

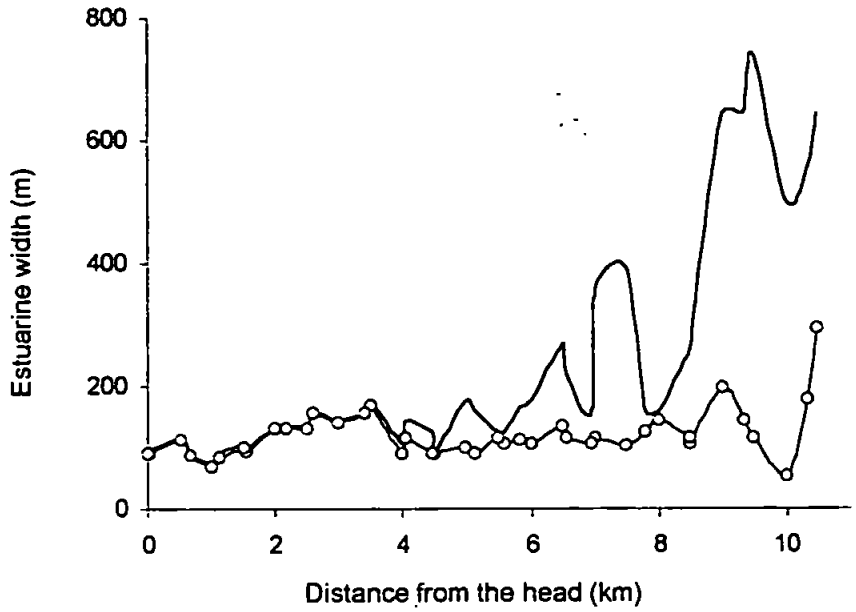

Figure 3.11 High (—) and low (-o-) water estuarine widths data from Ordnance Survey map 438.

In view of this, transverse sections of bed bathymetry were surveyed using an echo sounder and recorder aboard the LOIS semi-rigid inflatable boat. Bathymetric surveys were conducted on spring tides as near to high tide as possible. The boat was manoeuvred across the estuary at a constant speed perpendicular to the axis of the estuary typically moving from northern to southern banks. Where the boat was unable to complete a transect across the full width of the estuary due to insufficient water depth, the remaining distance was estimated and the bathymetry interpolated. Transects were performed between stations 4 and 20. A transect was not conducted at station 3 due to rough weather and the availability of bathymetry data from admiralty charts.

The vessel was not taken further up river than station 20 due to the problems of water depth and grounding. The bathymetry surveys required more time to complete than monitoring of standard suite variables and surveying had to be divided between two runs up the estuary. Transects were complete at even numbered stations on 7 February 1997 and at odd numbered sites on 5 April 1997. The echo sounder was calibrated using a sounding line and gave highly reproducible readings (R^2 = 0.98, n = 18, p = 0.001) for hard bottomed substrates. In a limited number of cases, the bottom consisted of fluid mud and

led to less accurate readings, as it was difficult to identify the water – sediment boundary with the sounding line. The Tweed Estuary is however, predominately hard bottomed and this was only encountered during the calibration procedure within the harbour area. Rapid fluctuations in depth due to wave swell were averaged out using a line of best fit and the bathymetry relative to the water surface is shown in Figure 3.13.

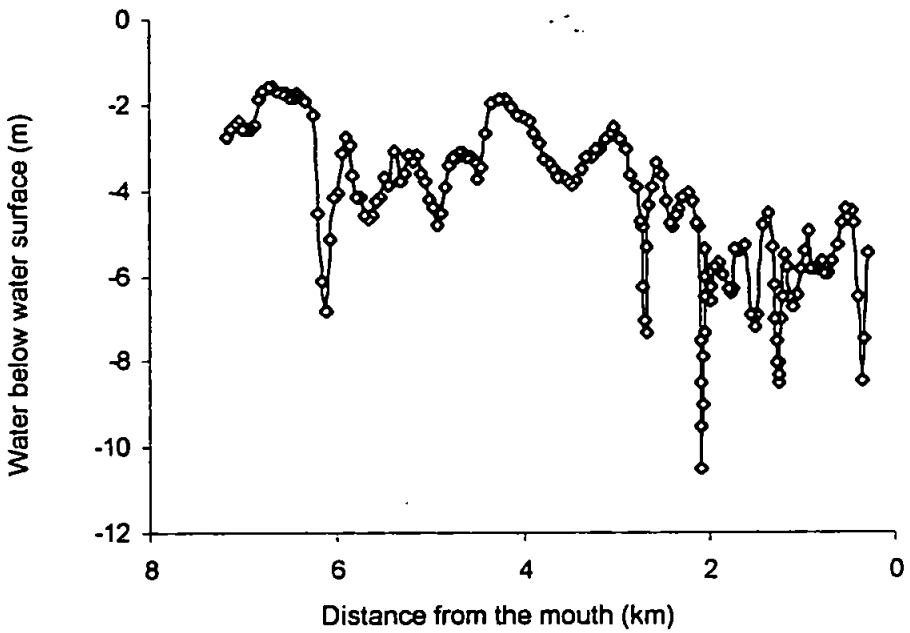

Figure 3.12 Deep channel depths in the lower 7 km of the Tweed Estuary (Uncles, 1996 *per. comm.*).

The variation in cross-sectional area was determined by dividing each bathymetry profile into slices of depth, d (0.5 m) as illustrated in Figure 3.14 and calculating the area within each slice according to Equation 3.1:

$$\text{Cross-sectional area of each slice} = (w_2 * d) + \left(\frac{b_1 * d}{2}\right) + \left(\frac{b_2 * d}{2}\right) \quad \textbf{(3.1)}$$

The areas of each slice have then be integrated and the results are plotted against total depth^2 in Figure 3.15 to derive the quadratic relationship expressed in Equation 2.11. This regression provides an R^2 value > 0.98 in over half the cross-sections and considering some of the uncertainties involved was deemed sufficient to describe the depth-area relationship through out the estuary.

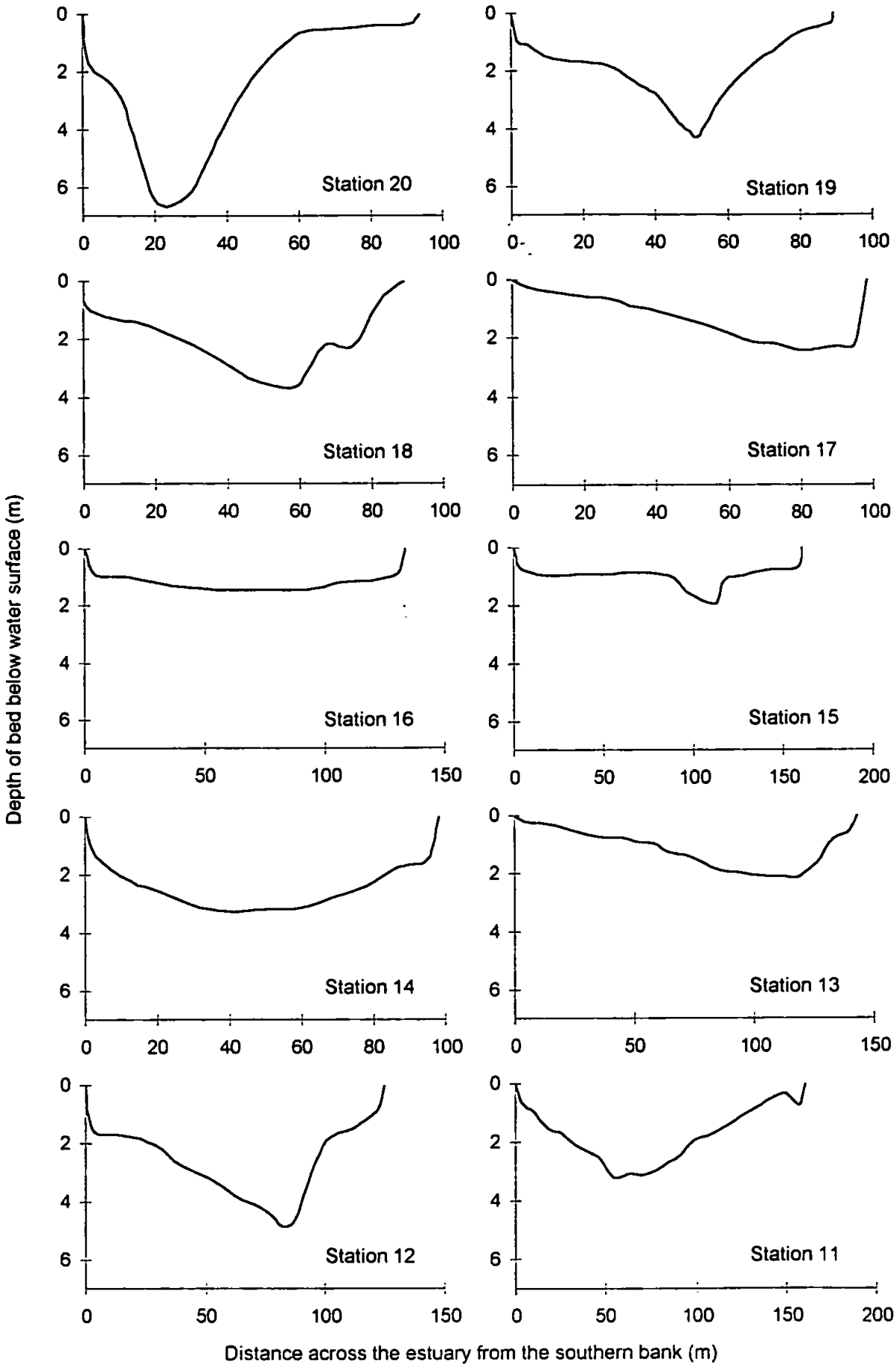

Figure 3.13 Bathymetry of the River Tweed relative to high water determined by echo sounder study.

Figure 3.13 Continued.

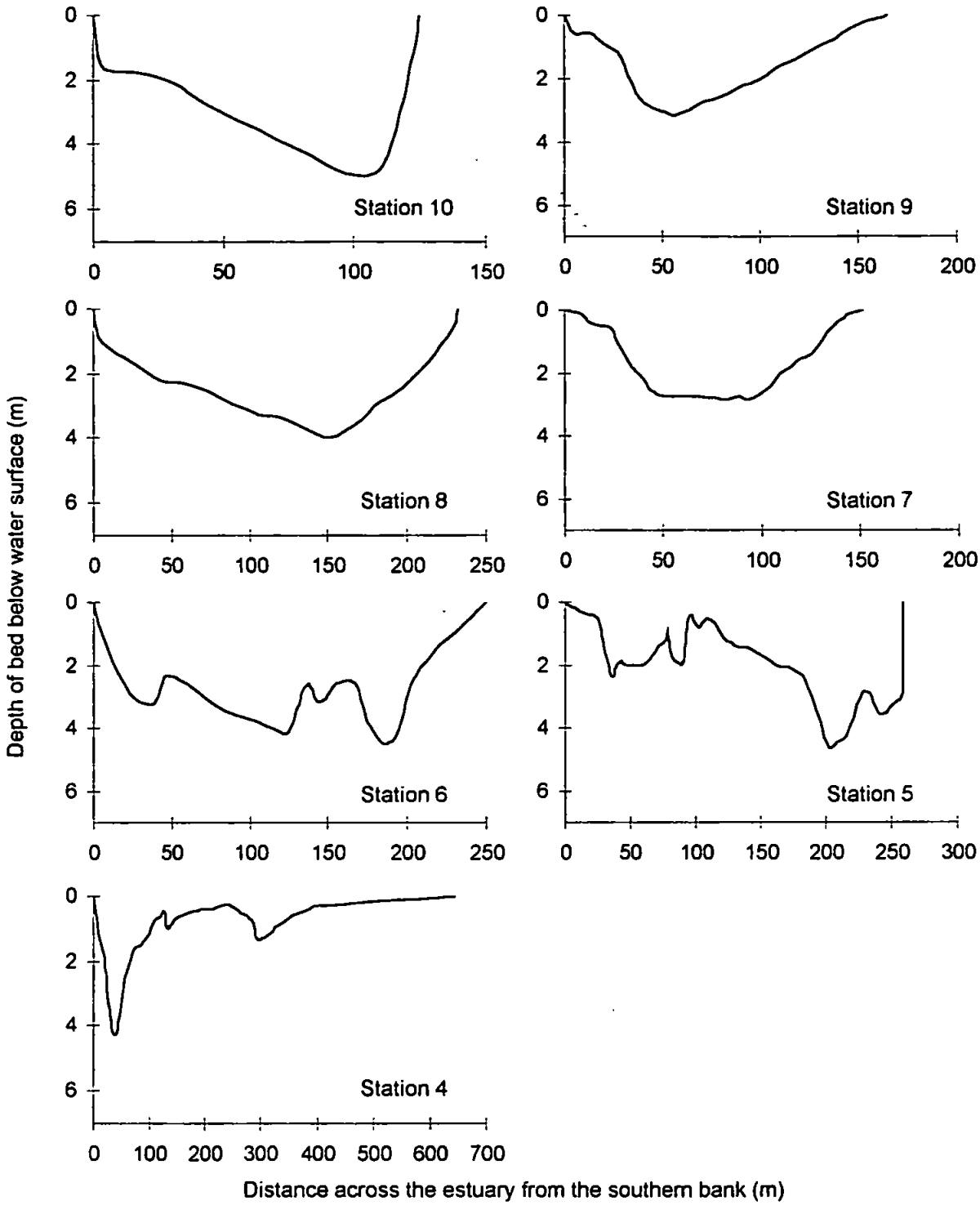

Where the cross-sectional area, A is related to depth, D employing the parameter x that is tabulated as a function of distance. The bed area was also calculated using the relationship:

$$\text{Bed area} = w_2 + \sqrt{b_1^{\,2} + d^2} + \sqrt{b_2^{\,2} + d^2} \qquad \textbf{(3.2)}$$

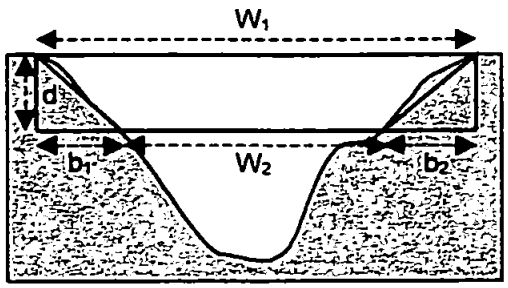

Figure 3.14 Division of estuarine cross-sectional area into 0.5 m slices to calculate cross-sectional area as a function of water depth.

where in this instance w_2 represents the estuarine bed. Figure 3.16 shows how the high water cross-sectional and bed area changes along the estuary. By multiplying these areas by segment length the high water volume of the Tweed Estuary between stations 3 and 20 was estimated as 3.4×10^9 l and the total bed area as 1.9×10^6 m^2.

If tidally averaged depths are used, a volume, V, of 2.0×10^9 l is derived. At flows, Q, of 20, 80 and 200 m^3 s^{-1} the associated flushing times were 28, 7 and 3 hours respectively. Uncles & Stephens (1996b) calculated for typical freshwater inflow of the Tweed an associated residence time of varying from 12 to 24 h during spring and neap tides respectively. Balls (1994) also estimated the flushing time and quotes values varying from between 22 to 67 h depending on river flow. Even though these estimates vary it is obvious that the Tweed is rapidly flushed and this may have important consequences for chemical reactions that occur over the order of hours or longer.

3.8. Salinity intrusion in the Tweed

The Tweed Estuary ranged from partially mixed to stratified depending on tidal state and freshwater inflow, and saline intrusion is a strong function of the spring-neap tidal cycle (Uncles & Stephens, 1996b). Under stratified conditions in the lower estuary, areas of high salinity water abut onto waters of much lower salinity, with the formation of a front often characterised by a distinct foam line. This front represented the leading upper edge of a salt wedge. Under fairly low flow (35 m^3 s^{-1}) and a spring tidal range of 4.7 m Uncles & Stephens (1996a) found that the salt wedge (salinity >30) moved more than 1 km up estuary by 2.6 h after low water and that the halocline was about 1 m thick. By 3.3 h after low water the salt wedge had advanced a further 1 km. The advancing salt wedge pushed the lower salinity surface waters as a buoyant plume back up the estuary. In addition to vertical stratification this resulted in transverse variations in salinity

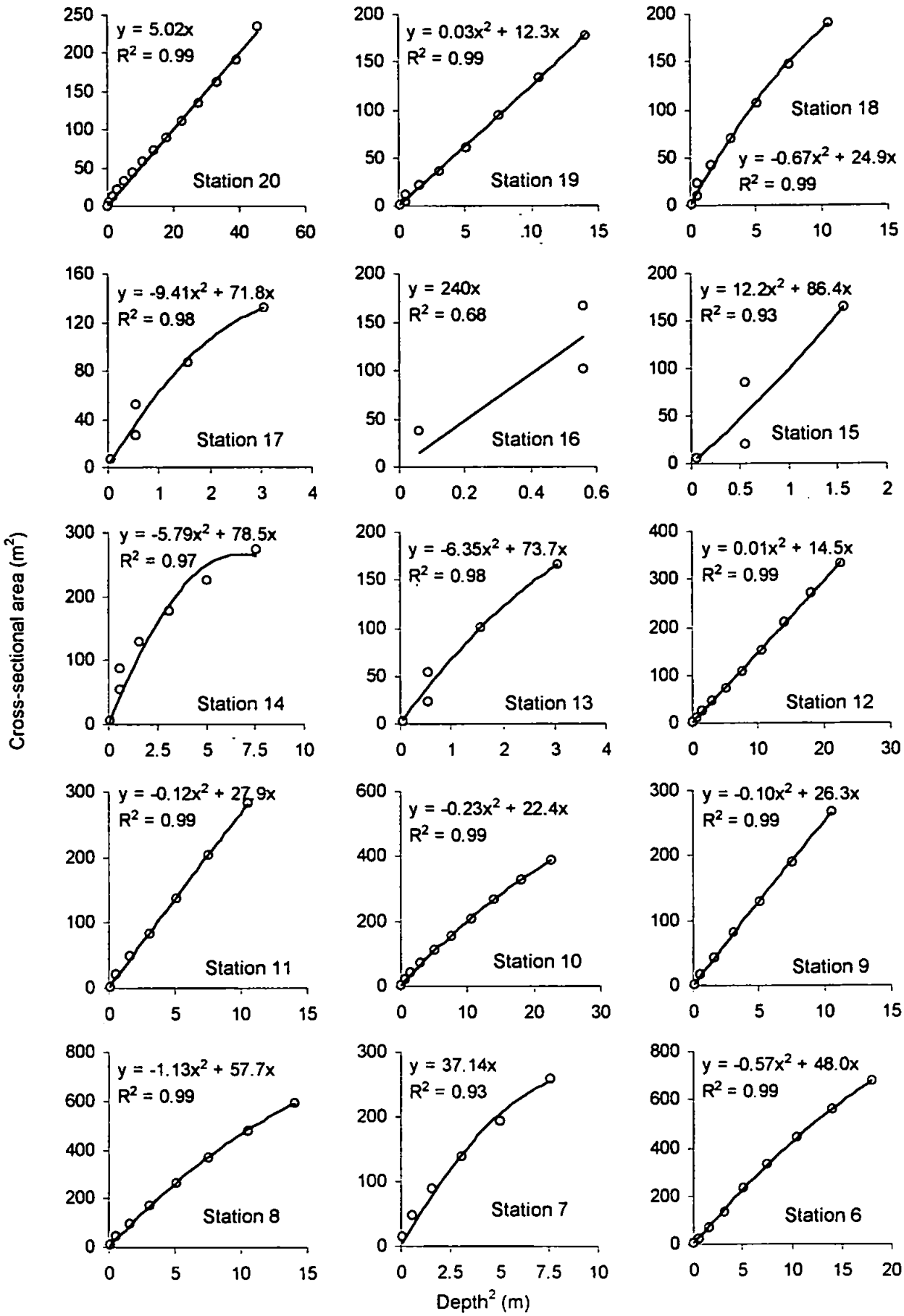

Figure 3.15 Quadratic depth-area relationship determined from Tweed Estuary cross-sectional areas.

Figure 3.15 continued.

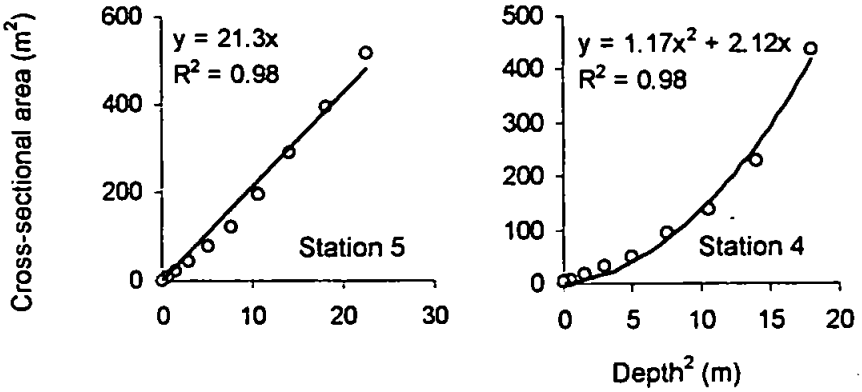

in the lower reaches as lower salinity surface waters were forced to the edges of the main channel where these abutted wide flanking shoals.

3.8.1. Axial variation in salinity

Uncles & Stephens (1996b) observed that salinity intrusion varied from 4.7 to 7.6 km from the mouth during their field work period and Uncles *et al.* (2000) found that variation in river flow could explain 80 % of the variation the location of the surface freshwater saltwater interface. The surface salinity profiles recorded during the LOIS field work campaign are shown in Figure 3.17. Surface saline intrusion varied from a maximum of 8.2 km on the 17 July 1996 during a low flow of 14 $m^3 s^{-1}$ and a spring tide of 4.4 m, to a minimum on the 9 December 1996 during flows of 304 $m^3 s^{-1}$ with a similar tidal range, when a maximum surface salinity of 0.13 was measured at the mouth of the estuary.

Between these two extremes the axial profiles show a range of features that not only indicate the physical variability of the estuary in response to tidal and river flow forcing, but are also influenced by the surveying protocol. This is important as the time that the survey was conducted relative to high water and the direction of the sampling must be considered when interpreting the results and comparing these to model predictions. For instance during September 1996 the second axial survey was started 1.85 h before high water and the limit of saline intrusion was reduced by about 2.3 km compared to a subsequent survey conducted later in the tide cycle under similar flow conditions with a smaller tidal range. Conversely, results gained during consistent times and conditions in August 1997 show similar profiles.

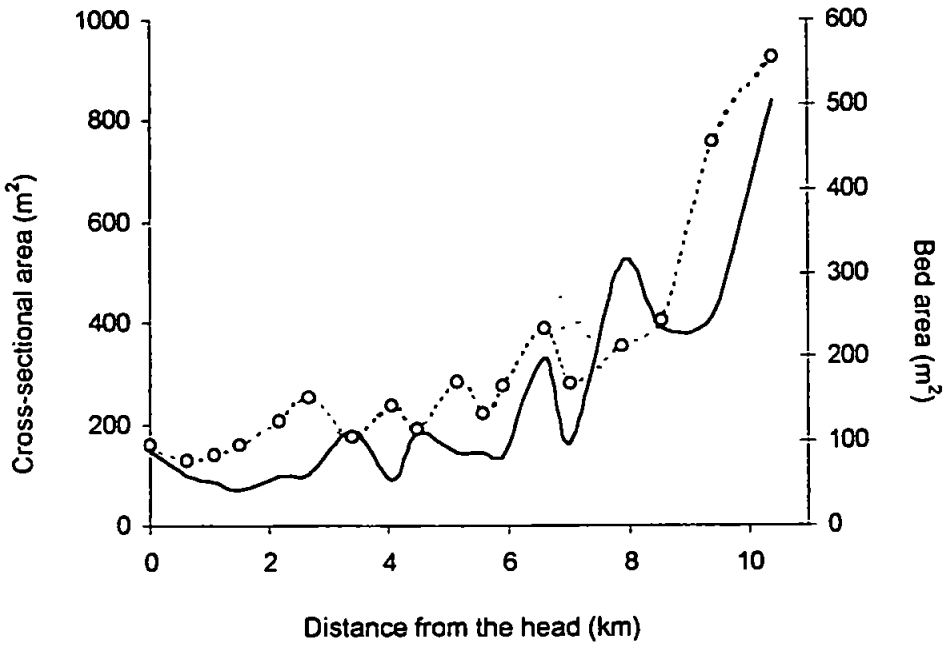

Figure 3.16 Cross-sectional (—) and bed area (-o-) between stations 3 and 20 in the Tweed Estuary.

In May 1997, there is an obvious reduction in saline intrusion in response to an increased flow from 21 to 78 $m^3 s^{-1}$. Only considering the mean daily flow fails to take account of the history of the hydrograph and Figure 3.5 showed that the flow on the preceding day was 109 $m^3 s^{-1}$ and may still have had some influence of the hydrodynamics of the estuary. The effect of increased tidal range on saline intrusion can be seen in June 1997, where under similar flows an increase in tidal range from 3.6 to 4.1 m led to an increased salt wedge intrusion of approximately 1 km. Uncles & Stephens (1996b) note the importance of the spring-neap variation in tidal range on saline intrusion. Only one survey was conducted during neap tides, September 1997 with a tidal range of 1.9 m. Even though the river flow was low (19 $m^3 s^{-1}$) the saline intrusion was greatly reduced and was more reminiscent of flow of the order of 80 to 100 $m^3 s^{-1}$ under spring tidal conditions.

A rapid increase in surface salinity from 20 to 25 to < 5 in 1.1 to 1.7 km was recorded in August 1997 as the survey vessel passed the upper edge of the salt wedge. A similar rapid increase in surface salinity over 0.7 to 1.5 km also occurred in June 1997. The salinity stratification was calculated as the difference between surface and bottom salinity and is plotted in Figure 3.18.

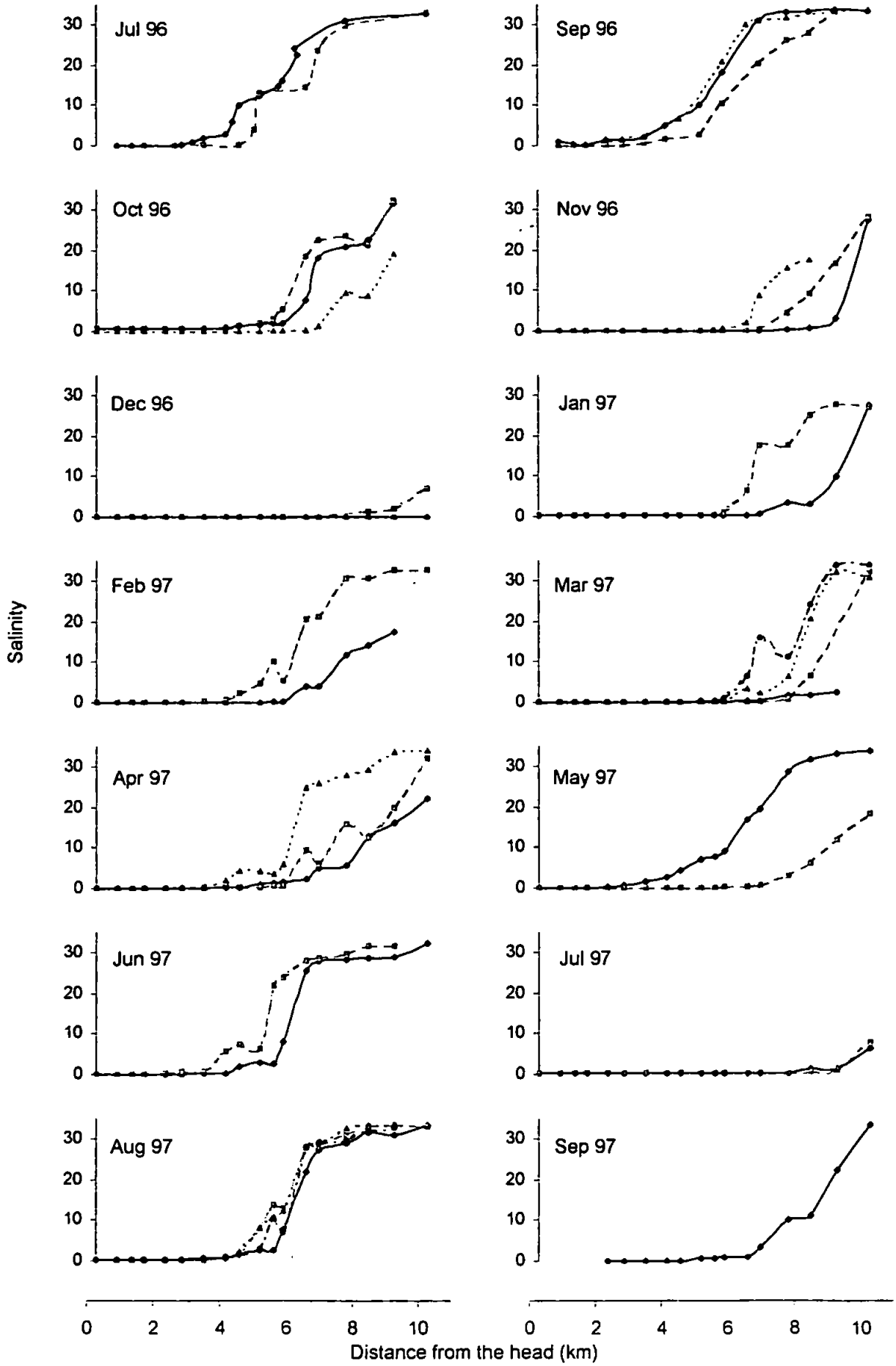

Figure 3.17 Axial profiles of salinity in the Tweed Estuary. The surveys are plotted chronologically as 1st (◆), 2nd (■), 3rd (▲) and 4th (--) profile per survey.

Figure 3.18 shows differences between surface and bottom salinity that can be up to 32 units. The maximum stratification is situated at the toe of the advancing salt wedge behind which the water is well mixed. The June and August data showed a localised region of stratification and very sharp change in the axial profile while the May axial profile was more drawn out and the stratified tip of the salt wedge was also more diffuse. The May, June and August surveys were conducted under similar flow and tidal conditions and were all sampled in the down estuary direction at comparable times relative to high water. There was also no significant difference in mean daily wind velocity and direction and it therefore difficult to explain these difference. They probably arise due to the cumulative effects of small difference in sampling time, flow, tidal elevation and wind speed further

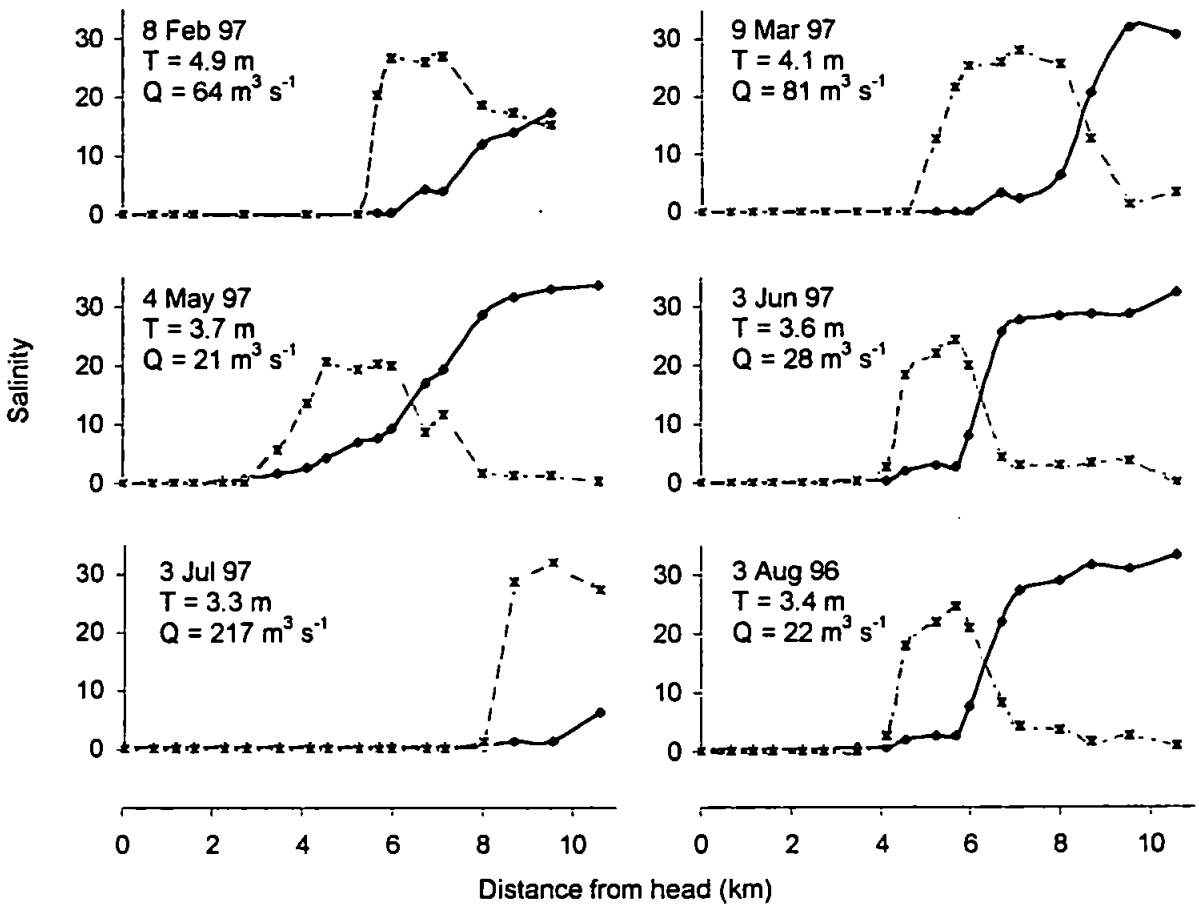

Figure 3.18 Comparison of surface salinity profile (—) with salinity stratification (---), *i.e.*, the difference between surface and bottom salinity. The tidal range (T) and Tweed mean daily flow (Q) are shown.

illustrating the difficulties in understanding and hence modelling a highly dynamic system. The February data showed the effect of a moderately high flow combined with a high spring tide. The limit of saline intrusion was reduced as was the surface salinity at the mouth (~17). In comparison to the other surveys illustrated there was still a high degree of

stratification in the lower part of the estuary. The bottom water of salinity 30 to 32 had propagated up to nearly 4 km from the mouth while a significant proportion of the freshwater flow passed over the salt wedge. In this instance, entrainment and mixing had led to increased salinity, while Figure 3.17 showed that during the high flows in December 96 and July 97 almost the entire surface flow consisted of freshwater.

A localised reduction in surface salinity in the region of the confluence with the Whiteadder can be seen during the February 1996 and April, June and August 1997 surveys. It is hard to relate this to particular flows in either river and probably occurred when the salt wedge penetrates into the mouth of the Whiteadder and under low dispersion conditions a buoyant flow from the tributary entered the main channel of the estuary. Some of the other variability may have arisen due to lower salinity water collecting at the flanks of the estuary as observed by Uncles & Stephens (1996a). Uncles & Stephens (1996b) also noted pooling of saline waters into deep holes in the estuary. Entrainment of this water may then lead to localised variations in salinity.

3.8.2. Salinity variation over a tidal cycle

Results which are easier to interpret are those from the anchor station illustrated in Figure 3.19. These show the wide range in surface salinity at a site only 1.9 km from the mouth. The April, June and August 1997 surveys were conducted under relatively low flows (MDF = 22 to 35 $m^3 s^{-1}$) and salinity reached 33 during the tidal cycle. Conversely, the flows during October to December 1996 and January and July 1997 were higher (MDF = 79 to 227 $m^3 s^{-1}$) and surface salinity was very low or zero during the majority of the tidal cycle. Comparing the observations to mean daily flow produces two anomalies; February and May 1997 both of which have high flows, (MDF = 248 and 109 $m^3 s^{-1}$ respectively), but both of which also show a wide salinity range. Although the tidal range in February was larger than during the other surveys it is unlikely to have had such a significant effect and the May tidal range was below the spring tidal mean. If we consider the quarter hourly flow, see Figure 3.20 it becomes obvious that the daily means are an overestimate of the flow prior to high water.

The increase in salinity measured at station 5 lagged behind the predicted increase in tidal elevation at the mouth by approximately 3 hours. The salinity then increased gradually up to approximately 5 units over the period of an hour then rapidly increased to full marine

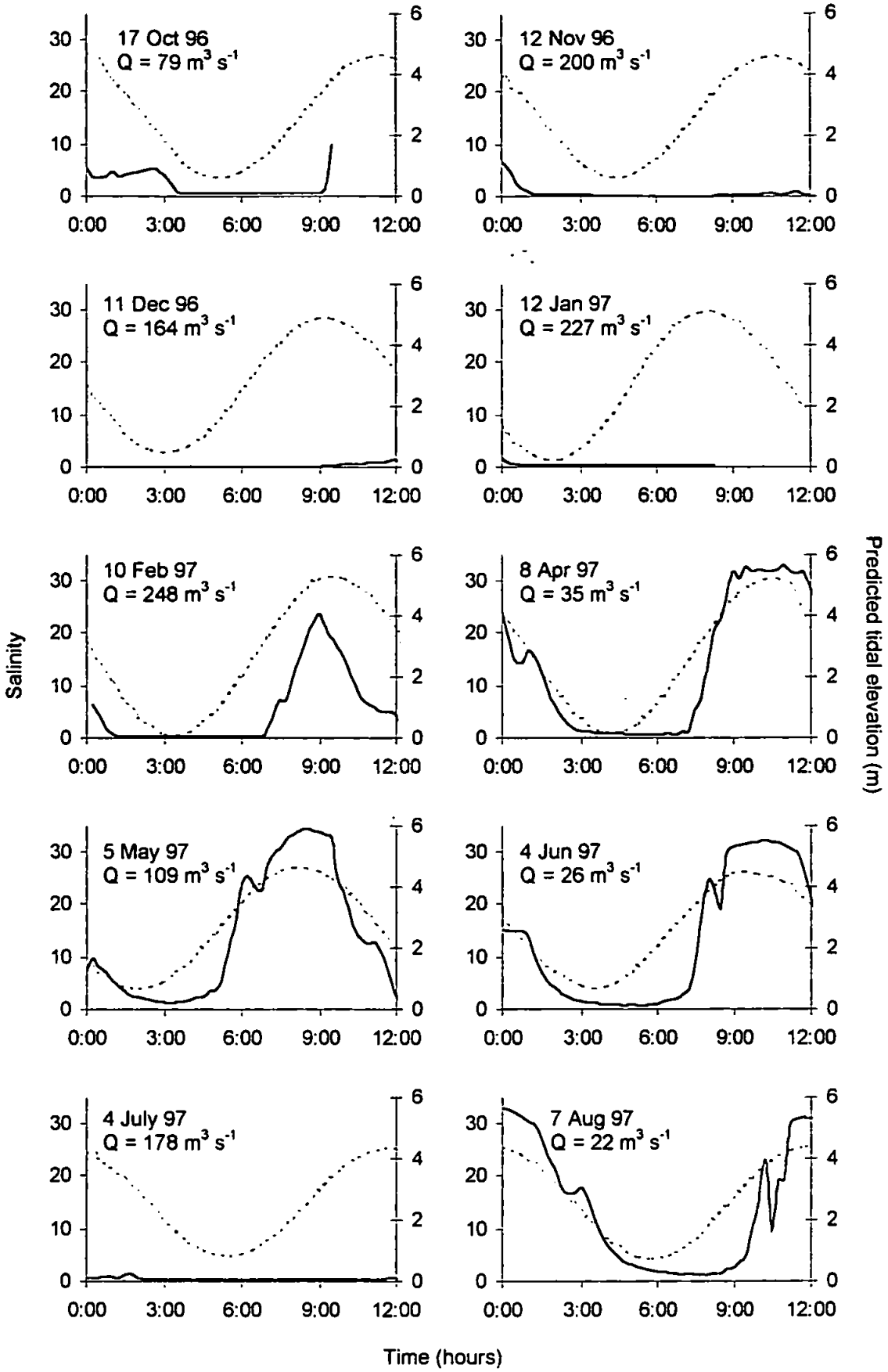

Figure 3.19 Surface salinity (—) recorded during the anchor station surveys at station 5. The predicted tidal range (Hydrographic Office, 1989) at the mouth is also shown (----) and Q is the mean daily flow of the Tweed.

salinity in approximately 3 hours. Increased river flow had the effect of increasing the lag time not only reducing surface salinity, but also reducing the period over which salinity was at its maximum.

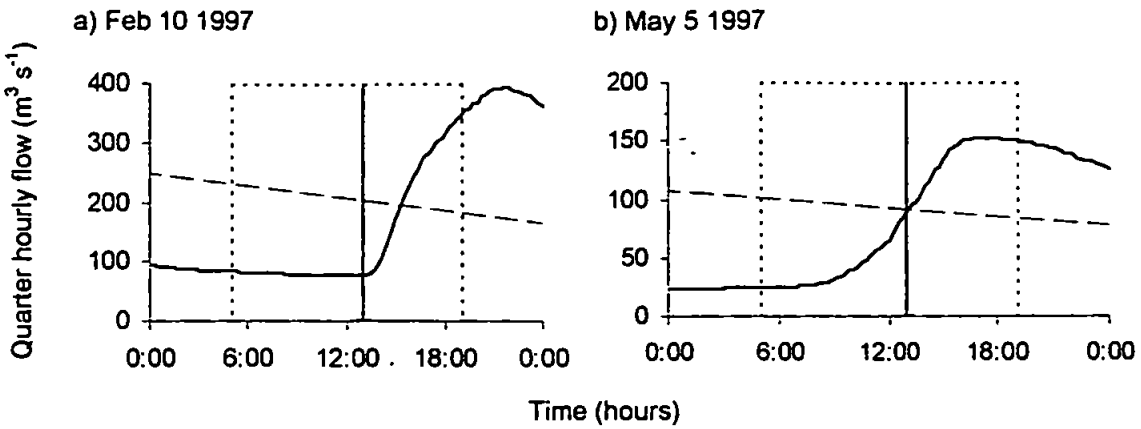

Figure 3.20 Quarter hourly flow of the Tweed during the a) February and b) May 1997 anchor station surveys (—) compared to the MDF (— —). The dashed box indicates the period during which the survey was conducted while the solid line indicates time of high water.

3.9. Suspended solids in the Tweed Estuary

A sediment flux of 5 x 10^4 T yr^{-1} through the Tweed Estuary catchment has been estimated according to the equation devised by Wilmot & Collins, (1981). The Tweed has a relatively large river flow for its catchment size and correspondingly low suspended sediment concentrations. If we assume an annual discharge of 2.4 km^3 yr^{-1} the mean suspended sediment concentration of Tweed river water is approximately 18 mg l^{-1}. Balls (1994) observed SPM concentrations in the range of 2 to 20 mg l^{-1} while Uncles & Stephens (1997) and Uncles *et al.* (2000) observed a slightly wider range of turbidity (2 to 30 mg l^{-1}). In rivers, suspended sediment concentrations increase rapidly with flow and values between 100 to 300 mg l^{-1} are reported for the Tweed during high flow (Robson *et al.*, 1996; Neal *et al.*, 1997; Bronsdon, & Naden, 2000).

It is then important to consider how this particle load is transported through the estuary. This will depend on the density of the sediment particles that determine its settle rate and hence probability of deposition and the tidal and river flow characteristics of the estuary. Walling *et al.* (2000) found that in the lower Tweed 97.5 % of suspended sediment particle were < 63 μm. The estuary is however characterised by a lack of fine grained bed sediment thorough out the system compared to a range of other macro-tidal estuaries. Uncles & Stephens (1997) and Uncles *et al.* (2000) noted conservative behaviour of turbidity at

salinities <30 and there are no reported observations of a turbidity maximum zone. The tidal elevation data showed that tides in the Tweed were relative symmetrical and that it is therefore unlikely to experience significant tidal pumping of fine grained sediment up estuary. This coupled with a short flushing time and periodic high flows that flush sedimentary material out of the estuary prevent the accumulation of significant quantities of bed sediment. Turbidity in the estuary will therefore be primarily controlled by the particle load carried in with either sea or river water.

3.9.1. Axial variation in turbidity

The turbidity concentrations measured during the EATs are shown in Figure 3.21. During low flow conditions, values were typically low (2.5 to 5 mg l^{-1}) and relatively consistent through out the majority of the estuary, *e.g.*, August, 1997. As flows increased, turbidity of the river increased (5 to10 mg l^{-1}), *e.g.*, January and July 1997 and May 1997 showed an increase in river turbidity from 6 to14 mg l^{-1} between the two surveys. Multiplying the turbidity measured at station 20 with the MDF has been used to generate mean sediment flux estimates for each of the survey periods, see Figure 3.22. If the mean turbidity from these measurements (5.4 mg l^{-1}) is extrapolated over a year using the average MDF (78 m^3 s^{-1}) an annual sediment flux of 0.13 x 10^5 T yr^{-1} is derived. This is approximately 25 % of the predicted sediment flux using the method of Wilmot & Colins (1981). This underestimation may arise due to the assumption that particle flux varies linearly with water flow and does not account for the fact that particle flux must increases faster than the water flow.

Although a mid-estuarine turbidity maximum zone is absent elevated levels of turbidity are observed at the mouth during September to December 1996 and February to April 1997. The region of the Tweed between stations 3 and 5 is characterised by broad shallow bathymetry and sandy bed sediment. In their study Uncles & Stephens (1997) found that wave swell explained over 90 % of the variation in turbidity at the mouth and recorded near-mouth turbidities of 28 and 16 mg l^{-1} associated with onshore winds of 091° and 064°. Comparing the turbidity data with wind velocity and direction showed that in September 1996 winds speeds were moderate (10 to11 knots), but onshore between 50 to 120°. In other instances the winds may not have been onshore, but were apparently sufficiently strong to resuspended bed sediment, *e.g.*, November and October 1996 and February 1997. A consistent relationship could not however be identified in April 1997.

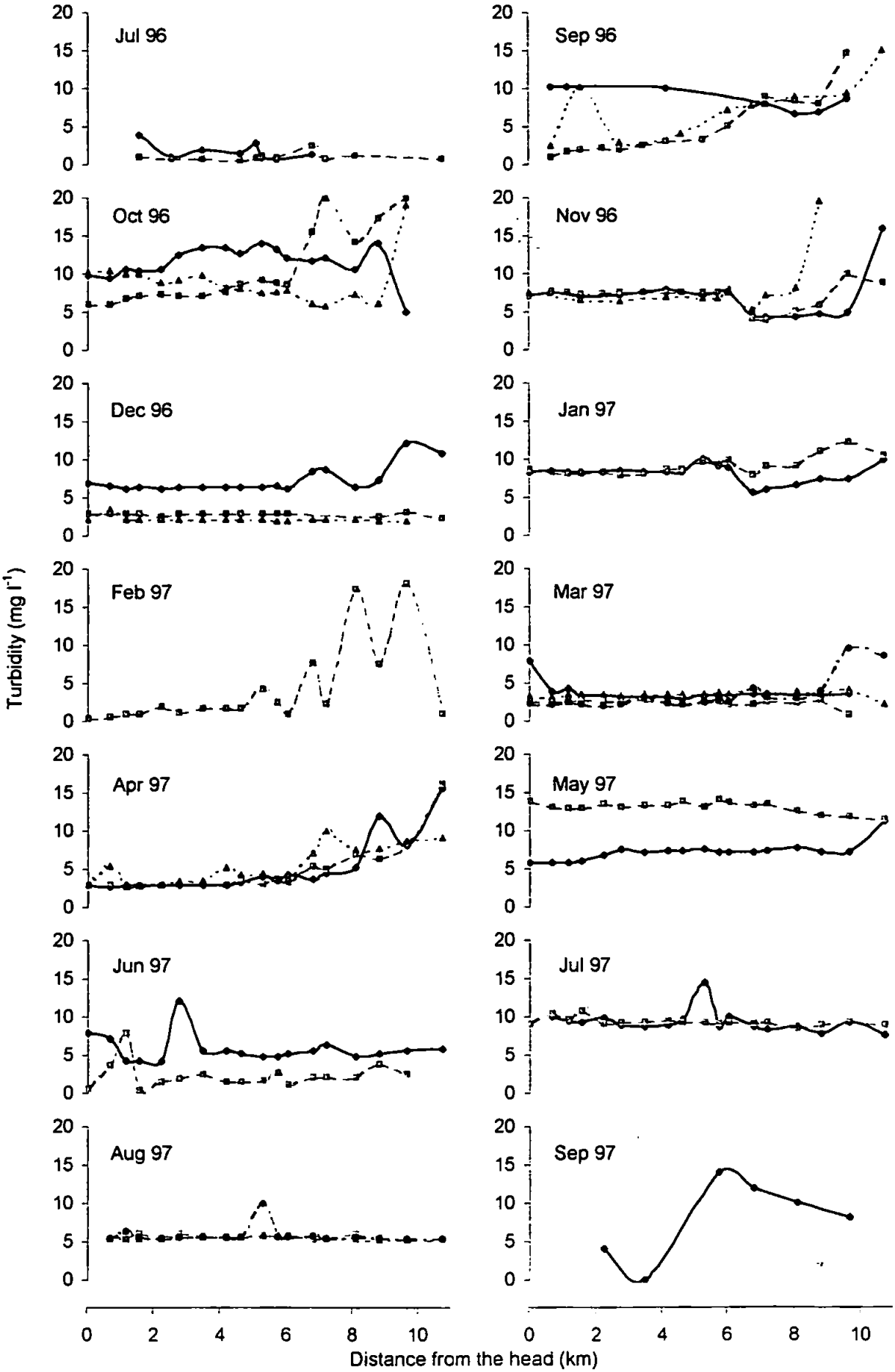

Figure 3.21 Axial profiles of surface turbidity in the Tweed River Estuary.

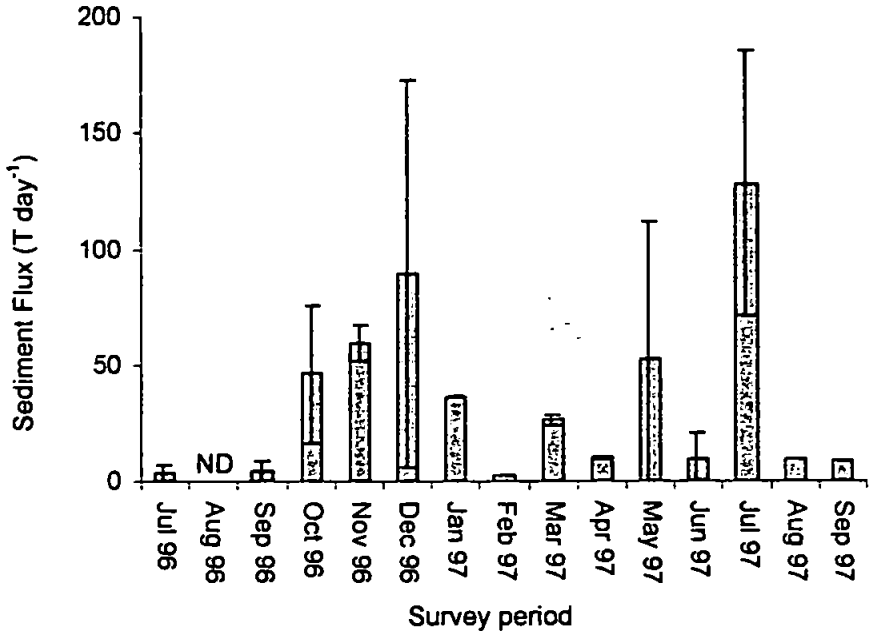

Figure 3.22 Mean and standard deviation of the daily sediment flux during the survey periods. Calculations based on the turbidity measured at station 20 and the MDF. No data was collected in August 1996.

3.9.2. Turbidity variation over a tidal cycle

The turbidity data recorded during the anchor ranged from 1 to 264 mg l^{-1} and is shown in Figure 3.23. With the exception of May and July 1997 surveys the mean concentrations recorded during the survey were comparable to those measured during the extended axial transects on preceding or subsequent days and for examples concentrations are low and consistent during December 1996 and February and August 1997.

In November 1996 and April and June 1997 peaks in turbidity occurred during mid ebb tide when concentrations increased from 10 to 25, 13 to 28 and 5 to12 mg l^{-1} respectively. This may represent the flushing of material out of the estuary as water velocity increased during the ebb tide. With the exception of the initial ebb tide, surface salinity during the November survey remained below 1. There was however, a rapid increase in turbidity from 7 to 56 mg l^{-1} just after high water and this is likely to represent changes in the freshwater turbidity not tidal flushing. Hourly flow data peaked at approximately 250 m^3 s^{-1} 2 to 3 hours before the increase of turbidity occurred at station 5. The increased turbidity probably relates to the transport of material out of the local catchment and head of the estuary in response to this rising hydrograph. High turbidity associated with low salinity water also occurred during October 1996 when there was an increase in turbidity during low water.

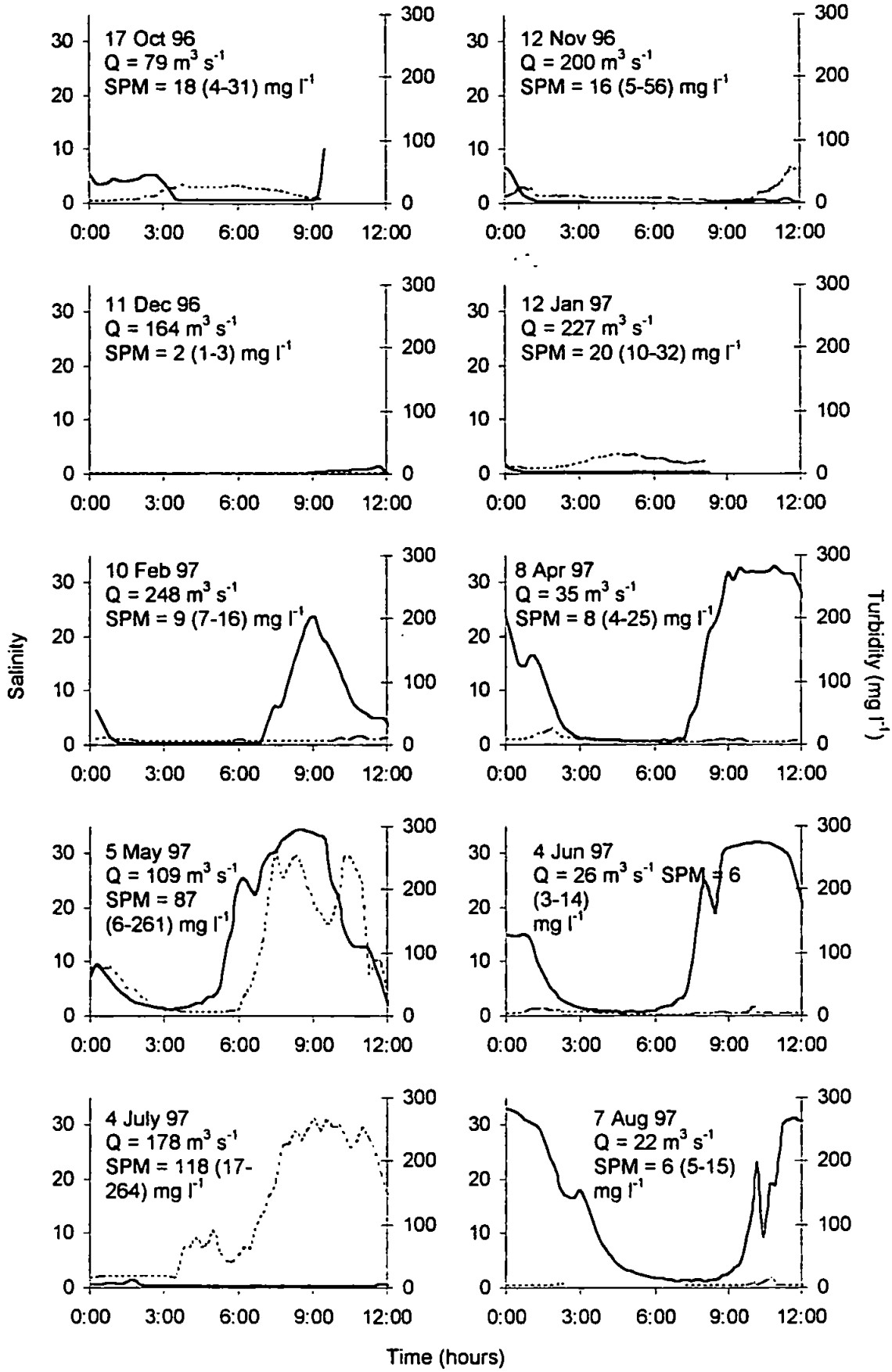

Figure 3.23 Surface salinity (—) and turbidity (—) recorded during the anchor station surveys at station 5. The mean daily flow of the Tweed (Q) and the mean concentration and range of turbidity are also shown.

During January, May and July 1997 surveys turbidity increased during the flood tide from 10 to 32, 11 to 261 and 40 to 264 mg l^{-1}. This was not however observed during the extended axial surveys. The January survey was conducted on a rising hydrograph after 10 days of flows between 52 to 65 m^3 s^{-1}. The May survey was also conducted during a period of rising flow after 19 days of low flows between 18 to 25 m^3 s^{-1}. In a similar case to November this probably represents the initial flushing of material out of the estuary as flow increased. The higher turbidity occurred in May because of the long period of low flows during which both biogenic and lithogenic material can accumulate in and around the water ways of the catchment.

The July survey was conducted on a falling hydrograph after 6 days of flow rates between 130 to 240 m^3 and 4 days after maximum flood. The suspended sediment pulse probably passed through the estuary 1 to 2 days prior to the axial surveys which showed that the estuary is dominated by freshwater and that turbidity is approximately 10 mg l^{-1} though out the system. The suspended load may then become deposited in the broad shallow region between station 5 and 3 as flow velocity decreased. The increased turbidity on the flood tide probably represented the resuspension of this material into the low salinity water overlying the shallow areas to either side of the main channel which is then carried back in on the advancing tide.

3.10. Summary

The estuary was relatively shallow at any point and the cross-sectional area varied as approximately the square of the tidally variable water depth. The estuary was shown to respond rapidly to changes in river flow and tidal state and a maximum saline intrusion of 8.2 km from the mouth was recorded as was salinity stratification of up to 32 units. No turbidity maximum was observed in surface waters and suspended sediment concentrations were low (< 10 mg l^{-1}) and often invariant through the estuary. Evidence of brief, but higher (264 mg l^{-1}) turbidity was however found. The data collected has provided an invaluable source for the calibration and verification of the ECoS hydrodynamic model of the Tweed presented in the Chapter 4.

Chapter 4

Calibration & validation of the hydrodynamic model

4 Calibration & validation of the hydrodynamic model

The field data showed that the Tweed Estuary is a rapidly changing system. For a model to reproduce this it must be capable of fine spatial and temporal resolution. Tidally averaged scenarios are not therefore considered appropriate and a tidally resolving hydrodynamic model, as opposed to one based on cubature calculations potentially provides a more realistic representation of movement of water in a tidal system. It also provides distinct stages in model development each of which can be tested separately and the problems associated with each step identified.

Calibration is an iterative process designed to tune the model output so that it matches a set of observed data (Hess *et al.*, 1999). The model results should then be compared to an independent data set to identify errors in the equations or parameters used. Agreement between modelled and observed results does not necessarily indicate that all relevant processes have been included or correctly described (Oreskes *et al.*, 1994). It is therefore important that during the validation stage that the model performance be assessed and if a model is to be used for assessment purposes some measure of the uncertainty in model output must be included (IAEA, 1989). There is however no widely accepted method to calibrate and validate numerical models of estuarine hydrodynamics and predictions of estuarine transport are often reported with little explanation of which coefficients have been tested and adjusted. The calibration and validation of the numerical model was therefore conducted using the recommendations of Hsu *et al.* (1999).

The modelling process has been divided into distinct stages and calibration and validation at each stage is discussed. Firstly the calibration and validation of tidal propagation through the estuary, determined by tidal range and river run off will be considered. Secondly modelling the distribution of salinity will assess the advection-dispersion of a conservative tracer. Finally the advection-dispersion of suspended particulate matter in the estuary will also be considered.

4.1 Predicting tidal range at the mouth

The two main driving variables in determining the volume and movement of water in an estuary are the river flow at the head of the estuary, together with tributaries, and the tidal elevation at the mouth. The river flow is monitored on the Tweed and Whiteadder rivers and has been discussed in Chapter 3. Tidal elevation is not however routinely

recorded at the mouth of the Tweed, although some measurements were made during the surveys of the estuary, see Figure 3.11.

Berwick-upon Tweed is not a standard port for tidal prediction purposes and times and heights of high and low water are related to those for North Shields on the Tyne Estuary, approximately 100 km to the south (Hydrographic Office, 1989a). The tidal ranges at the mouth of the Tweed and at North Shields are shown in Table 4.1. The times of high and low water compared to North Shields are -53 minutes and -1 hour 9 minutes respectively.

Table 4.1 Spring and neap tidal data for North Shields on the Tyne Estuary and Berwick-upon-Tweed (Hydrographic Office, 1989a).

	Z_0 (m)	MHWS (m)	MLWS (m)	Spring tidal range (m)	MHWN (m)	MLWN (m)	Neap tidal range (m)
North Shiels	2.91	5.0	0.7	4.3	3.9	1.8	2.1
Berwick	2.53	4.7	0.6	4.1	3.8	1.3	2.5

Mean sea level-Z_0, Mean high water springs-MHWS, mean low water springs-MLWS, mean high water neaps-MHWN and mean low water neaps-MLWN.

Six harmonic constituents are supplied by the Hydrographic Office for tidal predictions in standard and secondary ports and those reported for the Tweed are shown in Table 4.2.

Table 4.2 Tidal frequency and amplitude for the Tweed Estuary (Hydrographic Office, 1989a). No data is available for the M_4 and M_6 over tides.

Harmonic Constant	M_2	S_2	K_1	O_1
Frequency, T_F (° hour^{-1})	57	118	202	88
Amplitude, T_A (m)	1.60	0.51	0.04	0.07

Using these harmonic constants Tidecalc V1.1 (Hydrographic Office, 1992b) was used to generate hourly values of tidal elevation throughout each survey period (Figure 4.1). These results were tabulated as a time series and were used to provide the tidal elevation boundary condition in the model. This provided a more convenient method of incorporating date and time specific tidal elevation than either the 2 or 6 tidal component templates in ECoS3. The method for generating time specific astronomical angles and associated tidal ranges is presented by Schwiderski (1983) and although not approached during this project would provide a useful addition to the ECoS templates supplied with the software.

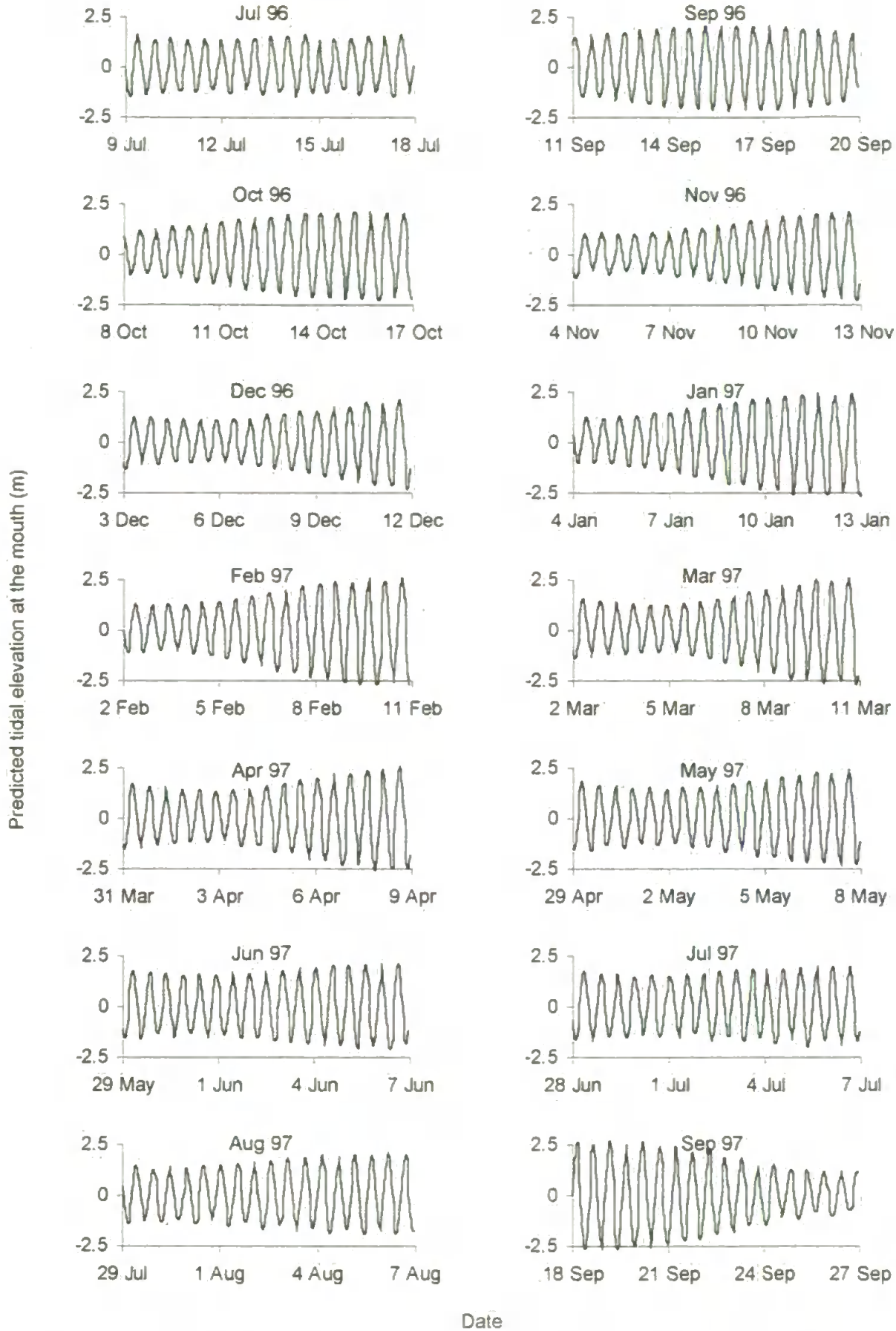

Figure 4.2 Tidal elevation at the mouth of the Tweed Estuary predicted using Tidecalc V1.1 (Hydrographic office, 1992b)

4.2 *Predicting tidal propagation through the estuary*

The hydrodynamic and tidally variable cross-sectional area templates (Harris & Gorley, 1998b) were used during model set-up as described in Chapter 2. The model was driven by mean daily flows of the Tweed at the head of the estuary and mean daily flows of the Whiteadder which was defined as a transfer into the estuary at 5.5 km from the mouth.

In tidal rivers where the bottom elevation rises gently and the tidal limit is determined by tidal range and river flow, the model boundary should be set beyond that of the tidal limit (Hsu *et al.*, 1999). The normal tidal limit of the Tweed Estuary is approximately 13 km from the mouth (Uncles & Stephens, 1996b), but field data was only available for a distance of 10.5 km from the mouth. The ECoS model of the estuary was therefore extended beyond the survey area by an additional 2 km (*i.e.*, to 12.5 km). The model was also extended seaward beyond station 3 by 0.6 km. This has the advantage of providing more stable boundary conditions for other model parameters, *i.e.*, salinity, which can be quite variable in the mouth of an estuary. Riverine input of water and sediment was encoded as a transfer across a closed boundary. Salinity was however encoded as an open boundary with a set value because there was insufficient data to determine the variation in depth averaged salinity at the marine limit of the model. The 13 km of the estuary covered by the model was divided into 35 segments each of 371.4 m length. The segment length was kept as small as possible in relation to the time step to prevent the generation of numerical dispersion. This segment length required a time step of 43 seconds (*i.e.*, 5 x 10^{-4} days) to maintain numerical stability and the calculations were solved using an UPWIND implicit scheme. Computational time increases dramatically as the time step was reduced, increasing by a factor of 3 as the time step was reduced from 20 to 10 seconds. The increased computational time was felt sufficient to limit further reduction in the segment length.

4.1.1 Bathymetry and cross-sectional area

The tidally variable cross-sectional area of the model was defined by two tables, observed bathymetry in relation to a mid-tide datum and the relationship of area to depth as described in Section 3.7. The cross-sectional areas showed the bathymetry of the Tweed to be variable with an asymmetrical profile particularly at stations 17, 10, 9 and 4. Additionally, the maximum water depth did not decrease in a simple manner up the estuary. The cross-sectional areas intercepted several deep regions in the upper part of the

estuary, *i.e.*, a maximum water depth of approximately 7 m under the bridge at station 20 and a series of deep holes in the lower estuary were also noted by Uncles & Stephens (1996b). Preliminary model set up had shown that the tidal propagation up the estuary was highly sensitive to changes in bathymetry. In a sectionally averaged model an appropriate value for the bathymetry and relationship to the mid-tide datum needs to be defined. Hsu *et al.* (1999) used a smoothed longitudinal profile of bathymetry, but under what criteria this was defined is unclear. The method developed in this work was to use the tidal elevation measurements at stations 9, 16 and 20 to correct the water depth measured at high water to that of a datum defined as the mid-tide. To ensure that the water represented a level surface within the tidal limit of the estuary reference could only be made during high and low water slack periods.

In a one dimensional model, bathymetry is defined by a single value at cross-section measurement. Each cross-section curve below the mean sea level was averaged to provide a mean depth. Although echo sounder measurements were not available the estuary was known to be particularly shallow between stations 19 and 20. Linear interpolation between the cross-sectional areas of stations 20 and 19 was not thought to be representative of that stretch of river and an additional point between stations 20 and 19 was therefore added based on visual estimates. The resulting bathymetry is shown in Figure 4.2.

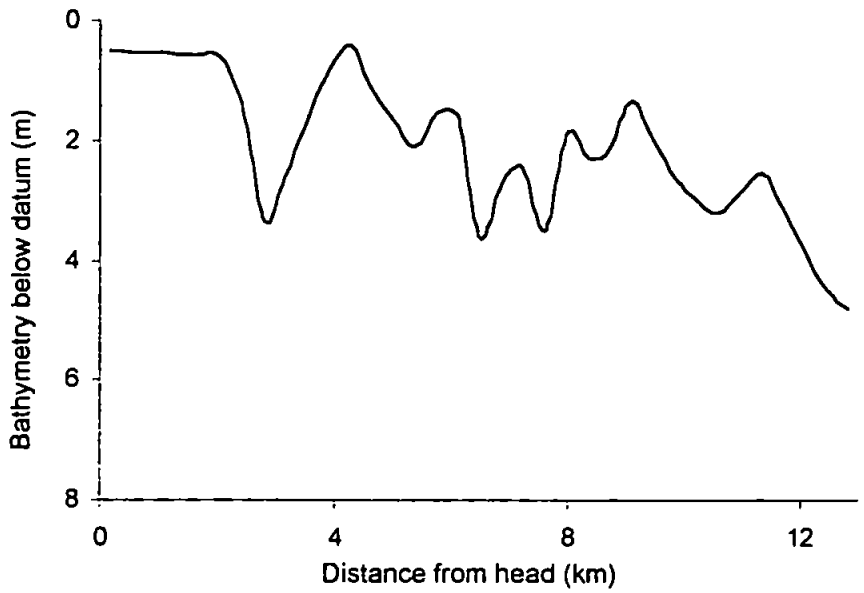

Figure 4.2 Mean bathymetry below the mid-tide datum.

Tidal elevation data during variable river flow and tidal ranges was available at points through the estuary, concurrent tidal elevation data at stations 4, 9, 16 and 20 was

however, only available during two tidal cycles, in February 11, and April 5, 1997. The April data covered a period with a predicted tidal range of 3.9 m and a relatively constant mean daily river flow of 40 $m^3 s^{-1}$. In comparison the river flow during February 11 was elevated and more variable (160 to 363 $m^3 s^{-1}$). The April data was chosen for calibration of the model and the model output has been validated using the February data.

An initial period of 48 h was used to allow the simulation to stabilise and then data was extracted at ~3 h intervals at low water, flood tide, high water and ebb tide at points in the model corresponding to stations 4, 9, 16 and 20 were tidal elevation data was recorded. The tidal propagation along the estuary was then determined by subtracting low water depth from that at high water. The resulting tidal propagation is compared to that measured in Figure 4.3.

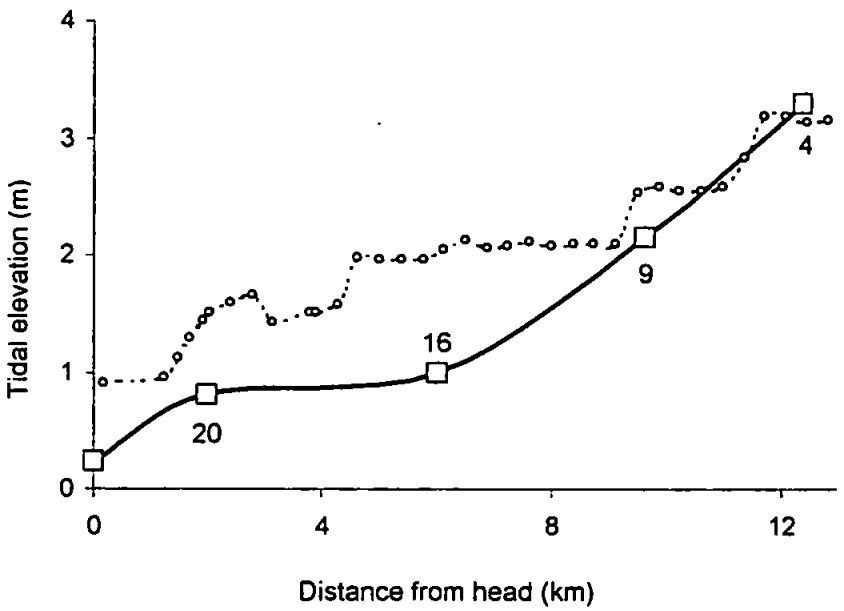

Figure 4.3 Predicted tidal elevation (-○-) compared to measured data at stations 20, 16, 9 and 4 (-□-). Tidal elevation is assumed to decrease towards zero at the model head.

The rapid reduction in the tidal propagation associated with the reduction in water depth within the first 4 km from the mouth is in agreement with Uncles & Stephens (1996b) who noted a rapid decline in tidal velocity in this area.

Inaccuracies in water depth will lead to inaccuracies in the predicted volume of water, its velocity and tidal propagation. The data shown in Chapter 3, (Figure 3.20) indicated a good correlation between cross-sectional area and depth. The measurement of cross-sectional areas may however have been insufficient to properly describe the bathymetry

of the estuary. ECoS will interpolate linearly between each cross-sectional value and as the stations were on average 500 m apart significant variation in the cross-sectional area may not have been recorded. At station 7 a substantial area of adjacent low lying ground becomes flooded at high water, but was not included during the bathymetry surveys. To allow for this the depth-area parameter at station 7 was increased and the values beyond the mouth set so that they would generate cross-sectional area of the order of 1 to 2 km. The depth-area relationship (A2) determined from the cross-sections is compared to that used in subsequent model runs in Figure 4.4.

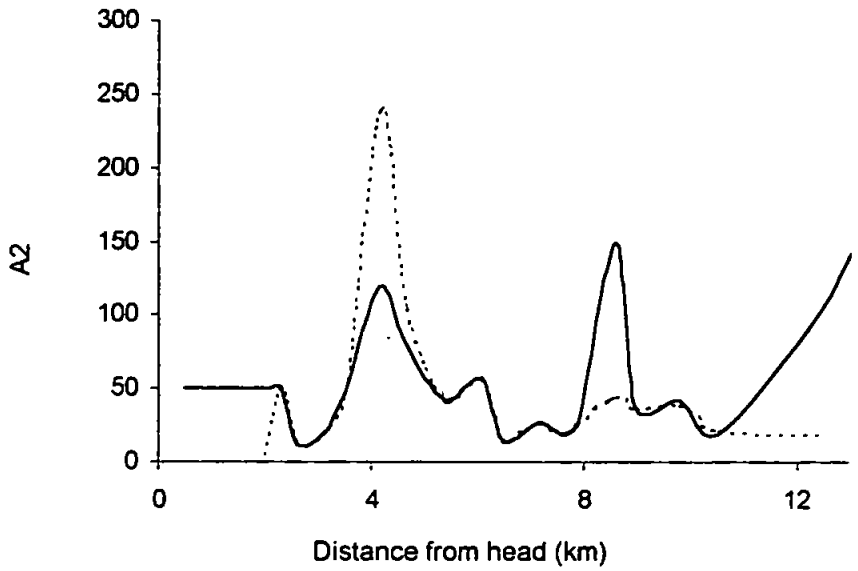

Figure 4.4 Defining the depth cross sectional area function A2. Values derived from the field data (—) and those gained during model calibration (—).

The depth-area relationship is also used to determine estuarine width and model predictions are compared to values derived from the 1:25,000 Ordnance Survey map of the area, see Figure 4.5. The width of the water surface may become significant when dealing with water-atmosphere exchange processes and the results for high water show an agreement of $R^2 = 0.3$, $p > 0.01$, and the model tended to over predict the width around 4 km from the head.

The inaccuracies in the model results arose due to the inherent limitations of the survey technique. The bathymetry was investigated by echo sounding and only considered the cross-sectional area below the water surface at the time of survey. The depth area parameter, A2 is therefore only accurate to the maximum water depth at this time. Although surveys were conducted on spring tides greater water depths may occur during extreme tidal or river flow conditions. When this occurs or when the model over predicts

tidal elevation the calculation of cross-sectional area may be inaccurate especially if there is a retaining river bank which was not accounted for in the original survey. This is illustrated in Figure 4.6.

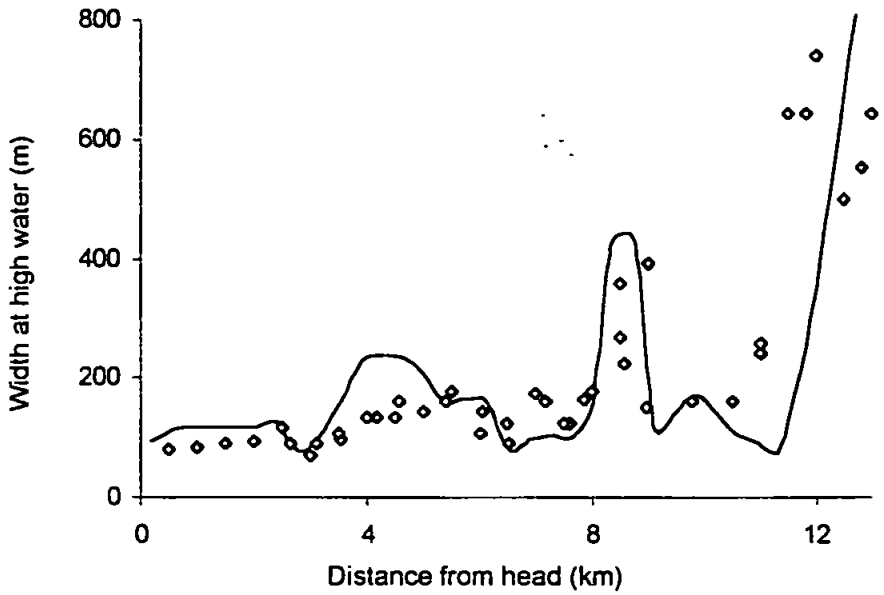

Figure 4.5 Model predictions of surface width of water in the Tweed Estuary (—) compared to those determined from the Ordnance Survey Map No. 438.

If the model over predicted cross-sectional area there would be a corresponding reduction in water velocity. It may therefore be necessary to define maximum limits to the cross-sectional area or to use a second or third order polynomial in the depth-cross-sectional area algorithm to include a retaining bank.

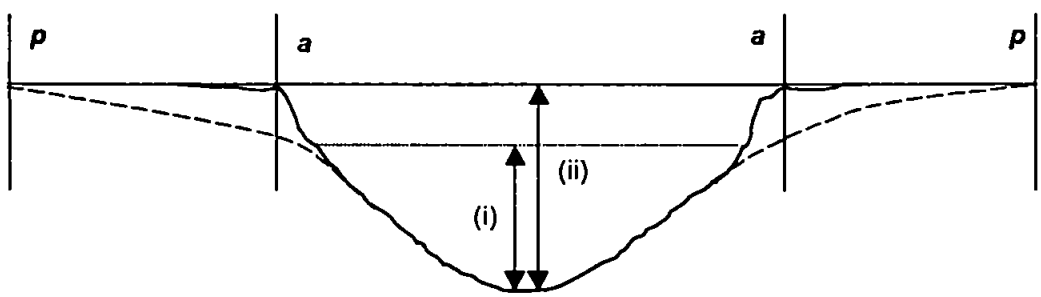

Figure 4.6 Model interpretation of the depth cross-sectional function. Water depth (i) represents the maximum depth during the survey period while (ii) shows a possible higher water elevation and how the model would over predict cross-sectional area (p) relative to the actual area (a).

In some modelling studies, time series data of velocity is included in the calibration processes (Gleizon, 1999). This may be important when erosion and deposition of sediments are critical components of the model. Although the EMP 2000 instrument rigs deployed in the Tweed were equipped with current meters, data were not recorded because the instruments could not be correctly placed due to the shallow water depth

(Howland, 1998 *per. comm.*). Hsu *et al.* (1999), however advised that surface elevation data be used because it is generally more stable, as opposed to highly variable current velocity. Sediment transport in the Tweed does not involve significant amounts of sediment exchange with the bed sediment and this approach was therefore adopted.

4.1.2 Calibrating bed friction

Having defined the bathymetry and cross-sectional area the Manning coefficient can be used to refine the model predictions of tidal excursion. Increasing the coefficient will reduce the tidal range and increase the phase lags for both high and low tides (Hsu *et al.*, 1999). The sensitivity of the model to changes in the Manning coefficient was assessed by comparing tidal propagation along the estuary with spatially invariant Manning coefficients of 0.015, 0.020, 0.025, 0.030, and 0.035. These values are comparable with those of Gillibrand & Balls (1998) where values between 0.02 and 0.06 were used in a one dimensional model of the Ythan Estuary and a range of 0.02 to 0.05 used in a MIKE 11 model of the Forth Estuary (Wallis & Brockie, 1997). Values ranging between 0.015 and 0.033 were also used by Hsu *et al.* (1999). The results are shown in Figure 4.7.

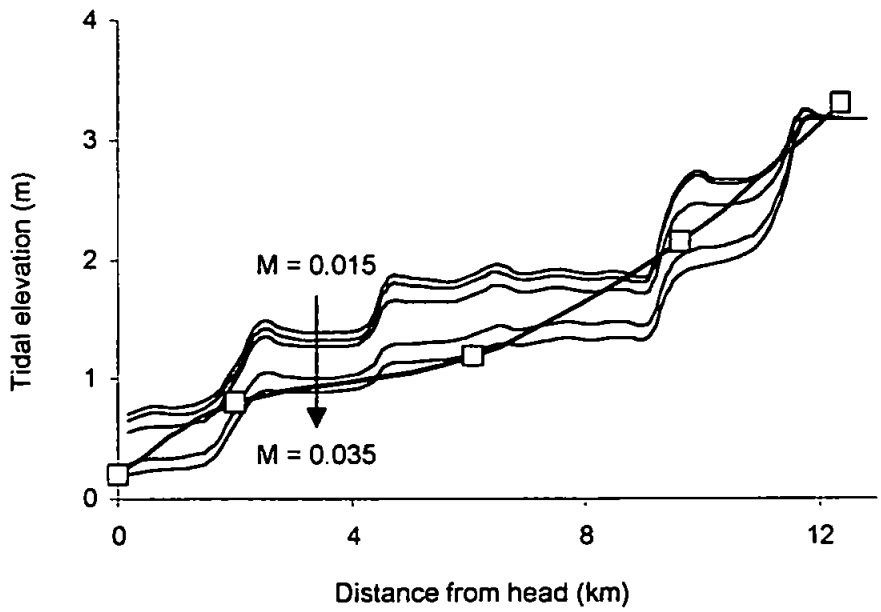

Figure 4.7 Reduction in tidal propagation up estuary when the Manning coefficient (M) is increased from 0.015 to 0.035. The predictions are compared to measured tidal propagation during April 1997 (-□-).

Increasing the Manning coefficient from 0.015 to 0.035 resulted in a maximum of 0.8 m reduction in tidal amplitude. Larger values of the coefficient however reduced the velocity of the river flow and as a consequence of reduced riverine flushing excessive

salinity values occurred. Figure 4.7 also shows that the model results towards the mouth of the estuary were closer to observed values when the Manning coefficient was low, while those at the head were closer to observed values when the Manning coefficient was high. Reeds and other vegetation upstream of station 13 will have increased the bed friction as will the meander of the channel between station 17 and 20 so this is not unreasonable. The Manning coefficient was therefore varied inversely with distance. Values tabulated as a function of distance were initially used and manually adjusted to obtain the best fit. As the model was more sensitive to the overall trend and magnitude of the Manning coefficient than to small variations the tabulated values were replaced with a linear function of distance. The resulting Manning coefficient and tidal propagation results are shown in Figure 4.8. predicted elevation differed from that measured by a maximum of 0.3 m at station 16 and less than 0.15 m at the other stations.

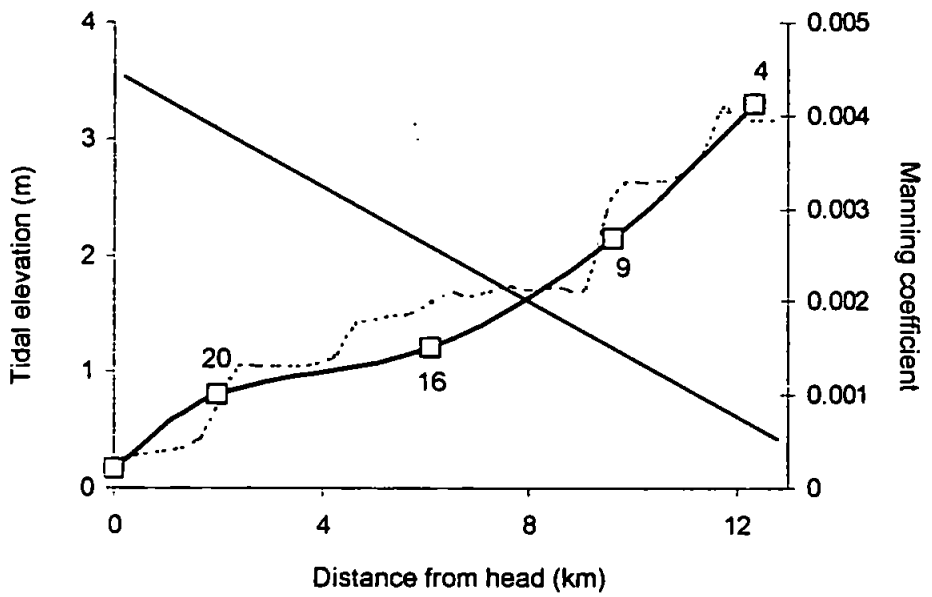

Figure 4.8 Model predictions of tidal elevation (—) compared to observed values (-□-) using a spatially varying Manning coefficient (—), inversely related to distance from the head (-0.0003x+0.0045 where x is the distance from the head in km).

4.1.3 Validation of the hydrodynamic model

The model was initially tested to determine the run up time required for the hydrodynamic simulation to stabilise. Figure 4.9 showed that within the first 12 hours of simulation time the model was unstable, but after 24 hours the model predictions over each tidal cycle were constant. A one day minimum warm up time was therefore used during the testing of the hydrodynamic model. To assess the performance of the model

under a range of river flow and tidal conditions validation runs were conducted for February, March, April and July 1997 surveys.

By using the ECoS sampler function it was possible to extract data from the model at specific locations. Samplers were set up to conform to the locations of the stations 9, 16 and 20 where tidal elevation data had been collected. The model was then run and the data extracted at 60 minute intervals over a 5 day period. The results are shown in Figure 4.10.

The results show that although the model was calibrated under one set of conditions it is responding well to changes in river flow and tidal range. In comparing the model output with field data three factors need to be considered: i) the amplitude and symmetry of tidal elevation; ii) the change in minimum water depth at low water and the iii) the phase of the tidal elevation.

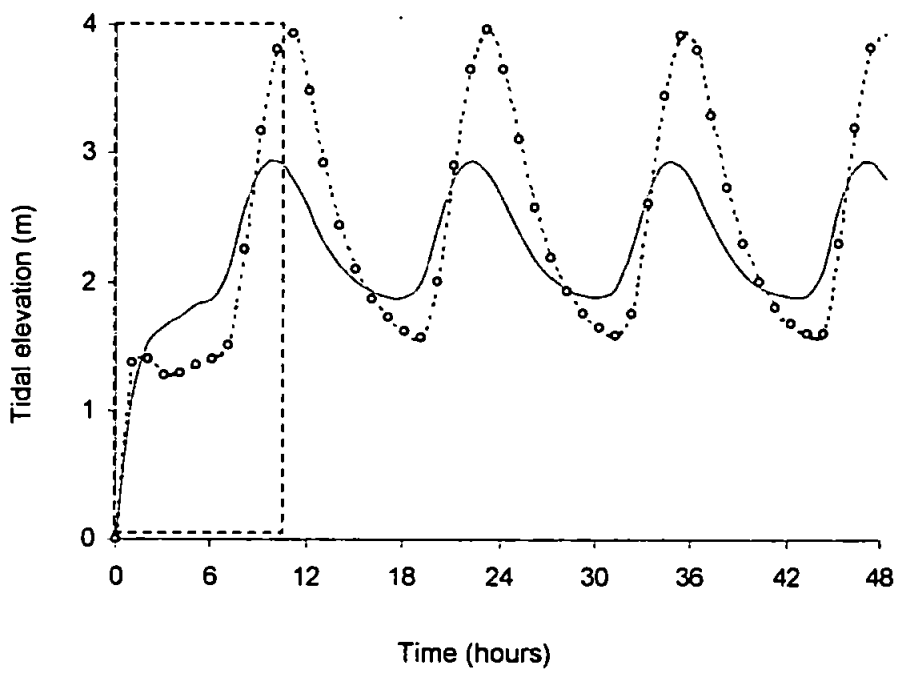

Figure 4.9 Determining the required warm-up period for the hydrodynamic simulation during spring (-o-) and neap (—) tides. The dashed box indicates the period during which the model had not fully stabilised.

The model simulated the reduction in tidal amplitude up the estuary from between 2 and 3 m at station 9 to between 1 and 1.5 m at station 20. The model showed a good fit for maximum tidal elevation at station 9, but had a tendency to over predict tidal elevation by up to 0.5 m at stations 16 and 20. This had been identified as a problem during the calibration process and although improvements had been implemented it has not been

fully resolved. However, the hydrodynamic template is providing a good approximation to the changing water depth given the uncertainties in the coding of the bathymetry.

The model responded to river flow in addition to tidal range at the mouth and the river flow is also shown in Figure 4.10. The model was driven by mean daily flows and it

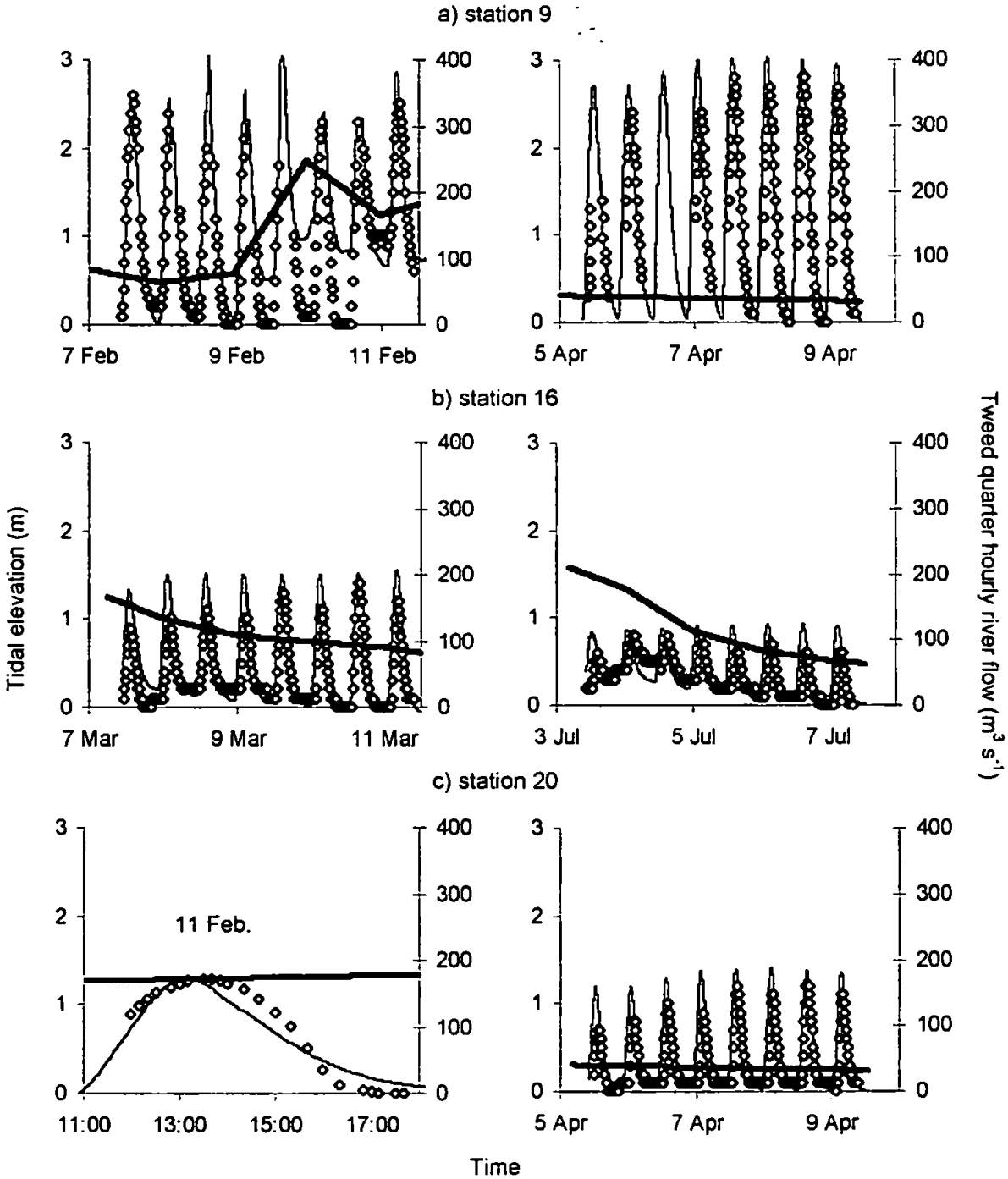

Figure 4.10 A comparison of modelled (—) and observed (◇) tidal elevation at stations 9, 16 and 20. The quarter hourly river flow is also shown by the thick line. The results have been normalised relative to minimum low water.

interpolated linearly between these flow values, while those shown in Figure 3.12 are quarter hourly flows. The quarter hourly flows are much more variable and differ from the model interpolation of flow by up to 130 $m^3 s^{-1}$ during February 1997. Mean daily flows were used as these are generally more accessible and it was felt that the performance of the model should be assessed with the range of data normally available. The main influence of river flow was upon the low water depth and this was in part reproduced by the model. During the April simulations, low water depth was relatively constant and this corresponds to the observations at stations 9 and 20. During March and July surveys the river flow decreased and the model showed a reduction in low water depth which was in agreement with the observations. During the February survey there was a rapid rise in river flow and an increase in the observed low water depths at station 9. The model response was too rapid and over predicted low water depth. This period was however marked by a 130 $m^3 s^{-1}$ difference in the flow interpolated between mean daily values and that of the quarter hourly flow. When the model was rerun using tabulated values of quarter hourly flow the agreement between model and observed data was greatly improved, see Figure 4.11. Rerunning the model with quarter hourly flows for the other surveys did not produce any significant increase in model accuracy because the discrepancies between hourly and daily flows were much smaller.

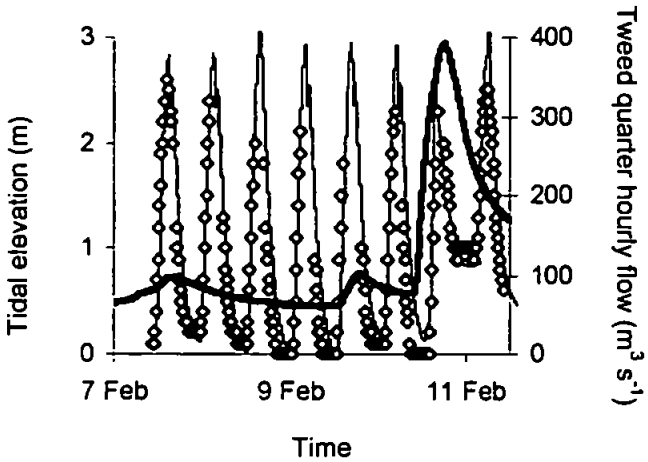

Figure 4.11 Model predictions of tidal elevation (—) at station 9 compared to observed values (◇) during February 1997 using quarter hourly river flow.

The agreement in tidal phase is good, although the flood tide tends to be early and again this is probably due to excessive propagation of the flood tide. The model also predicted a small degree of tidal asymmetry, which is in agreement with the data from stations 9 and 16.

4.2 Calibration and validation of saline intrusion

Calibration and validation of the saline intrusion into the estuary is the second stage of the hydrodynamic model development and testing. Salinity can be used as a conservative tracer to assess the advection-dispersion processes within the estuary as the river water, with zero salinity, mixes with seawater with typical coastal values of 34 to 34.5 units. Having calibrated and validated the water levels, adjusting and testing the saline intrusion into the estuary is a simpler process which if saline boundary conditions at the mouth are assumed to be constant will only involve the water dispersion parameter. The riverine salinity boundary was set to zero. The marine boundary was defined as mean salinity at the mouth during flows less than 100 $m^3 s^{-1}$, *i.e.*, 33 units. Once the model predictions of salinity distribution have been assessed this can be extrapolated to other conservative elements.

The model stability and warm-up time for advection and dispersion was first tested by running the model over several tidal cycles with identical tidal range and river flow conditions, see Figure 4.12.

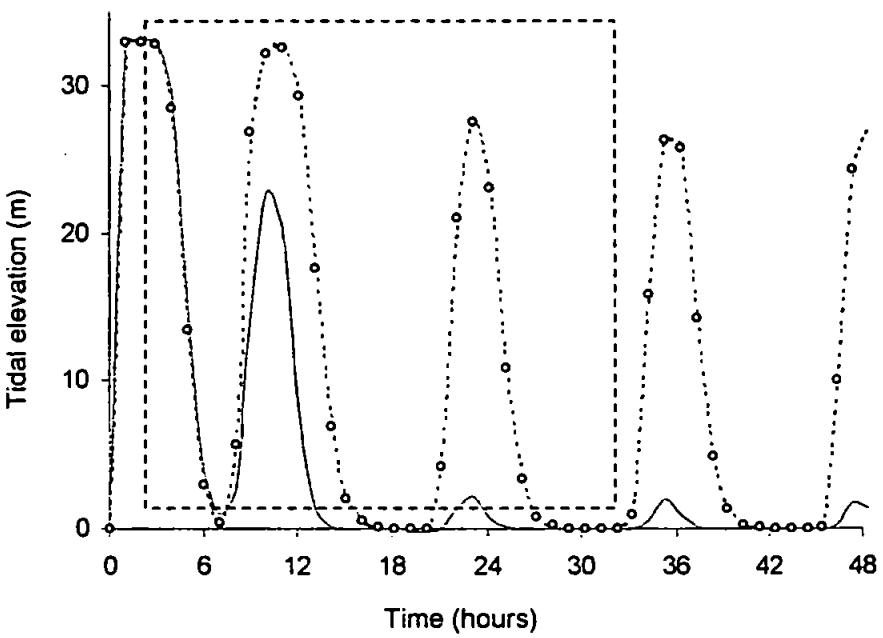

Figure 4.12 Determining the warm-up period required for the advection dispersion of salinity under spring (—) and neap (—) tidal conditions. The dashed box indicates the period during which the model had not fully stabilised.

This showed that the distribution of a solute required longer to reach equilibrium than the hydrodynamic process and there is a slight difference between the predictions for a third and fourth tidal cycle. All subsequent simulations were therefore run with a 48 hour run

up period. Using this, the initial conditions for salinity had very little effect on the simulation output and were therefore set at zero.

4.2.1 Predicting axial distribution of salinity

One extended axial survey was chosen from each survey period to cover a range of river flow and tidal conditions and the model run for a warm up period of 48 hours. Due to the variability in sampling time the ECoS sampler function was used to extract model values of salinity at each sampling site over a period of one hour prior to, and one hour after high water. Model predictions expressed as mean, minimum and maximum salinity over the 2 hour period around high water are compared to surface salinity measurements in Figure 4.13.

Calculation of dispersion coefficients from salinity data assumes that the system is in a steady state and an alternative approach is to calibrate the model output directly with observed data. The generation of numerical dispersion was also discussed in Section 2.3.6 and the model output was first tested with water dispersion set as zero.

The model appeared to be over predicting salinity in the mid estuary in all, but the highest flow situations. The predicted limit of saline intrusion was up to 6 km beyond that measured in January 1997 and predicted salinity values in excess of 25 units over those measured are made in October and November 1996 and January 1997. Chapter 3 presented a large data set of axial and tidal station measurements of salinity in the Tweed Estuary under a range of river flow and tidal conditions. The vast majority of these measurements were of surface salinity, but, as noted by Uncles & Stephens (1996b) and as illustrated in Figure 3.23, the Tweed can show substantial salinity stratification during the flood tide. Under these circumstances , depth averaged salinity would be expected to be higher than those measured in the surface water. The model predictions must therefore be compared to depth averaged salinity values.

Depth profiles of salinity were made during a limited number of axial surveys between February and August 1997. The number of measurements made below the surface ranged from between one and four and with this limited data set some assumptions had to be made. Firstly, that salinity varied linearly between each measurement and secondly that the deepest measurement represented salinity close to the estuarine bed. The estuarine cross-

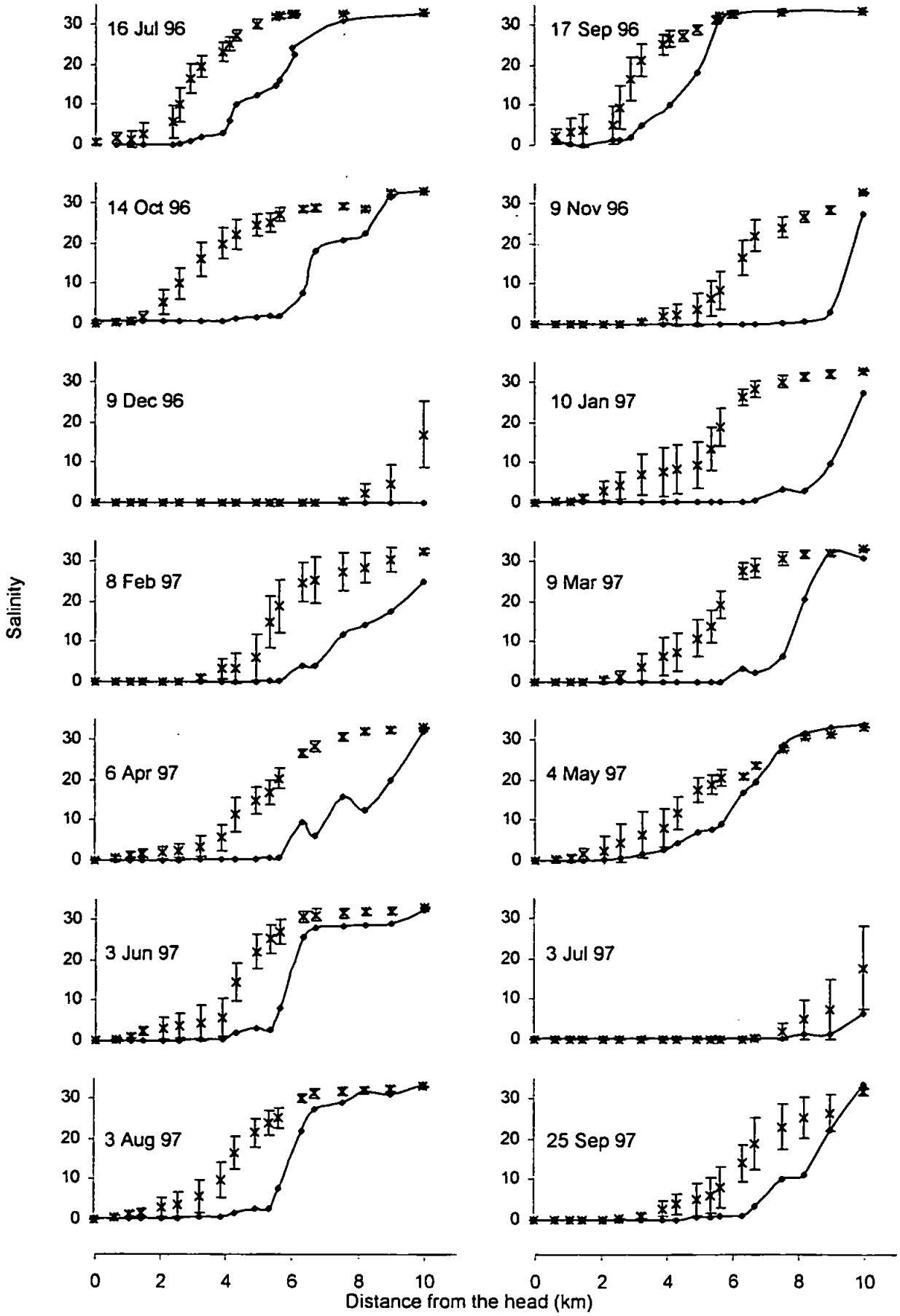

Figure 4.13 Comparison of observed (—♦—) with predicted (x) salinity in the Tweed Estuary. The error bars indicated the predicted salinity range 1 hour either side of high water at the mouth.

section was assumed to be rectangular to simplify the calculation. As the cross-sectional width reduces with depth at most sites this will lead to a slight over estimation of cross-sectional averaged salinity, but in view of the approximations already made this was felt acceptable. Points were interpolated at 0.1 m distance between the measurements and the mean of these was taken as the depth averaged salinity. Following Uncles *et al.* (2000), but using depth averaged salinity the location of the depth averaged FSI (km from the mouth) was found to be related ($R^2 = 0.88$, $p < 0.01$) to river flow, Q ($m^3 s^{-1}$) by the parameters a = 7.4 and b = 0.02:

$$FSI = a - b*Q \quad (4.1)$$

Depth averaged salinities are plotted against model predictions in Figure 4.14. These is a much better agreement between predicted and measured values than in Figure 4.13, with the overall shape of the curves being reproduced. The correlation between surface and depth averaged measurements and model output is shown in Table 4.3

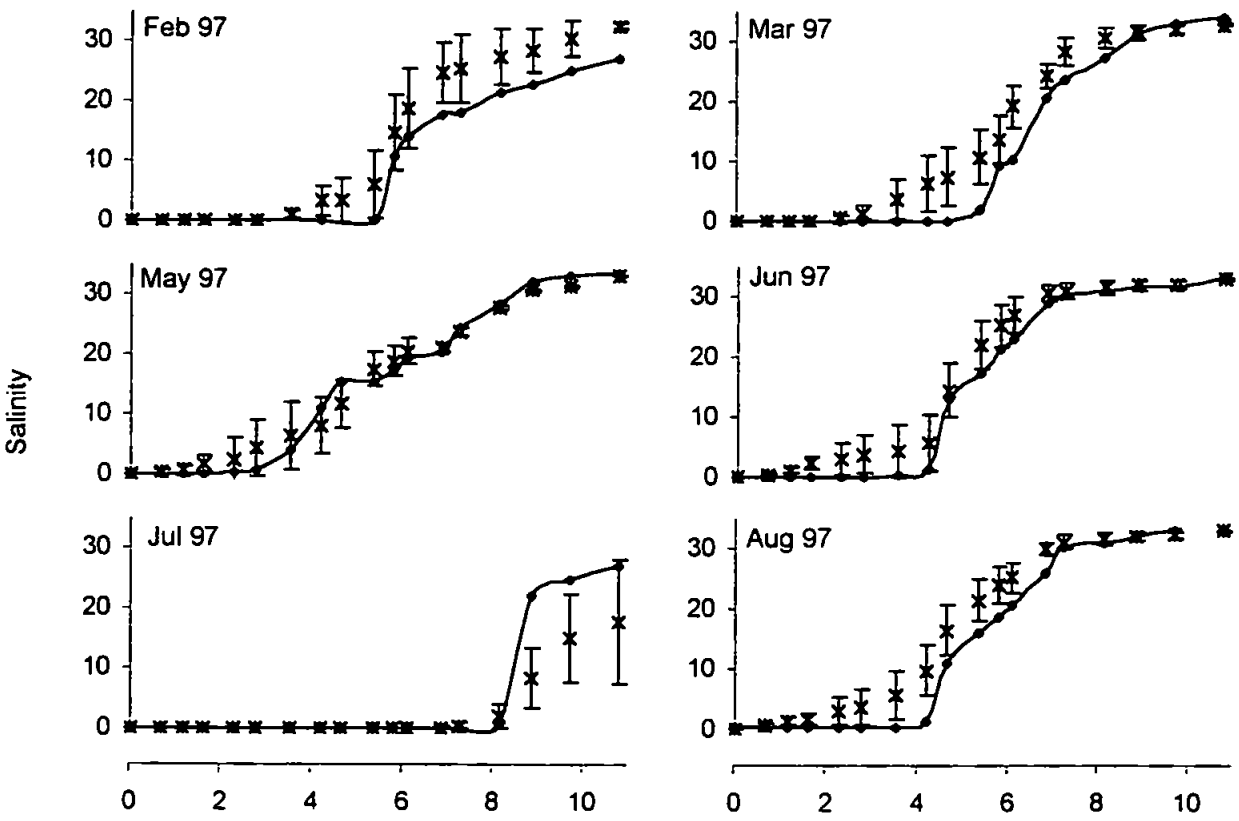

Figure 4.14 Comparison of depth averaged salinity (—◆—) with predicted salinity (x). The error bars indicated the predicted salinity range 1 hour either side of high water.

The model still showed a tendency to over predict saline intrusion in the mid to upper region of the estuary and this is related to the model over estimation of tidal propagation

as discussed in Section 4.2. Saline intrusion was influenced by the water dispersion coefficient in addition to advection processes. The dispersion coefficient is typically in the range of 100 to 300 $m^2 s^{-1}$ (Dyer, 1997) and the effects of changing the coefficient on model output was shown in Figure 2.10. The water and saline dispersion coefficients were set to zero during these model runs in an attempted to compensate for the over prediction of dispersion processes. The UPWIND scheme used to solve the differential equations will however generate some degree of numerical dispersion. Although in reality a dispersion coefficient of zero would be unrealistic this is acceptable as a model parameter value and was used through out this study.

Figure 4.3 Comparison of model predictions with surface and depth averaged salinity measurements.

Survey	Surface salinity measurements		Depth averaged salinity	
	R^2 (n = 18)	p	R^2 (n = 18)	p
Feb 8 1997	0.69	< 0.01	0.98	< 0.001
Mar 9 1997	0.53	< 0.05	0.94	< 0.001
May 4 1997	0.63	< 0.01	0.98	< 0.001
Jun 3 1997	0.75	< 0.001	0.99	< 0.001
Jul 3 1997	0.72	< 0.001	0.95	< 0.001
Aug 3 1997	0.74	< 0.001	0.96	< 0.001

4.2.2 Predicting anchor station salinity

Model predictions of salinity can also be compared with the anchor station measurements. These are important as they show how the model responded not just around high water, but also throughout the tidal cycle. They also have the advantage that the proximity of station 5 to the mouth meant that with the exception of high flow events the water column was relatively well mixed through out the majority of the tidal cycle. The model results are shown in Figure 4.15 and the agreement between predicted and observed measurements is good ($R^2 = 0.87$, $p < 0.001$) during low river flow in April, June and August 1997 and during high flow in February and May 1997. During the other anchor stations the mean daily flows ranged from 79 to 227 $m^3 s^{-1}$ and the model predicted salinities higher than measured values. In these instances the measured data only represented the overlying freshwater flow. Depth profiles of salinity were not available during these high flows. The depth averaged salinity at station 5 was calculated in section 4.2.1 as 23 and 22 units during high flows in February and July 1997 respectively. The model however predicted salinity between 28 and 33 at flows up to 248 $m^3 s^{-1}$. The marine salinity boundary

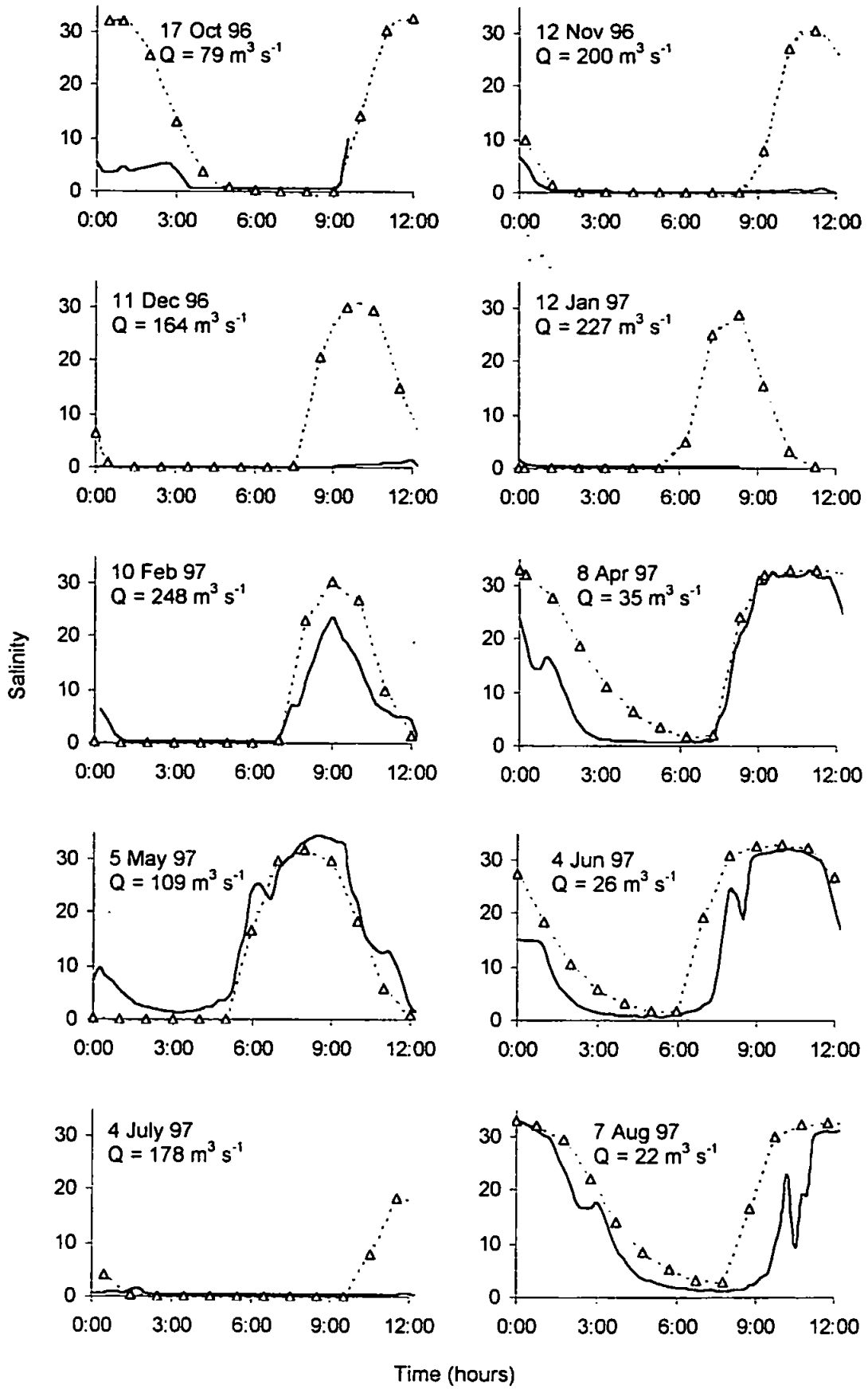

Figure 4.15 A comparison of surface salinity (—) recorded during the anchor station surveys at station 5 with depth averaged model predictions (--△--). Q is the mean daily flow of the Tweed.

condition was set at 33 (based on salinity data during flows below 100 $m^3 s^{-1}$) and although the model was extended out beyond the mouth by 0.6 km the depth averaged, salinity may still have been reduced by high river run off. By reducing the marine boundary salinity it was found that a value of 30 produced model predictions of 20 to 25 units at station 5 agreeing with the findings in Section 4.2.1.

The agreement between observed surface salinity and depth averaged predictions in May 1997 may seem surprising. At a MDF of 109 $m^3 s^{-1}$ stratification of the water column should have resulted in significant differences between surface measurements and depth averaged predictions. Section 3.8 showed that because the actual river flow only increased after high water, the flow values interpolated by the ECoS from the mean daily flows would be too high. As a consequence the lower salinity predictions were in agreement with the observed data. If QHF were used model predictions resemble those of June 1997 and over predict salinity during the flood tide. The model also over predicted salinity by up to 15 units during the flood and ebb tides. This is similar to that observed during the axial surveys and elates to the difference between surface and depth averaged salinity as the salt wedge advances past station 5. This also implies that the Tweed was partially stratified on the ebb tides as well as the flood.

4.3 Calibration and validation of SPM distributions

Calibration and validation of the sediment transport component is the third and final stage of developing the transport model. The model of SPM in the Tweed Estuary not only considers the exchange and dispersion processes of sediment transport of sediment within the estuary, but also aims to provide an estimate of the flux of sediment through the system. The water-sediment model can then be used to model more complex biogeochemical processes (Chapters 5 and 6) and provide estimates of the transport of particle reactive elements from the land to the sea.

4.3.1 Predicting turbidity at the riverine boundary.

Unlike salinity where the riverine boundary can be set to zero the turbidity of the Tweed river water can vary substantially and values between 2 mg l^{-1} and 300 mg l^{-1} have been reported (Ball, 1994; Robson *et al.*, 1996; Neal *et al.*, 1997; Uncles & Stephens 1997; Bronsdon & Naden, 2000; Uncles *et al.*, 2000). Uncles & Stephens (1997) derived a linear

regression ($R^2 = 0.62$) between river flow (Q) and suspended load, SPM (mg l^{-1}) in Tweed river water:

$$SPM = -a + b * Q_{30} \quad (4.2)$$

where a and b are 1.0 and 0.16 respectively and Q_{30} (m^3 s^{-1}) is the river flow 30 h previously.

Three data sets of freshwater turbidity were available during the survey period 1996 to 1997, i) data from Norham on the Tweed (n = 23); ii) data from Hutton Castle on the Whiteadder (n = 24) and iii) data from station 20 at the head of the estuary (n = 35). A linear regression was fitted to log turbidity on log Q (MDF) for the Tweed and Whiteadder data:

$$\text{Log } SPM = a + b*(\text{Log } Q) \quad (4.3)$$

where the constants a and b are −1.47 and 1.22 for the Tweed ($R^2 = 0.81$, $p < 0.001$) and 0.02 and 0.87 for the Whiteadder (0.69, $p < 0.001$). These predictions can be compared to the regression determined by Uncles & Stephens (1997), see Figure 4.16. As the time of sampling is unknown the Q_{30} is assumed to equivalent to the mean daily flow on the preceding day. The regression of Uncles & Stephens (1997) predicted higher turbidity than that indicated by the data. Their analysis was based on measurements made within the tidal reaches of the estuary and may include some degree of tidal resuspension of bed sediment.

At comparable flow rates the turbidity of the Whiteadder is approximately double that of the Tweed. The mean flow of the Whiteadder is 6 m^3 s^{-1} and the ratio of flow to catchment size is about half that of the Tweed. This corresponds to the gradient in rainfall between upland areas in the west and lowland areas in the east (Neal *et al.*, 1997) and to differences in land use (Robson *et al.*, 1996). The Whiteadder therefore has a potentially higher suspended solid flux in relation to the flow when compared to either the Tweed or Tamar rivers and plumes of higher turbidity water from the Whiteadder have been observed at the confluence with the Tweed (Millward, 1999 *per. comm.*).

Unfortunately, where automated samplers are absent, manual collection, often restricted to predetermined periods has limited the probability of capturing high turbidity events. The relationship between turbidity at station 20 and flow is not however statistically significant. Station 20 is also still with in the tidal limits of the Tweed and the recorded turbidities may

be complicated by tidal movements. Sediment flux calculations have therefore been conducted using the flow-turbidity relationship determined at the river monitoring stations. Due to the lack of fine grained sediment deposits in the Tweed Estuary or tidal reaches of the river this relationship can be used to determine net fluxes through the estuary to the North Sea.

The anchor station surveys identified pulses of material passing through the estuary and it is unfortunate that the axial surveys failed to sample at the head of the estuary during these periods. Conversely, turbidity measured during low flow summer conditions was higher than expected and may represent a significant proportion of biogenic as opposed to lithogenic material and diatoms have been note as forming a significant proportion of the suspended load (Bronsdon & Naden, 2000).

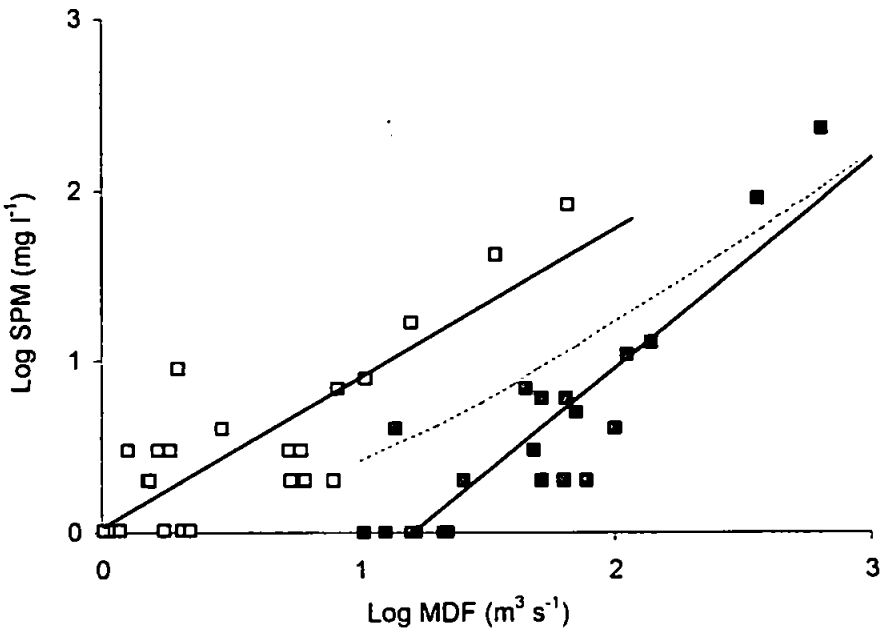

Figure 4.16 Comparison of the flow turbidity relationships of Uncles & Stephens (1997) (—) with regressions based on data from the Tweed (■) and Whiteadder (□) river monitoring stations.

Uncles *et al.* (1990) used the flow-turbidity relationship of Harris *et al.* (1984) to predict the flux of material through the Tamar Estuary. The lack of fine grained sediment deposits in the estuaries implies that it is neither a source nor sink for suspended particulate matter. Assuming conservative transport of sediment and using the relationship expressed in Equation 4.3 mean daily sediment flux for the Tweed and Whiteadder Rivers has been calculated between 1970 and 1997. Daily fluxes have then been summed and are shown as an annual flux of through the estuary in Figure 4.17. The annual mean flux of 4.7 ± 0.2 x 10^4 T yr^{-1} is similar to the value (4.5 x 10^4 T yr^{-1}) derived following Wilmot & Colins

(1981) and within the range 3.8 to 9.0 x 10^4 T yr^{-1} estimated by Bronsdon & Naden (2000), although lower than that of 6.4 x 10^4 T yr^{-1} and 6.6 x 10^4 T yr^{-1} estimated by McManus & Duck (1996) and Owens *et al.* (1999). If the sediment flux over a range of flows is calculated 95 % of the flux is found to occur during flows in excess of 400 m^3 s^{-1}. During the period 1970 to 1997 Tweed River flows in excess of 400 m^3 s^{-1} accounted for approximately 1 % of the time. In the Humber, 92 % of the sediment is transport in 11 % of the time (Neal *et al.*, 2000) illustrating the importance of the brief spate conditions in the flux of sediment from the Tweed catchment to the North Sea.

Neal *et al.* (1997) noted that although suspended sediments increased with flow in the Tweed there was a large scatter in the flow-turbidity relationship. The flow-turbidity algorithm may therefore need to be more complex and include the history of the changing hydrograph. Mulder *et al.* (1998) noted that river discharge tended to increases exponentially to the maximum flood then decrease linearly and Syvitski & Morehead (1999) noted that the rising limb of a flood carried more sediment than the falling limb. The changing hydrograph may also be responsible for delivery of different particle fractions. Course particles may be entrained during the rising limb when fluvial energy is high and then rapidly deposited as the fluvial energy drops (Wass *et al.*, 1997). These particles tend to have a high organic content due to surface soil erosion during high precipitation effects (Tipping *et al.*, 1997). Naudin *et al.* (1997) reported that in peak flood the Rhone River plume contained approximately 60 % of temporarily suspended material, but at the end of the flood this had reduced to approximately 30 %. The initial pulse of sediment resulting from remobilization of material from the channel beds in the catchment during the rising hydrograph may contain relative coarse particle. The occurrence of these particles may not only be related to the transport capability or flow hydrualics of the water, but also to changes in the relative contribution from different sediment sources. As this source becomes exhausted, contributions of finer material from more distal sources may then become more important (Walling *et al.*, 2000). The rates and magnitude of these changes in addition to the balance between biogenic and lithogenic material will affect the flux estimates of particulate matter. Chemical composition and surface area of the particle, possibly related to the sediment source, will influence the chemical reactivity and the ratio of dissolved to particulate metals transported through the system. The nature of the particles in addition to their concentration, may therefore need to be included in the flow-turbidity relationship in future studies.

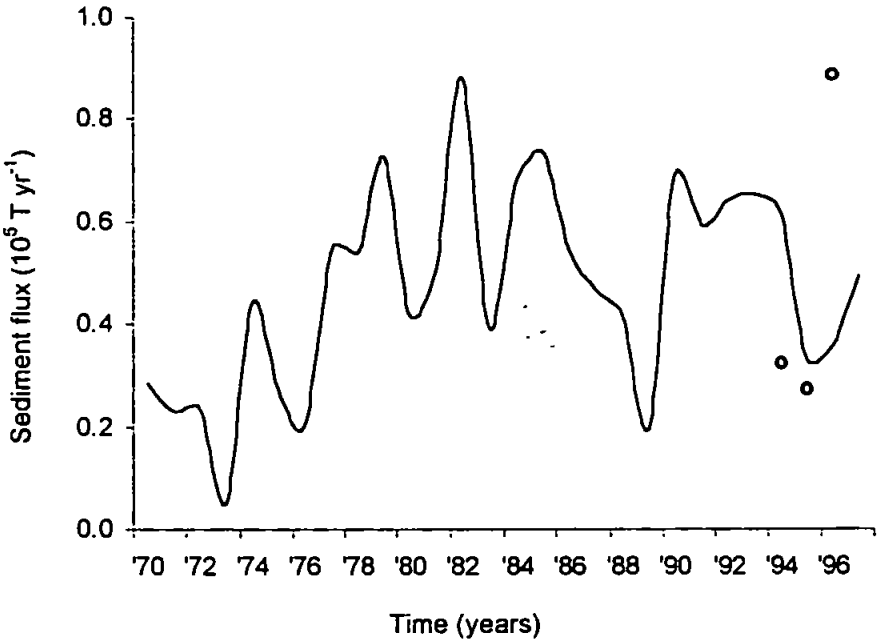

Figure 4.17 Annual sediment flux from the Tweed Estuary determined from Equation 4.4 and MDF of the Tweed and Whiteadder Rivers. Flux estimates of Bronsdon & Naden (2000) are also shown (o).

4.3.2 Predicting turbidity at the marine boundary.

Uncles & Stephens (1997) noted near linear behaviour between salinity and turbidity within the central reaches of the estuary, but turbidity at the mouth can be elevated by 10 to 20 mg l^{-1} relative to the rest of the estuary. They also found that simulated swell-wave height explained over 90 % of the variance in turbidity at the mouth. The resuspension of sediment due to wave swell could be encoded as a transfer function from the bed sediment compartment to the temporarily suspended sediment within the water column as a function of wind velocity. Resuspension at the mouth predominately consists of course sand particles. Course grained sediments however play a minor role in water-sediment sorption processes and encoding wind resuspension in to the model was beyond the scope of this project.

4.3.3 Axial distribution of turbidity

To assess how accurately the model predicted the transport of suspended sediments through the Tweed Estuary the marine and freshwater turbidity were defined using the observed end member values. Unlike salinity which will advect and disperse with the water in the estuary the transport of particulate matter may be very different from that of the water. The Tweed is characterised by the lack of fine grained bed sediment. Bed resuspension is therefore unlikely to play a significant part in the suspended sediment

distributions and compared to estuaries such as the Tamar, the Tweed has no mid-estuarine turbidity maximum. A model of the Tamar should be calibrated to simulate these processes, but it is equally important that a model of the Tweed behaves realistically and does not generate sediment deposits under current hydrological scenarios. The lack of any substantial deposits of sediment in the estuary also implies that what ever material is derived from the catchment is transported to the coastal zone within a limited number of tidal cycles.

Surveys were chosen which provided the widest salinity ranges and where possible the model was run for the same periods used when predicting axial distributions of salinity. A similar methodology was used to allow the model to warm up and to extract data. As very little data existed on cohesive sediment properties in the Tweed the model was run using the sediment transport parameters for the Tamar model (Harris & Gorley, 1998b), see Table 4. 5.

Table 4.5 Parameterisation of sediment transport in the Tweed simulations.

Sediment transport parameter	Value used in Tweed model
Depositional threshold, U_D	0.2 m s^{-1}
Erodability constant, M	0.003 kg m^2 s^{-1}
Erosion threshold, U_E	0.5 m s^{-1}
Settling velocity, V_S	1 x 10^{-3} m s^{-1}
Riverine PSP / TSP ratio	0.9
Marine PSP / TSP ratio	1
Riverine bed sediment	0.15 x Riverine TSP
Marine bed sediment	0
Initial bed sediment	0
Riverine TSP	From data
Marine TSP	From data

The initial bed sediment concentrations were set to zero to correspond to the lack of fine grained material deposited in the estuary. The boundary conditions were extracted from the field data and applied during the model warm up and simulation runs. The results from the model are shown in Figure 4.18.

The turbidity measured during the axial surveys showed a linear relationship with salinity throughout most of the surveys chosen. The model reproduced this conservative behaviour well in response to the generally high predicted velocities. Preliminary runs showed that insufficient material was deposited during slack water to generate any significant ebb flushing effect and comparisons to anchor station observations are not present as they fail

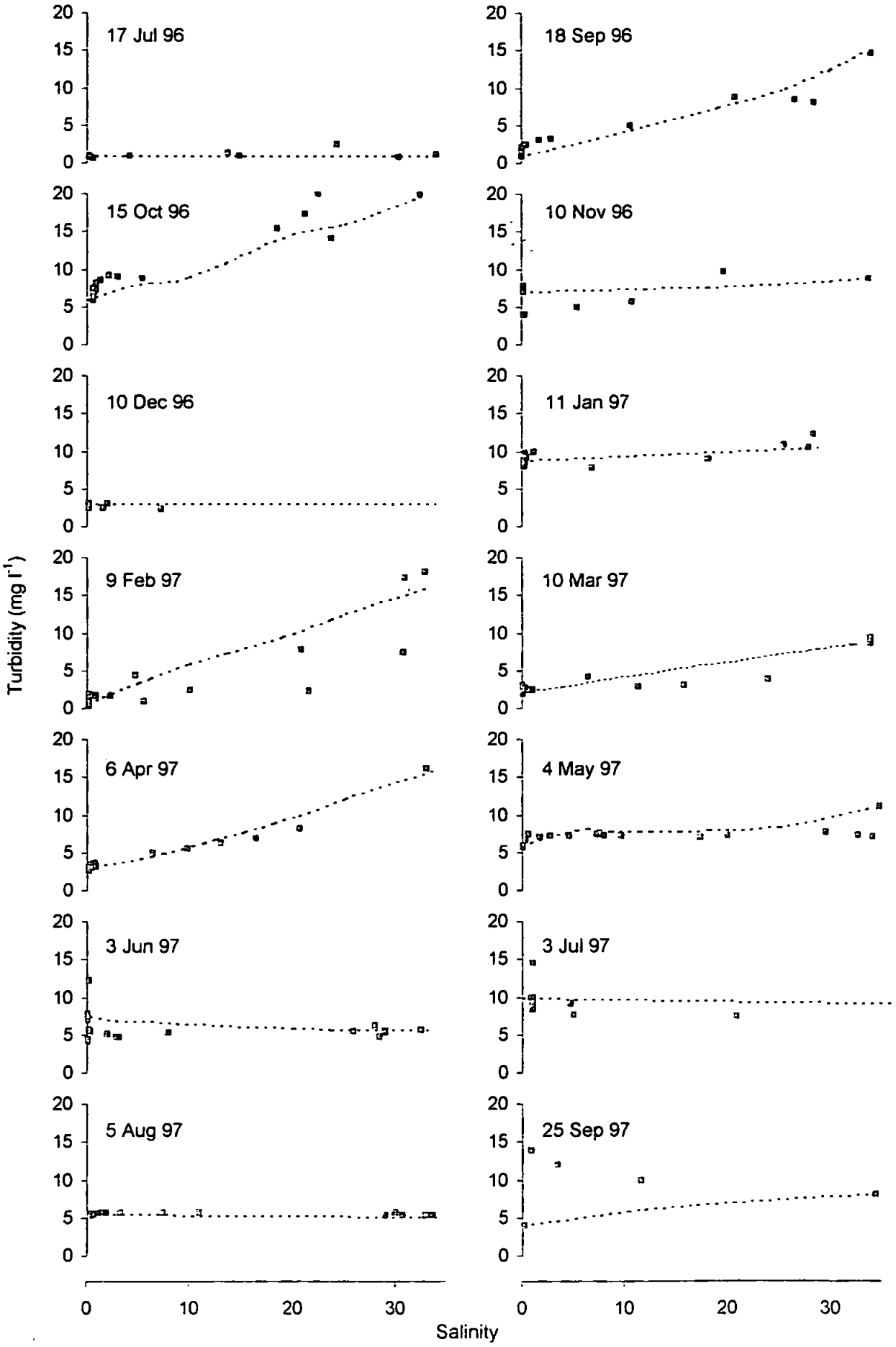

Figure 4.18 Observed (■) and predicted (----) axial distribution of turbidity in the Tweed Estuary.

to illustrate anything further and marine and riverine boundary values were not available. Erosion and deposition could be enhanced in the model by varying the riverine PSP / TSP ratio. The ratio is unlikely to remain the same under a range of flow conditions and high flows might be expected to contain a greater proportion of larger TSP particles. These may then accumulate during low tidal velocity conditions to subsequently be resuspended.

4.4 Summary and suggested model improvement

The application of a hydrodynamic modelling method has allowed the effects of short term (< day) changes in the tidal state and river flow to be simulate. During the parameterisation of the ECoS hydrodynamic templates, defining the bathymetry and tidal propagation into the estuary were the first and most critical process in the model set up.

It may be inappropriate to compare tidally averaged models with salinity measured at one state of the tide. In a similar fashion, results from a depth averaged model must be compared with depth averaged measurements and not just those at the surface. In a stratified estuary, a depth averaged model can not therefore reproduce the spatial distribution of data from surface measurements. The model results, when compared to the depth averaged salinity were good and explained over 90 % of the variation in salinity. The model however tended to over predict salinity by up to 7 units in the mid estuary and may indicate a need to refine the bathymetry data. This could be achieved through additional bathymetric surveys and the use of a higher order polynomial to represent the depth-area relationship.

Suspended sediment behaviour was predominately conservative in the estuary (Uncles *et al.*, 2000) and over 95 % of the variation was reproduced by the model. The salinity and turbidity predictions have not, however, been validated against an independent data set because no additional calibration process was needed to fit the model predictions to survey results. In view of the stratification present in the Tweed it is important that any further comparisons of model output are made against depth averaged measurements. These could be gained by depth profile studies with an optical turbidity meter, such as the YSI 6000. It would also be useful to determine the changing concentrations of suspended solids throughout a tidal cycle, particularly during spate conditions. This would best be achieved by the use of an *in situ* turbidity meter that could be placed in the upper estuary for periods such as a spring-neap tidal cycle.

Chapter 5

Abiotic and biotic controls of estuarine pH

5 Abiotic and biotic control of estuarine pH

The extended axial surveys of the Tweed identified a region of elevated pH in the tidal reaches of the river. These pH profiles were presented by Howland *et al.* (2000), this chapter reports additional observations and attempts to identify the abiotic and biotic processes that were responsible for the variability in pH in the estuary. A highly process orientated method for modelling the abiotic controls pH in the Tweed Estuary is outlined and has been implemented as an ECoS3 group, fully compatible with the existing estuarine quality template (Harris & Gorley, 1998b). The biological controls of pH will be discussed with reference to the dissolved oxygen saturation and dissolved nutrient concentrations.

5.1 Measurement of pH and dissolved oxygen in the Tweed River-Estuary

During extended, repetitive axial and anchor station surveys, measurements of pH and dissolved oxygen were made with a YSI 6000 instrument probe, see Table 1. Measurements were taken concurrently with those of salinity, temperature and turbidity using similar methodologies to those discussed in Section 3.7. Surface water samples were also collected and analysed for chlorophyll *a* (Uncles *et al.*, 2000).

5.1.1 Measurement of pH

The YSI 6000 employed a combination electrode consisting of a proton selective glass reservoir filled with buffer at ~ pH 7 and a Ag / AgCl reference electrode with gelled electrolyte. A three-point calibration (4, 7 and 10) was conducted using BDH Colourkey buffer solutions at the beginning of each survey day. The pH and temperature probes were slowly and carefully immersed into each buffer and a minimum of 1 minute was allowed to ensure temperature equilibrium, calibration was then accepted when readings were stable for 30 seconds. The electrode was rinsed and gently dried between different pH solutions. Temperature equilibration was essential to ensure that the instrument could automatically and accurately adjust for differences in temperature between the calibration standard and field measurements. Electrode drift was assessed at the end of each day, and was found to be minor.

Liquid junction potential changes with salinity and can effect the pH by 0.1 or more (Whitfield & Turner, 1985). The NISP Standard buffers used were of a fixed salinity (Howland *et al.*, 2000) and consequently can result in errors from about 0.01 pH units

under-estimation in saline waters to about 0.04 pH units over-estimation in freshwater (Millero, 1986). The pH in the Tweed ranged from about 7 to10 units and will not therefore be significantly effected by these potential errors.

Table 5.1 YSI 6000 instrument parameters showing the range, accuracy and resolution of pH and dissolved oxygen measurements (Yellow Springs Instrument Incorporated, 1993).

Parameter	Sensor type	Range	Accuracy	Resolution
pH	Combination glass electrode	2 to 14 units	± 0.2 units	0.01 units
Oxygen	Rapid pulse – polarographic	0 to 200 % air saturation	± 2 % air saturation	0.1 % air saturation

Organic ligands have a high affinity for glass surfaces and may cause a change to surface potential or modify the ion exchange capacity of the electrode. This is particularly problematic when DOC concentrations are higher than those of DIC and may cause erroneous pH measurements (Herczeg & Hesslein, 1984; Cai & Wang, 1998). Neal *et al.* (1998c) reported maximum DOC concentrations at Norham of 13.8 mg l^{-1} and values of between 2 and 6 mg l^{-1} were measured in the estuary (Martino, 1999 *per. comm.*). When compared to a mean of 85 mg l^{-1} (range 31 to 191 mg l^{-1}) of HCO_3^- (n = 103) concentration at Norham between 1994 and 1997 (Tappin, 1999 *per. comm.*), this is unlikely to be a significant problem to pH measurement in the Tweed River or Estuary.

In addition to the YSI 6000 instrument, the EMP 2000 bed rigs were also used to recorded pH, but these instruments were not fitted with dissolved oxygen sensors. The pH sensor parameters of the EMP 2000 are similar to those shown in Table 5.1. The EMP 2000 does not, however compensate for temperature variations and the sensor output had to be post calibrated according to:

$$pH_T = 7-(7-pH_{20})/(1+(T-20) * 3.41 \times 10^{-3}) \quad (5.1)$$

where for any temperature T, the corrected pH_T is related to the sensor output pH_{20} using the linear relationship expressed above (Applied Microsystems Ltd., 1993).

5.1.2 Measurement of dissolved oxygen

Prior to calibration, the Teflon membrane covering the oxygen probe electrodes was examined for damage and the KCl electrolyte solution checked to ensure than none had

leaked out and that no bubbles were present. The membrane and solution were also changed at regular intervals. During calibration the sensor was allowed to thermally equilibrate and stabilise for 10 to15 minutes in 100 % water-saturated air and then set to current barometric pressure in mm Hg (available from meteorological reports). The rapid pulse system employed by the YSI 6000 was affected by temperature (approximately 1 % per °C), although the software will automatically compensate for this, it was essential to calibrate the instrument at temperatures as close to those of the samples to be measured. This was achieved by immersion of the calibration cup into a bucket of water collected from the estuary. Between surveys the dissolved oxygen probe was kept damp to prevent the Teflon membrane from dying out.

The O_2 meter in the flow through cell aboard R. V. *Tamaris* generated spurious results during January and April 1997 anchor station and repetitive axial surveys. These were omitted during further analysis. Problems with the data set were identified by large (50 to 100 %) and rapid (15 to 30 second) changes in meter output. Further technical problems with the probe prevented O_2 saturation data collection during September 1996 and June 1997 extended axial surveys.

5.2 Variation of pH in the Tweed

Data was available from the EMP rig at station 4 for the period January to March 1997 and measurements of seawater pH (salinity between 33 and 35) are compared to those of freshwater (salinity <1) recorded at station 4 in Figure 5.1. Marine values of pH were relatively constant (8.2 ± 0.07) while those of freshwater varied from 7.5 to 8.7. The freshwater pH is reduced in mid February in response to high river flow and then showed a rapid rise through March as river flows decreased. As a consequence of these changes pH of river water was either higher, lower or similar to that of the seawater. To assess how the behaviour of pH in the Tweed changed in response to these variations two sets of results are presented:

- The first data set (October 1996 to August 1997) plots pH measured during anchor station and repetitive axial surveys (between stations 3 and 8) against salinity. Data from the repetitive axial transects have been combined to provided a broader coverage of salinity than that offered by the anchor station data alone.

- The second set of data (July 1996 to September 1997) describes the pH measurements made during the extended axial transects of the estuary. These data are plotted against distance because all of the surveys extended into the freshwater tidal reaches of the river and during high river flows, low salinity measurements were taken at the majority of stations. Plotting the results against distance is also used to identify any processes that are specific to a particular area of the river or estuary, as opposed to a specific salinity.

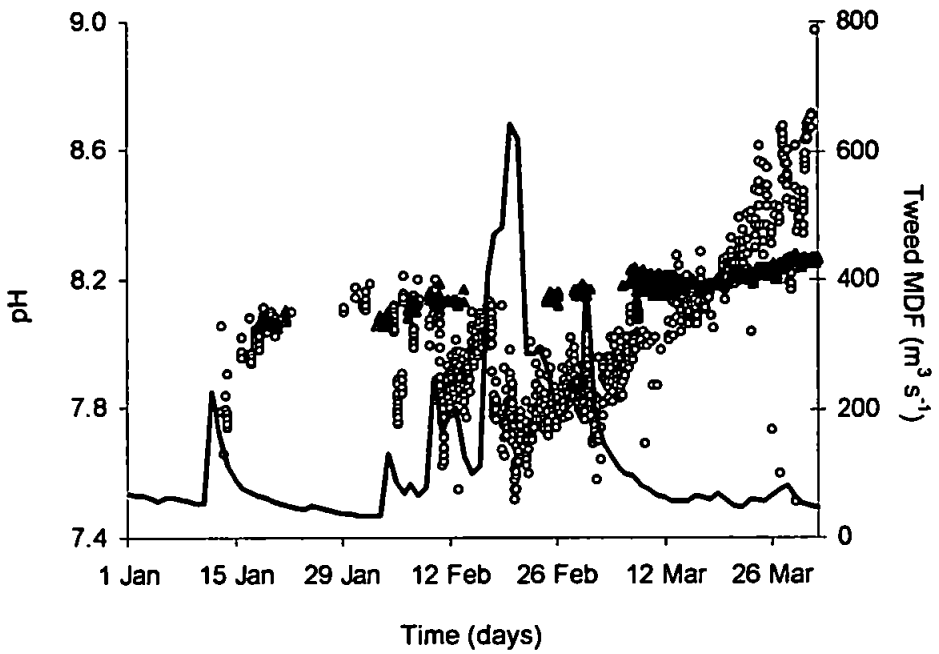

Figure 5.1 Freshwater (salinity < 1) pH (○) and seawater (salinity 33 to 35) pH (▲) recorded by the EMP rig at station 4. Tweed River MDF is also shown (—).

5.2.1 pH in the lower estuary between stations 3 and 8

The pH in the lower estuary measured during the repetitive and anchor station surveys is shown in Figure 5.2. The pH ranges of maximum and minimum salinity measurements during each survey are summarised in Table 5.2. The mean pH of fresh and low salinity water measured during these surveys ranged from 7.40 to 7.85 between October 1996 to February 1997 and from 8.64 to 9.00 between April 1997 and August 1997. There were two exceptions to the latter group which corresponded to high river flows in May and July 1997. During these periods the freshwater pH was reduced to 7.69 and 7.77 respectively, values more typical of the winter period. Due to the buffering capacity of seawater the pH at salinity of 27 to 34 varied from a minimum of 7.97 in February 1997 to a maximum of 8.21 in August 1997.

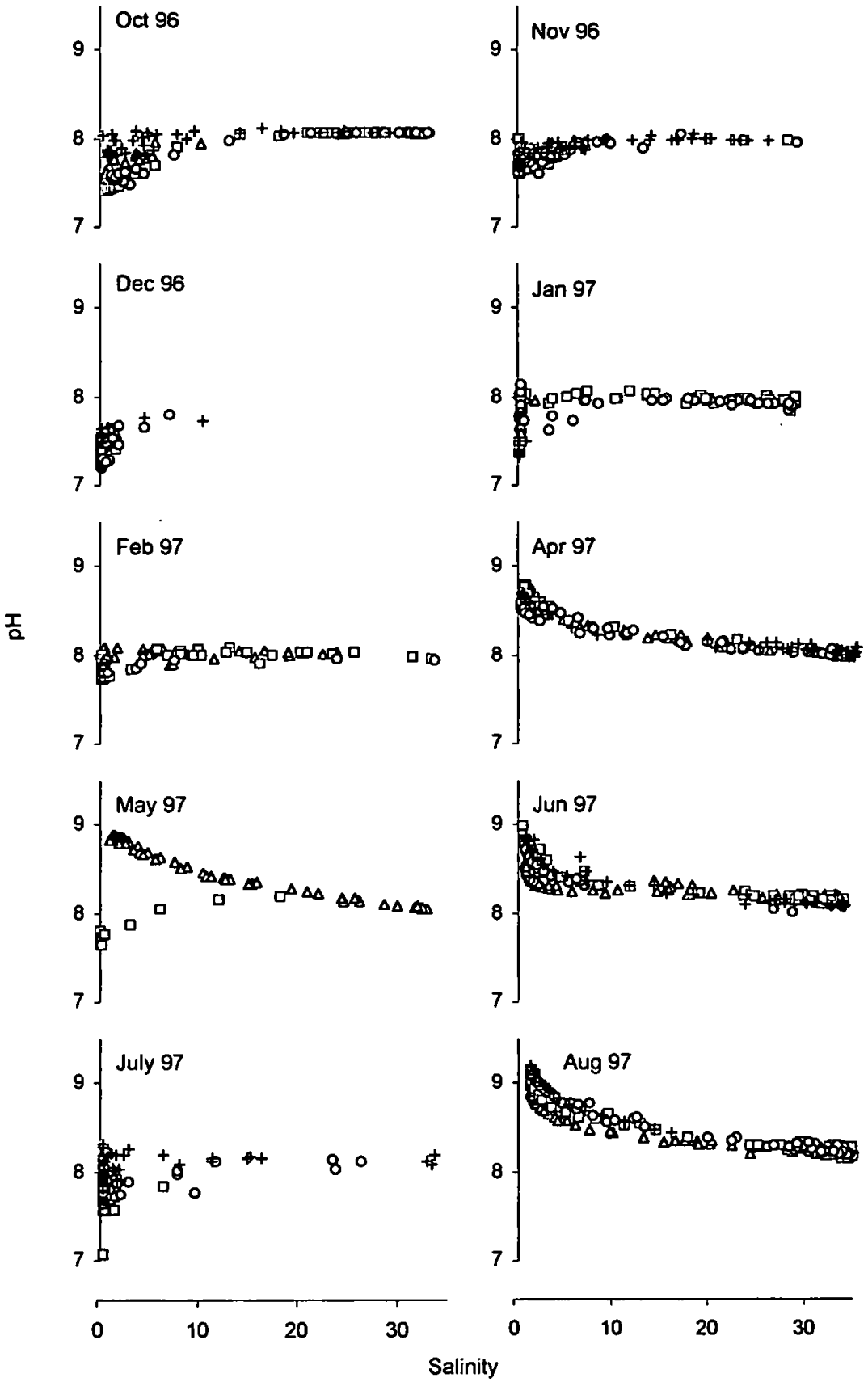

Figure 5.2 pH data recorded during repetitive axial and anchor station surveys in the Tweed Estuary. The data are plotted chronologically as 1st (◇), 2nd (□), 3rd (△) and 4th (+) profile per survey.

Within each survey period the pH of the freshwater varied by a maximum of 0.7 units. A linear relationship between river flow and pH explained 42 % of the variation in pH in the Vaal Estuary (Roos & Pieterse, 1995) and a regression of pH at Norham (see Appendices) on flow in the Tweed explained 58 % of the variation in pH. October 1996 to February 1997 and July 1997 survey periods were characterised by variable river flow and consequently the pH varied between days and potentially with each day.

When the freshwater pH was higher than that of the seawater (*e.g.*, April, June and August 1997) there was a rapid reduction in pH as salinity increased. If the pH of both end members was similar (*e.g.*, February 1997) the pH remained relatively constant throughout the estuary. When the freshwater pH was lower than that of marine values, there was a pH minimum followed by rapid increase of pH as the salinity increased from 0 to approximately 10. This is consistent with Mook & Koene (1975) and Whitfield & Turner (1986) predictions of pH when considering the effect of changes in salinity.

5.2.2 pH in the River-Estuary

The data in Figure 5.2 was limited to that collected between station 3 and 8. In Figure 5.3 the results from the extended axial surveys between stations 3 and 20 are shown. The R.V. *Tamaris* was not available at certain times and the extended axial transect data includes four additional surveys periods. The pH data from the upper stations of the survey area are summarised in Table 5.2.

Table 5.2 Riverine and marine end member pH during extended and repetitive axial surveys.

	Anchor station and repetitive axial survey data		Extended axial survey
	Salinity <1-2 pH mean ± SD	Salinity 27-34 pH mean ± SD	Riverine pH mean ± SD
Jul 96	R.V. *Tamaris* not available		9.00 ± 0.11
Sep 96			9.98 ± 0.29
Oct 96	7.64 ± 0.17	8.06 ± 0.05	7.63 ± 0.13
Nov 96	7.71 ± 0.07	7.79 ± 0.02	7.75 ± 0.05
Dec 96	7.40 ± 0.10	7.73	7.50 ± 0.12
Jan 97	7.70 ± 0.24	7.90 ± 0.04	7.94 ± 0.02
Feb 97	7.85 ± 0.08	7.97 ± 0.02	8.00 ± 0.07
Mar 97	R.V. *Tamaris* not available		7.86 ± 0.06
Apr 97	8.64 ± 0.09	8.02 ± 0.02	8.72 ± 0.12
May 97	8.04 ± 0.54	8.05 ± 0.01	8.13 ± 0.63
Jun 97	8.69 ± 0.14	8.10 ± 0.02	8.59 ± 0.40
Jul 97	7.77 ± 0.17	8.15 ± 0.05	8.02 ± 0.26
Aug 97	9.00 ± 0.12	8.21 ± 0.04	9.13 ± 0.19
Sep 97	R.V. *Tamaris* not available		8.90

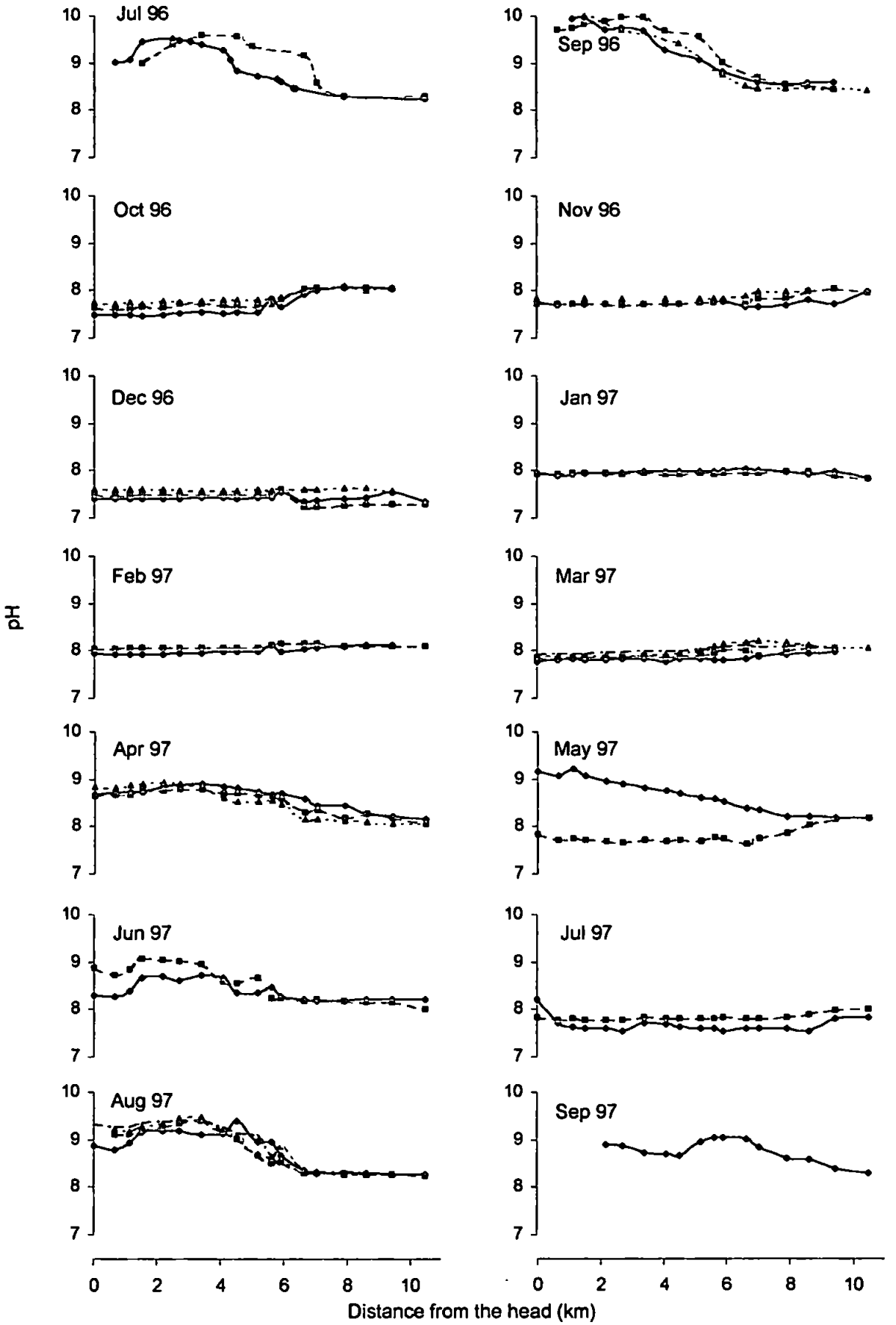

Figure 5.3 Axial profiles of pH in the Tweed Estuary. The data are plotted chronologically as 1st (◆), 2nd (■), 3rd (▲) and 4th (—) profile per survey.

The pH showed a gradual rise through the spring to mid to late summer values of pH 9 to 10, followed by a rapid decrease between September and October to winter values of pH 7 to 8. These were similar to the seasonal trends observed at Norham and in the lowest salinity measurements collected during the repetitive and anchor station surveys.

During July 1996, June and August 1997 and to a lesser extent September 1996 and April 1997 the extended axial surveys showed an increase in pH between 2 and 4 km from station 20. To test how closely the observed pH distributions conformed to those predicted, using the approach of Mook & Koene (1975), a model was developed to account for the influence of salinity, temperature and the variation in end member pH and alkalinity. This has been applied to both data sets described above.

5.3 Predicting abiotic controls of pH

Morris *et al.* (1982), de Mora (1983) and Muller *et al.* (1994) compared thermodynamically predicted values of pH with observed measurements, but did not fully describe the methodology they used to generate the theoretical dilution curve of pH. Harris *et al.* (1993) suggested a method for modelling the carbonate system in the ECoS V2 user manual, but a pH template was not included in ECoS3.

The following section describes the development of a code to predict the change in pH with salinity following the methods described by Mook & Koene (1975). The model assumed that although the partial pressures of CO_2 may vary from that in the atmosphere there was no gaseous exchange across the water-air interface. The model also assumed that the alkalinity was in the form of bicarbonate and carbonate ions in certain ratios for a given salinity and temperature, and that carbonate alkalinity (A_C) and total inorganic carbon (C_T) were conserved. This is discussed more fully in Section 5.3.2. The pH evolution with salinity was then dependent upon the alkalinity, temperature and the pH of the freshwater and marine end members. The model calculated intermediate carbonate ratios and pH for given salinity and temperature values. The model was initially compiled within a spreadsheet and then subsequently encoded as a template for use in ECoS3.

5.3.1 Predicting alkalinity in the Tweed Estuary

End member and intermediate values of temperature and salinity were collected concurrently with pH measurements during all surveys. Measurements of alkalinity were

however only made during 11 surveys in July and November 1996 and April, February and July 1997 (Howland *et al.*, 2000). Water samples were first filtered through GF/F filters and alkalinity (mequiv. l^{-1}) was then determined by acidimetric titration (Gran procedure) following the method described by Leek *et al.* (1997). A method of estimating the alkalinity of riverine and estuarine water during the other surveys was therefore required before the model could be applied.

The mean and range of alkalinity in the Tweed was 1.3 (0.8 to 2.2) mequiv. l^{-1} and in the Whiteadder 2.1 (1.4 to 2.7) mequiv. l^{-1} and Figure 5.4 shows a correlation ($p < 0.001$) between flow and alkalinity in both rivers. The higher alkalinity of river water in the Whiteadder may be due to the different river flow-catchment size ratio as discussed in Section 4.4, but may also represent the higher proportion of carboniferous limestone (McAdam, 1993, Jarvie *et al.*, 2000) in the Whiteadder catchment.

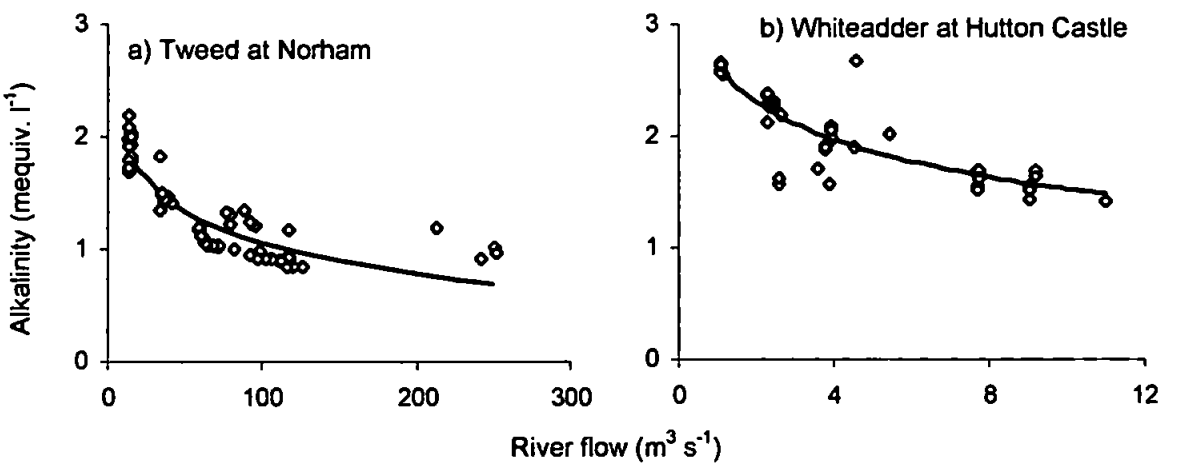

Figure 5.4 Flow – alkalinity relationship for (a) the Tweed (n = 65) and (b) the Whiteadder Rivers (n = 50). Data supplied by Tappin (*per. comm.* 1999) and covers the period 1996-1997. The regression of $a - b$*ln(Q) where a = 2.91 and b = 0.40 in the Tweed and a = 2.64 and b = 0.49 in the Whiteadder explains 76 % and 83 % of the variability of the alkalinity in the two rivers respectively.

Measurements of alkalinity were also made at Norham, station 20 and station 16 during the survey period and the mean and standard deviation of these results for 6 periods are shown in Table 5.3.

The results showed that there was no statistical difference between the data from the three sites at the 95 % confidence level. Biological or geochemical mediation of total alkalinity between Norham and the upper part of the estuary was therefore minimal and it was assumed that predictions made at Norham could be extrapolated to the head of the estuary. A comparison of predictions of flow determined alkalinity at Norham with values

measured at station 16 gave an R^2 regression of 0.73 ($p < 0.001$). Alkalinity values were also reported for the Tweed by Howland *et al.* (2000). They noted that alkalinity ranged from 0.8 to 1.9 mequiv. l^{-1} in the low salinity tidal reaches and was relatively constant within a given survey. Some variation may however arise due to rapid fluctuations in river flow and corresponding changes in source waters or through biological mediation. A comparison of predictions using the flow-alkalinity relationship determined at Norham with values reported by Howland *et al.* (2000) gave an R^2 regression of 0.76 ($p < 0.001$) again indicating the usefulness of this relationship.

Table 5.3 A comparison of the mean and standard deviation of alkalinity measured at Norham with that in the Tweed Estuary. Data supplied by Tappin (*per. comm.* 2000). ND = No data.

	Alkalinity (mequiv. l^{-1})		
	Norham	Station 20	Station 16
14-17 Jul 1996	1.88 ± 0.15 (n = 15)	1.82 ± 0.02 (n = 9)	ND
8-12 Nov 1996	0.93 ± 0.08 (n = 19)	0.86 ± 0.09 (n = 2)	ND
7-10 Feb 1997	1.12 ± 0.10 (n = 14)	ND	1.13 ± 0.09 (n = 15)
6-9 Apr 1997	1.44 ± 0.03 (n = 16)	ND	1.46 ± 0.03 (n = 10)
6-7 Jul 1997	1.25 ± 0.58 (n = 6)	ND	1.25 ± 0.57 (n = 6)
17 July 1997	ND	1.80 (n = 1)	1.82 (n = 1)

Alkalinity of seawater is typically higher and more constant than that of the Tweed River water ranging from 2.0 to 3.0 mequiv. l^{-1} (Wong, 1979; de Mora, 1983; Cifuentes *et al.*, 1990; Benoit *et al.*, 1994; Muller *et al.*, 1994). At salinity of 30 to 33 Howland *et al.* (2000) reported alkalinity to range from 2.0 to 2.3 mequiv. l^{-1} in the Tweed although it is hard to determine any kind of seasonal or flow driven signal in this variation. A marine boundary alkalinity of 2.3 mequiv. l^{-1} was therefore used in the model runs.

Howland *et al.* (2000) also noted a linear relationship between carbonate alkalinity and salinity and found that the carbonate alkalinity was never less than ~96.5 % of the total alkalinity. Initial model runs to investigate the variation in pH with salinity therefore assumed conservative mixing between marine and riverine end member alkalinity and used values of total alkalinity.

The Whiteadder may introduce waters of different alkalinity and pH into the mid region of the Tweed Estuary. Although a flow-alkalinity relationship has been determined for the Whiteadder its incorporation into the model would have added additional degrees of freedom and made interpretation of the results more difficult. The influence of the Whiteadder was therefore not encoded at this stage of model development.

5.3.2 Equilibrium modelling of carbonate speciation

During estuarine mixing of fresh and seawater the individual dissolved inorganic carbon fractions of CO_2, HCO_3^- and CO_3^{2-} do not behave conservatively due to the chemical rearrangement in the following dissociation equilibria:

$$H_2O + CO_2 \overset{K_1}{\Leftrightarrow} H^+ + HCO_3^- \overset{K_2}{\Leftrightarrow} CO_3^{2-} + H^+ \quad \textbf{(5.2)}$$

Following Mook & Koene (1975) the calculation of carbonate equilibria assuming no CO_2 exchange with the atmosphere or biota can be described by:

$$[a_H]^2 + [a_H]K_1(1-N) + K_1K_2(1-2N) = 0 \quad \textbf{(5.3)}$$

where a_H is the concentration of hydrogen ions (moles), defined by pH, *i.e.*, -log a_H. N represents the ratio of total dissolved inorganic carbon, C_T, *i.e.*, the sum of CO_2, HCO_3^- and CO_3^{2-}, to that of carbonate alkalinity, A_C:

$$N = \frac{C_T}{A_C} = \frac{[CO_2] + [HCO_3] + [CO_3]}{[HCO_3] + [2CO_3]} \quad \textbf{(5.4)}$$

and K_1 and K_2 are the first and second dissociation constants of carbonic acid. The ratio (N) of total dissolved inorganic carbon to the carbonate alkalinity for the freshwater and marine end members respectively is calculated according to Mook & Koene, (1975) Equation 8:

$$N = \frac{a_H^2 + a_H K_1 + K_1K_2}{a_H K_1 + 2K_1K_2} \quad \textbf{(5.5)}$$

where a_H is the hydrogen ion activity of the freshwater and marine end members determined from the pH and K_1 and K_2 dissociation constants. The carbonate alkalinity was

assumed to have changed linearly with salinity and the ratio, J, between freshwater (N_f) and marine (N_m) values was calculated according to:

$$J = \frac{N_f}{N_m} = \frac{((1-b)N_f Z + bN_m)}{((1-b)Z + b)} \quad \textbf{(5.6)}$$

where b and Z are the salinity and alkalinity ratios respectively. The salinity ratio varied from zero in freshwater to 1 at full marine salinity while Z is a constant defined by the riverine / marine carbonate alkalinity ratio. The pH is then calculated according to Mook & Koene, (1975) Equation 15:

$$\text{pH} = \quad -\log\left(\frac{(-(1-J)K_1 + \sqrt{((1-J)K_1)^2 - 4(1-2J)K_1K_2)}}{2}\right) \quad \textbf{(5.7)}$$

5.3.3 Carbonate dissociation constants

Wanninkhof *et al.* (1999) noted that there have been four independent determinations of the carbonate dissociation constants since the first sets of apparent dissociation constants for seawater were prepared in the 1950s, *i.e.*, Hansson (1973); Mehrbach *et al.* (1973); Goyet & Poisson (1989) and Roy *et al.* (1993). Mehrbach *et al.* (1973) was the only worker to conduct experiments using real, opposed to artificial seawater, and to have determined constants at low partial pressures of CO_2. The combination and refit of the Hansson (1973) and Mehrbach *et al.* (1973) constants by Dickson & Millero, (1987) led to a formulation suitable for salinity of 0 to 35 and temperatures 2 to 35°C. Ghosh & Janna (1994) calculated the dissociation constants of carbonic acid in estuarine water (salinity 0.1 to 31.7 and temperature 5 to 35°C). The results were found to be comparable with those obtained using the Dickson & Millero (1987) refitted constants with average differences being less than 4.4 %. Wanninkhof *et al.* (1999) also found that the formulation of Dickson & Millero (1987) provided the best fit for their results. These constants, as presented by Regnier *et al.* (1997) in their model simulations of pH in the Scheldt Estuary and used in this study are:

$$-\log K_1 = \quad \frac{6320.81}{T_K} - 126.3405 + 19.568\ln T_K + \left(19.894 - \frac{840.39}{T_K} - 3.0189\ln T_K\right)\sqrt{S} + 0.0068S \quad \textbf{(5.8a)}$$

$$-\log K_2 = \quad \frac{5143.69}{T_K} - 90.18329 + 14.613\ln T_K + \left(17.176 - \frac{690.59}{T_K} - 2.6719\ln T_K\right)\sqrt{S} + 0.0217S \quad \textbf{(5.8b)}$$

where S is salinity and T_K is the absolute temperature (K).

5.3.4 Sensitivity analysis of pH predictions

To test the sensitivity of model predictions freshwater pH, temperature and alkalinity were systematically altered and the effect on intermediate pH observed. Marine pH and alkalinity were kept constant at 8 and 2 mequiv. l^{-1} respectively during this testing, see Figures 5.5 to 5.7.

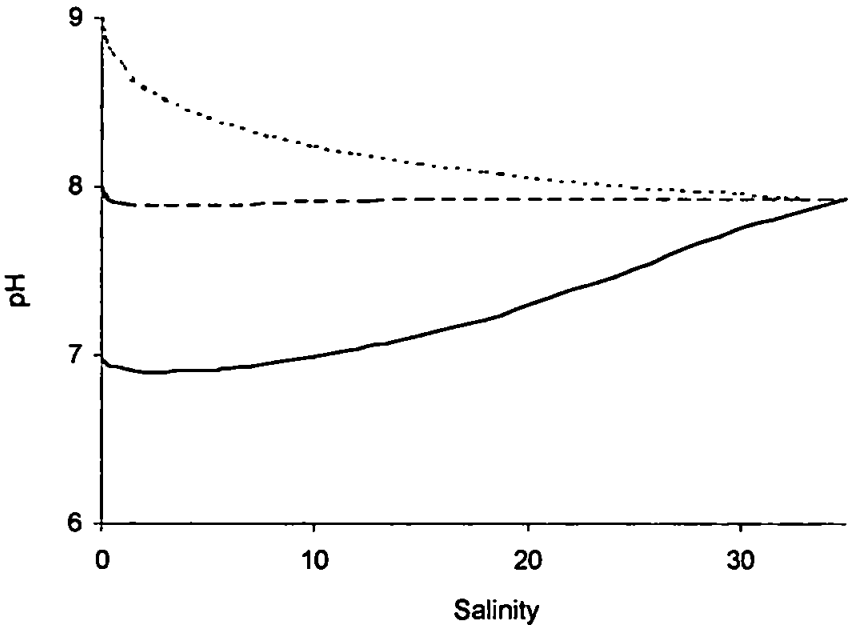

Figure 5.5 Predicted pH at 10°C and N_f / N_m = 0.5 for freshwater pH of 7 (—), 8 (— —) and 9 (—·—) units.

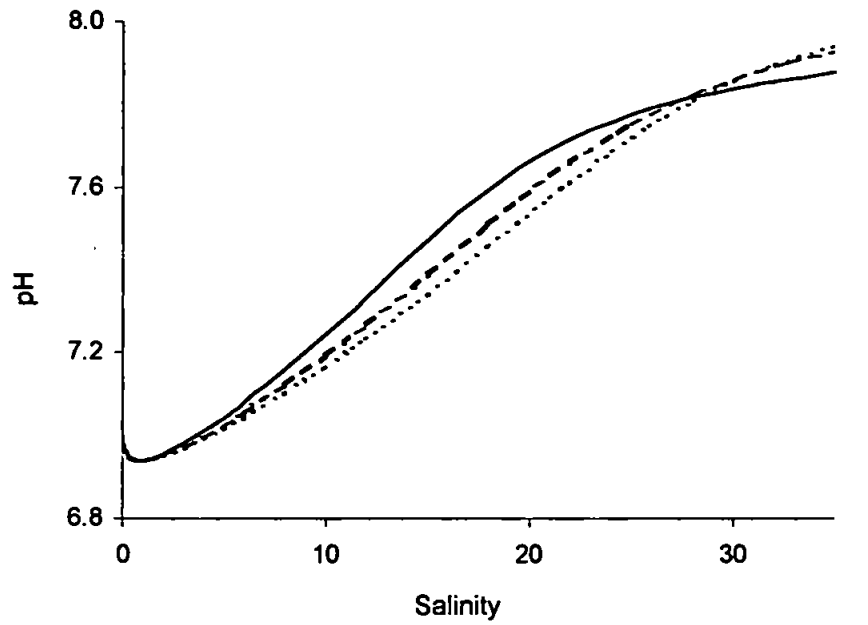

Figure 5.6 Sensitivity of pH predictions with salinity to temperature of 5°C (—), 10°C (— —) and 20°C (—·—). N_f/N_m = 0.25.

Changes in temperature generated a maximum difference of 0.14 units between salinity of 15 and 20 when freshwater pH and N_f/N_m were 7 and 0.25 respectively. This difference became smaller as the freshwater pH and alkalinity was increased. These small differences are below the level of accuracy of the YSI 6000 so could not be clearly resolved in the observed data.

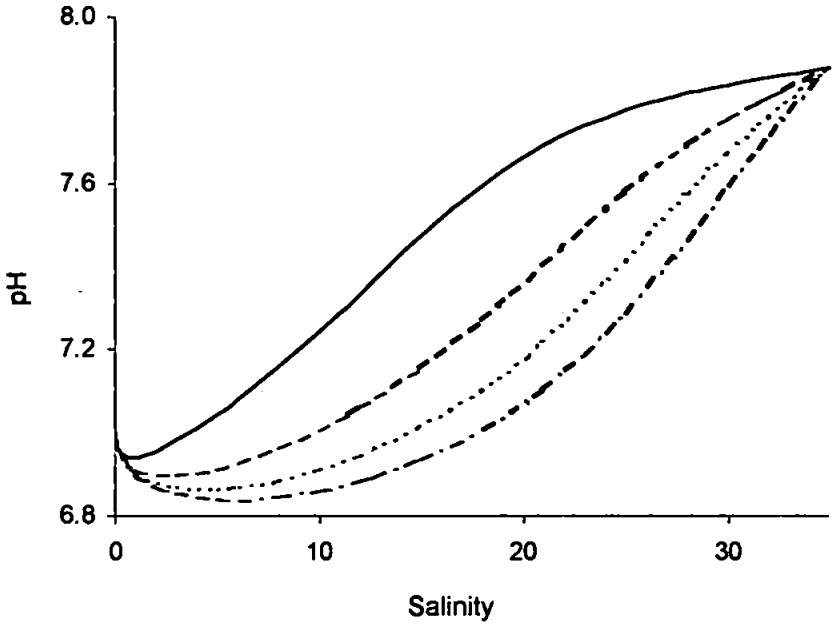

Figure 5.7 Sensitivity of pH predictions with salinity to alkalinity N_f/N_m of 0.25 (—), 0.5 (— —), 0.75 (----) and 1.00 (— · —). Temperature = 20°C.

Variation in the alkalinity ratio had the greatest effect when freshwater pH was also low, and the temperature high and accounted for up to 0.59 pH units difference between salinity of 15 and 20.

As the temperature was reduced and freshwater pH increased, the change in intermediate pH became smaller. A change in freshwater alkalinity from 0.5 to 2.0 mequiv. l^{-1} can therefore have a significant effect on the pH prediction. Incorrectly defining the end member alkalinity and also the assumption of conservative behaviour with salinity may therefore be a potential source of error in model predictions.

5.4 Model predictions of abiotic control of estuarine pH

The model was first applied to the data from the repetitive and anchor station surveys to verify the approach. Once the performance on one data set had been assessed, the model was then used to investigate the pH distribution observed during the extended axial surveys.

5.4.1 Validation of model predictions

The time series data from each survey was sorted so that measurements of temperature and observed pH were tabulated against salinity. The model set up assumed that the end members represented salinity of 0 and 35. Where the field data did not extended to 0 or 35 salinity the end member pH and temperature were estimated. For the majority of the surveys temperature showed a linear correlation with salinity and the end member temperatures were determined by extrapolating a linear regression to the data. Where data was restricted to low salinity measurements, marine end member pH and temperatures were determined from another day in the survey period. The model was run for each day that repetitive axial or anchor station data was available and the predicted pH for each intermediate temperature and salinity value compared to the observed pH measurement, see Figure 5.8.

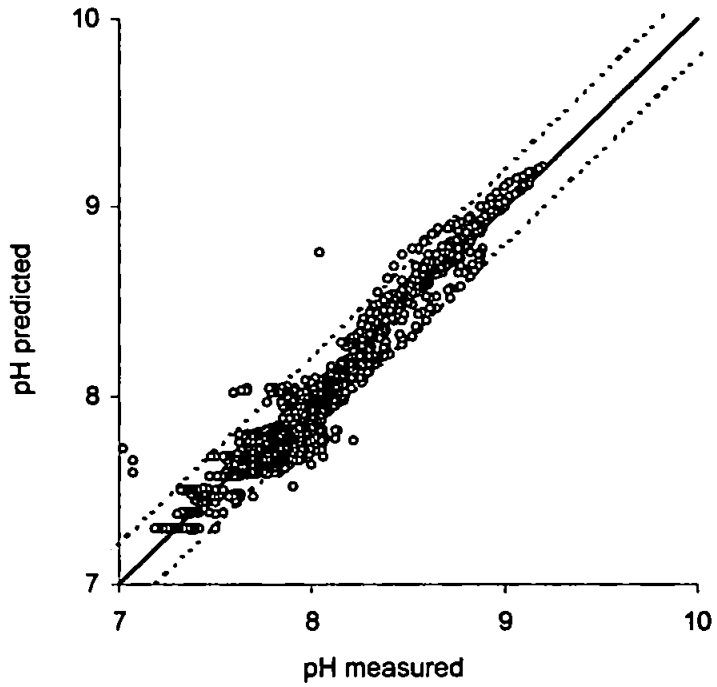

Figure 5.8 Comparison of observed and predicted pH for all of the anchor station and repetitive axial surveys. R^2 = 0.94 (n = 1750) when forced through the origin (—).The ± 0.2 unit precision of the YSI 6000 pH sensor is indicated by the dashed lines.

The model predicted 94 % of the variability in the data. To determine how the model responded to different conditions the results have been broken down into each survey period. Data from one day per survey period has been chosen to best illustrate model performance and is shown in Figure 5.9.

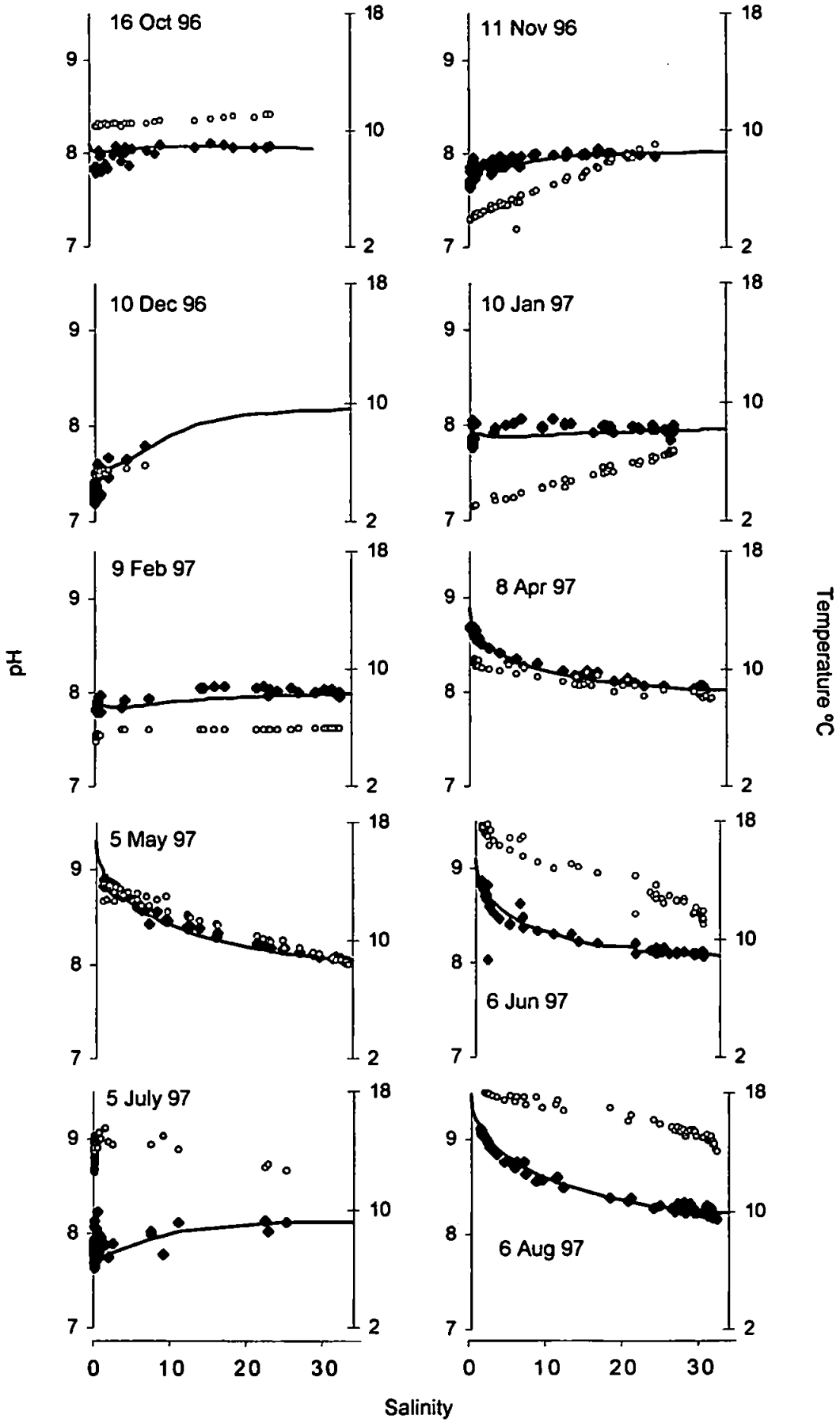

Figure 5.9 Predicted (—) and observed (◆) pH recorded during the repetitive and anchor station surveys in the Tweed Estuary. Temperature (○) is also shown.

The model predictions during higher freshwater pH of 8.5 to 9.5 (*e.g.*, April, May, June and August 1997) more closely match the observed values ($R^2 = 0.88$). Sensitivity testing however showed that during high freshwater pH the predictions were relatively insensitive to inaccuracies in determining alkalinity and this may in part account for the better model fit to observed data during high freshwater pH. These results implied that an assumption of conservative behaviour of alkalinity and total inorganic carbon could be applied to the pH variation with salinity in the lower reaches of the estuary (stations 8 to 3) under most conditions. They also show that the formulation of the model is adequate to describe the pH variation with alkalinity, temperature and salinity.

In January and February 1997 the model under predicted pH by up to 0.2 units at mid salinity. A reduction in alkalinity of 25 % is required to account for these differences. This may indicate inaccuracy in determining the end member alkalinity or non-conservative behaviour within the estuary. Between October 1996 and February 1997 and in July 1997 the variability in freshwater pH during each survey was not reproduced by the model. Single values of river water pH and alkalinity were used each day and may not have been appropriate during rapidly changing hydrographs.

5.4.2 Model application to the extended axial surveys

Using similar methodologies to those outlined above, the model was then applied to the extended axial transect data to determine whether a conservative behaviour of alkalinity and total inorganic carbon assumption could be used during the modelling of pH throughout the tidal reaches of the Tweed.

The model predictions are compared with observed data in Figure 5.10. The overall performance of the model explained 88 % of the variability in measured values, a lower agreement that that found for the previous data set. The results showed that the model under predicted pH when observed values were between 8.5 and 9.5. To determine how the model responded to different conditions model runs were conducted for each extended axial survey and data from one day per survey period was chosen to best illustrate model performance, see Figure 5.11.

The model predictions during October 1997 and March 1997 again under-predicted pH at mid-salinity by up to 0.4 units This could be a due to incorrect estimation of the alkalinity

as suggested during the repetitive axial survey. These differences may also represent the influence of the Whiteadder, possibly introducing higher pH water into the Tweed, which has not been account for by the model.

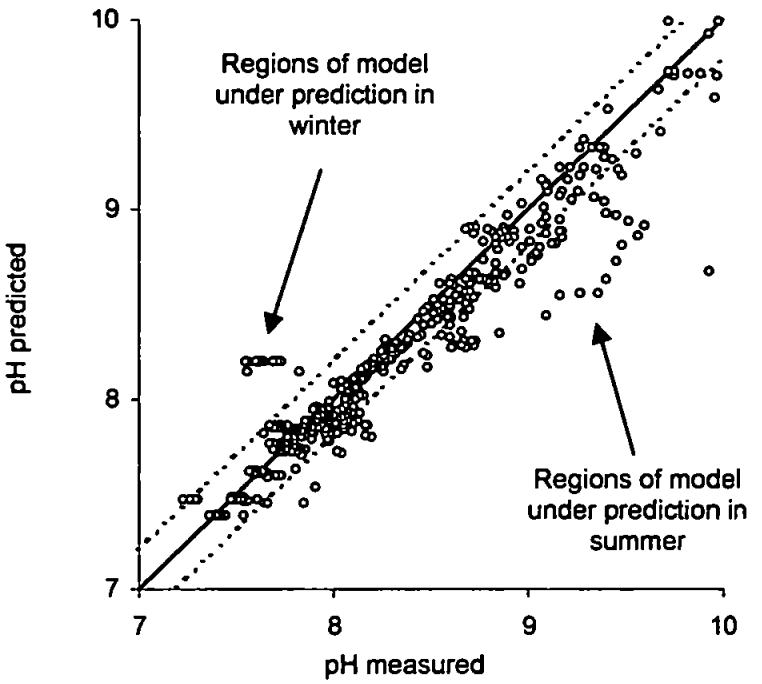

Figure 5.10 Comparison of predicted and observed pH for all of the extended axial surveys. An R^2 correlation (—) forced through the origin = 0.88, (n = 550). The ± 0.2 unit precision of the YSI 6000 pH sensor is indicated by the dashed lines.

Mook & Koene (1975) predicted a pH minimum at a specific mixing ratio of fresh and seawater. To a small degree in April and more obviously in July and September 1996 and June and August 1997, these data showed a peak in pH in the freshwater and low salinity region of the upper estuary. The difference between modelled and observed results could not be accounted for by differences in the alkalinity and the model predictions made during high pH for the previous data set were good ($p < 0.001$) and did not show this deviation. The difference between modelled and observed pH increased between stations 18 and reached a maximum of up to 1.25 units between stations 15 and 14 at 3 to 4 km from the head. Increasing the riverine pH boundary value in model simulations to that of the pH maximum showed that the reduction in pH beyond this point was due to dilution and increasing salinity. There is also discrepancy between modelled and observed pH in October 1996 and March 1997. The difference however occurs further down the estuary and the pH increase occurred at higher salinity. The location is coincident with the Whiteadder and may indicate some influence from the tributary.

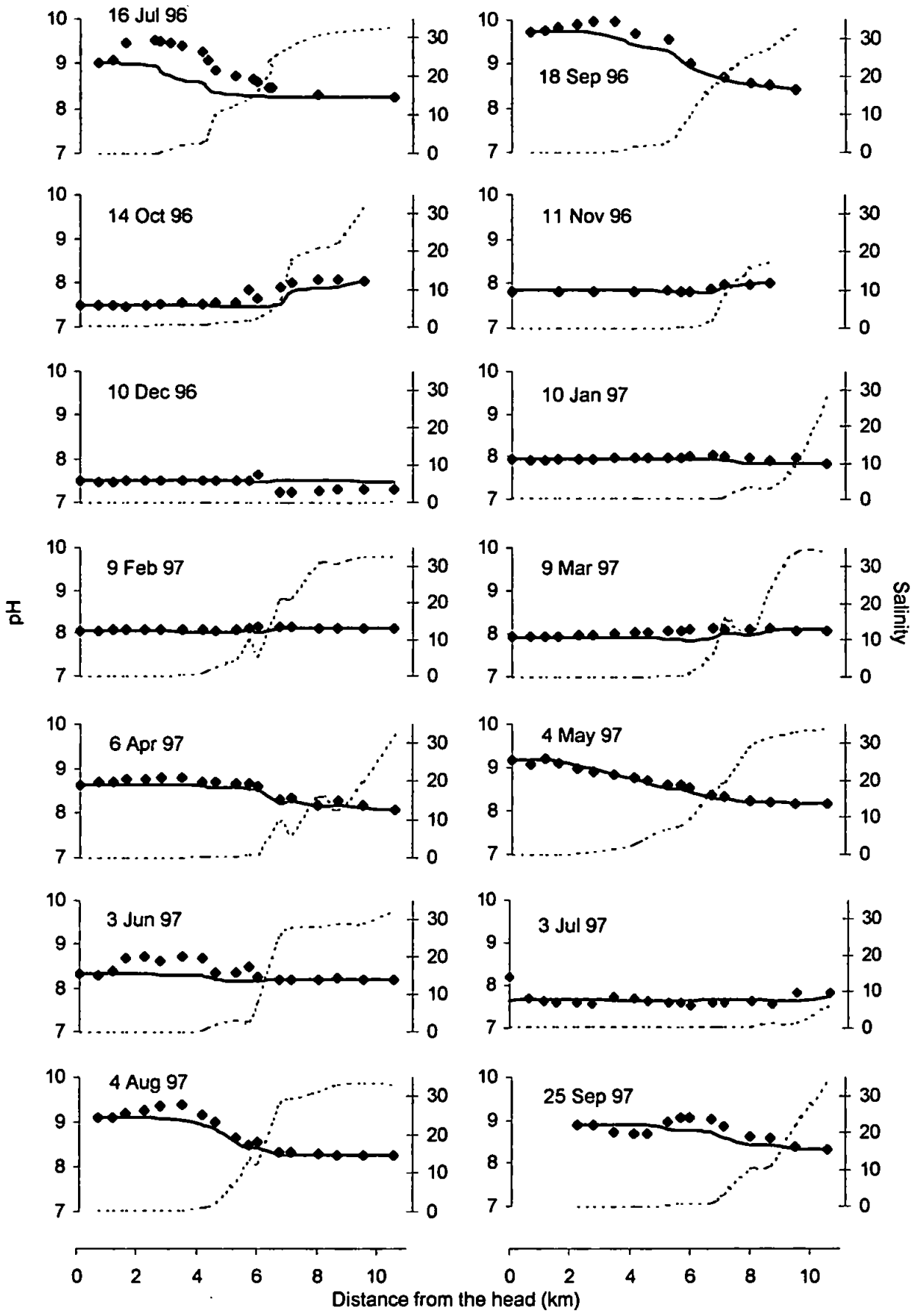

Figure 5.11 Predicted (—) and observed pH (◆) recorded during the extended axial surveys of the Tweed Estuary. Salinity is also shown (—).

5.4.3 pH variation with depth

So far discussions have focused on surface measurements of pH. The pH variation with depth was also investigated. Due to salinity stratification the results are plotted against salinity and are shown along with model predictions in Figure 5.12.

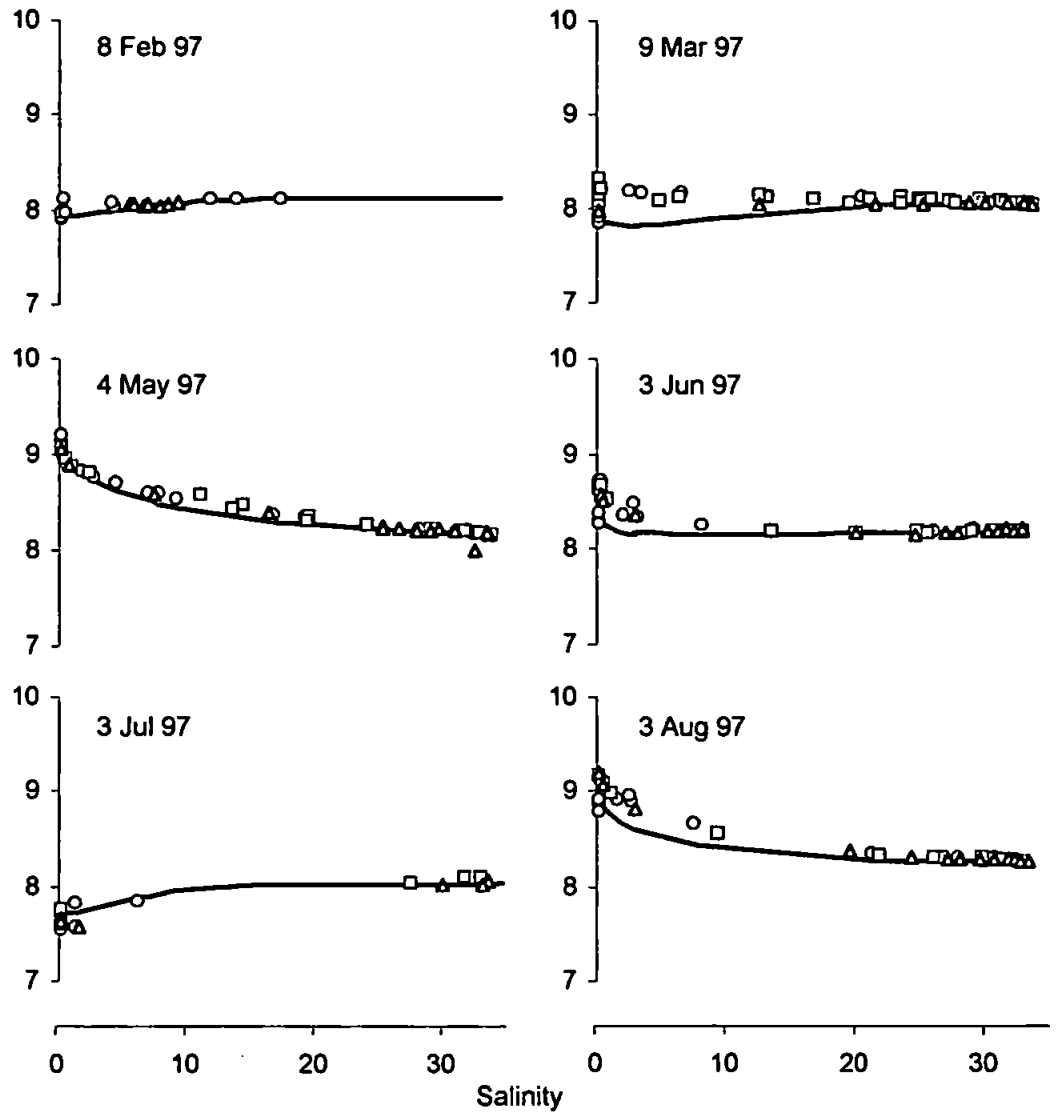

Figure 5.12 Comparison of pH measurements at the surface (o), in the middle of the water column (□) and above the bed (Δ). Model prediction based on surface pH of the end members are also shown (—).

The pH data from surface waters, within the water column and at or above the bed showed a consistent behaviour with salinity, with a region of elevated pH at salinity < 1. Depth measurements were not however made above station 15 and although no salinity stratification was present pH variation with depth may have occurred. This implies that between stations 3 and 15, regardless of position in the water column, the effect of salinity

on ion activity is a driving influence on the CO_2 system and hence on the H^+ concentration and pH.

5.4.4 Diurnal variation in the pH

Diurnal variability in pH has been reported within the Tweed River (Jarvie *et al.*, 2000), but could not be resolved through the EATs. Records of the diurnal variation in pH within the upper estuary were however available from the EMP rig at station 16. Data available over several consecutive days, when there was no saline intrusion up to station 16 was unfortunately limited to the April 1997 survey. The results are shown in Figure 5.13.

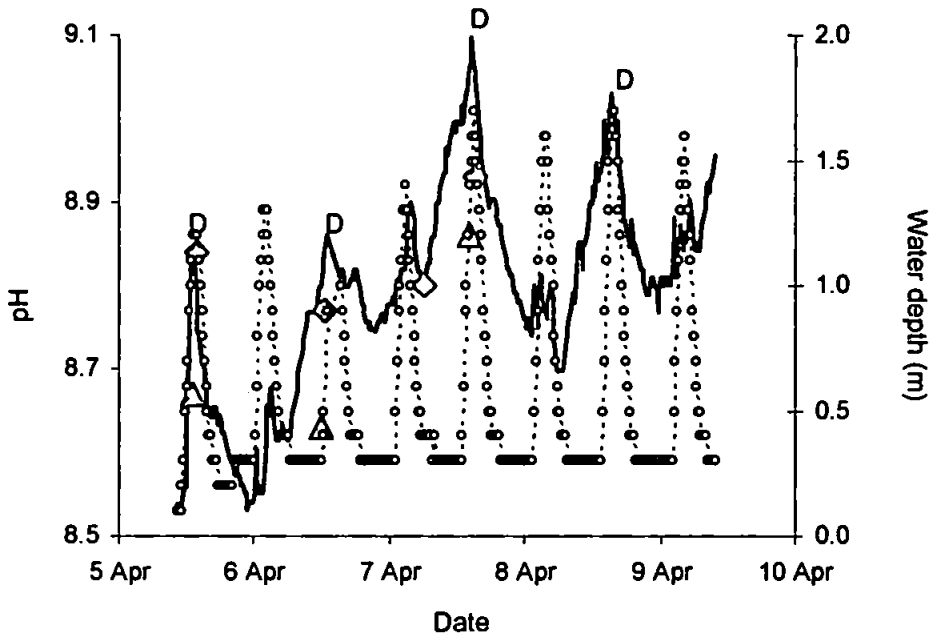

Figure 5.13 Comparison of pH measurements made by the EMP rig at station 16 (—) and surface measurements taken in the vicinity (◆). The tidally variable water depth is also shown (–o–). The instrument recorded zero salinity during this period. The pH peaks that are coincident with the high water around mid-day to early afternoon are marked by the D.

The increasing trend in pH (8.5 to 8.9) and water temperature (9.5 to 11.5°C), Figure 5.14 can be related to a gradual reduction in the river flow (42 to 33 $m^3 s^{-1}$) and increased hours of bright sunshine (0.5 to 10) during this period, Figure 5.15. The more striking feature of the pH and temperature data is however that of the diurnal variability, both of which showed peaks that are at a maximum during the day. The peaks are not however coincident with maximum irradiance (Figure 5.14), but are correlated ($p < 0.001$) with high water. The daily pH increase began during low water and then rose at a relatively constant rate through the remainder of the low water and flood tide, reaching a maximum at high water. Peaks in temperature only occurred at high water during the day. Peaks in pH were at a

maximum during the day, but also showed secondary peaks during high water at night. The mean increase during the day was 0.30 ± 0.03 units while that at night 0.13 ± 0.03 units. The increase during the day was comparable to a maximum difference of 0.23 unit between modelled and predicted results for the EATs in April.

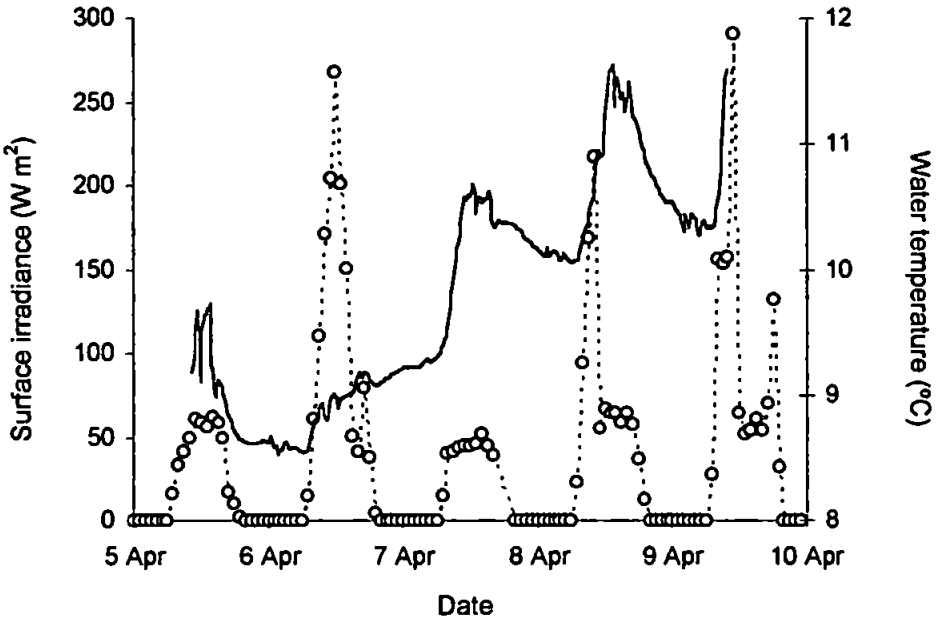

Figure 5.14 Comparison of surface irradiance (—) W m^2 measured at Charterhall and water temperature recorded by the EMP rig at station 16 (—).

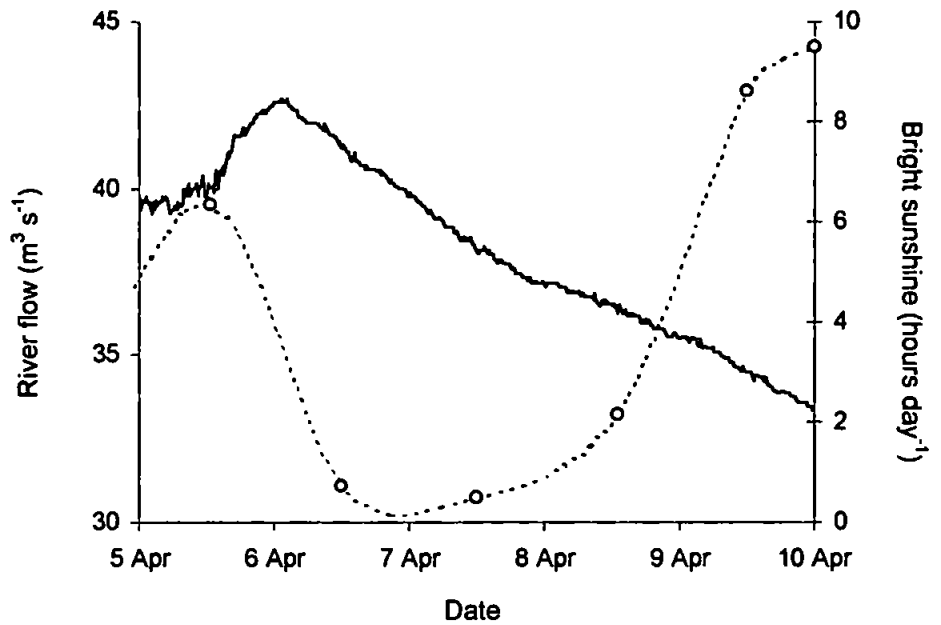

Figure 5.15 Comparison of river flow (—) measured at Norham and hours of bright sunshine, taken as a mean of data from the Galashiels and Boulmer monitoring stations (—).

The increase of pH in response to light availability implies that biological processes, *i.e.*, photosynthesis are important, but that an additional hydrodynamic control is also acting.

The increase in pH during high water at night is on average 43 % of that during the day. This may represent a water mass, where the pH had been elevated previously, that had not been flushed from the estuary and was being forced back up stream by the advancing salt wedge. Increasing salinity is the main control on reducing the pH and low concentrations of phytoplankton (Shaw *et al.*, 1998) and DOC (Martino, 1999 *per. comm.*) ensure that there would be minimal production of respiratory CO_2 and reduction of the pH in this water.

5.5 Biotic controls of pH in the Tweed River-Estuary

To determine whether the pH variations from the thermodynamically predicted value could be attributed to photosynthetic activity the dissolved oxygen saturation and nutrient concentrations in the estuary were investigated.

5.5.1 O_2-CO_2 balance and photosynthesis in the Tweed Estuary

Dissolved oxygen concentrations exceeding saturation have been recorded in the Tweed Estuary during April, July and September 1991 and February 1992 (Balls, 1994) and the dissolved oxygen saturation recorded during the repetitive surveys and extended axial surveys are shown in Figures 5.16 and 5.17. These show that the O_2 saturation tended to be lower in the winter and higher in the summer, but was reduced by high river flows in the summer, and this is similar to the pH distributions discussed in the previous section. There is not however a statistically significant relationship at the 90 % or higher confidence limit between the two variables at the head of the estuary.

Between stations 3 and 8 O_2 saturation varied from mean values of 84 to114 % with minimum and maximum values of 70 and 128 % in May and August respectively. During the extended axial surveys the mean saturation ranged from 79 to 123 % with minimum and maximum values of 71 to 160 % in January 1997 and July 1996. During the extended and repetitive axial transects in October, November and December 1996 and from March to May oxygen was at or near 100 % saturation and was quite invariant throughout the salinity range. Saturation between 70 to 80 % was restricted to surveys in January, February and May 1997. The low values in May coincided with increased river flow from 21 to 78 $m^3\ s^{-1}$ and resulted in a decrease of oxygen saturation from 138 to 86 %. There and was also an associated decrease in pH from 9.2 to 7.9. The high saturation measured in October and December 1996 and March 1997 may have resulted from physical aeration of

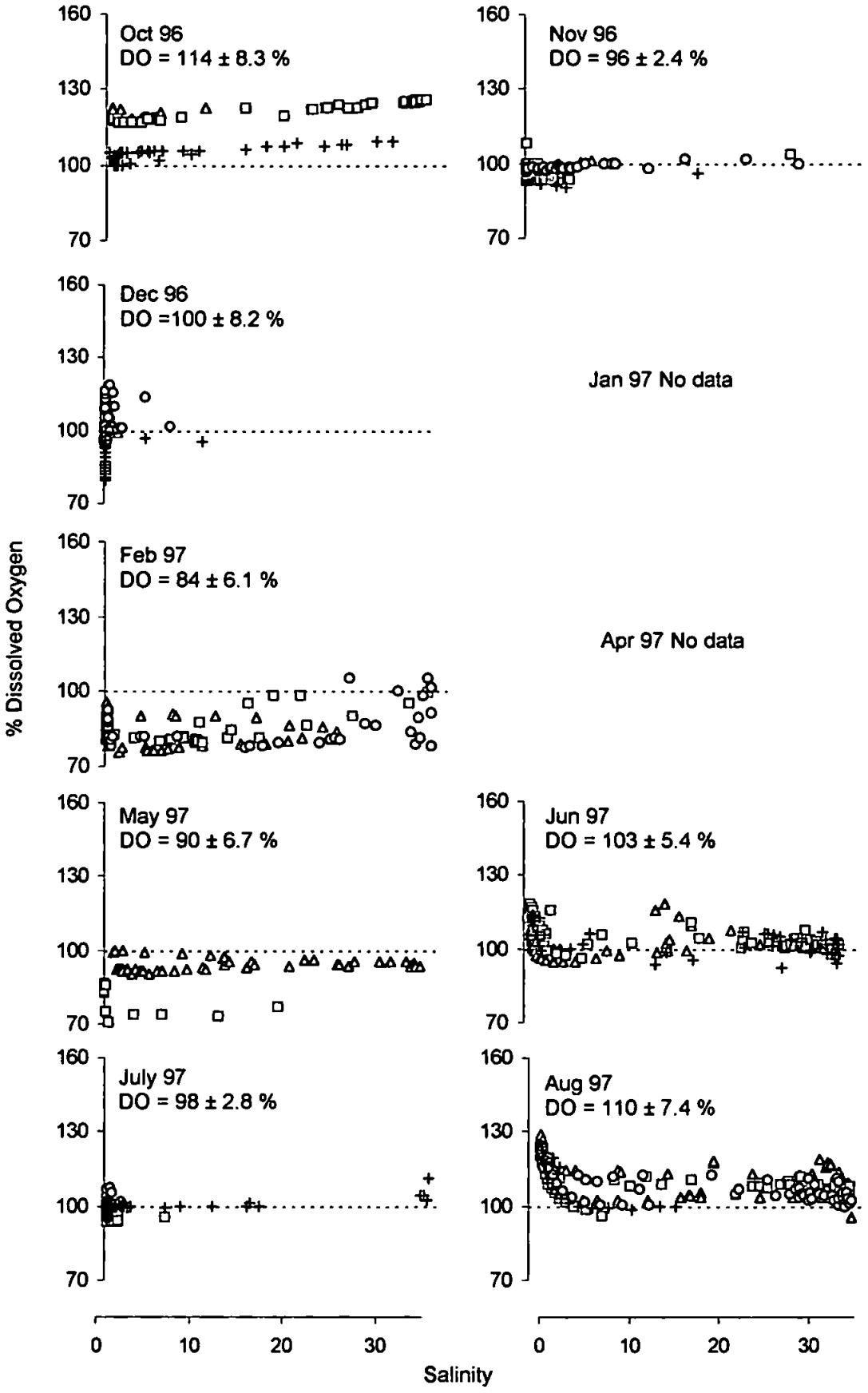

Figure 5.16 Percentage dissolved oxygen measured during the anchor station surveys and repetitive axial transect surveys between stations 3 and 8 in the Tweed Estuary. 100 % saturation is marked (—) for reference and the mean and standard deviation of the survey results shown. The different symbols represent different days in the surveys.

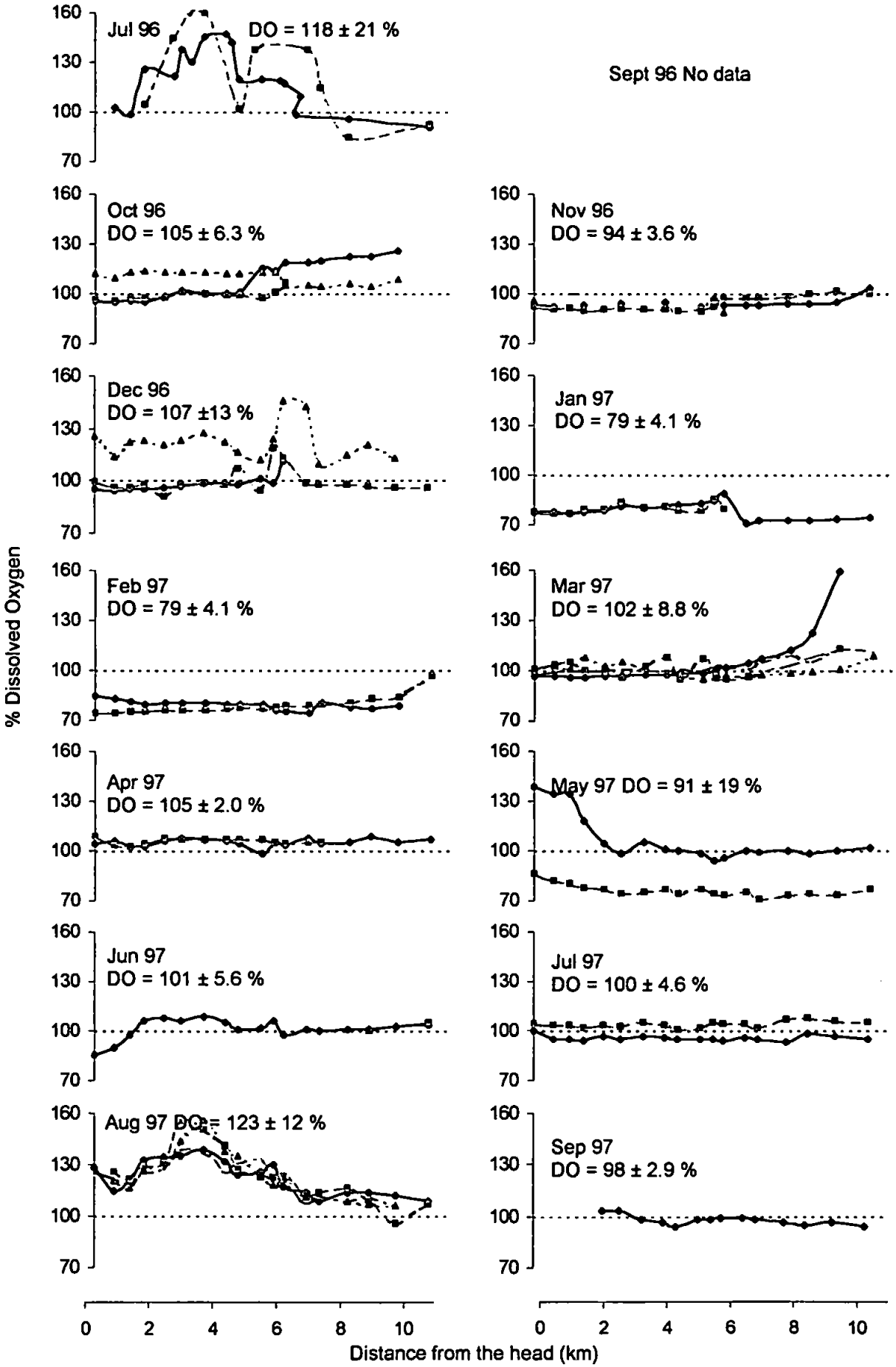

Figure 5.17 Axial profiles of oxygen saturation in the Tweed Estuary. 100 % saturation is marked for reference (—) and the mean and standard deviation of the survey results shown.

the water through wave swell action (Balls, 1994). The supersaturation measured in July 1996 and August 1997 and to a lesser extend in June 1997 however increased in the upper reaches of the estuary coincident with the peaks in pH from approximately 100 to between 120 and 130 % at salinity below 2 units. The co-variance of pH and dissolved oxygen implies that primary production may have affected the pH.

5.5.2 Photosynthetic carbon uptake

To determine how much inorganic carbon would have needed to be removed in order to elevate the pH the model was adapted to predict concentrations of the inorganic carbon fractions. These have then been compared to oxygen saturation and chlorophyll *a* concentrations (Uncles *et al.*, 2000).

The carbon fractions can be expressed in terms of the hydrogen ion activity (a_H), carbonate alkalinity (A_C.) and carbonic acid dissociation constants (K_1, K_2) using the relationship determined by Mook and Koene (1975, Equation 5):

$$D = \frac{A_C}{a_H K_1 + 2K_1 K_2} \qquad \textbf{(5.9)}$$

where (D) is used to calculate the molar concentration of CO_2, HCO_3^- and CO_3^{2-} using the following relationships:

$$[CO_3^{2-}] = K_1 K_2 D \qquad \textbf{(5.10a)}$$

$$[HCO_3^-] = a_H K_1 D \qquad \textbf{(5.10b)}$$

$$[CO_2] = (a_H)^2 D \qquad \textbf{(5.10c)}$$

Assuming conservative behaviour of carbonate alkalinity the concentration of total inorganic carbon was calculated for the observed and predicted pH measurements. The difference between the two values indicates the concentration of CO_2 that needs to be removed from the water to elevate the pH has been compared to the percentage oxygen saturation. Due to problems with the oxygen probe comparisons were limited to data from July 1996 and June and August 1997 surveys. The results of which are shown in Figure 5.18. There was a statistical significant ($p < 0.001$) relationship between these two variables, the slope of the regression however identified two groups within the data; a) July

1996 and June 1997 and b) August 1997. Compared to the August 1997 data a corresponding increase in O_2 saturation was associated with over a three-fold increase in C_T removal during the July 1996 and June 1997 surveys.

It is difficult to identify why the difference in regressions occurred. The O_2 saturation at the head of the estuary was higher in August 1997 (125 %) compared to that in July 1996 (103 %) or June 1997 (86 %), although there was little difference in the pH between the August and July surveys. The water temperature in the upper estuary during the August surveys was 18.7 ± 0.36°C. The corresponding temperature during June 1997 was lower (14.6 ± 0.06°C), but that recorded during July 1997 was higher (20.3 ± 0.6°C). The differences in the O_2-C_T uptake regression does not therefore seem have resulted from the effects of temperature on the dissociation of carbonic acid or the solubility of either O_2 or CO_2 in the water.

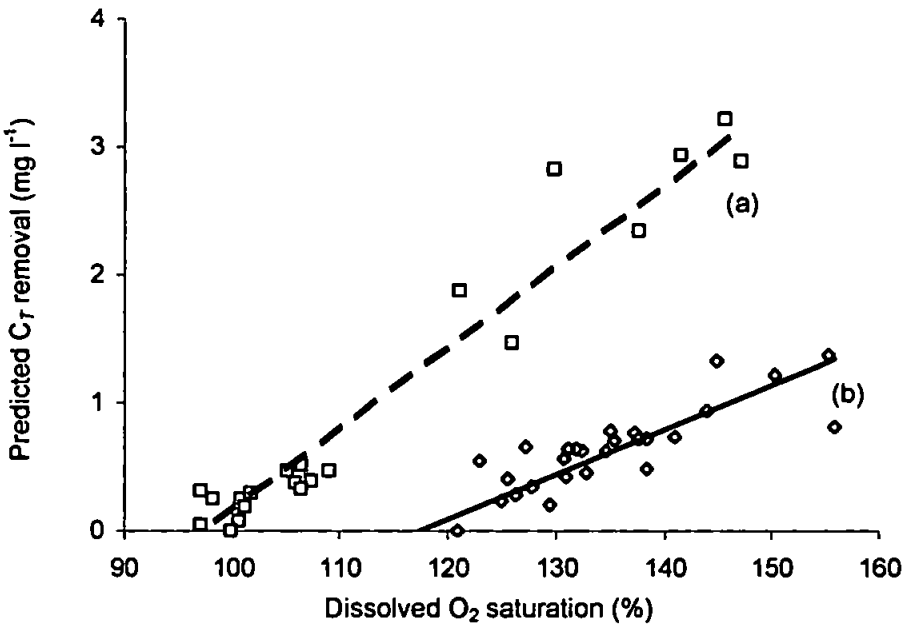

Figure 5.18 Comparison of dissolved O_2 saturation and predicted inorganic carbon uptake in the upper reaches of the Tweed Estuary. (a) $R^2 = 0.94$, ($n = 24$) in July 1996 and June 1997 (□). (b) $R^2 = 0.78$, ($n = 31$) in August 1997 (◇).

The model has so far assumed that carbonate alkalinity is conserved within the estuary. Photosynthetic removal of CO_2 does not affect the net charge balance (which defines the alkalinity) of the estuarine water. In reality though photosynthesis is accompanied by the assimilation of ions such as nitrate and ammonium the removal of which will alter the charge balance and hence alkalinity. The August 1997 predictions of inorganic carbon removal were tested by decreasing the freshwater alkalinity by 1 %, although this had no effect on the pH prediction the estimated carbon removal in the estuary was reduced by 13

%. These predictions are therefore sensitive to this parameter and the difference between the regressions shown in Figure 5.18 may be due to incorrect estimation of end member alkalinity or non-conservative behaviour of alkalinity in the estuary.

5.5.3 Chlorophyll *a* concentration and photosynthetic rate in the water column

The correlation between O_2 and pH in the summer months and the clearly defined peaks in both variables imply that primary productivity and CO_2 assimilation was localised in the upper river estuary. Chlorophyll *a* concentrations determined from surface water samples (see Appendices) showed that mean chlorophyll *a* concentrations through out the Tweed were low (0.19 to 0.93 $\mu g\ l^{-1}$) except for May 1997 when concentrations reached 14 $\mu g\ l^{-1}$ ($6.3 \pm 4.0\ \mu g\ l^{-1}$). There was no indication of any seasonal variability and this confirms the findings of Shaw *et al.* (1998). Neither was there any indication of phytoplankton blooms coincident with the peaks in pH and O_2. The absences of a turbidity maximum zone in estuaries such as the Tweed is indicative of systems where the hydrodynamic processes prevent the development of plankton blooms (Fichez *et al*, 1992). Phytoplankton divide ~ 0.5 to 3 times per day and in estuaries with a residence time of less than two to three days, such as the Tweed there may be insufficient time for phytoplankton blooms to develop (Valiela, 1997). Uncles *et al.*, (2000) suggest that the elevated chlorophyll *a* concentration in May are due to a spring bloom. Phytoplankton biomass tends to be inversely related to flow rate (Madariaga, 1995), but significant washout may occur during high river flow (Boyer *et al*, 1993; Iriarte *et al*, 1996). The high concentrations of chlorophyll *a* measured during the May survey corresponded to increased river flow and a reduction in both pH and O_2 saturation. These higher than normal concentrations may therefore represent plant debris and suspended and benthic algae that have been flushed out of the Tweed River system above the limit of the survey area opposed to natural growth of the population in the lower Tweed River.

Although the chlorophyll *a* concentrations were relatively invariant, the rate of primary productivity may have varied in response to light availability. The time available for CO_2 assimilation to effect the carbon balance in the water will also depend on flow rate and the peaks in pH and O_2 were both associated with high irradiance and low flow conditions.

The mean water temperature recorded during the surveys showed a peak coincident with the pH and O_2 maximums. The maximum temperatures were elevated by 1.4°C (July

1996), 0.87°C (June 1997), and 0.65°C (August 1997) relative to the temperature at station 20. The region upstream of station 20 was shaded, but between stations 18 and 15 the surrounding topography is more level and there was less shading of the water by banks or vegetation. The bathymetry of the river was broader and shallower in this region. This implies that more light was available and that corresponding rates of primary productivity would have been higher in the area associate with the pH and O_2 peaks.

To determine whether primary productivity based on the measured chlorophyll *a* concentrations would be sufficient to account for the increased pH, photosynthetic rates were estimated. Photosynthetic rates of 0.011 to 0.034 μg C_T (μg Chl *a*)$^{-1}$ h^{-1} (μE m^2 s)$^{-1}$ have been reported for a range of estuarine systems (Harding *et al*, 1986; Madariaga, 1995; Kromkamp *et al.*, 1995). Using the maximum value of 0.034 μg C_T (μg Chl *a*)$^{-1}$ h^{-1} (μE m^2 s)$^{-1}$ and an estimated residence time of five hours productivity was determined from incident light levels and water column Chlorophyll *a* concentrations. Maximum values of irradiance data (W m^{-2}) during each transect was converted to photosynthetic active radiation (PAR) of units μE m^2 s^{-1} by using a conversion factor of 2.168 (Kirk, 1994). Corrections were not however made for loss of light by reflection from the surface or attenuation through the water column, so that productivity estimates were over estimated in these calculations. Potential carbon uptake by phytoplankton is compared to the mean of values calculated in the region of the pH peak in Table 5.4.

Table 5.4 Comparison of mean carbon assimilation between 2 to 5 km from the head and that estimated from chlorophyll a concentrations in the water column for a 5 hour period. *No chlorophyll a data was available in July 1996 and values are estimated as the average of June and August 1997 data.

Survey	Chl *a* (μg l^{-1})	Maximum irradiance (μE m^2 s^{-1})	Phytoplankton C assimilation (mg C_T l^{-1})	Total C assimilation (mg C_T l^{-1})	% attributed to phytoplankton
Jul 96	*0.55	1655	0.15	2.7	5.6
Sep 96	0.67	952	0.11	1.5	7.3
June 97	0.59	1350	0.14	0.8	18
Aug 97	0.50	1025	0.09	0.5	18

Despite the potential over estimation of parameters used, assimilation of C_T by phytoplankton could not account for more than 20 % in the difference between modelled and observed pH. The repetitive occurrence of the pH maximum and oxygen supersaturation at the same locality implies photosynthetic processes, although is also hard to attributed this to plankton communities transported within the water column at a velocity equal to that of the water.

5.5.4 Dissolved nutrient concentrations in the Tweed River-Estuary

The dissolved nitrite, nitrate and date are shown in the Appendices. The nitrate and nitrite concentrations at the head of the estuary per survey ranged from 38 ± 5 to 320 ± 70 μM l^{-1} nitrate and 0.6 ± 0.1 to 1.5 ± 0.04 μM l^{-1} nitrite. In both cases the largest concentrations occurred in January and the smallest in March 1997.

A linear regression of nutrient concentration against pH at salinity < 1during the summer months showed a weak (p = 0.05) negative correlation with nitrite and total organic nitrogen (TON). There was however a stronger negative correlation (p = 0.02) between dissolved oxygen saturation and TON. Shaw *et al.*, (1998) found that phytoplankton activity in the Tweed Estuary resulted in low rates of dissolved nitrogen uptake (<0.4 nM N l^{-1} h^{-1}) and caused small changes in the dissolved oxygen saturation. Assuming a conservative estimated of a 36 hour residence time during low summer flows and 5 μg l^{-1} chlorophyll *a*, the water column uptake would then only account for up to 0.04 μM l^{-1} reduction in dissolved concentrations. The variation in nitrogen concentration at salinity < 1 that could not be accounted for by mixing processes ranged from 3.5 to 35 μM l^{-1} nitrate. Phytoplankton activity therefore accounted for less than 0.3 % of the mean (17 μM l^{-1}) variation in nitrate. This strengthens the hypothesis that benthic and not water column photosynthesis is affecting the water chemistry.

In the absence of carbonate precipitation, nitrification consumes 2 equivalents of alkalinity per nitrogen transformed (Regnier *et al.*, 1997). Even with a relatively low river water alkalinity of 1 mequiv. l^{-1} a 35 μM l^{-1} nitrate removal would result in less than a 4 % reduction in the alkalinity and an associate 0.03 unit change in pH, an order of magnitude less than that observed and below the limit of instrument detection. This confirms Howland *et al.* (2000) findings that alkalinity is likely to behave conservatively in the estuary regardless of where the primary productivity is situated.

Freshwater silicate concentrations ranged from 23 ± 4 μM l^{-1} in July 1996 to 98 ± 1 μM l^{-1} January 1997 and showed an increasing trend with river flow (R^2 = 0.3, n = 17). A 25 % reduction in the dissolved silicate concentrations during the summer months was negatively correlated (p = 0.02) with dissolved oxygen saturation and may indicate autotrophic uptake. Having established that phytoplankton are likely to play a minor role in this process silicate uptake may be due to epibenthic algae or siliceous macrophytes).

Silica forms 95 % of diatom cell structure and reduction in dissolved silica corresponding to diatom blooms in the Tweed has been noted by Bronsdon & Naden (2000). Diatom growth can be large and relatively high values of pH have been attributed to the diatom *Navicular lanceolata* by Clayton (1997) and Neal *et al.* (1997). In October 1996 a rapid reduction of silicate from 40 to 13 $\mu M\ l^{-1}$ was also coincident with the elevated pH below station 11 and may indicate an input from the Whiteadder opposed to *in situ* biological uptake.

In the remainder of the estuary conservative mixing explained 89 % of the variation in dissolved nitrate and nitrite data and 91 % of the variation in dissolved silicate. This implies that photosynthetic uptake is not significantly affecting the concentration of these nutrients in the lower estuary and would not therefore be likely to lead to non-conservative behaviour of alkalinity. Abiotic processes were found to be the main control of pH in the lower estuary also indicating that photosynthesis either in the water column or on the bed is minimal.

Dissolved phosphate and dissolved ammonia concentration, see Figure 5.19 are more variable in the upper estuary than those of nitrite and nitrate and are less well correlated with salinity (R^2 = 0.76 and 0.61 respectively). Both nutrients show peaks in the mid-estuary in low salinity water around station 9. Some of the dissolved phosphate variability may arise due to desorption from particles as salinity increases (Balls, 1992) although this can not explain the co-variance of ammonia. The location of the peaks in the vicinity of the Tweed sewage works discharge point may however indicate anthropogenic input which may have affected the surface waters when the estuary was stratified. Discharges were detectable in the summer through their odour and discoloration of the water. The ammonia and phosphate show no significant correlation with pH. An input from the swage works in addition to the Whiteadder may however lead to changes in alkalinity or pH explaining the discrepancy between model and observed results in this region during certain times of the year.

5.5.5 Benthic productivity in the Tweed River-Estuary

Although the carbon-oxygen balance of the water is being altered in a localised region of the tidal reaches of the Tweed there is no indication that this is due to phytoplankton in the water column. An alternative explanation is that benthic and not water column processes

are important in controlling the O_2-CO_2 balance in the Tweed Estuary. High productivity in the river has also been attributed to benthic algae and macrophyte colonisation in the shallow clear waters (Clayton, 1997; Neal *et al*, 1997; Robson & Neal, 1997). Un-shaded lowland streams often support abundant submerged plants (Sand-Jensen & Frost-Christensen, 1998) and oxygen levels have been dominated by benthic processes in shallow estuaries (Valiela, 1997). The presence of benthic macrophytes in the upper reaches of the estuary was reported Howland *et al.* (2000). This region of the estuary is un-shaded by high vegetation, has reed communities along the banks and on and around shallow islands in the channel.

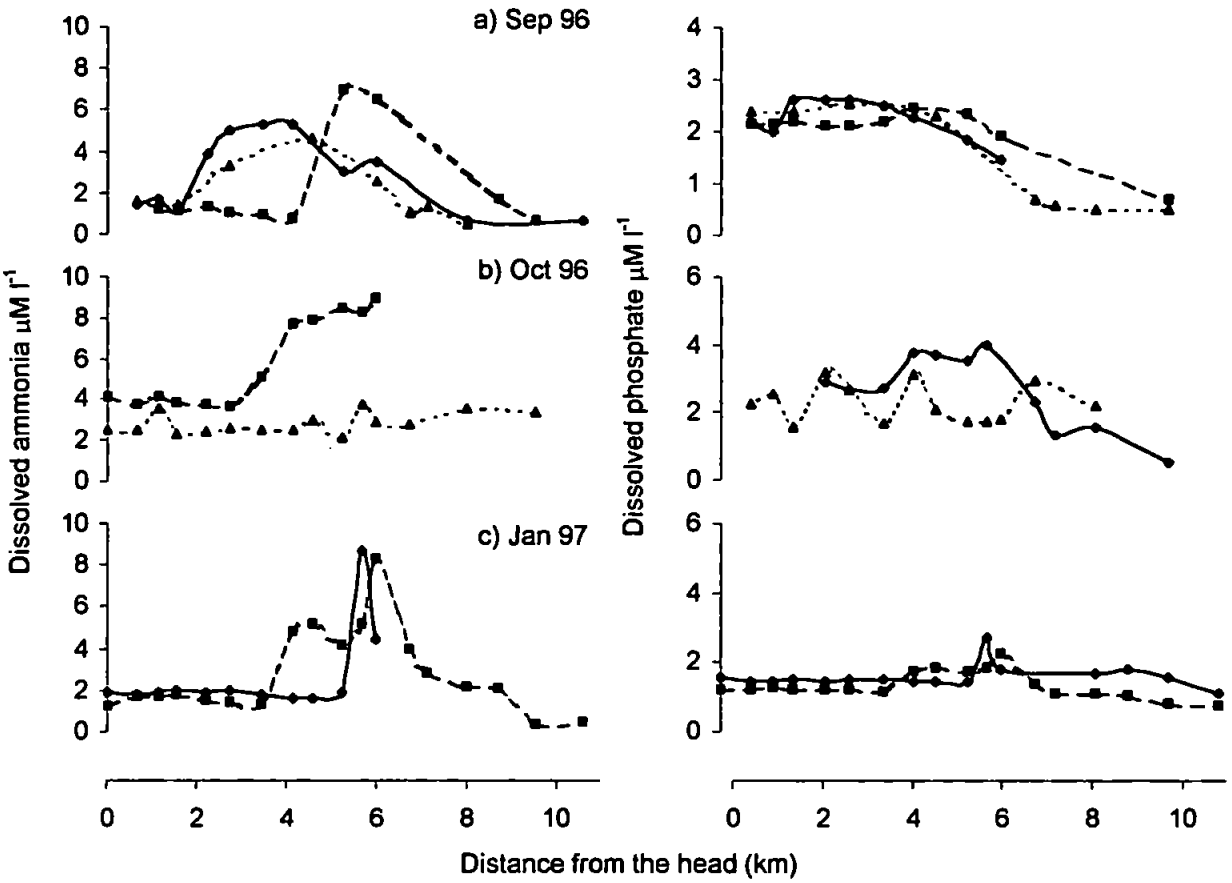

Figure 5.19 Dissolved ammonia and phosphate during a) September 1996, b) October 1996 and c) January 1997. The different symbols indicate different days within each survey period.

The Tweed Estuary as a whole was shallow (mean 2 m, with maximum depths rarely exceeding 7 m), particularly between stations 18 and 15 where the water depth ranged from 0.5 to 2.0 m depending on tidal state and freshwater flow. The increase in pH with water depth has not yet been explained, especially as increased water depth would be expected to reduce light intensity and hence reduce benthic photosynthesis. Possible explanations may include:

- As the water level rises vegetation (reed, other macrophytes and benthic diatoms) along the bank margins are submerged. Photosynthesis and the abstraction of CO_2 from the water elevates the pH. As the water level drops this effect is reduced. This implies that the pH increase will probably be at a maximum when high water is coincident with maximum irradiance (*i.e.*, spring tides). As the time of high water advances each day it will move out of phase with maximum irradiance and the pH peaks may then decrease (*i.e.*, neap tides). This effect may however only be apparent in the slow moving water at the channel margins.
- At low tide the shallow water depth may allow sufficient oxygen and carbon dioxide exchange with the atmosphere to prevent photosynthetic activity modifying the carbon dioxide balance and affecting the pH. As the water level increases the ratio of surface area to volume is approximately halved. This will reduce the clearance time and allow photosynthetic activity to reduce the carbon dioxide concentrations.
- Tidal state will influence the flow velocity and corresponding residence time. High water slack may correspond to minimum flow velocity increasing the amount of time that carbon dioxide can be extracted from any particular unit of water.

5.6 Summary

Extensive measurements of pH in the Tweed River-Estuary has shown that the freshwater pH is seasonally variable and ranged from approximately 7 under high river flow in the winter up to 10.5 during low flow summer conditions. The variability in freshwater pH compared to that of seawater resulted in a wide range of pH profiles through the estuary. The Mook & Koene (1975) model of estuarine pH variation has been successfully used to help distinguish abiotic from biotic processes when investigating the extensive database of pH measurements presented.

Comparison of modelled and observed pH showed that with the exception of the tidal reaches, seaward of station 15 the main control on the pH was due to the change in salinity. This implies that there is minimal biological mediation (photosynthesis or respiration) either from the benthos or within the water column in the lower part of the estuary. This also implies that atmospheric exchange does not significantly effect the pH and this may be expected from the relatively rapid flushing rate and excess partial pressures of CO_2 at or greater than equilibrium (Howland *et al.*, 2000).

Between stations 18 and 15 there was an increase in pH during summer conditions which could not be reproduced when conservative behaviour of total inorganic carbon was assumed. Dissolved oxygen and nutrient data supports the hypothesis that this is due to photosynthetic uptake of CO_2, although this cannot be attributed to phytoplankton. It has been proposed that macrophytes and diatoms along the channel margins and bed may account for approximately 80 % of the carbon and 99 % of the nitrate removal from the water when immersed.

A localised region just above the extent of saline intrusion therefore appears to critical in controlling processes within the estuary. High pH in the river, further elevated in the tidal reaches of the estuary may deter migrating salmonoids (Clayton, 1997). To investigate these processes further, more detailed studies in the upper reaches of the river estuary are therefore suggested. The algae *Hydrodictyon reticulatum* has been present in the Tweed since at least the mid-1970s (Neal *et al.*, 2000) and may become more prevalent if summer water temperatures are high and flows low. These may also elevate the pH affecting fish stocks and also warrants investigation.

Chapter 6

Measurement and prediction of axial metal concentration and fluxes

6 Measurement and prediction of trace metal concentrations and fluxes

The partitioning of Cd and Zn onto chemically-characterised SPM from the Tweed Estuary, has been determined in laboratory and *in situ* radiotracer experiments and through analytical determination of dissolved and particulate concentrations in the estuary. The effect of salinity, SPM concentration, pH and particle type on the partition coefficient has determined and a K_d-salinity relationship encoded to model the axial distribution of dissolved and particulate metals in the Tweed Estuary. The predictions of metal behaviour in the estuary have then been used to estimate how the fluxes of Cd and Zn from the River Tweed catchment are modified as they are transported through the estuary to the North Sea.

6.1 Radiochemical experiments

Unlike partial or total extraction of metals from particles using mineral acids replicating the exchangeable metal fraction using radioisotopes under controlled laboratory conditions has the advantage that only the fraction of metal adsorbed is subsequently analysed. Analysis is also relatively simple and reproducible, and many contamination problems are avoided. Laboratory studies are however conducted in discrete, parallel experiments that fail to reproduce the continuous nature of estuarine chemical gradients. Short term incubation studies also fail to identify how the reaction kinetics may affect the ultimate location of the metal on the particles.

6.1.1 Estuarine mixing experiment

Radiotracer studies of K_d as a function of salinity and turbidity have been performed (February, April, June and September 1997) following the method of Turner *et al.*, 1993. Unfiltered samples of marine and riverine end members were collected and mixed to provide 6 to 8 aliquots at salinity of approximately 0, 2, 5, 10, 15, 25 and 30 to 35. Concentrations of SPM were low (< 15 mg l^{-1}), but did vary by up to a factor of 10, increasing with salinity. Using the same end member samples three replicates of each sample were generated and reactor vessels were conditioned by rinsing with the appropriate aliquot before use, the final volume in each reactor was then made up to 50 ml. Each aliquot was then labelled with a 10 µl cocktail of ^{109}Cd and ^{65}Zn. Two additional tracers were also used to determine, firstly, Mn-oxide formation (^{54}Mn) and secondly, the

uptake of a non-bioactive metal due solely to geochemical partitioning (^{137}Cs). A 0.1 to 0.2 ml aliquot of 10 % NH_3 was then used to restore the original pH. Samples were periodically agitated to maintain the SPM in suspension and equilibrated for 24 hours in the dark. The contents of each reactor was then filtered through pre-weighed 0.45 μm pore size Sartorius filters mounted in a glass vacuum filtration unit. Filters were then placed in Petri dishes and filtrate in 50 ml containers and acidified to pH ≈ 1 with HNO_3 prior to gamma spectroscopy analysis.

Bulk water samples were also collected from the end members to determine a range of master variables and particle characteristics (Table 6.1). The mass of suspended sediment in each estuarine mixing aliquot was low (0.06 to 0.7 mg) compared to the filter weight (~ 25 mg). The turbidity and salinity of each estuarine mixing aliquot was therefore calculated based on the proportion of each end member sample used.

Table 6.1 Details of the riverine and marine end member water samples used during the estuarine mixing experiments.

Survey & end member		Salinity	pH	Temp (°C)	SPM (mg l^{-1})	Particle characteristics				
						*Chl *a* (μg l^{-1})	*C %	*C:N	[Fe] (mg g^{-1})	[Mn] (mg g^{-1})
Feb 97	R	0.1	8.05	4.8	5.3	0.40	5.3	4.5	1.6	0.82
	M	21.6	8.10	6.8	9.4	0.83	2.6	13.3	8.0	0.39
Apr 97	R	0.1	8.67	8.7	1.1	2.1	11	10.2	2.3	0.31
	M	22.2	8.14	8.4	12.5	0.57	4.1	11.8	8.2	0.45
Jun 97	R	0.1	8.87	17.8	2.0	0.68	15	8.9	6.6	1.83
	M	32.4	8.16	11.6	3.2	0.53	3.8	10.8	12.4	1.68
Sep 97	R	0.1	8.90	12.5	0.9	ND	11	9.1	12.2	0.85
	M	33.2	8.31	12.7	14.5	ND	3.6	11.8	10.3	0.56

(R = riverine end member, M = marine end member, *data collected as part of LOIS, ND = no data)

6.1.2 Biological uptake experiment

To determine what effect biotic driven processes had on the K_d biological uptake experiments were also performed during April and June 1997 surveys in freshwater, low salinity and high salinity regions of the estuary following a method adapted from that of Shaw *et al.* (1998). A further experiment using a modified protocol was also conducted in September 1997.

At dawn bulk water samples were collected to determine a range of master variable and particle characteristics (Table 6.2). From the bulk water sample 60 ml aliquots were placed in polycarbonate bottles, transparent to ambient radiation and porous to dissolved oxygen and then labelled with 10 µl cocktail of ^{109}Cd, ^{54}Mn, ^{137}Cs and ^{65}Zn and 0.1 to 0.2 ml of 10 % NH_3 used to restore the original pH. Three replicates were suspended in the water column at 50 cm below the surface, either tethered to an EMP rig (stations 9 and 16) or suspended from a boom extended from the gunwale of R.V. *Tamaris* (station 5).

Table 6.2 Details of water samples used during the biological uptake experiment.

Survey & Station		Salinity	pH	Temp (°C)	SPM (mg l^{-1})	Particle characteristics				
						*Chl a (µg l^{-1})	C %	C:N	[Fe] (mg g^{-1})	[Mn] (mg g^{-1})
Apr	16	0.1	8.80	7.4	1.1	1.91	7.3	9.4	1.4	0.31
97	9	0.1	8.27	7.9	1.7	2.54	9.0	9.8	9.9	0.96
Jun	16	0.1	8.57	15.5	2.8	0.77	12.5	7.8	14.6	1.83
97	9	3.5	8.81	13.5	3.7	0.51	7.4	9.1	22.4	4.75
	5	17.6	8.16	11.2	3.5	0.76	5.4	10.1	17.6	2.58
Sep	14	0.1	8.73	12.2	2.5	ND	7.1	9.1	6.9	0.96
97	8	1.0	9.02	12.7	7.7	ND	6.4	9.4	11.2	2.40
	4	22.1	8.39	12.5	9.8	ND	4.4	11.8	12.3	0.96

(*Chlorophyll *a* concentrations were kindly supplied by P. Shaw (*per. comm.* 1998). ND = no data)

These samples were exposed to ambient light and temperature conditions within the water column through out the daylight period. Three replicates were poisoned with 200 µl of 3 % mercuric chloride (added as a metabolic inhibitor) and placed with three non-poisoned replicates in a dark plastic bag that was then immersed within the water column to maintain ambient temperatures. The addition of mercuric chloride to incubating samples therefore provided a means of distinguishing chemical from biological mediated adsorption onto particles (Vojak *et al.*, 1985). The samples were retrieved during the late evening and maintained in dark and cool conditions overnight.

A modified version of this protocol was employed during the September survey. Water samples collected during the axial survey from stations 14, 8 and 4 were prepared as described above then placed in a water tank situated by an open window in the laboratory and exposed to ambient light conditions. Temperature was maintained close to that observed in the estuary by the addition of chilled water to the tank.

In both methods, 24 hours after the spike had been added samples were filtered through 0.2 μm pore size Nuclepore membrane filters. The filtrate was acidified with 50 μl NHO_3 and filter and filtrate retained for gamma spectroscopy determination. Due to the potentially low SPM mass within each 60 ml aliquot (0.07 to 0.6 mg) compared to filter weight (~15 mg), SPM concentrations were determined from the bulk water sample.

6.1.3 Determination of the partition coefficient

Gamma spectroscopy analysis of filters and filtrate were performed using a high purity coaxial germanium detector coupled to a multi-channel analyser (Canberra Ltd.). The partitioning coefficient (K_d) was derived from the ratio of activity on the filter to activity in the filtrate calculated as:

$$K_d(l\ g^{-1}) = \frac{Pa.V}{Da.m.f} \qquad (6.1)$$

where *Pa* and *Da* are the particulate and dissolved counts (per 1000 s), *V* is the volume of dissolved fraction (l) and *m* the mass of particulate matter (g). The geometric correction factor (*f*) is determined from the ratio of measured activity per spike absorbed in a blank filter and dissolved in filtered water (Turner & Millward, 1994).

Background activity of the four radiotracers used were found to be below the limit of detection. Spiked samples were initially counted for 1000 s and for most this was sufficient to produce a percentage error of < 10 %. Low activity samples were recounted for 10,000 s and then normalised to 1000 s. The percentage error indicated the statistical uncertainty in the peak area calculation of sample activity and the analysis of replicates yielded the following RSD. Dissolved phase counts: Cd; 1.11 %, Cs; 0.35 %, Mn; 2.46 %, Zn; 1.09 %, 25 mm filter particulate counts: Cd; 3.11 %, Cs; 4.33 %, Mn; 1.60 %, Zn; 2.46 % and the 47 mm filter particulate counts: Cd; 3.90 %, Cs; 1.50 %, Mn; 2.08 %, Zn; 1.74 %.

The relative standard deviation of the three replicates used during the estuarine mixing and biological uptake experiments ranged from 20 to 30 %. This was higher than reported previously for radiotracer experiments (Turner, 1996) and may have resulted from the uncertainty in determining the SPM mass under these low turbidity conditions.

To investigate how the K_d of the metals changed in the different estuarine mixing samples a linear regression of log K_d on log (S+1) was used, following the method of Bale (1987). The intercept and gradient of the regression were then used to determine the freshwater K_d (K_0) and the rate at which the K_d decreased as the salinity increased (b). Due to the low SPM concentration and lack of fine grained bed sediment it was not possible to collect sufficient SPM to adjust the turbidity of the estuarine mixing aliquots. The influence of the particle concentration effect due to the co-variance of SPM with salinity could not therefore be investigated in the radiotracer experiments. The SPM concentrations in the estuarine mixing experiments were however typical of those normally observed in the estuary.

6.1.4 K_d variation in radiotracer experiments

Results from estuarine mixing and biological uptake experiments showed that the K_d varied between radiotracers and surveys. The freshwater partitioning coefficient varied between 2 to 3 orders of magnitude between Cs and Mn and the particle reactivity of the metals studied could be generalised in the order of Cs < Cd ≤ Zn < Mn. The results from the estuarine mixing and biological uptake experiments are shown in Figures 6.1 and 6.2. The K_0 and b values of ^{109}Cd, ^{137}Cs and ^{65}Zn determined by Turner, (1996) for the Tweed during 120 h incubations using riverine and marine SPM concentrations of 173 and 28.7 mg l^{-1} are shown for comparison in Table 6.3. Despite the shorter incubation period and lower SPM concentration the K_0 and b values of ^{109}Cd and ^{137}Cs reported by Turner (1996) were within the range established in this study. The K_0 of ^{65}Zn was however larger by a factor of three than the seasonally averaged value determined in this work.

Table 6.3 Partition coefficient parameters determined by Turner (1996) in the Tweed Estuary.

	K_0 (l g^{-1})	b
^{109}Cd	59.9	1.33
^{137}Cs	10.5	1.14
^{65}Zn	133	0.7

The K_d values determined through the estuarine mixing experiment are plotted against salinity in Figure 6.1. A regression fitted through the data showed that the K_d of all metals decreased in the higher salinity samples. The minimum R^2 coefficient of the regression during each experiment (n = 5 to 7) was 0.81 (p = 0.05), but in the majority of cases R^2 > 0.95 (p < 0.001). The biological uptake experiments included only 2 or 3 different salinity samples, the results do however indicate that as with the estuarine mixing experiment the

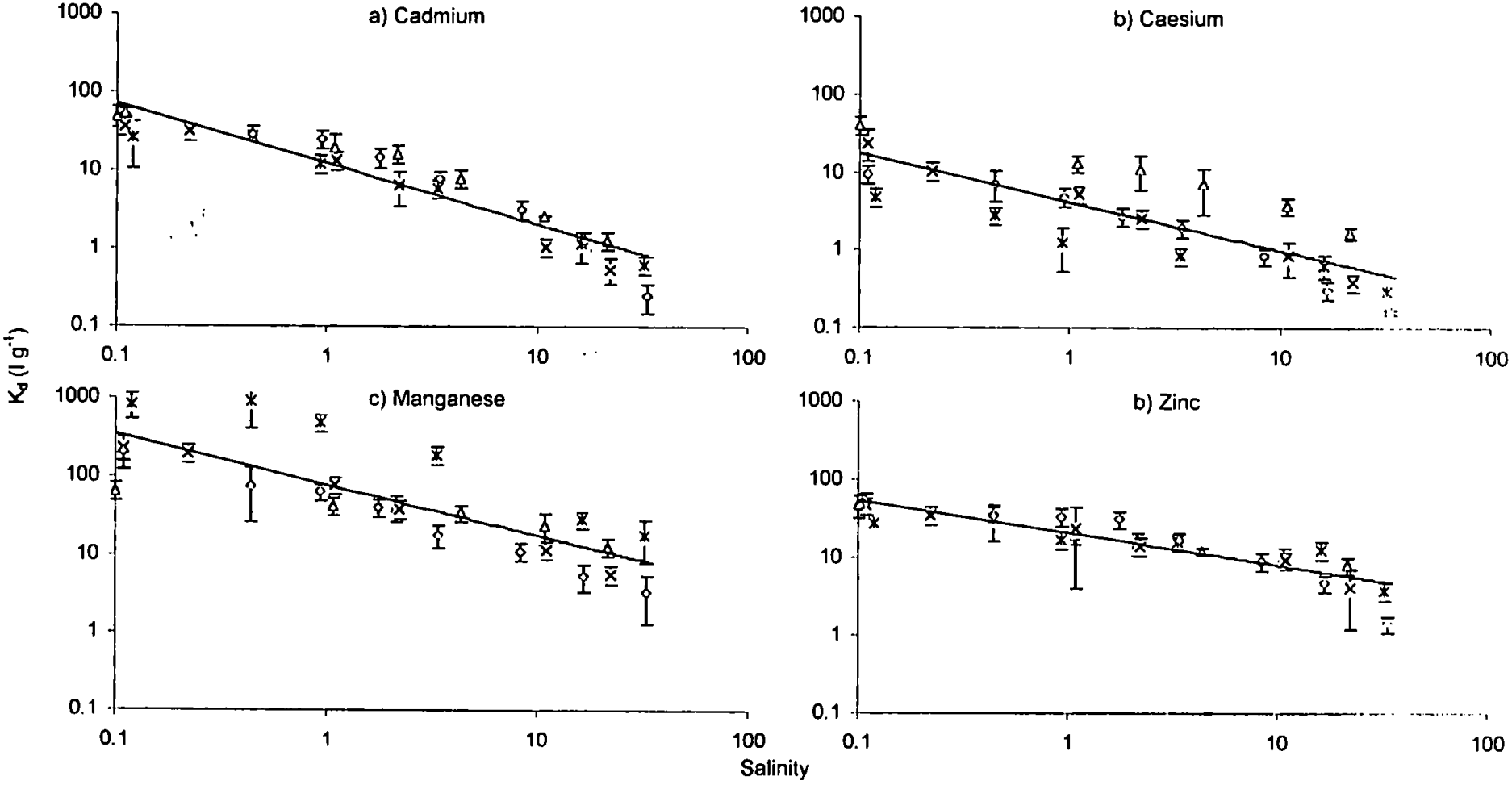

Figure 6.1 Mean and standard deviation of partition coefficient values determined during the estuarine mixing experiments in February (△), April (x), June (✳) and September (◇) 1997. The seasonally averaged regression shows the reduction in K_d with salinity (*b*) and the intercept (K_0). Individual regressions for each period are summarised in Table 6.5.

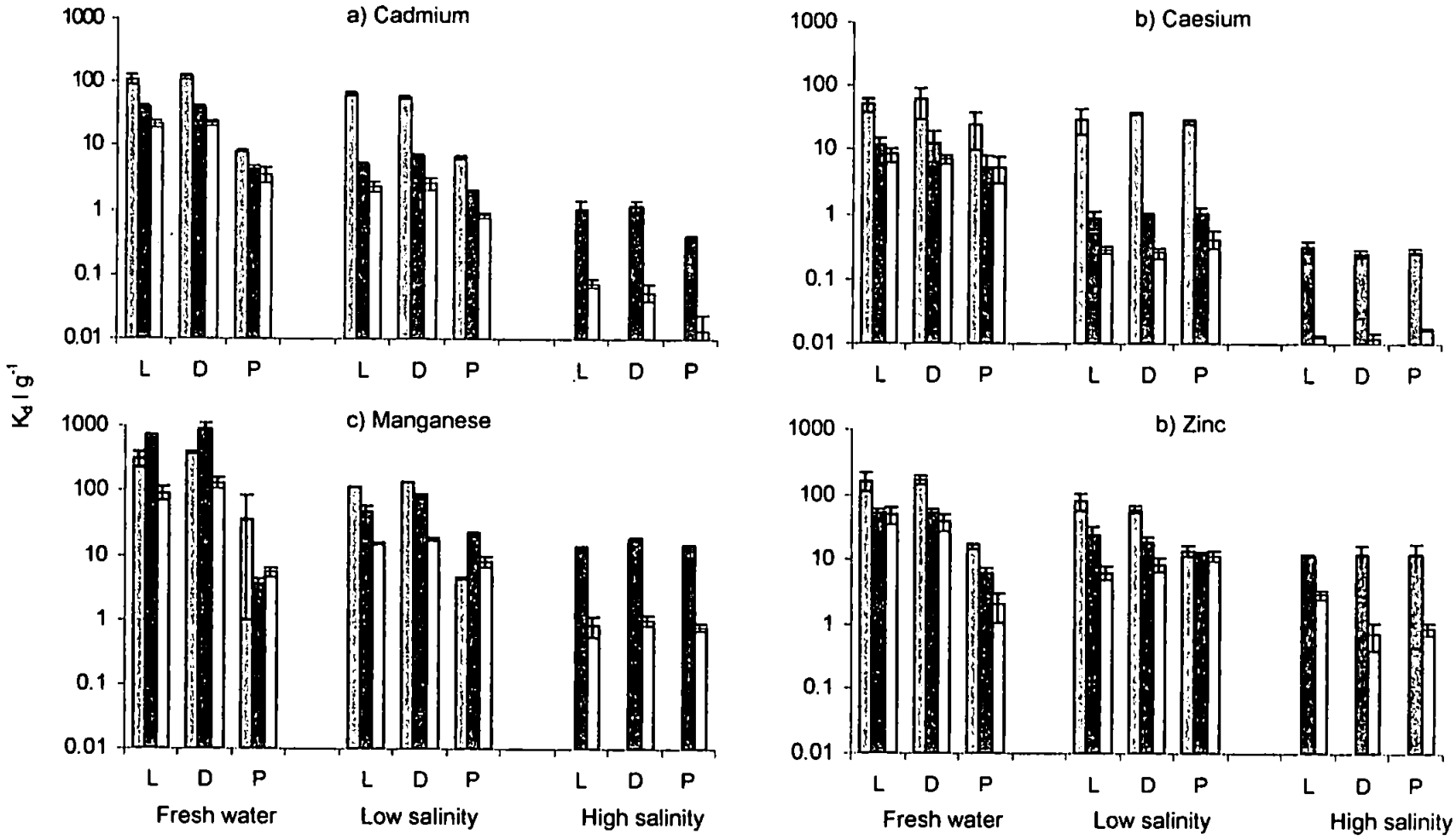

Figure 6.2 Mean (bar height) and standard deviation of partition coefficient values determined during the biological uptake experiment in freshwater, low salinity (0.1-3.5) and high salinity (18-22) water. Samples were incubated either in the light (L), dark (D) or dark and poisoned (P) during April (▬), June (■) and September 1997 (□). Non-poisoned K_0 values are summaries in Table 6.5.

K_d of all four metals decreased as salinity increased. Dissolved Cd and Zn are increasingly complexed by chloride ions down estuary, hence sorption and the K_d is reduced as the salinity increases (Kuwabara *et al.*, 1989; Turner *et al.*, 1993; Paalman *et al.*, 1994; Turner, 1996). Cadmium has a higher chlorocomplex stability constant than Zn ($\log_{10} K(CdCl_2)$ = 2.59 cf. $\log_{10} K(ZnCl_2)$ = 0.62) so that the change in the partitioning between river and marine end-members was greater (Turner *et al.*, 1981). Zinc adsorption is also influenced by competition with seawater ions (particularly Ca and Mg) for particle adsorption sites that reduce the rate and extent of adsorption (Ackroyd *et al.*, 1986). This effect however appears less significant than the chlorocomplexation capacity of Cd.

The relationship between the radiotracer determined K_0(Cd) and K_0(Zn) and SPM concentration are shown in Figure 6.3. Millward *et al.* (1992) found that increases in SPM concentration had no appreciable effect on the removal of Zn from the dissolved phase while Turner *et al.* (1992b) observed that K_d(Zn) was reduced with increasing SPM concentration. Although neither radiotracer shows a statistically significant correlation with SPM concentration at the 90 % or higher confidence limit, there does appear to be a reduction in K_0 at higher SPM concentrations, particularly for Zn.

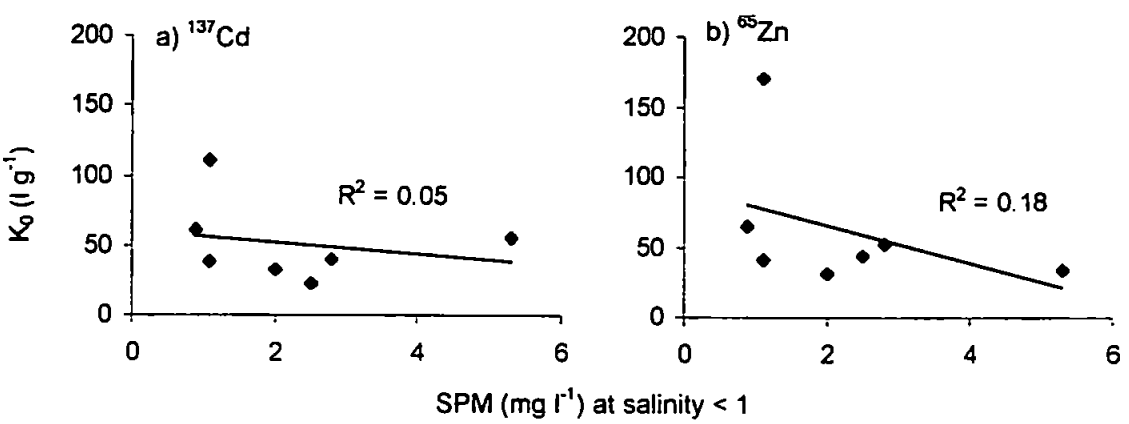

Figure 6.3 Relationship of radiotracer K_0(Cd) and K_0(Zn) to SPM concentration at salinity < 1.

The K_d relationship of Cd and Zn with salinity is sensitive to pH (Turner *et al.*, 1993; Bourg & Bertin, 1996) and desorption is depressed as the pH rises (van Gils *et al.*, 1993; Zwolsman *et al.*, 1997). The relationship between the freshwater radiotracer determined K_0(Cd) and K_0(Zn) and pH are shown in Figure 6.4. Neither relationship is statistically significant, there is however a trend of increasing K_0 at higher pH.

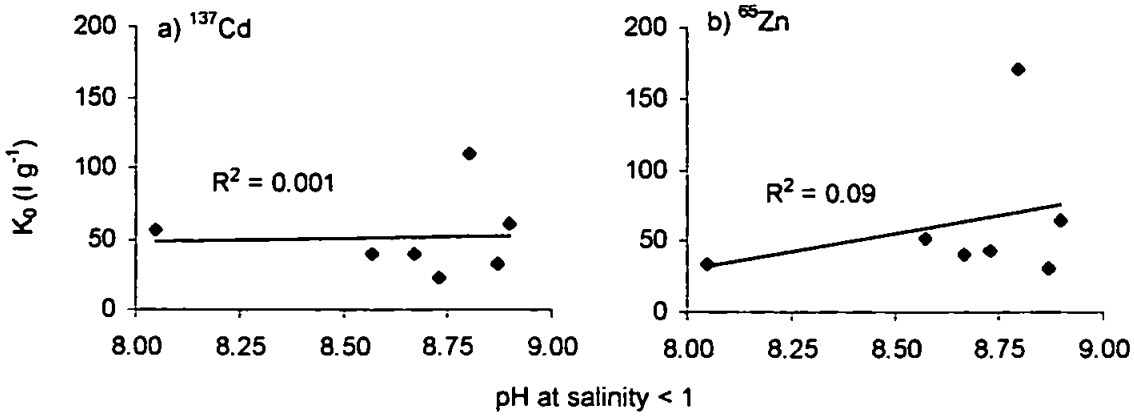

Figure 6.4 Relationship of radiotracer K_0(Cd) and K_0(Zn) to pH at salinity < 1.

The seasonal variability in particle characteristics may also be important in determining the K_d. Cadmium has a higher affinity for biological particulate organic matter (diatoms and dinoflagellates) than Zn and is more concentrated in biogenic particle than in non-biogenic particles (Noriki *et al.*, 1985; Balls, 1990). Zinc however has a slightly less preferential distribution between organic and clay minerals (Martin *et al.*, 1993) and its adsorption by clays is enhanced by Mn oxide coatings (Li *et al.*, 1984b).

Following Turner (1996) the K_0 results have also been plotted against the ratio of (Fe+Mn)/carbon, see Figure 6.5. The trend in K_0 is similar to that observed by Turner (1996), although the relationship is not statistically significant at the 90 % or higher confidence limit. The K_0 results from the estuarine mixing and biological uptake experiments are also plotted against riverine particle characteristics from a range of estuaries in Figure 6.7.

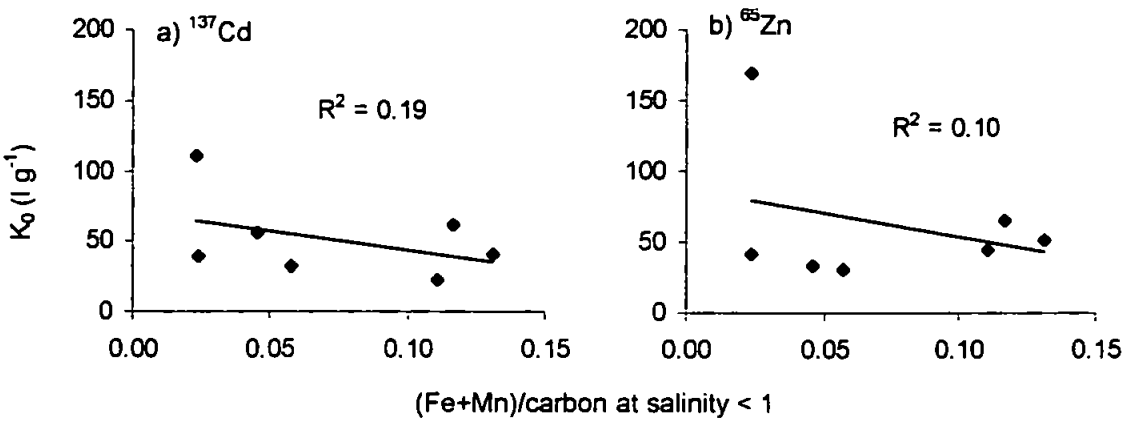

Figure 6.5 Relationship of radiotracer K_0(Cd) and K_0(Zn) to particulate (Fe+Mn)/carbon at salinity < 1.

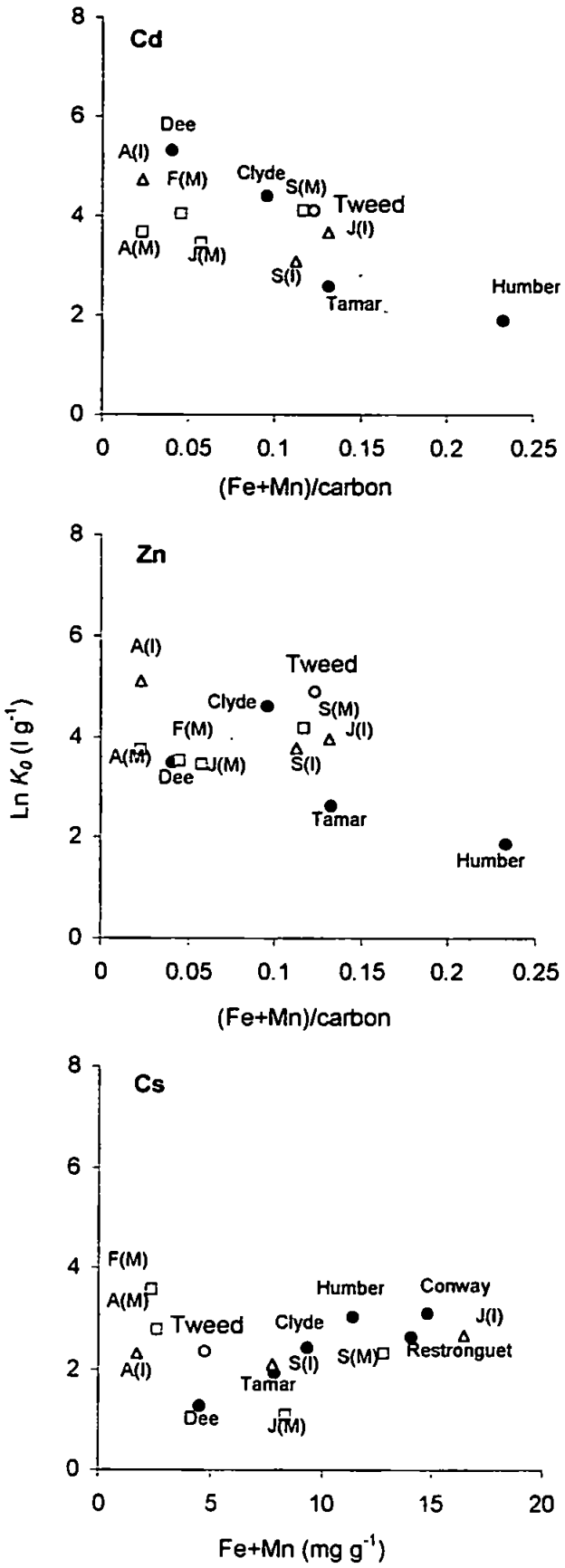

Figure 6.6 Relationship between Cd, Zn and Cs K_0 with riverine particle characteristics in the mixing (M) series (□) and biological uptake (I) experiments (△) in February (F), April (A), June (J) and September (S). Results are compared to those of Turner (1996).

The variability in the ratio of particulate Fe and Mn to carbon in the Tweed spans the measurements made in the Dee, Clyde and Tamar rivers. The K_D results also confirm that Cd ($R^2 = 0.53$, n = 13, $p = 0.01$) and to a lesser extend Zn ($R^2 = 0.26$, n = 14, $p = 0.1$) adsorption was inversely related to the ratio of acid extractable Fe and Mn to total carbon and comparable to previous findings (Turner, 1996).

There was no statistically significant difference between samples incubated in the light or dark in the biological uptake experiment. This implies that there was no *in situ* photosynthetically mediated control on the partitioning processes and this concurs with the low chlorophyll *a* concentrations (< 2.5 $\mu g\ l^{-1}$). In the freshwater poisoned samples there was however a reduction in K_d of 98 % (^{109}Cd), 91 % (^{65}Zn) 95 % (^{54}Mn), but no significant difference between poisoned and non-poisoned samples at salinity > 18. The effects of chloro-complexation and cation competition may then have been more significant than any biological effect (Vojak *et al.*, 1985). Caesium is not a bioactive metal and metabolic inhibition had little effect on ^{137}Cs uptake and the K_d determined in light, dark and poisoned samples was similar.

Particle sorption of Mn is strongly influenced by redox processes (Turner & Millward, 1994) and Laslett (1995) cited oxygenated conditions as responsible for high particulate concentrations (< 6.6 Mn mg g^{-1}) despite the low dissolved concentrations in the Tweed compared with the Tees, Wear and Tyne. Higher K_d(Mn) values were observed in both the estuarine mixing and biological uptake experiments during the summer, there was however no statistically significant seasonal variation in the poisoned samples. This implies that the variation in K_d(Mn) is predominately driven by *in situ* biological processes and high water temperatures in June may be associated with higher rates of bacterial oxidation and precipitation of ^{54}Mn onto pre-existing particulate Mn (Turner *et al.*, 1993). Bacterial mediation has been noted as an important processes during Mn oxidation in low salinity regions (Vojak *et al.*, 1985; Turner *et al.*, 1992b) and may also enhance the removal from the dissolved phase of the other metals.

6.2 Dissolved and particulate metal concentration and K_d variation

6.2.1 Determining particulate trace metal concentrations

To determine Fe-Mn oxide and Zn concentrations in suspended sediment, surface water samples were collected using acid cleaned carboys during February, April, and June 1997

EATs. Within 24 h of collection up to 15 l from each sample was filtered through pre-weighed, acid cleaned 0.4 μm Nuclepore polycarbonate filters using a metal-free Teflon pressure filtration apparatus. End member samples filtered relatively rapidly, however samples from between stations 16 to 10 during April and June surveys were slow to filter, requiring several hours, despite low SPM concentrations (< 5 mg l^{-1}). Due to time constraints it was not always possible to ensure sufficient volume was filtered to provide a 10 % increase in membrane weight. The membranes were washed free of salt with 20 to 50 ml of Milli-Q water, removed from the filtering apparatus and sealed in plastic Petri dishes and stored frozen until ready for analysis. Filters were then air dried, re-weighted and sample digests conducted using 1M HCl over 24 hours. Following Liu (1996) samples were analysed using flame atomic absorption spectroscopy (Varian SpectrAA 300/400 Plus). Samples (200 μl) were aspirated into an air-acetylene flame using the micro-cup method combined with peak height measurement. The method was calibrated in the linear range using 4 standards and the coefficient of variation determined by running triplicate sample analysis in each batch of samples. Particulate concentrations of Cd were supplied by Tappin (*per. comm.*, 2000).

6.2.2 K_d determined using analytical methods

The K_d values have been determined from dissolved and particulate concentrations of Tappin (*per. comm.* 2000) using a similar methodology to that described in Section 6.3.3. The results of which are shown in Figure 6.7.

The K_d variation with salinity is best described by an exponential function proposed by Harris (1987):

$$K_d = K_0 \, EXP(-b*S) \qquad \textbf{(6.2)}$$

there the seasonally averaged K_0(Cd) = 140 l g^{-1} and K_0(Zn) = 160 l g^{-1} and the seasonally averaged value of b = 0.1 for both metals. The K_0 values in this experiment are more variable than those determined in the radiotracer experiments and this appears to be partly due to the effect of pH and SPM concentration.

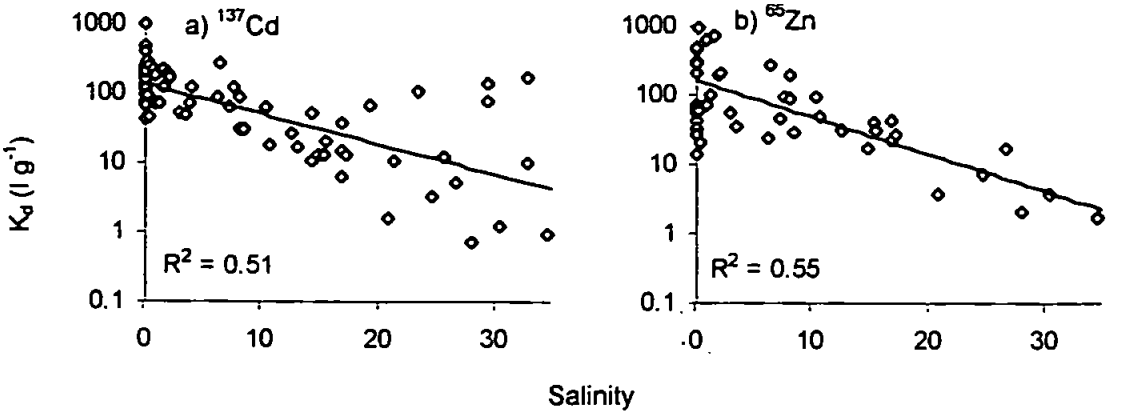

Figure 6.7 Relationship of K_d(Cd) and K_d(Zn) to salinity. Both relationships are statistically significant ($p < 0.001$).

Analytically determined K_0(Zn) (Figure 6.5) showed an order of magnitude increase as the pH increased from 7.8 to 9.5. The K_0(Cd) however showed no significant change with pH. These findings show similar trends to those identified in the radiotracer experiments and the steeper Zn gradient results from the stability constants $K(Zn(OH)_2) > K(Cd(OH)_2)$. The change in K_0(Zn) was however greater than that observed in the radiotracer experiments.

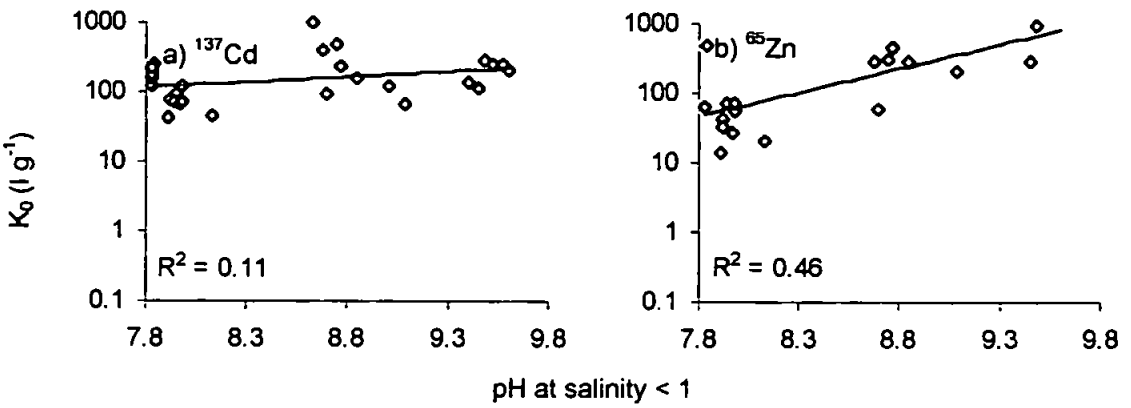

Figure 6.5 Relationship of K_0(Cd) and K_0(Zn) to pH at salinity < 1. K_d(Cd) $p > 0.1$ and K_d(Zn) $p = 0.01$.

This may arise because the wider pH variations were not captured during the radiotracer experiment. The greater increase in K_d with pH observed from the actual measurements may also be due to increased colloidal flocculation and filter retention as the pH increased.

The analytically determined K_0 results showed a significant reduction of 1 to 2 orders of magnitude as the SPM concentration increased from 2 to 6 mg l^{-1}, see Figure 6.9. This particle concentration effect may therefore result from a combination of: i) The aggregation of particles as the SPM concentration increases, reducing the specific surface area ii) The co-variance of pH that is negatively correlation ($R^2 = 0.51$, n = 34, $p < 0.001$)

with particle concentration and iii) colloidal retention on the filter discussed in Section 6.2.3.

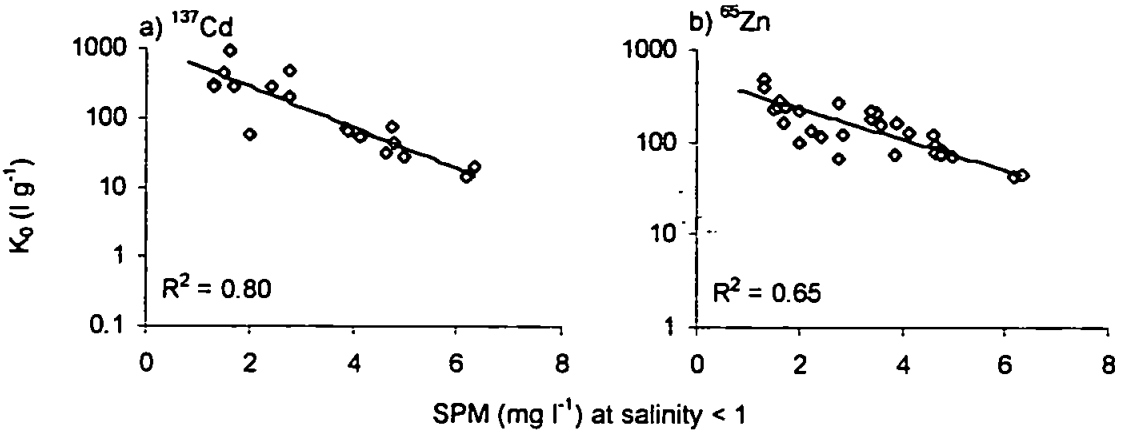

Figure 6.9 Relationship of K_0(Cd) and K_0(Zn) to SPM concentration at salinity < 1. K_d(Cd) p < 0.001 and K_d(Zn) p < 0.001.

Particulate Mn and carbon values were not available for comparison of the (Fe+Mn)/carbon ratio with analytically determined K_ds values. Particulate Fe concentrations were however available and particulate Cd and Zn showed a significant linear correlation with particulate Fe concentrations throughout the estuary during a range of surveys, see Table 6.4.

Table 6.4 Results of a linear regression forced through the origin of particulate Cd and Zn concentration on particulate Fe concentration.

Survey	Cd			Zn		
	R^2	n	p	R^2	n	p
Jul 96	0.92	26	< 0.001	0.80	26	< 0.001
Nov 96	0.71	16	< 0.001	0.84	15	< 0.001
Feb 97	0.94	13	< 0.001	0.40	12	0.05
Apr 97	0.79	29	< 0.001	0.81	30	< 0.001
Jul 97	0.69	20	< 0.001	0.66	20	< 0.001

The K_0 has also been compared to particulate Fe concentration and shows that the partitioning is also controlled by the co-variance of these metals at low salinity, see Figure 6.10.

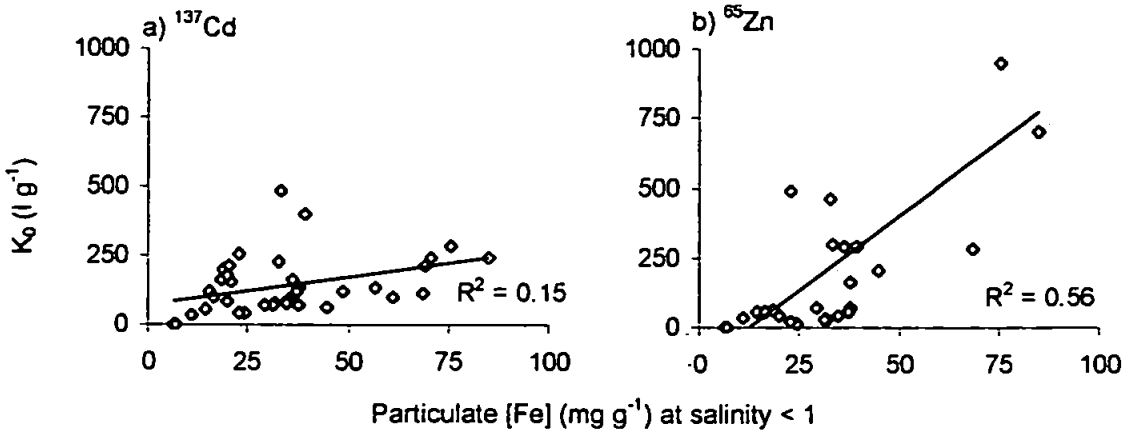

Figure 6.10 Relationship of K_d(Cd) and K_d(Zn) to particulate Fe concentration at salinity < 1. K_d(Cd) p = 0.05 and K_d(Zn) p < 0.001.

6.2.3 Comparison of methods and analytical uncertainty

The results from the radiotracer experiments and actual measurements show that the K_d varied substantially depending upon the methodology used and are summaries in Table 6.5. In both experiments the variation in partitioning was however consistent between Cd and Zn and the slope of the regression was 1.5 (a) and 1.1 (b), see Figure 6.11.

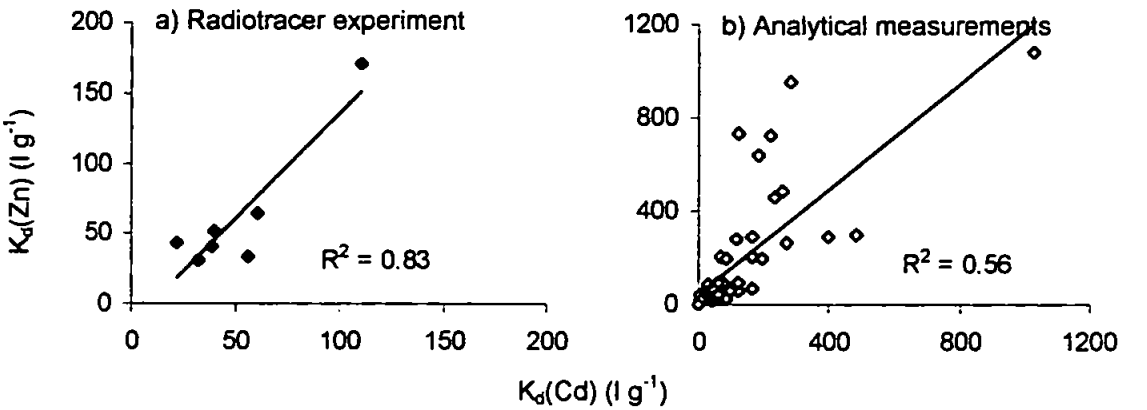

Figure 6.11 Relationship between K_d(Cd) and K_d(Zn) determined through a) radiotracer experiments and b) analytical measurements.

No statistically significant correlation could, however, be established between the two sets of K_d, for values of similar salinity, SPM concentration and pH. This illustrates the complexity in environmental controls of the K_d.

Analytical factors may also be important in measurement of trace metal concentrations and subsequent K_d determination. Concentrations of dissolved Fe are above the saturation limit for Fe oxide-hydroxide precipitation and micro-particulate oxides may be important in the both the Tweed and Whiteadder Rivers (Jarvie *et al.*, 2000). In the summer when dissolved

Table 6.5 Mean ± standard deviation of radiotracer K_d parameters determined during the estuarine mixing and biological uptake experiments (mean of non-poisoned light and dark samples) in 1997. The regression coefficient of K_d on (S+1) determined during the analytical measurements is also shown.

^{109}Cd	Experiment 1 Estuarine mixing		Experiment 2 Biological uptake	Experiment 3 Actual measurements	
Survey (1997)	K_0 (l g^{-1})	*b*	K_0 (l g^{-1})	K_0 (l g^{-1})	*b*
Feb	56 ± 11	1.2	110 ± 15	750	0.75
Apr	39 ± 8.4	1.4	40 ± 2.4	250	0.5
Jun	32 ± 3.6	1.2	22 ± 2.6	500	0.5
Sept	61 ± 19	1.4			
Seasonally averaged	47	1.3	57	500	0.6
^{137}Cs					
Feb	35 ± 4.1	1.0	ND		
Apr	16 ± 3.2	1.2	55 ± 21		
Jun	3 ± 0.9	0.7	12 ± 4.9	ND	
Sept	10 ± 1.2	1.2	8 ± 1.6		
Seasonally averaged	43	1.0	50		
^{65}Zn					
Feb	34 ± 9.3	0.7	ND	500	0.1
Apr	41 ± 12	0.5	170 ± 41	1000	0.1
Jun	31 ± 9.4	0.5	52 ± 8.4	375	0.5
Sept	65 ± 18	0.9	44 ± 13		
Seasonally averaged	43	0.7	89	625	0.2
^{54}Mn					
Feb	70 ± 12.6	1.2	ND	250	0.1
Apr	220 ± 27	1.2	340 ± 50	1000	0.5
Jun	1100 ± 287	0.5	750 ± 190	150	0.5
Sept	140 ± 31	1.2	110 ± 24		
Seasonally averaged	383	1.0	400	467	0.2

(ND = no data)

oxygen saturation often exceeded 100 %, and bacterial activity is high, oxidation and precipitation of Mn may generate Fe-Mn colloids. Flocculation of these micro-particles in the region of elevated pH may have resulted in the 'clogging' of the filter membrane pores and account for the associated difficulties in filtration. This would have reduced the effective pore size of the filter membrane and have resulted in the retention of colloidal material and micro-particle oxide co-precipitated metals. Analytically determined concentration of particulate Cd and Zn have been shown to co-vary with that of particulate

Fe. Particulate Fe concentrations used to determine the correlation with Cd and Zn concentration in Table 6.4 have been plotted against SPM concentration in Figure 6.12.

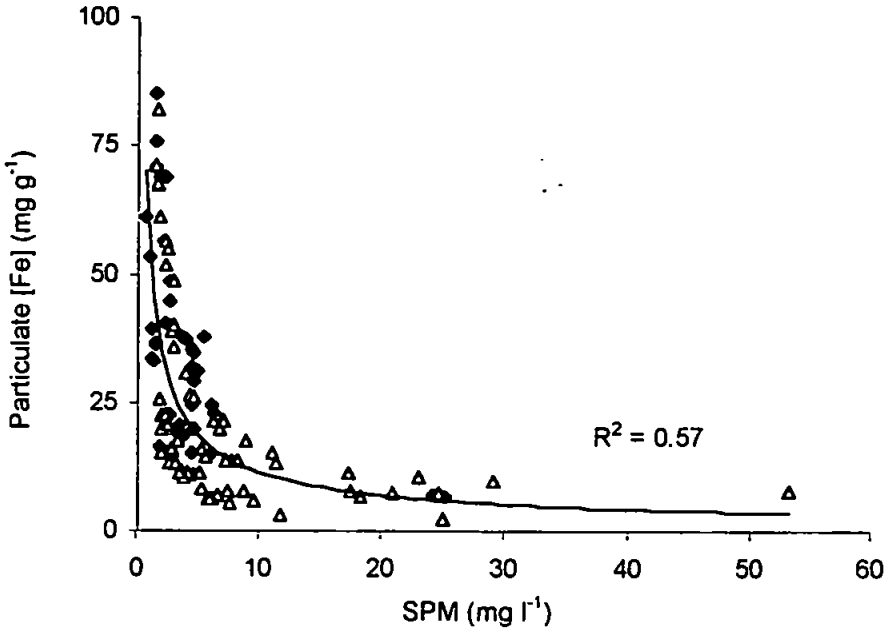

Figure 6.12 Relationship between Particulate Fe concentration and SPM concentration at salinity < 1 (◆) and salinity 1 to 34 (△).

Particulate Fe concentrations were greatest when the SPM concentration were below 3 mg l^{-1} in July 1996 and April 1997. This corresponds to low river flows, high pH and the period when filtration was most problematic. In these instances it would appear that although there may be some actual variation in particle composition the results for Fe, Cd, Zn and potentially other geochemically reactive metals, may be strongly biased by excessive filter retention. The resulting increase in the analytical determined particulate phase will then result in the calculation of higher K_d values. This explains the relationship with pH and SPM concentration shown in Figure 6.8 and 6.9. The K_d(Cd) and K_d(Zn) values determined from the actual measurements at higher freshwater SPM concentrations were 44 and 20 l g^{-1} and these are comparable to K_ds determined during the radiotracer experiments and probably represent a more realistic estimate.

Higher K_ds may also arise due the poor selectivity of mineral acid extractions liberating a proportion of metal ions bound in internal matrix sites and not normally available for exchange with the dissolved phase. In the Tweed Zn is mainly derived from geological sources (Jarvie *et al.*, 2000) and it is unlikely that metal derived from aged deposits will exchange between dissolved and particulate phases as rapidly as radiotracers under short term laboratory studies. In this case, particularly when the flushing rate through the estuary

is in the order of a tidal cycle or less there may be insufficient time for the metals to be released from the particles.

6.2.4 Influence of K_d and SPM concentration on the dissolved phase

Despite the problems identified in determining particulate concentrations in the Tweed all three experiments have shown that the K_d of Cd and Zn was reduced as the salinity increased. Even in a rapidly flushed estuary such as the Tweed it is therefore likely that a proportion of the metal will desorb from particulate or micro-particulate mater as the salinity increases.

Assuming that the particle concentration effect is an analytical error, the percentage of metal retained in the dissolved phase as a function of SPM concentration has been calculated using the radiotracer determined K_ds:

$$\% \text{ Dissolved metal} = \frac{100}{1 + K_d * SPM} \qquad \textbf{(6.3)}$$

As a general rule K_d values < 100 l g^{-1} implies that the majority of the metal will remain in the dissolved phase, see Figure 6.13.

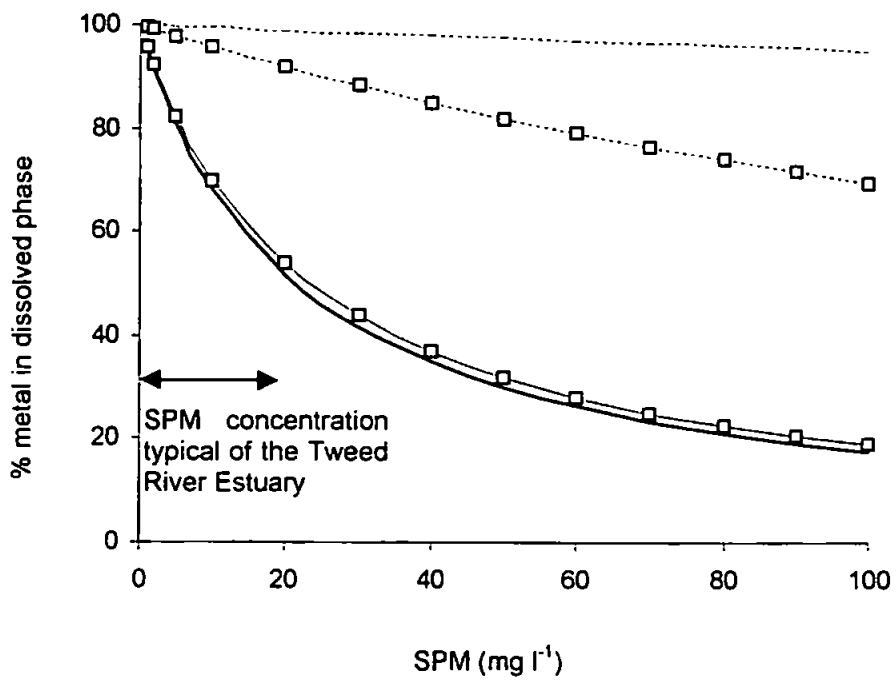

Figure 6.13 Percentage of Cd (no symbol) and Zn (□) retained in the dissolved phase at salinity = 0 (—) and salinity = 35 (--) predicted from the seasonally average K_d determined from the radiotracer experiments as a function of SPM concentration.

Figure 6.13 shows that during typical SPM concentrations (< 20 mg l^{-1}) in the estuary over 50 % of Cd and Zn will remain in the dissolved phase in the freshwater and over 90 % at salinity = 35. Brief, but high turbidity events occur in the Tweed which may however significantly reduce the percentage metal held in the dissolved phase and this is likely to be more significant for Zn than Cd. Adsorption and desorption during these high flow events can not however be quantified without further information of the exchange kinetics under high SPM concentrations of time scales of minutes to hours.

6.3 Modelling axial distribution of Cd and Zn

The ECoS metal transport model has been used to determine to what extent the K_ds derived from the estuarine mixing experiment and analytical measurements could be used to predict the axial distribution of dissolved and particulate Cd and Zn in the Tweed Estuary.

6.3.1 Encoding the K_d-salinity relationship in ECoS

Salinity was the most consistent factor controlling the K_d in the three experiments and a linear regression of log K_d on log (S+1) was represent within the ECoS model using the expression of i) Harris & Gorley, (1998b) and ii) Harris (1987):

$$\text{i) } K_{d(\text{Radiotracer})} = K_0^*(S+1)^{-b} \quad \text{and} \quad \text{ii) } K_{d(\text{Analytical})} = K_0^*\text{EXP}(S^{*-b}) \tag{6.4}$$

The process of adsorption and desorption is encoded as an exchange transfer between the dissolved and particulate (permanent and temporarily suspended) constituents. Following Harris & Gorley (1998b) it has been assuming that desorption is the exact reverse of adsorption and no metal is sequestered internally. Adsorption is also assumed to be proportional to the concentration of suspended particles (g l^{-1}) and desorption proportional to the concentration of metal on the particles and the K_d (l g^{-1}):

$$[Particle] \underset{Adsorption=A^*SPM}{\overset{Desorption=A/K_D}{\rightleftharpoons}} [Dissolved] \tag{6.5}$$

where A is a rate coefficient of litres of water cleared of dissolved metal per unit time per gram of suspended particle. If the rates of adsorption and desorption are known then realistic values of A can be incorporated and linked to other model parameters such as salinity or particle composition. Kinetic studies were not conducted upon the Tweed samples and an equilibrium approach has been applied during the modelling. The rate

parameter A was therefore set to 10^6 l g^{-1} s^{-1} implying that the adsorption and desorption processes were effectively instantaneous.

Marine and riverine boundary conditions used are shown in Table 6.6 and the model was run-up for a period of 48 hours. The predicted dissolved and particulate Cd and Zn concentrations were then extracted at high water and compared to an independent data set of dissolved concentration data of Tappin (*per. comm.*:2000) and particulate concentrations determined in this study, see Figure 6.14 and 6.15.

Table 6.6 Riverine (REM) and marine (MEM) boundary conditions of turbidity, and dissolved and particulate concentrations of Mn, Zn and Cd used in the ECoS model simulations.

	Feb 97		Apr 97		Jun 97	
	REM	MEM	REM	MEM	REM	MEM
Q (m^3 s^{-1})	64		39		25	
SPM (mg l^{-1})	0.5	18	2.9	16	0.5	2.4
Zn (µg l^{-1})	0.56	0.37	0.60	0.53	0.39	0.14
Zn (µg g^{-1})	285	218	259	138	800	350
Cd (µg l^{-1})	0.004	0.004	0.006	0.006	0.014	0.014
Cd (µg g^{-1})	2.17	0.83	5.00	0.23	2.58	0.82

6.3.2 Model predictions of Cd and Zn concentration

The results show that when the radiotracer determined K_0 values were used the model over predicted the dissolved concentrations and under predicted the particulate metal concentrations with an average difference between modelled and observed values of 80 %. This large discrepancy is however expected due to the problems associated with the analytical determination of the particulate phase. If the K_ds determined from the actual measurements are used the model results are in better agreement with the observed values (an average difference between modelled and observed results of 24 %).

Although the overall performance of the model appeared to be increased using the K_ds from the actual measurements the variability in both the dissolved and particulate concentrations measured through the estuary and tidal reaches have been difficult to reproduce. In comparison to the predictions of SPM transport and pH only one of several factor (*i.e.*, the salinity dependence and not the potential effect of pH or SPM concentration) has been included.

Problems in extrapolating laboratory K_d values to natural systems have also been noted by Balls (1989) and Turner (1996) where the radiotracer determined K_d values were insufficient to explain the analytically determined dissolved and particulate phases. Radiotracer experiments may provide a clearer understanding of exchange processes and are therefore a valuable tool in model predictions of trace metal flux. Comparison of model results with analytically

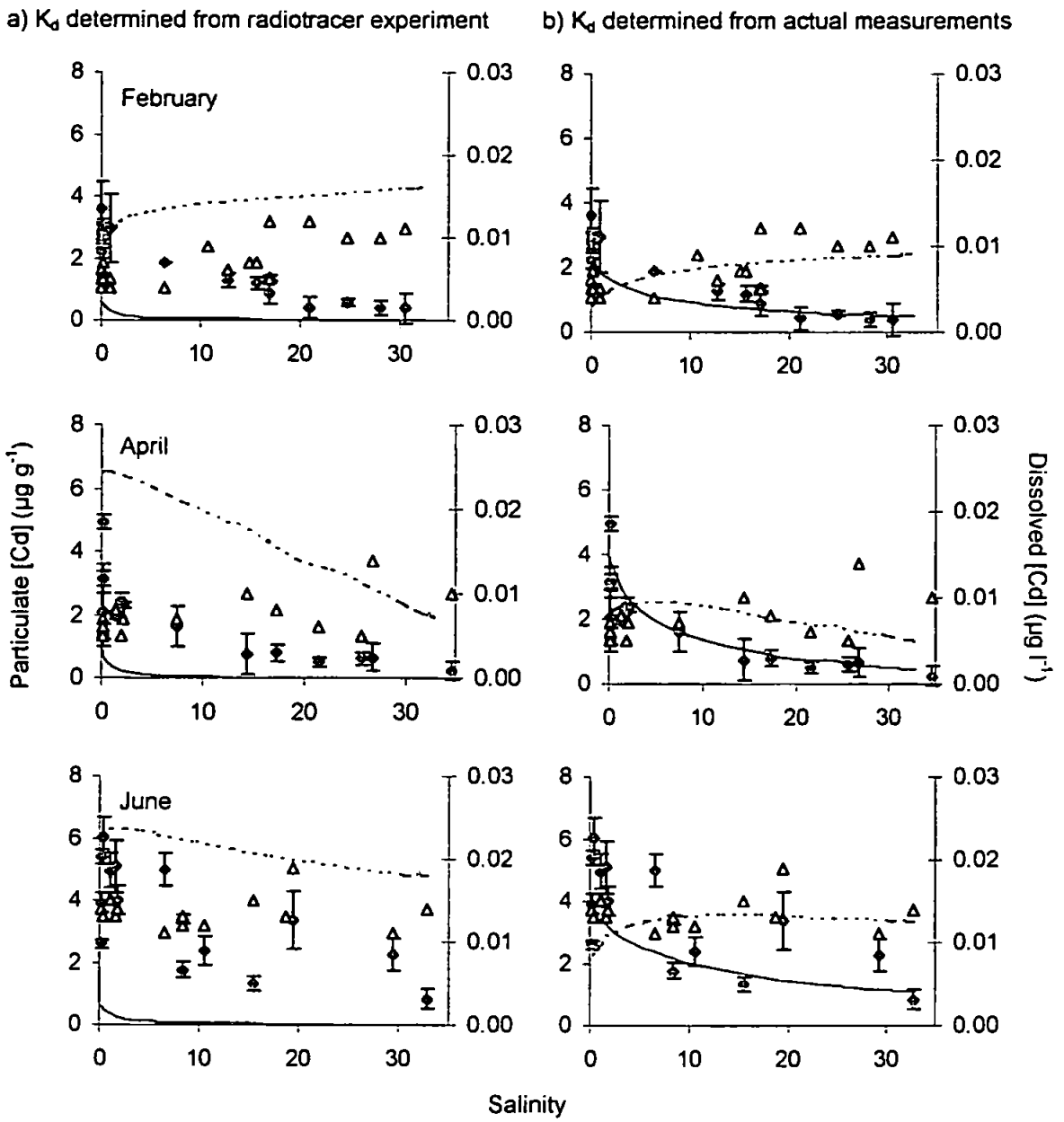

Figure 6.14 Comparison of model predictions of dissolved (—) and particulate (—) Cd concentration with dissolved (Δ) and particulate (♦) measurements during a) February, b) April and c) June. Model predictions using the a) K_d determined from the radiotracer experiments and b) those determined from analytical measurement. Error bars indicate standard deviation of the particulate concentration. Dissolved data supplied by Tappin (*per. comm.*, 2000).

determined concentrations either for calibration or validation purposes can not however be made when the K_d determined from the radiotracer experiments and analytical measurements differ.

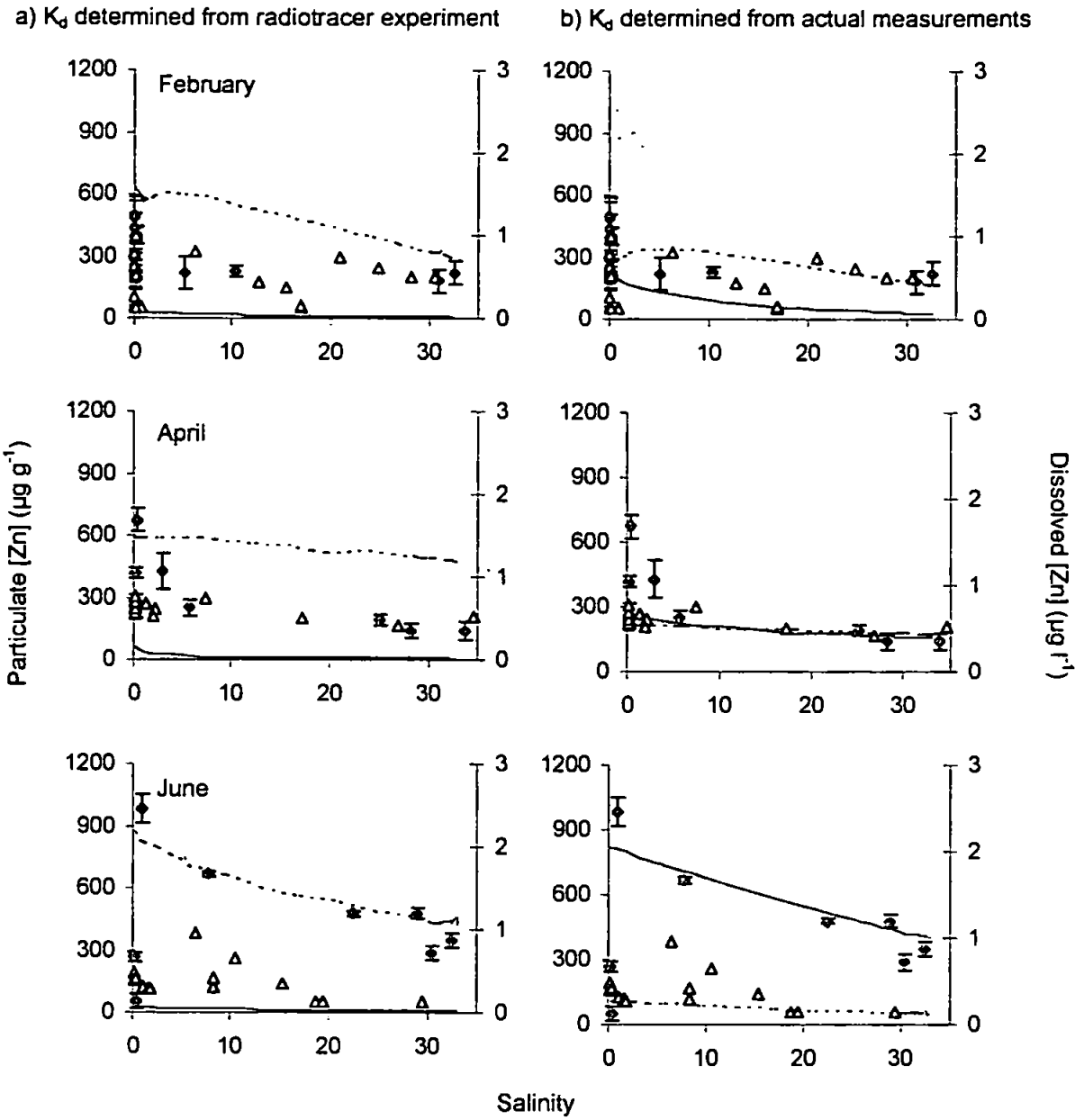

Figure 6.15 Comparison of model predictions of dissolved (—) and particulate (—) Zn concentration with dissolved (Δ) and particulate (♦) measurements during a) February, b) April and c) June. Model predictions using the a) K_d determined from the radiotracer experiments and b) those determined from analytical measurement. Error bars indicate standard deviation of the particulate concentration. Dissolved data supplied by Tappin (*per. comm.*, 2000).

Although successful calibration and validation of a model does not imply that it is a correct representation of a system (Oreskes *et al.*, 1994) it is an important stage in bench marking the models capability. Further work must therefore be directed at achieving comparable results from radiotracer and analytically determined K_ds.

6.4 *Flux of Cd and Zn to the North Sea*

One of the major objectives of the LOIS programme was to determine the flux of trace elements from the land to the sea (NERC, 1994). Hydrodynamic models are suitable when modelling short term events in dynamic systems. The long simulation times mean that they are not however practical for predicting estuarine fluxes over periods of months or years and as outline above calibration and validation may be problematic. The expertise gained from the hydrodynamic modelling can however be applied through empirical protocols to estimate how trace metal fluxes are modified through an estuary.

The flow weighed mean riverine fluxes of total Cd and Zn determined from the LOIS core monitoring programme were 0.016 $\mu g\ l^{-1}$ Cd and 31.6 $\mu g\ l^{-1}$ Zn (Neal & Robson, 2000). The lack of any historical contamination or current anthropogenic discharge and the rapid flushing rate of the estuary implies that the net flux of Cd and Zn out of the estuary will be equivalent to the riverine input. There may however be an exchange between dissolved and particulate phases within the estuary.

Due to the problems identified with the analytically determined K_d the seasonally averaged radiotracer determined K_d has been used to assess the exchange of metal between dissolved and particulate phases during transport through the Tweed Estuary. The change in K_d with salinity within the estuary will determine the flux of dissolved and particulate metal out of the estuary and the radiotracer studies indicated that at salinity of 33 the mean K_d of Cd and Zn was 0.3 and 2.6 g^{-1} respectively.

The SPM-flow relationship (Equation 4.4) has been used to estimate the freshwater SPM concentration. The concentration at the mouth, (salinity = 33) was then calculated assuming conservative mixing between the freshwater concentration and an assumed constant marine value of 5 $mg\ l^{-1}$. This protocol has been applied to period 1996 to 1997 the results of which are plotted in Figure 6.16.

This shows that although the net flux remains unchanged through the estuary approximately 75 % of the particulate Cd and Zn flux out of the estuary occurred in 5 % of the time while approximately 75 % of the dissolved Cd and Zn flux out of the estuary occurred in 40 % of the time. Overall 75 % of the total metal flux was predicted to occur in 39 % of the time. The flux estimates of Cd and Zn out of the estuary, assuming that all the

metal is exchangeable and that desorption is sufficiently rapid compared to the flushing time are shown in Table 6.7.

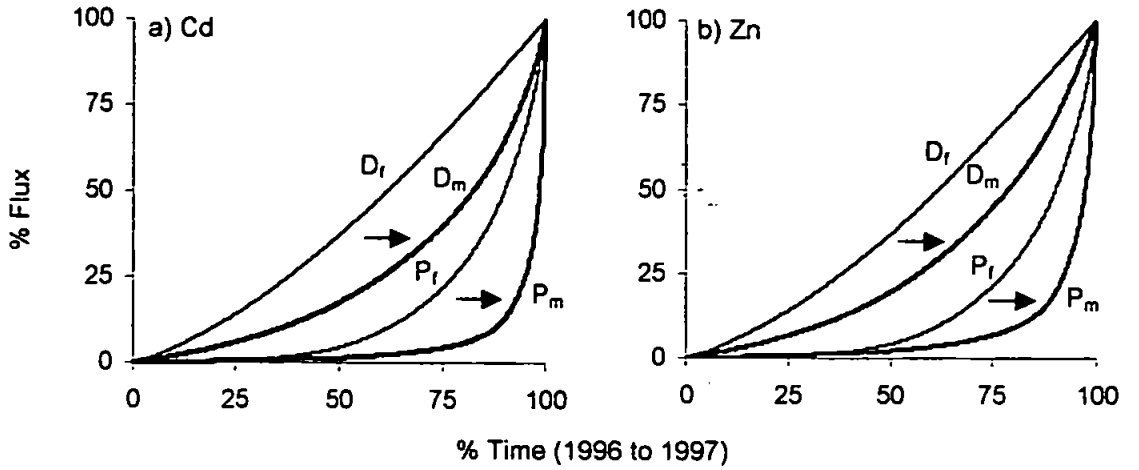

Figure 6.16 Freshwater flux of dissolved (D_f) and particulate (P_f) a) Cd and b) Zn into the Tweed Estuary and dissolved (D_m) and particulate (P_m) flux out of the estuary into the North Sea.

Table 6.7 Calculated annual flux of particulate and dissolved Cd and Zn from the Tweed Estuary to the North Sea based on SEPA and LOIS monitoring data between 1991 and 1997.

	Cd		Zn	
	Particulate	Dissolved	Particulate	Dissolved
Annual Flux ($T\ yr^{-1}$)	2.5×10^{-5}	0.04	0.51	70

6.5 Summary

Comparison of radiotracer and analytically determined K_d are problematic in the Tweed and may in part be due to filter retention of colloidal and micro-particulate materiel normally considered a component of the dissolved phase. The low turbidity, and high pH and dissolved oxygen saturation means this phenomena is likely to be more significant in estuaries like the Tweed compared to more turbid systems such as the Humber, particularly during low summer flows.

Flux estimates of Cd and Zn have shown that > 99 % of the metal flux occurred in the dissolved phase and that 75 % of this was flux occurred in 40 % of the time. Due to the low SPM concentration in the Tweed Estuary anthropogenic input of trace metals are therefore likely to have a higher impact on the dissolved concentration than in areas with higher SPM concentration. The particulate flux accounted for less than 1 % of the total metal flux, but the majority of the particulate transport occurred during short flood events characterised by high turbidity.

Chapter 7

Conclusions and recommendations

7 Conclusions and recommendations

Estuarine modelling provides a means of helping to understand and predict the behaviour of a system or a component within it to a range of variables e.g., river flow, tidal state, effluent discharge or geochemistry. However, measurement and monitoring programmes of estuarine physico-chemical variable are all to frequently based on long established field study methods that may not necessarily provide the most appropriate data for current modelling capabilities. Increasing legislative requirements and the need to be able to predict environmental response to climatic change have promoted modelling studies and shown that they may at times be the only practical means of investigating estuarine processes (Lane *et al.*, 1997). Commercially available estuarine models such as ECoS are an invaluable tool allowing environmental managers to develop models of various complexity. The most appropriate model design for any management issues in question are hard to define, what is however clear is that different model designs have different data requirements for their development and testing. Measurement and monitoring programmes must therefore be driven by the model requirements and this work has developed and tested generic protocols for the integration of estuarine measurement and modelling strategies.

7.1 Measurement and modelling in the Tweed Estuary

During this work the tidal, daily and seasonal variation in salinity, turbidity, pH and trace metal partitioning has been investigated and modelled and this work represents the first reported application of the ECoS3 hydrodynamic template to a tidal system. Throughout the research programme extensive field studies have been compliment by laboratory analysis to provide data required to develop the ECoS model, the results of which have been linked directly to observations in the field. The integration of an extensive field work programme and a tidal model of estuarine transport, pH and trace metal distribution has critical examined previous modelling protocols. Key requirements for the development of sampling and modelling strategies in stratified, dynamic and low turbidity systems have been identified. The major objective of the research have been accomplished, in particular:

- New bathymetry data has been collected at 17 stations in the estuary and used to generate tidally variable cross-sectional areas. These areas have then been encoded into a hydrodynamic model of the Tweed Estuary using ECoS3. The model is driven by tidal elevation at the mouth and mean daily or quarter hourly freshwater flows at the

head and through the tributary the Whiteadder. The model has been calibrated and validated against water elevation data at four sites through the estuary under variable river flow and tidal state. A Manning Coefficient of 0.005 to 0.045, increasing toward the head of the estuary and a constant water dispersion coefficient of 0 m^2 s^{-1} were found to give the best agreement between modelled and observed water depths. The model however over predicted tidal elevation by up to ~ 30 % in the mid to upper estuary. This has been attributed to insufficient resolution of the model (371.4 m) and problems in defining an average bathymetry and common datum in a rapidly rising estuary. A time step of 43 seconds (Courant Number ~ 1) was required to maintain model stability, but further reductions in segment size, required to resolve the complex bathymetry would have approximately doubled the computational time. This has shown that hydrodynamic modelling of a short rapidly rising estuaries may require greater resources in set up and running than a larger estuary.

- Salinity and turbidity distributions have been recorded during axial and tidal surveys and been shown to change rapidly in response to variation in river flow and tidal state. The estuary varied from partially stratified to salt wedge and the limit of surface saline intrusion was reduced from 8.2 to < 1 km as a function of increasing river flow from 14 to 304 m^3 s^{-1}. During 1996 and 1997 river flow changed by up to 25 m^3 s^{-1} over a 15 minute period. Concentrations of SPM were typically low (< 20 mg l^{-1}), but increases in flow of up to 300 m^3 s^{-1} in approximately 7 hours were associated with brief spates of higher (< 260 mg l^{-1}) SPM concentrations that peaked 2 to 3 hours after maximum river discharge. Transport of SPM was mainly conservative and assuming no net deposition or erosion within the estuary the mean annual flux was calculated as 4.7 ± 0.2 x 10^4 T yr^{-1}. 95 % of the sediment flux was estimated to occur during flows in excess of 400 m^3 s^{-1}. This represents 1 % of the time and shows that rapid flushing events are more significant in controlling the flux of sediment and particle bound contaminants in the Tweed than in the Humber.

- The advection and dispersion of salinity and suspended sediment critical to understanding the behaviour of particle reactive trace metals has been modelled and compared to data collected during each survey period. The dispersion of salinity was set equal to that of the water and model results compared to surface measurements. Initial comparisons showed that on averaged the model reproduced 67 % of the variation and over predicted salinity by < 25 units in the mid reaches of the estuary.

Comparison of model predictions to depth averaged salinity data increased the agreement between modelled and observed results to 97 %. This has shown that 1-D models cannot be calibrated and validated using surface measurements of salinity in stratified systems. Agreement between modelled and observed surface results in stratified systems may therefore indicate the need to re-evaluate model performance. The conservative salinity-SPM relationship was well reproduced when settling, erosion and deposition parameters of the Tamar Estuary were used (Harris & Gorley, 1998b), despite the fact that the sediment regime in the Tamar Estuary is different. These sediment transport parameters may also be applicable to other estuarine systems. The spatial distribution of surface salinity and hence any solute or particle advected along the axis of a stratified estuary can not however be reproduced by a 1-D model. This has implications for water quality modelling where the concentration at a particular location opposed to salinity need to be predicted.

- An extensive database of seasonal, daily and spatial variation of pH in the estuary has been established. The pH in the Tweed Estuary varied between 7 and 10 and a highly process orientated model of pH distribution in an estuary has been successfully developed based on the conservative transport of total inorganic carbon and alkalinity (Mook & Koene, 1975). The formulation of the model is presented and has been encoded as a new template fully compatible with ECoS3. The model has been used to separate abiotic from biotic controls on the pH in the Tweed. During the winter the conservative model of total inorganic carbon and alkalinity reproduced the observed data indicating that the main estuarine controls on pH were variations in alkalinity and salinity. During summer low flow conditions a localised region of elevated pH between stations 18 and 15 could not be explained by the model. Corresponding supersaturation of dissolved oxygen, reduction in nutrient concentrations and diurnal variation in the pH indicated that photosynthetic process are important in controlling the pH in the upper estuary during these periods. Inorganic carbon and nutrient assimilation can not however be accounted for by the low concentrations of algae in the water column. Benthic algae and macrophytes therefore appear to be the main biotic controls on water chemistry and may be significant in other rapidly flushed estuaries where there is insufficient time for phytoplankton communities to develop in the water column. These are however only likely to occur in shallow low turbidity systems where enough light can penetrate to the bed. Seaward of station 15 the model reproduced the variation in pH throughout the year indicating that photosynthetic processes were less significant in

the mid to lower estuary. Prediction of pH in the estuary was however dependent upon the availability of end member concentrations of alkalinity and the ability to predict how these concentrations changed through the estuary. Non-conservative behaviour of total inorganic carbon due to high biological activity further complicated the prediction of estuarine pH. ECoS3, however, includes a productivity template and has the potential to be combined with the pH template to produce an extensive water quality module which could be used to model photosynthetic and respiratory controls on the inorganic carbon system and hence pH. Preliminary testing of the productivity template showed that all the parameters were not however operating synergistically. Productivity has not therefore been modelled in this work, but warrants further study.

- Radiotracer sorption experiments to assess the partition coefficients of Cd and Zn were conducted during February, April, June and September 1997 and compared to those determined analytically and the effect of salinity, pH, SPM concentration, and biological activity assessed. All experiments showed a reduction in K_d with increased salinity. The analytically determined K_ds were however an order of magnitude larger that those measured in the radiotracers experiments. The analytically determined K_d(Zn) also showed an order of magnitude increase with increased pH between 7.8 and 9.5 that was not apparent in the radiotracer studies. The K_d(Cd) showed no significant variation with pH through either method. The analytically determined K_d of both metals also showed an order of magnitude decrease with increasing SPM concentration from 1 to 8 mg l^{-1} that was less significant in the radiotracers experiments. It has been hypothesised that the co-variation of particulate Cd and Zn concentrations with that of Fe is due to filter retention of Fe-Mn colloids, precipitated in response to the elevated pH and dissolved oxygen saturation in the estuary and similar processes have been identified in the Danube River (Guieu *et al.*, 1998) and River Rhine (Admiraal *et al.*, 1996). Metabolic inhibition of radiotracer studies showed that this may in part be biologically mediated, although not photosynthetically related. Seasonally variable K_d–salinity relationships determined through analytically and radiotracer studies have been encoded into ECoS3 and model results compared to field measurements. This has shown that model predictions based on radiotracer determined K_ds can not be calibrated or validated against observed data when these K_ds differ from those determined analytically. The analytically determined K_d-salinity relationship explained 76 % of the variation in surface measurements. The variability of the data may be more fully modelled by the inclusion of K_d-pH and K_d-SPM parameters, these relationships

may however be artifactual and the validity of model predictions and measurements may therefore be questionable. Assuming no net gain or loss of metal during transport through the estuary and that all particle bound metal was exchangeable, the radiotracer determined K_d has been used to predict that 99 % of the metal will be flushed from the estuary in the dissolved phase. The remaining 1 % is transported during flood events characterised by high concentrations of SPM.

7.2 *Integration of estuarine measurement and modelling: implications for environmental management*

Key issues identified in the choice of modelling strategy and the collection of data have implications for the management and interpretation of processes in a broad range of estuarine systems.

7.2.1 Sediment and contaminant flux

In estuaries such as the Elbe (Turner *et al.*, 1991) or Tay Estuaries (Balls, 1992) the short flushing time implies that the hydrodynamic response time of water and sediment transport to river flow may be rapid. River flow may also be highly variable and in Weser Estuary maximum flows are an order of magnitude greater than the mean flow (Turner *et al.*, 1991). Tsonis (1996) proposed that "extreme" precipitation events are becoming more frequent and this may lead to increased "flashiness" of river-estuary systems. Short term flood events are therefore likely to become more significant in controlling the flux of sediment and particle reactive contaminants into the coastal zone. In low turbidity estuaries where there is limited particle exchange with the bed such as in some Arctic estuaries *e.g.*, the Chupa Estuary (Howland *et al.*, 1999) flux estimates to the sea can be derived directly from those in the river. On average 90 % of riverborne particulate matter is removed to bed sediments during estuarine mixing in temperate estuaries (Balls, 1988) and when there are natural or anthropogenic sources or sinks in the estuary this approach can not be taken. As industrial inputs to coastal seas and river systems decrease historical contamination in estuarine sediments will become increasing more important as contaminant sources. The erosion, deposition and eventual transport of this contaminated sediment out of an estuary such as the Mersey (NRA, 1995) can only be assessed through modelling of the variation in water velocity in response to tide and river flow. It is however impractical to run detailed hydrodynamic models over periods of years. Models could alternatively be run for

representative periods (high flow, low flow, spring tide, neap tide) and the results extrapolated to provide flux estimates under various climatic scenarios.

The modelling of highly particle reactive or conservative elements may only need to concentrate on accurately defining either the water or sediment transport through an estuary. When, however, the contaminant exchanges between solid and dissolved phases the flux of both water and sediment needs to be encoded. Experimentally deriving K_d values and their response to estuarine geochemical gradients may be problematic when salinity, pH and SPM concentrations co-vary. It is therefore important that the effect of each of these variables be assessed separately. The flux of a contaminant is also dependent upon the rate at which it will adsorb or desorb from suspended particulate mater. During low river flows and high tidal ranges the FSI will be shifted up estuary (Figure 7.1a).

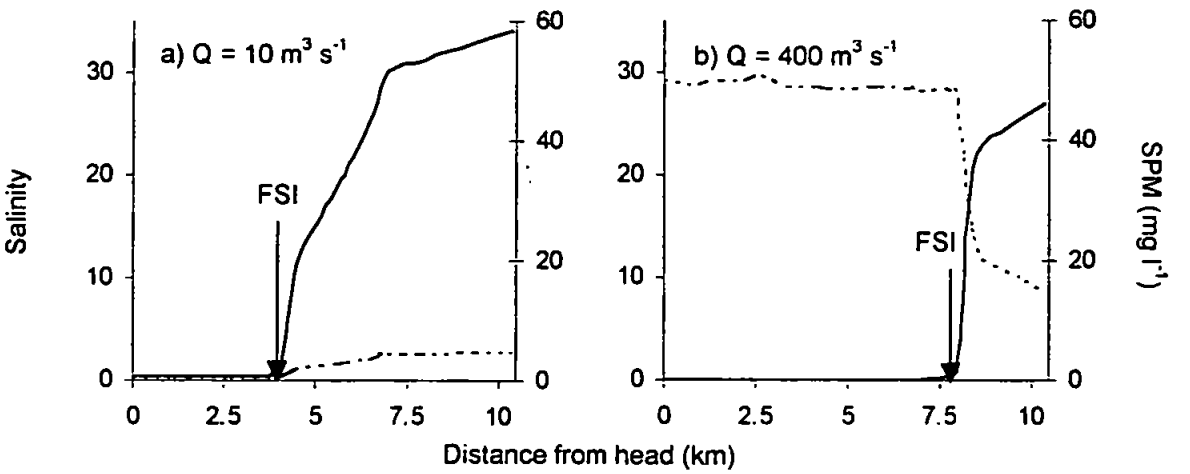

Figure 7.1 Prediction of axial distribution of salinity (—) and SPM concentration (—) under a) low flow and b) high flow conditions in the Tweed Estuary. The limit of saline intrusion is marked (FSI) to illustrate the shift towards the mouth as river flow increases.

If low flow conditions are associated with low SPM the majority of the metal will be transported in the dissolved phase and high concentrations of colloidal and precipitate metals may be important components within the dissolved phases when the pH is high (Figure 7.2a). As river flow increase the FSI is shifted toward the mouth, SPM may increase and pH decrease, (Figures 7.1a and 7.1b).

This significantly reduced the time available for geochemical reactions in response to changes in water chemistry to occur. As the majority of sediment flux occurs during brief flood events sorption kinetics and their incorporation into models that can produce realistic transport times is therefore important in determining exchange processes during these events.

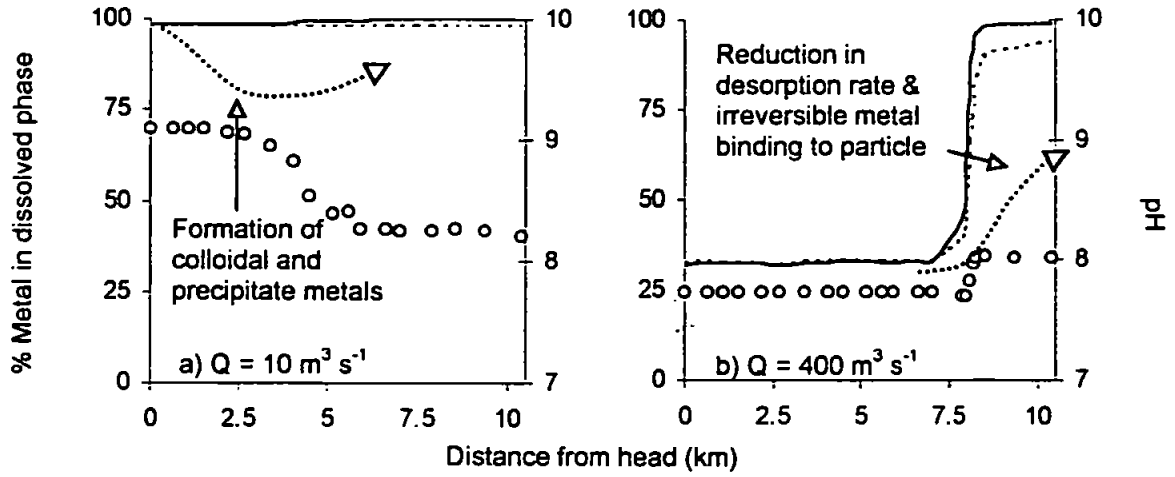

Figure 7.2 Prediction of axial distribution of Cd (—) and Zn (—) based on partitioning data derived from the radiotracer studies as a function of salinity and SPM concentration during a) low flow and b) high flow conditions. The effect of the formation of metal precipitates (a) and reduced desorption (b) are also shown.

7.2.2 Spatial variability and limitation of 1-D models

Determining the flux from estuaries to the sea was a major objective of LOIS (NERC, 1994). Measurement of these fluxes requires a detailed knowledge of the vertical, lateral and temporal variation in current velocity (Dyer, 1997) and Lance *et al.* (1997) concluded that modelling was the only practical means of determining this. Where density currents and lateral variability occur, *e.g.*, Hudson River Estuary (Chant & Wilson, 2000), the use of models to estimate the fluxes is also a very complex issue. The application of tidally average, and tidal 1, 2 or 3-D models to flux estimates can only be made if the effects of model averaging have been fully investigated and are appropriate to the system. The balance between data and computational requirements, and the need to resolved estuarine processes at various levels are summarised in Figure 7.3. For instance the three layer vertical stratification and renewal of deep waters in Arctic systems such as the Chupa Estuary (Howland *et al.*, 1999) could not be reproduced by a 1-D model. The application to fjords and deep estuaries in modelling problems such as biocide accumulation associate with fish farming must therefore be limited to models that can resolve depth stratification. Vertical stratification in water velocity in the Ribble Estuary is important in control sediment transport (Burton, 1994) and could not be reproduced by depth averaged models (Gleizon, 1999). Lateral variation in broad shallow estuaries may also be important and wind forcing and the effect of coastal trapping in broad estuaries such as the Terrebonne Estuary, Louisiana requires the horizontal resolution of flow by 2-D models with detailed bathymetry and coastal topography (Inoue & Wiseman, 2000). A further consequence of

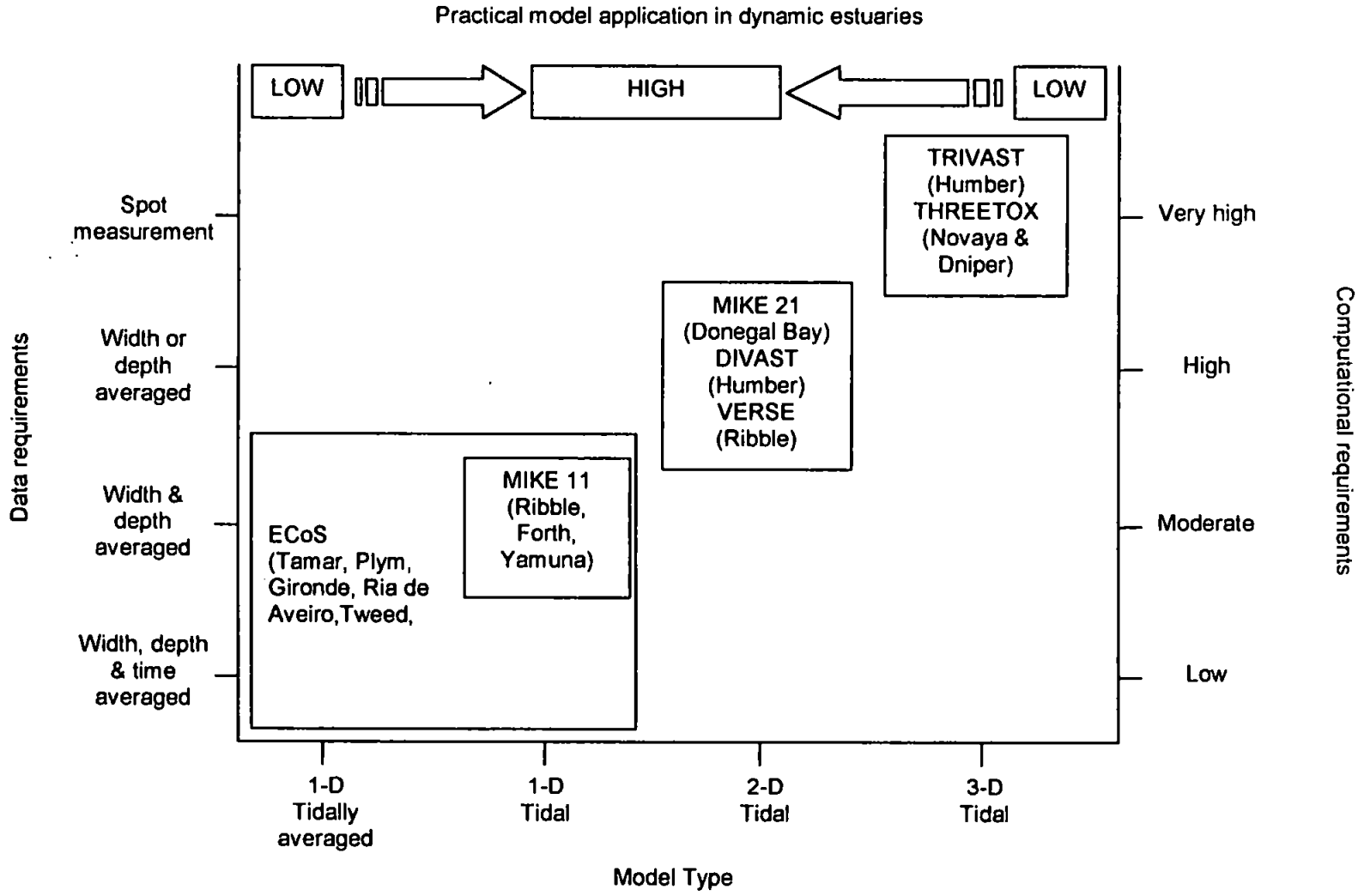

Figure 7.3 Practical application of estuarine models strategies. A selection of model types grouped as a function of data and computational requirement.

climatic change is sea level rise. This will result in increased water depth and models will response by predicting further tidal intrusion into the estuary. The bathymetry surveys in of the Tweed did not however take account of the bank topography and as shown in Figure 4.6 the cross-sectional area-depth prediction at greater water depths (during flood events or through sea level rise) may be inaccurate. The topography of the banks and river valley sides is however quite steeply rising though out the majority of the current tidal limit, but increased tidal inundation of low lying surrounding ground may occur along the southern bank between stations 6 and 8 and 13 and 17. Inundation of salt marsh and over bank flooding onto agricultural land as a function of river flow, tidal state and wind forcing are important issues, but modelling studies of this nature are however more suited to 2-D horizontally resolving models such as MIKE 21.

7.3 Future work and recommendations

To increase estuarine modelling capabilities in dynamic tidal systems requires a better understanding of how physical, chemical and biological processes operate on the time scales involved. In rapidly flushed estuaries with little bed sediment deposits and no anthropogenic inputs fluxes can be derived from riverine measurements. In the majority of estuaries, identifying the importance of source and sinks of contaminants is however critical in modelling the flux through the system.

1) The discrepancy between modelled and observed water elevation has been attributed to insufficient resolution of the bathymetry. Bathymetry surveys, either related to the refinement of the Tweed model or the parameterisation of a new area should include i) the area up to and preferably just beyond the tidal limit, ii) a longitudinal transect along the deep channel to asses the variation between cross-sections and iii) the bank topography so that the effect of extreme flood events and sea level rise can be modelled.

2) The use of the same input data into other 1 or 2-D models (*e.g.*, MIKE 11, MIKE 21 and VERSE) and comparison of models results could be used to establish minimal requirements for model parameters and to define what are acceptable levels of model performance.

3) The accumulation of sediment and sediment bound contaminants within a riverine system and episodic flux from the catchment in response to rapidly changing hydrographs need to be more fully investigated so that flux models can be generated. Seasonal and flow related variation in particle size, composition and the effect that this has on the geochemical reactivity of the particles also needs to be more fully understood if the effects of extreme precipitation events are to be modelled.

4) High concentrations of Fe and Mn colloids and precipitates may be critical in controlling metal partitioning in low turbidity high pH systems. Increased water temperatures and primary productivity during summer months may lead to the elevation of pH in river and estuarine systems. Kinetic studies of the effect of pH, dissolved oxygen and bacterial mediation on the distribution of metals between dissolved, colloidal or micro-particulate and particulate phases should be investigated. Differences between radiotracer and analytically determined K_ds should also be investigated to increase the understanding and modelling of these processes.

5) The determination of particulate or dissolved concentrations for purposes such as discharge authorisation by regulatory bodies or the generation of K_d values for modelling studies is critically dependent on the operational definition between particulate and dissolved phases. This work has drawn into question the reliability of standard filtration techniques. Future work should be aimed at determining how filter pore size and particle separation techniques affect the determination of dissolved and particulate concentrations and hence K_d, and the consequences of this for the regulatory authorities.

A model is only a numerical representation of a concept and model results will always be limited by the quality and quantity of data available for model parameterisation and testing. Using the guidelines outlined in this work proposed measurement and modelling strategies should be critically examined to determine whether they are appropriate to the management or research issue in question.

References

References

Abreu, S. N., Pereira, M. E. & Duarte, A. C. 1998 The use of a mathematical model to evaluate mercury accumulation in sediments and recovery time in a coastal lagoon (Ria de Aveiro, Portugal). *Water Science Technology* **37**, 33-38.

Ackroyd, D. R., Bale, A. J., Howland, R. J. M., Knox, S., Millward, G. E. & Morris, A. W. 1986 Distribution and behaviour of dissolved Cu, Zn and Mn in the Tamar Estuary. *Estuarine, Coastal and Shelf Science* **23**, 621-640.

Admiraal, W., Tubbing, G. M. J. & Breebaart, L. 1995 Effects of phytoplankton on metal partitioning in the lower River Rhine. *Water Research* **29**, 941-946.

Amin, M. & Flather, R. A. 1996 Calibration of a numerical model with a limited number of tidal constituents. *Estuarine, Coastal and Shelf Science* **43**, 637-652.

Applied Microsystems Limited 1993 *Model EMP 2000 Multi-parameter Water Quality Monitoring Instrument Users Manual Version 1.03.* Applied Microsystems Ltd, Sidney, Canada, 67 pp.

Baeyens, W., Elsken, M., Gillain, M. & Goeyens, L. 1998 Biogeochemical behaviour of Cd, Cu, Pb and Zn in the Scheldt Estuary during the period 1981-1983. *Hydrobiologia* **366**, 15-44.

BADC (British Atmospheric Data Centre) 1998 Application for Access to Restricted Datasets. http://www.badc.rl.ac.uk/cgi-bin/conditions/conditions.pl.

Bale, A. J. 1987 *The Characteristics, Behaviour and Heterogeneous Chemical Reactivity of Estuarine Suspended Particles.* Ph.D. Thesis Plymouth Polytechnic, Devon, UK.

Bale, A. J., Morris, A. W. & Howland, R. J. M. 1985 Seasonal sediment movement in the Tamar Estuary. *Oceanologica Acta* **8**, 1-6.

Bale, A. J., Barrett, C. D., West, J. R. & Oduyemi, K. O. K 1989 Use of *in-situ* laser diffraction particle sizing for particle transport studies in estuaries. In: *Developments in Estuarine and Coastal Study Techniques.* McManus, J. & Elliot, M. (Eds.), Olsen & Olsen, Denmark, 133-138.

Balls, P. W., 1988 The control of trace metal concentrations in coastal seawater through partition onto suspended particulate matter. *Netherlands Journal of Sea Research* **22**, 213-218.

Balls, P. W., 1989 The partition coefficient of trace metals between dissolved and particulate phases in European coastal waters: a compilation of field data and comparison with laboratory studies. *Netherlands Journal of Sea Research* **23**, 7-14.

Balls, P. W. 1990 Distribution and composition of suspended particulate material in the Clyde Estuary and associated sea lochs. *Estuarine, Coastal and Shelf Science* **30**, 475-487.

Balls, P. W. 1992 Nutritional behaviour in two contrasting Scottish estuaries, the Forth and Tay. *Oceanologica Acta* **15**, 261-277.

Balls, P. W. 1994 Nutrient inputs to estuaries from nine Scottish east coast rivers: Influences of estuarine processes on inputs to the North Sea. *Estuarine, Coastal and Shelf Science* **39**, 329-352.

Balls, P. W., Laslett, R. E. & Price, N. B. 1994 Nutrient and trace metal distributions over a complete semi-diurnal tidal cycle in the Forth Estuary, Scotland. *Netherlands Journal of Sea Research* **33**, 1-17.

Benes, P. Kuncova, M., Slovak, J. & Lam Ramos, P. 1988 Analysis of the interaction of radionuclides with solid phase in surface waters using laboratory model experiments: methodical problems. *Journal of Radioanalytical and Nuclear Chemistry* **125**, 295-315.

Benoit, G., Oktay-Marshall, S. D., Cantu II, A., Hood, E. M., Coleman, C. H., Corapcioglu, M. O. & Santschi, P. H. 1994 Partitioning of Cu, Pb, Ag, Zn, Fe, Al and Mn between filter-retained particles, colloids, and solution in six Texas estuaries. *Marine Chemistry* **45**, 307-336.

Bewers, J. M., Blanton, J. O., Davies, A. M., Gurbutt, P. A., Hofmann, E. E., Jamart, B. M., Lam, D. C. L., Takahashi, M. & Verboom, G. K. 1992 A conceptual model of contaminant transport in coastal marine systems. *Ambio* **21**, 166-169.

Bilos, C., Colombo, J. C. & Presa, M. J. R. 1998 Trace metals in suspended particles, sediment and Asiatic clams (*Corbicula fluminea*) of the Rio de la Plata Estuary. *Environmental Pollution* **99**, 1-11.

Blom, G. & Winkels, H. J. 1998 Modelling sediment accumulation and dispersion of contaminants in Lake Ijsselmeer (the Netherlands). *Water Science Technology* **37**, 17-24.

Bourg, A. C. M. 1988 Physicochemical speciation of trace elements in oxygenated estuarine waters. In: *Determination of Trace Metals in Natural Waters*. West, T. S. & Numberg, H. W. (Eds.), Blackwell Scientific, Oxford, UK, 287-321.

Bourg, A. C. M. & Bertin, C. 1996 Diurnal variations in the water chemistry of a river contaminated by heavy metals: natural biological cycling and anthropic influence. *Water, Air and Soil Pollution* **86**, 101-116.

Boyer, J. N., Christian, R. R. & Stanley, D. W. 1993 Patterns of phytoplankton primary productivity in the Neuse River Estuary, North Carolina, USA. *Marine Ecology Progress Series* **97**, 287-297.

Braungardt, C., Achterberg, E. R. & Nimmo, M. 1998 On-line voltammetric monitoring of dissolved Cu and Ni in the Gulf of Cadiz, south-west Spain. *Analytica Chimica Acta* **377**, 205-215.

Bronsdon, R. K. & Naden, P. S. 2000 Suspended sediment in the Rivers Tweed and Teviot. *The Science of the Total Environment* **251/252**, 95-113.

Brown, A. (Ed.), 1992 *The UK Environment*, HMSO, London, 258 pp.

Bryan, G. W., Gibbs, P. E., Hummerstone, L. G. & Burt, G. R. 1987 Copper, zinc and organotin as long-term factors governing the distribution of organisms in the Fal Estuary in southwest England estuaries. *Estuaries* **10**, 208-219.

Burton, D. 1994 *Modelling of Solute and Sediment Transport in the Ribble Estuary*. Ph.D. Thesis, University of Birmingham, West Midlands, UK.

Cai, W. & Wang, Y. 1998 The chemistry, fluxes, and sources of carbon dioxide in the estuarine waters of the Satilla and Altamaha Rivers, Georgia. *Limnology and Oceanography* **43**, 657-668.

Cai, W., Wang, Y. & Hodson, R. E. 1998 Acid-base properties of dissolved organic matter in the estuarine waters of Georgia. *Geochimica et Cosmochimica Acta* **54**, 1247-1254.

Camusso, M., Crescenzio, S., Martinotti, W., Pettine, M. & Pagnotta, R. 1997 Behaviour of Co, Fe, Mn and Ni in the Po Estuary (Italy). *Water, Air and Soil Pollution* **99**, 297-304.

Cancino, L. & Neves, R. 1995 Three-dimensional model system for baroclinic estuarine dynamics and suspended sediment transport in a mesotidal estuary. In: *Computer Modelling of Seas and Coastal Regions II*. Brebbia, C. A., Traversoni, L. & Wrobel, L. C. (Eds.), Computational Mechanics Publications, Southampton, 353-360.

Chant, R. J. & Wilson, R. E. 2000 Internal hydraulics and mixing in a highly stratified estuary. *Journal of Geophysical Research-Oceans* **105**, 14215-14222.

Chapelle, A., Lazure, P. & Menesguen, A. 1994 Modelling eutrophication events in a coastal ecosystem. Sensitivity analysis. *Estuarine, Coastal Shelf Science* **39**, 529-548.

Chester, R. 1990 *Marine Geochemistry*, Chapman & Hall, London, 698 pp.

Church, T. A. 1986 Biogeochemical factors influencing the residence time of microconstituents in a large tidal estuary, Delaware Bay. *Marine Chemistry* **18**, 393-406.

Cifuentes, L. A., Schemel, L. E. & Sharp, J. H. 1990 Qualitative and numerical analysis of the effects of river inflow variation on mixing diagrams in estuaries. *Estuarine, Coastal and Shelf Science* **30**, 411-427.

Clarke, S. & Elliott, A. J. 1998 Modelling suspended sediment concentrations in the Firth of Forth **47**, 235-250.

Clayton, J. W. 1997 The biology of the River Tweed. *The Science of the Total Environment* **194/195** 155-162.

Comans, R. N. J., Haller, M. & de Preter, P. 1991 Sorption of cesium on illite: Non-equilibrium behaviour and reversibility. *Geochimica et Cosmochimica Acta* **55**, 433-440.

Comber, S. D. W., Gunn, A. M. & Whalley, C. 1995 Comparison of the partitioning of trace metals in the Humber and Mersey Estuaries. *Marine Pollution Bulletin* **30**, 851-860.

Crawford, D. W. & Purdie, D. A. 1997 Increase of pCO_2 during blooms of *Emiliania huxleyi*: Theoretical considerations on the asymmetry between acquisition of HCO_3^- and respiration of free CO_2. *Limnology and Oceanography* **42**, 365-372.

Danish Hydraulic Institute 1995 DHI Software User Conference 1995, CD-ROM, Danish Hydraulic Institute, Denmark.

Danish Hydraulic Institute 1996 *MIKE 21 A Modelling System for Estuaries, Coastal Waters and Seas*. Danish Hydraulic Institute, Denmark.

Davison, W., Hill, M., Woof, C., Rouen, M. & Aspinall, D. 1994 Continuous measurements of stream pH. Evaluation of procedures and comparison of resulting hydrogen ion budgets with those from flow-weighted integrating samplers. *Water Research* **28**, 161-170.

Dickson, A. G. & Millero, F. J. 1987 A comparison of the equilibrium constants for the dissociation of carbonic acid in seawater media. *Deep-Sea Research* **34**, 1733-1743.

Dyke, P. 1996 *Modelling Marine Processes*, Prentice Hall, London, 152 pp.

Dyer, K. R. 1986 *Coastal Estuarine Sediment Dynamics*, John Wiley & Son, Chichester, 342 pp.

Dyer, K. R. 1991 Circulation and mixing in stratified estuaries. *Marine Chemistry* **32**, 111-120.

Dyer, K. R. 1994. Estuarine sediment transport and deposition. In: *Sediment Transport and Depositional Processes*. Pye, K. (Ed.) Blackwell Scientific Publications, Oxford, 193-218.

Dyer, K. R. 1997 *Estuaries: A Physical Introduction*, 2nd Edition, John Wiley & Son, Chichester, 195 pp.

Dyer, K. R. & Evans, E. M. 1989 Dynamics of turbidity maximum in a homogeneous tidal channel. *Journal of Coastal Research* **5**, 23-30.

Eatherall, A., Naden, P. S. & Cooper, D. M. 1998 Simulating carbon flux to the estuary: The first step. *The Science of the Total Environment* **210/211**, 519-533.

van Eck, G. Th. M. & de Rooji, N. M. 1990 Development of a water quality and bio-accumulation model for the Scheldt Estuary. In: *Estuarine Water Quality Management Coastal and Estuarine Studies*. Vol. 36. Michaelis, W. (Ed.) Springer-Verlag, Berlin, 95-102.

Edinger, J. E., Buchak, E. M. & Kolluru, V. S. 1998 Modelling flushing and mixing in a deep estuary. *Water, Air, and Soil Pollution* **102**, 345-353.

Edwards, A. M. C., Freestone, R. J. & Crockett, C. P. 1997 River management in the Humber catchment. *The Science of the Total Environment* **194/195**, 235-246.

Elbaz-Poulichet, F., Martin, J. M., Huang, W. W. & Zhu, J. X. 1987 Dissolved Cd behaviour in some selected French and Chinese estuaries. Consequences on Cd supply to the ocean. *Marine Chemistry* **22**, 125-136.

Elbaz-Poulichet, F., Garnier, J. M., Guan, D. M., Martin, J. –M. & Thomas, A. J. 1996 The conservative behaviour of trace metals (Cd, Cu, Ni and Pb) and As in the surface plume of stratified estuaries: examples of the Rhone River (France). *Estuarine, Coastal Shelf Science* **42**, 289-310.

Elbaz-Poulichet, F., Morley, N. H., Cruzado, A., Velasquez, Z., Achterberg, E. P. & Braungardt, C. B. 1999 Trace metal and nutrient distribution in an extremely low pH (2.5) river-estuarine system, the Ria of Huelva (south-west Spain). *The Science of the Total Environment* **227**, 73-83.

Environment Agency 1999 http://www.environment-aganecy.gov.uk.

European Commission 1999a http://www.europa.eu.int/comm/dg11/iczm/background.htm.

European Commission 1999b http://www.europa.eu.int/comm/dg11/policy_en.htm.

Falconer, R. A. 1992 Flow and water-quality modelling in coastal and inland waters. *Journal of Hydraulic Research* **30**, 437-452.

Falconer, R. A. & Lin, B. 1997 Three-dimensional modelling of water quality in the Humber Estuary. *Water Research* **31**, 1092-1102.

Ferrier, G. & Anderson, J. M. 1997 A multi-disciplinary study of frontal systems in the Tay Estuary, Scotland. *Estuarine, Coastal Shelf Science* **45**, 317-336.

Featherstone, A. M. & O'Grady, B. V. 1997 Removal of dissolved copper and iron at the freshwater-saltwater interface of an acid mine stream. *Marine Pollution Bulletin* **34**, 332-337.

Fichez, R., Jickells, T. D. & Edmunds, H. M. 1992 Algal blooms in high turbidity, a result of the conflicting consequences of turbulence on nutrient cycling in a shallow water estuary. *Estuarine, Coastal Shelf Science* **35**, 577-592.

Fox, I.A. and Johnson, R.C. 1997 The hydrology of the River Tweed. *The Science of the Total Environment*, **194/195**, 163-172.

Frankignoulle, M., Bourge, I. & Wollast, R. 1996 Atmospheric CO_2 fluxes in a highly polluted estuary (the Scheldt). *Limnology and Oceanography* **41**, 365-369.

Gagnon, C., Arnac, M. & Brindle, J. 1992 Sorption interactions between trace metals (Cd and Ni) and phenolic substances on suspended clay minerals. *Water Research* **26**, 1067-1072.

Garnier, J. –M., Martin, J. –M., Mouchel, J. –M. & Thomas, A. J. 1993 Surface properties characterisation of suspended matter in the Ebro Delta (Spain); with an application to trace metal sorption. *Estuarine, Coastal Shelf Science* **36**, 315-332.

GESAMP (Joint Group of Experts on the Scientific Aspects of Marine Pollution) 1987 *Land/Sea Boundary Flux of Contaminants: Contributions from Rivers*. GESAMP, **32**, 172 pp.

Gillibrand, P. A. & Balls, P. W. 1998 Modelling salt intrusion and nitrate concentrations in the Ythan estuary. *Estuarine Coastal and Shelf Science* **47**, 695-706.

van Gils, J. A. G., Ouboter, M. R. L. & de Rooij, N. M. 1993 Modelling of water and sediment quality in the Scheldt Estuary. *Netherlands Journal of Aquatic Ecology* **27**, 257-265.

Glegg, G. A., Titley, J. G., Millward, G. E., Glasson, D. R. & Morris, A. W. 1988 Sorption behaviour of waste-generated trace metals in estuarine waters. *Water Science Technology* **20**, 113-121.

Gleizon, P. 1999, VERSE, a vertically resolving model of sediment transport for the Ribble Estuary. Abstract in *Coast and Estuaries of North-West England, ECSA Local Meeting, Lancaster University, 8-9 April, 1999.*

Gomez-Reyes, E. & Blumberg, A. F. 1995 Pollution transport in coastal water bodies. In: *Computer Modelling of Seas and Coastal Regions II.* Brebbia, C. A., Traversoni, L. & Wrobel, L. C. (Eds.), Computational Mechanics Publications, Southampton, 87-94.

Gorley, R. N. & Harris, J. R. W. 1998 *ECoS3 User Guide.* Centre for Coastal and Marine Sciences Plymouth Marine Laboratories, Plymouth, 35 pp.

Gosh, S. K. & Jana, T. K. 1994 Apparent dissociation constants of carbonic acid in estuarine water at different salinities and temperatures. *Indian Journal of Marine Sciences* **23**, 126-128.

Goyet, C. & Poisson, A. 1989 New determination of carbonic acid dissociation constants in seawater as a function of temperature and salinity. *Deep-Sea Research* **36**, 1635-1654.

Grabemann, I., Uncles, R. J., Krause, G. & Stephens, J. A. 1997 Behaviour of turbidity maxima in the Tamar (U.K.) and Weser (F.R.G.) Estuaries. *Estuarine, Coastal Shelf Science* **45**, 235-246.

Guasch, H., Armengol, J., Marti, E. & Sabater, S. 1998 Diurnal variation in dissolved oxygen and carbon dioxide in two low-order streams. *Water Research* **32**, 1067-1074.

Guieu, C., Martin, J., Tankere, S. P. C., Mousty, F., Trincherini, P., Bazot, M. & Dai, M. H. 1998 On trace metal geochemistry in the Danube River and western Black Sea. *Estuarine, Coastal Shelf Science* **47**, 471-485.

Hall, I. R., Hydes, D. J., Statham, P. J. & Overnells, J. 1996 Dissolved and particulate trace metals in a Scottish sea loch: an example of a pristine environment? *Marine Pollution Bulletin* **32**, 846-854.

Hamilton-Taylor, J., Kelly, M., Titley, J. G. & Turner, D. R. 1993 Particle-solution behaviour of plutonium in the estuarine environment, Esk Estuary, UK. *Geochimica et Cosmochimica Acta* **57**, 3367-3381.

Hanley, N., Faichney, R., Munro, A. & Shortle, J. S. 1998 Economic and environmental modelling for pollution control in an estuary. *Journal of Environmental Management* **52**, 211-225.

Hansson, I. 1973 A new set of acidity constants for carbonic acid and boric acid in seawater. *Deep-Sea Research* **20**, 461-478.

Harding, Jr., L. W., Meeson, B. W. & Fisher, Jr., T. R. 1986 Phytoplankton production in two east coast estuaries: photosynthesis-light functions and patterns of carbon assimilation in Chesapeake and Delaware Bays. *Estuarine, Coastal and Shelf Science* **23**, 773-806.

Harris, J. R. W. 1987 Sink or drain: a simulation study of factors affecting the role of an estuary subject to toxic inputs. *Water Research* **8**, 975-981.

Harris, J. R. W. & Gorley, R. N. 1998a *An Introduction to Modelling Estuaries with ECoS3*. Centre for Coastal and Marine Sciences Plymouth Marine Laboratories, Plymouth, 43 pp.

Harris, J. R. W. & Gorley, R. N. 1998b *Estuarine Quality Templates for ECoS3*. Centre for Coastal and Marine Sciences Plymouth Marine Laboratories, Plymouth, 47 pp.

Harris, J. R. W., Bale, A. J., Bayne, B. J., Mantoura, R. F. C., Morris, A. W., Nelson, L. A., Radford, P. J., Uncles, R. J. Weston, S. A. & Widdows, J. 1984 A preliminary model of the dispersal and biological effects of toxins in the Tamar estuary, England. *Ecological Modelling* **22**, 253-284.

Harris, J. R. W., Gorley, R. N. & Bartlett, C. A 1993 *ECoS Version 2, User Manual Edition 2.1*. Plymouth Marine Laboratories, Plymouth, 146 pp.

Hegeman, W. J. M., van der Weijden, C. H. & Zwolsman, J. J. G. 1992 Sorption of zinc on suspended particles along a salinity gradient: a laboratory study using illite and suspended matter from the River Rhine. *Netherlands Journal of Sea Research* **28**, 285-292.

Herczeg, A. L. & Hesslein, R. H. 1984 Determination of hydrogen ion concentration in softwater lakes using carbon dioxide equilibria. *Geochimica et Cosmochimica Acta* **48**, 837-845.

Hess, T., Matthews, R. & Quinton, J. 1999 *Modelling Environmental Systems*. Silsoe College, Cranfield University, Bedford, 59 pp.

Hoffer-French, K. J. & Herman, J. S. 1989 Evaluation of hydrological and biological influences on CO_2 fluxes from a Karst stream. *Journal of Hydrology* **108**, 189-212.

Hoffmann, M. R. 1981 Thermodynamic, kinetic and extrathermodynamic considerations in the development of equilibrium models for aquatic systems. *Environmental Science & Technology* **15**, 345-353.

Howland, R. J. M., Pantiulin, A. N., Millward, G. E. & Prego, R. 1999 The hydrography of the Chupa Estuary, White Sea, Russia. *Estuarine, Coastal and Shelf Science* **48**, 1-12.

Howland, R. J. M., Tappin, R. J. Uncles, Plummer, D. H. & Bloomer, N. J. 2000 Distribution and seasonal variability of pH and alkalinity in the Tweed Estuary, U.K. *The Science of the Total Environment* **251/252**, 125-138.

Huthnance, J. M., Allens, J. I., Davies, A. M., Hydes, D. J., James, I. D., Jones, J. E., Millward, G. E., Prandle, D., Proctor, R., Purdie, D. A., Statham, P. J., Tett, P. B., Thomas, S. & Wood, R. G. 1993 Towards water quality models. *Philosophical Transactions of the Royal Society of London* **343**, 569-584.

Hsu, M-H., Kuo, A. Y., Kuo, J-T. & Liu, W-C. 1999 Procedure to calibrate and verify numerical models of estuarine hydrodynamics. *Journal of Hydraulic Engineering* **125**, 166-182.

Hydrographic Office 1989a *Admiralty Tide Tables*, Volume 1. Hydrographer of the Navy, Taunton, UK, 433 pp.

Hydrographic Office 1992a *Admiralty Chart No. 1612.* Hydrographer of the Navy, Taunton, UK.

Hydrographic Office 1992b *Hydrographic Office Tidal Prediction System Tidecalc V1.1.* Hydrographer of the Navy, Taunton, UK.

IAEA (International Atomic Energy Agency) 1989 *Evaluating the Reliability of Predictions made using Environmental Transfer Models* Safety Series No. 100, International Atomic Energy Agency, Vienna.

IAEA (International Atomic Energy Agency) 1991 *Coastal Modelling* Rep. 43, International Atomic Energy Agency, Vienna.

Ibanez, C. Pont, D. & Prat, N. 1997 Characterisation of the Ebro and Rhone Estuaries: A basis for defining and classifying salt-wedge estuaries. *Limnology and Oceanography* **42**, 89-101.

Inoue, M. & Wiseman, W. J. 2000 Transport, mixing and stirring processes in a Louisiana estuary: a model study. *Estuarine, Coastal and Shelf Science* **50**, 449-466.

Iriarte, A., Madariaga, I. Diez-Garagarza, F., Revilla, M. & Orive, E. 1996 Primary plankton production, respiration and nitrification in a shallow temperate estuary during summer. *Journal of Experimental Marine Biology and Ecology* **208** 127-151.

Istvanovics, V. 1994 Fractional composition, adsorption and release of sediment phosphorus in the Kis-Balaton reservoir. *Water Research*, **28**, 717-726.

Jannasch, H. W., Honeyman, B. D., Balistrieri, L. S. & Murray, J. W. 1988 Kinetics of trace element uptake by marine particles. *Geochimica et Cosmochimica Acta* **52**, 567-577.

Jarvie, H. P., Neal, C., Leach, D. V., Ryland, G. P., House, W. A. & Robson, A. J. 1997 Major ion concentrations and the inorganic carbon chemistry of the Humber rivers. *The Science of the Total Environment* **194/195**, 285-302.

Jarvie, H. P., Neal, C., Tappin, A. D., Burton, J. D., Hill, L., Neal, M., Harrow, M., Hopkins, R., Watts, C. & Wickham, H. 2000 Riverine inputs of major ions and trace elements to the tidal reaches of the River Tweed, UK. *The Science of the Total Environment* **251/252**, 55-81.

Johnson, C. A. 1986 The regulation of trace element concentrations in rivers and estuarine waters contaminated with acid mine drainage: The adsorption of Cu and Zn on amorphous Fe oxyhydroxides. *Geochimica et Cosmochimica Acta* **50**, 2433-2438.

Kazmi, A. A. & Hansen, I. S. 1997 Numerical models in water quality management: A case study for the Yamuna River (India). *Water Science Technology* **36**, 193-200.

Kern, U., Li, C. & Westrich, B. 1998 Assessment of sediment contamination from pollutant discharges in surface waters. *Water Science Technology* **37**, 1-8.

Kirk, J. T. O. 1994 *Light and Photosynthesis in Aquatic Ecosystems. 2nd Edition.* Cambridge University Press, Cambridge, UK, 509 pp.

Koelmans, A. A. & Radovanovic, H. 1998 Prediction of trace metal distribution coefficients (K_d) for aerobic sediments. *Water Science Technology* **37**, 71-78.

Koeppenkastrop, D. & de Carlo, E. H. 1993 Uptake of rare earth elements from solution by metal oxides. *Environmental Science & Technology* **27**, 1796-1802.

Koziy, L., Maderich, V., Margvelashvili, N. & Zheleznyak, M. 1998 Three-dimensional model of radionuclide dispersion in estuaries and shelf seas. *Environmental Modelling & Software* **13**, 413-420.

Kowalik, Z. & Murty, T. S. 1993 *Numerical Modelling of Ocean Dynamics*, Advanced Series on Ocean Engineering, Vol. 5, World Science, London, 481 pp.

Kraepiel, A. M. L., Chiffoleau, J., Martin, J. & Morel, F. M. M. 1997 Geochemistry of trace metals in the Gironde Estuary. *Geochimica et Cosmochimica Acta* **61**, 1421-1436.

Krapivin, V. F., Cherepenin, V. A., Phillips, G. W., August, R. A. & Pautkin, A. Y. 1998 An application of modelling technology to the study of radionuclear pollutants and heavy metal dynamics in the Angara-Yenisey river system. *Ecological Modelling* **111**, 121-134.

Kromkamp, J., Peene, J., van Rijswijk, P., Sandee, A. & Goosen, N. 1995 Nutrients, light and primary production by phytoplankton and micobenthos in the eutrophic, turbid Westerschelde Estuary (The Netherlands). *Hydrobiologia* **311**, 9-19.

Kurup, G. R., Hamilton, D. P. & Patterson, J. C. 1998 Modelling the effects of seasonal flow variation on the position of salt wedge in a macrotidal estuary. *Estuarine, Coastal and Shelf Science* **47**, 191-208.

Kuwabara, J. S., Chang, C. C. Y., Cloern, J. E., Fries, T. L., Davies, J. A. & Luoma, S. N. 1989 Trace metal association in the water column of south San Francisco Bay, California.

Lane, A., Prandle, D., Harrison, A. J., Jones, P. D. & Jarvis, C. J. Measuring fluxes in tidal estuaries: sensitivity to instrumentation and associated data analysis. *Estuarine, Coastal and Shelf Science* **45**, 433-451.

Laslett. R. E. 1995 Concentrations of dissolved and suspended particulate Cd, Cu, Mn, Ni, Pb and Zn in surface waters around the coasts of England and Wales and in the adjacent seas. *Estuarine, Coastal and Shelf Science* **40**, 67-85.

Laslett, R. E. & Balls, P. W. 1995 The behaviour of dissolved Mn, Ni and Zn in the Forth, an industrialised, partially mixed estuary. *Marine Chemistry* **48**, 311-328.

Lee, A. J. 1980 North Sea: Physical oceanography. In: *The North West European Shelf Seas: The Seabed and Sea in Motion*, Vol. 2. Banner, F., Collins, M. B. & Massie, K. S. (Eds.), Elsevier Scientific Publishing, 467-493.

Leeks, G. J. L., Neal, C., Jarvie, H. P., Casey, H. & Leach, D. V. 1997 The LOIS rivers monitoring network: strategy and implementation. *The Science of the Total Environment* **194/195**, 101-109.

Lerman, A. & Stumm, W. 1989 CO_2 storage and alkalinity trends in lakes. *Water Research* **23**, 139-146.

Li, Y., Burkhardt, L.Buchholtz, M. O'Hara, P. Santschi, P. H. 1984a Partitioning of radiotracers between suspended particles and seawater. *Geochimica et Cosmochimica Acta* **48**, 2011-2019.

Li, Y., Burkhardt, L. & Teraoka, H. 1984b Desorption and coagulation of trace elements during estuarine mixing. *Geochimica et Cosmochimica Acta* **48**, 1879-1884.

Lick, W., Chroneer, Z. & Rapaka, V. 1997 Modelling the dynamics of the sorption of hydrophobic organic chemicals to suspended sediments. *Water, Air and Soil Pollution* **99**, 225-235.

Liddicoat, M. I., Turner, D. R. & Whitfield, M. 1983 Conservative behaviour of boron in the Tamar Estuary. *Estuarine, Coastal and Shelf Science* **17**, 467-472.

Liu, Y. P. 1996 *Modelling Estuarine Chemical Dynamics of Trace Metals*. Ph.D. Thesis, University of Plymouth, Devon, UK.

Liu, Y. P., Millward, G. E. & Harris, J. R. W. 1998 Modelling the distribution of dissolved Zn and Ni in the Tamar Estuary using hydrodynamics coupled with chemical kinetics. *Estuarine Coastal and Shelf Science* **47**, 535-546.

Lofts, S. & Tipping, E. 1998 An assemblage model for cation binding by natural particulate matter. *Geochimica et Cosmochimica Acta* **62**, 2609-2635.

Lyons, M. G. 1997 The dynamics of suspended sediment transport in the Ribble Estuary. *Water, Air and Soil Pollution* **99**, 141-148.

Maberly, S. C. 1996 Diel, episodic and seasonal changes in pH and concentrations of inorganic carbon in a productive lake. *Freshwater Biology* **35**, 579-598.

MacCready, P. 1999 Estuarine adjustment to changes in river flow and tidal mixing. *Journal of Physical Oceanography* **29**, 708-726.

Madariaga, I. Photosynthetic characteristics of phytoplankton during the development of a summer bloom in the Urdaibai Estuary, Bay of Biscay. *Estuarine Coastal and Shelf Science* **40**, 559-575.

Mantoura, R. F. C. & Morris, A. W. 1983 Measurement of chemical distributions and processes. In: *Practical Procedures for Estuarine Studies*. Morris, A. W. (Ed.), Natural Environment Research Council, Swindon, UK, 55-100.

Mantoura, R. F. C., Dickson, A. & Riley, J. P. 1978 The complexation of metals with humic materials in natural waters. *Estuarine Coastal and Shelf Science* **6**, 387-408.

Margvelashvily, N., Maderich, V. & Zheleznyak, M. 1999 Simulation of radionuclide fluxes from the Dnieper-Bug Estuary. *Journal of Environmental Radioactivity* **43**, 157-171.

Marsh, T. J. & Sanderson, F. J. 1997 A review of hydrological conditions throughout the period of the LOIS monitoring programme-considered within the context of the recent UK climatic volatility. *The Science of the Total Environment* **194/194**, 59-69.

Martin, J., Dai, M. & Cauwet, G. 1995 Significance of colloids in the biogeochemical cycling of organic carbon and trace metals in the Venice Lagoon (Italy). *Limnology and Oceanography* **40**, 119-131.

Martin, J., Guan, D. M., Elbaz-Poulichet, F., Thomas, A. J. & Gordeev, V. V. 1993 Preliminary assessment of the distribution of some trace elements (As, Cd, Cu, Fe, Ni, Pb and Zn) in a pristine aquatic environment: the Lena River Estuary (Russia). *Marine Chemistry* **43**, 185-199.

Mayer, L. M. 1982 Retention of riverine iron in estuaries. *Geochimica et Cosmochimica Acta* **46**, 1003-1009.

McAdam, A. D. 1993 Whiteadder Water. In: *Scottish Borders Geology An Excursion Guide*. McAdam, A. D., Clarkson, E. N. K. & Stone, P. (Eds.), Scottish Academic Press, Edinburgh, 85-89.

McDowell, D. M. & O'Conner, B. A. 1977 *Hydraulic Behaviour of Estuaries*. Macmillan Press, London, 292 pp.

McManus, J. P. & Prandle, D. 1996 Determination of source concentrations of dissolved and particulate trace metals in the southern North Sea. *Marine Pollution Bulletin* **32**, 504-512.

McManus, J. & Duck, R. W. 1996 Regional variation of fluvial sediment yield in eastern Scotland. In: *Erosion and Sediment Yield: Global and Regional Perspectives*. Walling, D. E. & Webb, B. W. (Eds.), IAHS Publication 236, 157-161.

Millero, F. J. 1986 The pH of estuarine waters. *Limnology and Oceanography* **31**, 839-847.

Millward, G. E. 1995 Processes affecting trace element speciation in estuaries: a review. *Analyst* **120**, 609-614.

Millward, G. E. & Turner, A. 1995 Trace metals in estuaries. In: *Trace Metals in Natural waters*. Salbu, B. & Steinnes, E. (Eds.), CRC Press, London, 223-245.

Millward, G. E., Turner, A., Glasson, D. R. & Glegg, G. A. 1990 Intra- and inter-estuarine variability of particle microstructure. *The Science of the Total Environment* **97/98**, 289-300.

Millward, G. E., Glegg, G. A. Morris, A. W. 1992 Zn and Cu removal kinetics in estuarine waters. *Estuarine, Coastal and Shelf Science* **35**, 37-54.

Millward, G. E., Williams, M. R. & Clifton, R. J. 1994 Particle sources and trace element reactivity in the Humber Plume. *Netherlands Journal of Aquatic Ecology* **28**, 359-364.

Millward, G. E., Allen, J. I., Morris, A. W. & Turner, A. 1996 Distribution and fluxes of non-detrital particulate Fe, Mn, Cu, Zn in the Humber coastal zone, U.K. *Continental Shelf Research* **16**, 967-993.

Mehrbach, C., Culberson, C. H., Hawley, J. E., Pytkowicz, R. M. 1973 Measurement of the apparent dissociation constants of carbonic acid in seawater at atmospheric pressure. *Limnology and Oceanography* **18**, 897-907.

Moffett, J. W. & Ho, J. 1996 Oxidation of cobalt and manganese in seawater via a common microbially catalyzed pathway. *Geochimica et Cosmochimica Acta* **60**, 3415-3424.

Mook, W. G. & Koene, B. K. S. 1975 Chemistry of dissolved inorganic carbon in estuarine and coastal brackish waters. *Estuarine and Coastal Marine Science* **3**, 325-336.

Moore, R. M. & Millward, G. E. 1988 The kinetics of Th reactions with marine particles. *Geochimica et Cosmochimica Acta* **52**, 113-118.

de Mora, S. J. 1983 The distribution of alkalinity and pH in the Fraser Estuary. *Environmental Technology Letters* **4**, 35-46.

Morel., F. M. M., Hudson., R. J. M. & Price, N. M. 1991 Limitation of productivity by trace metals in the sea. *Limnology and Oceanography* **36**, 1742-1755.

Morgan, S. B., Yeats, P. A. & Balls, P. W. 1996 On the role of colloids in trace metal solid-solution partitioning in continental shelf waters: a comparison of model results and field data. *Continental Shelf Research* **16**, 397-408.

Morris, A. W. 1978 Chemical processes in estuaries: The importance of pH and its variability. In: *Environmental Biogeochemistry and Geomicrobiology. Vol. 1: The Aquatic Environment*. Krumbein, W. E. (Ed.) Ann Arbor Science, Michigan, 179-187.

Morris, A. W. 1986 Removal of trace metals in the very low salinity region of the Tamar Estuary, England. *The Science of the Total Environment* **49**, 297-304.

Morris, A. W. 1990 Kinetic and equilibrium approaches to estuarine chemistry. *The Science of the Total Environment* **97/98**, 253-266.

Morris, A. W. & Bale, A. J. 1979 Effects of rapid precipitation of dissolved Mn in river waters on estuarine Mn distribution. *Nature* **279**, 318-319.

Morris, A. W., Mantoura, R. F. C., Bale, A. J. & Howland, R. J. M. 1978 Very low salinity regions of estuaries: important sites for chemical and biological reactions. *Nature* **274**, 678-680.

Morris, A. W., Bale, A. J. & Howland, R. J. M. 1982 Chemical variability in the Tamar Estuary, South West England. *Estuarine, Coastal and Shelf Science* **14**, 649-661.

Morris, A. W., Bale, A. J., Howland, R. J. M., Millward, G. E., Ackroyd, D. E., Loring, D. H. & Rantala, R. T. T. 1986 Sediment mobility and its contribution to trace-metal cycling and retention in a macrotidal estuary. *Water Science Technology* **18**, 111-119.

Morris, A. W., Allen, J. I., Howland, R. J. M. & Wood, R. G. 1995 The estuary plume zone: source or sink for land-derived nutrient discharges? *Estuarine, Coastal and Shelf Science* **40**, 387-402.

Mulder, T., Syvitski, J. P. M. & Skene, K. I. 1998 Modelling of erosion and deposition by turbidity currents generated at river mouths. *Journal of Sedimentary Research* **68**, 124-137.

Muller, F. L. L., Tranter, M. & Balls, P. W. 1994 Distribution and transport of chemical constituents in the Clyde Estuary. *Estuarine, Coastal and Shelf Science* **39**, 105-126.

Murphy, D. G. & Odd, N. V. M. 1993 NORPOLL – A 3D North Sea Policy Model for Heavy Metal Discharges. Simulation of Cadmium and Lead in 1988/89 Based on Estimated Loads. *Report SR 304*. HR Wallingford, Oxfordshire, 18 pp.

Mwanuzi, F. & de Smedt, F. 1999 Heavy metal distribution under estuarine mixing. *Hydrological Processes* **13**, 789-804.

National Rivers Authority (NRA) 1995 *The Mersey Estuary – A Report on Environmental Quality*, Water Quality Series, No. 23, HMSO, London, 43 pp.

Naudin, J. J., Cauwet, G. Chretiennot-Dinet, M. –J., Deniaux, B., Devenon, J. –L. & Pauc, H. 1997 River discharge and wind influence upon particulate transfer at the land-ocean interaction: case study of the Rhone River Plume. *Estuarine, Coastal and Shelf Science* **45**, 303-316.

Neal, C. & Hill, S. 1994 Dissolved inorganic and organic carbon in moorland and forest streams: Plynlimon, Mid-Wales. *Journal of Hydrology* **153**, 231-243.

Neal, C. & Robson, A. J. 2000 A summary of river water quality data collected within the Land-Ocean Interaction Study: core data for eastern UK rivers draining to the North Sea. *The Science of the Total Environment* **251/252**, 585-665.

Neal, C., Robson, A.J., Harrow, M., Hill, L., Wickham, H., Bhardwaj, C.L., Tindall, C.I., Ryland, G.P., Leach, D.V., Johnson, R.C., Bronsdon, R.K., and Craston, M. 1997 Major, minor, trace element and suspended sediment variations in the River Tweed: results from the LOIS core monitoring programme. *The Science of the Total Environment* **194/195**, 193-205.

Neal. C., Fox, K. K., Harrow, M. & Neal. M. 1998a Boron in the major UK rivers entering the North Sea. *The Science of the Total Environment* **210/211**, 41-51.

Neal, C. Harrow, M. & Williams, R. J. 1998b Dissolved carbon dioxide and oxygen in the River Thames: Spring-summer 1997. *The Science of the Total Environment* **210/211**, 205-217.

Neal. C., House, W. A. & Down, K, 1998c An assessment of excess carbon dioxide partial pressures in natural waters based on pH and alkalinity measurements. *The Science of the Total Environment* **210/211**, 173-185.

Neal, C., House, W. A., Jarvie, H. P. & Eatherall, A. 1998d The significance of dissolved carbon dioxide in major lowland rivers entering the North Sea. *The Science of the Total Environment* **210/211**, 187-203.

Neal, C., House, W. A., Leeks, G. J. L., Whitton, B. A. & Williams, R. J. 2000 Conclusions to the special issue of *Science of the Total Environment* concerning 'TH water quality of UK rivers entering the North Sea'. *The Science of the Total Environment* **251/252**, 557-573.

NERC (Natural Environment Research Council) 1994 Land-Ocean Interaction Study (LOIS) Implementation Plan for a Community Research Project. Natural Environment Research Council, Swindon, UK, 60 pp.

Ng, B., Turner, A., Tyler, A. O., Falconer, R. A. & Millward, G. E. 1996 Modelling contaminant geochemistry in estuaries. *Water Research* **30**, 63-74.

Nilsson, N., Persson, P., Lovgren, L. & Sjoberg, S. 1996 Competitive surface complexation of *o*-phthalate and phosphate on goethite (α-FeOOH) particles. *Geochimica et Cosmochimica Acta* **60**, 4385-4395.

Niu., X. –F., Edmiston, H. L. & Bailey, G. O. 1998 Time series models for salinity and other environmental factors in the Apalachicola Estuarine system. *Estuarine, Coastal and Shelf Science* **48**, 549-563.

Nolting, R. E., Helder, W., de Baar, H. J. W. & Gerringa, L. J. A. 1999 Contrasting behaviour of trace metals in the Scheldt estuary in 1978 compared to recent years. *Journal of Sea Research* **42**, 275-290.

Noriki, S., Ishimori, N., Harada, K. & Tsunogai, S. 1985 Removal of trace metals from seawater during a phytoplankton bloom as studied with sediment traps in Funka Bay, Japan. *Marine Chemistry* **17**, 75-89.

Oakley, S. M., Nelson, P. O. & Williamson, K. J. 1981 Model of trace-metal partitioning in marine sediments. *Environmental Science & Technology* **15**, 474-480.

O'Neill, P. 1993 *Environmental Chemistry*, Chapman & Hall, London, 268 pp.

Oreskes, N., Shrader-Frechette, K & Belitz, K. 1994 Verification, validation and confirmation of numerical models in the Earth sciences. *Science* **263**, 641-646.

Ouboter, M. R. L., van Eck, B. T. M., van Gils, J. A. G., Sweerts, J. P. & Villars, M. T. 1998 Water quality modelling of the western Scheldt Estuary. *Hydrobiologia* **366**, 129-142.

Owens, P. N., Walling, D. E. & Leeks, G. J. L. 1999 Deposition and storage of fine-grained sediment within the main channel system of the River Tweed, Scotland. *Earth Surface Processes and Landforms* **24**, 1061-1076.

Owens, R. E. & Balls, P. W. 1997 Dissolved trace metals in the Tay Estuary. *Estuarine, Coastal and Shelf Science* **44**, 421-434.

Owens, R. E., Balls, P. W. & Price, N. B. 1997 Physicochemical processes and their effects on the composition of suspended particulate material in estuaries: implications for monitoring and modelling. *Marine Pollution Bulletin* **34**, 51-60.

Paalman, M. A. A., van der Weijden, C. H. & Loch, J. P. G. 1994 Sorption of cadmium on suspended matter under estuarine conditions; competition and complexation with major seawater ions. *Water, Air, and Soil Pollution* **73**, 49-60.

Pankow, J. F. & McKenzie, S. W. 1991 Parameterizing the equilibrium distribution of chemicals between the dissolved, solid particulate matter, and colloidal matter compartments in aqueous systems. *Environmental Science & Technology* **25**, 2046-2053.

Paucot, H. & Wollast, R. 1997 Transport and transformation of trace metals in the Scheldt Estuary. *Marine Chemistry* **58**, 229-244.

Perianez, R. & Martinez-Aguirre, A. 1997 Uranium and thorium concentrations in an estuary affected by phosphate processing: Experimental results and a modelling study. *Journal of Environmental Radioactivity* **35**, 281-304.

Perianez, R. Abril, J. M. Garcia-Leon, M. 1996a Modelling the dispersion of non-conservative radionuclides in tidal waters. Part 1: Conceptual and mathematical model. *Journal of Environmental Radioactivity* **31**, 127-141.

Perianez, R. Abril, J. M. Garcia-Leon, M. 1996b Modelling the dispersion of non-conservative radionuclides in tidal waters. Part 2: Application to Ra-226 dispersion in an estuarine system. *Journal of Environmental Radioactivity* **31**, 253-272.

Peters, H. 1997 Observations of stratified turbulent mixing in an estuary: neap-to-spring variation during high river flow. *Estuarine, Coastal and Shelf Science* **45**, 69-88.

Pettine, M., Camusso, M., Martinotti, W., Marchetti, R., Passino, R. & Queirazza, G. 1994 Soluble and particulate metals in the Po River: factors affecting concentrations and partitioning. *The Science of the Total Environment* **145**, 243-265.

Pham, M. K., Martin, J. M., Garnier, J. M., Li, Z. & Boutier, B. 1997 On the possibility of using the commercially available ECoS model to simulate Cd distribution in the Gironde estuary. *Marine Chemistry* **58**, 163-172.

Plymsolve 1991 *An Estuarine Contaminant Simulator User Manual Edition 1.01*, Plymsolve, Plymouth 91 pp.

Pollet, I. & Bendell-Young, L. I. 1999 Uptake of ^{109}Cd from natural sediments by the blue mussel *Mytilus trossulus* in relation to sediment nutritional and geochemical composition. *Archives of Environmental Contamination and Toxicity* **36** 288-294.

Portela, L. I. & Neves, R. 1994 Numerical modelling of suspended sediment transport in tidal estuaries: a comparison between the Tagus (Portugal) and the Scheldt (Belgium – the Netherlands). *Netherlands Journal of Aquatic Ecology* **28**, 329-335.

Postman, L. 1984 A two dimensional water quality model application for Hong Kong coastal waters. *Water Science Technology* **16**, 643-652.

Rajar, R. Cetina, M. & Zagar, D. 1995 Three-dimensional modelling of oil spill in the Adriatic. In: *Computer Modelling of Seas and Coastal Regions II.* Brebbia, C. A., Traversoni, L. & Wrobel, L. C. (Eds.), Computational Mechanics Publications, Southampton, 95-102.

Real, C., Barreiro, R. & Carballeira, A. 1993 Heavy metal mixing behaviour in estuarine sediments in the Ria de Arousa (NW Spain). Differences between metals. *The Science of the Total Environment* **128**, 51-67.

Rebsdorf, A., Thyssen, N. & Erlandsen, M. 1991 Regional and temporal variation in pH, alkalinity and carbon dioxide in Danish streams, related to soil type and land use. *Freshwater Biology* **25**, 419-435.

Regnier, P., Wollast, R. & Steefel, C. I. 1997 Long-term fluxes of reactive species in macrotidal estuaries: Estimates from a fully transient, multicomponent reaction-transport model. *Marine Chemistry* **58**, 127-145.

Reynolds, B., Neal, C., Hornung, M. & Stevens, P. A. 1986 Baseflow buffering of streamwater acidity in five mid-Wales catchments. *Journal of Hydrology* **87**, 167-185.

Robson, A. J. & Neal, C. 1997 Regional water quality of the River Tweed. *The Science of the Total Environment* **194/195**, 173-192.

Robson, A. J., Neal, C., Currie, J. C., Virtue, W. A. & Ringrose, A. 1996 *The Water Quality of the Tweed and its Tributaries.* Tweed River Purification Board, IH Report No. 128.

Roos, J. C. & Pieterse, A. J. H. 1995 Nutrients, dissolved gases and pH in the Vaal River at Balkfontein, South Africa. *Archiv Fur Hydrobiologie* **133**, 173-196.

Roy, R. N., Roy, L. N., Vogel, K. M., Porter-Moore, C., Pearson, T., Good, C. E. 1993 The dissociation constants of carbonic acid in seawater at salinities 5 to 45 and temperatures 0 to 45°C. *Marine Chemistry* **42**, 249-267.

Sand-Jenson, K. & Frost-Christensen, H. 1998 Photosynthesis of amphibious and obligately submerged plants in CO_2-rich lowland streams. *Oecologia* **117**, 31-39.

Saliot, A., & Martin, J. 1997 Fourth international symposium on model estuaries: 'The biogeochemistry of organic compounds and trace metals in macrotidal estuaries'. *Marine Chemistry* **58**, 1-2.

Sarin, M. M. & Church, T. M. 1994 Behaviour of uranium during estuarine mixing in the Delaware and Chesapeake Estuaries. *Estuarine, Coastal Shelf Science* **39**, 619-631.

Schiwiderski, E. W. 1983 Atlas of ocean tidal charts and maps. Part I: the semidurnal principal lunar tides M2. *Marine Geodesy* **6**, 219-265.

Shafer, M. M., Overdier, J. T., Hurley, J. P., Armstrong, D. & Webb, D. 1997 The influence of dissolved organic carbon, suspended particulates, and hydrology on the concentration, partitioning and variability of trace metals in two contrasting Wisconsin watersheds (U.S.A.). *Chemical Geology* **136**, 71-97.

Shafer, M. M., Overdier, J. T., Phillips, H., Webb, D., Sullivan, J. R. & Armstrong, D. E. 1999 Trace metal levels and partitioning in Wisconsin rivers. *Water, Air and Soil Pollution* **110**, 273-311.

Shaw, P. J., Chapron, C., Purdie, D. A. & Rees, A. P. 1998 Impact of phytoplankton activity on dissolved nitrogen fluxes in the tidal reaches of the Tweed, UK. *Marine Pollution Bulletin* **37**, 280-294.

Skogen, M. D., Svendsen, E., Berntsen, J., Aksnes, D. & Ulvestad, K. B. 1995 Modelling the primary productivity in the North Sea using a coupled three-dimensional physical-chemical-biological ocean model. *Estuarine, Coastal Shelf Science* **41**, 545-565.

de Smedt, F., Vuksanovic, V., van Meerbeeck, S. & Reyns, D. 1998 A time dependent flow model for heavy metals in the Scheldt Estuary. *Hydrobiologia* **336**, 143-155.

Smith, J. A. 1995 *Ecological Management Strategies for Impounded Harbours*. Ph.D. Thesis, University of Plymouth, Devon, UK.

Sung, W. 1995 Some observations on surface partitioning of Cd, Cu and Zn in estuaries. *Environmental Science & Technology* **29**, 1303-1312.

van Straten, G. 1998 Models for water quality management: the problem of structural change. *Water Science Technology* **37**, 103-111.

Sutcliffe, D. W. & Carrick, T. R. 1988 Alkalinity and pH of tarns and streams in the English Lake District (Cumbria). *Freshwater Biology* **19**, 179-189.

Sylaisos, G. & Boxall, S. R. 1998 Residual currents and flux estimates in a partially-mixed estuary. *Estuarine, Coastal and Shelf Science* **46**, 671-682.

Syvitski, J. P. & Morehead, M. D. 1999 Estimating river-sediment discharge to the ocean: application to the Eel margin, northern California. *Marine Geology* **154**, 13-28.

Talling, J. F. 1976 The depletion of carbon dioxide from lake water by phytoplankton. *Journal of Ecology* **64**, 79-121.

Tappin, A. D., Burton, J. D., Millward, G. E. & Stratham, P. J. 1997 A numerical transport model for predicting the distribution of Cd, Cu, Ni, Pb and Zn in the southern North Sea: the sensitivity of model results to the uncertainties in the magnitudes of metal inputs. *Journal of Marine Systems* **13**, 173-204.

Thouvenin, B. Gonzalez, J. L. Boutier, B. 1997 Modelling of pollutant behaviour in estuaries: Application to cadmium in the Loire Estuary. *Marine Chemistry* **58**, 147-161.

Tindall, C. I. & Moore, R. V. 1997 The rivers database and the overall data management for the Land Ocean Interaction Study programme. *The Science of the Total Environment* **194/195**, 129-135.

Tipping, E., Marker, A. F. H., Butterwick, C., Collett, G. D., Cranwell, P. A., Ingram, J. K. G., Leach, D. V., Lishman, J. P., Pinder, A. C., Rigg, E. & Simon, B. M. 1997 Organic carbon in Humber Rivers. *The Science of the Total Environment* **194/195**, 345-355.

Tipping, E., Lofts, S. & Lawlor, A. J. 1998 Modelling the chemical speciation of trace metals in the surface waters of the Humber system. *The Science of the Total Environment* **210/211**, 63-77.

Tsonis, A. A. 1996 Widespread increases in low-frequency variability in precipitation over the past century. *Nature* **382**, 700-702.

Turner, A. 1990 *Chemical Dynamics in North Sea Estuaries and Plumes*. Ph.D., Polytechnic South West, Devon, UK.

Turner, A. 1996 Trace metal partitioning in estuaries: importance of salinity and particle concentration. *Marine Chemistry* **54**, 27-39.

Turner, A. 1999 Diagnosis of chemical reactivity and pollution sources from particulate trace metal distributions in estuaries. *Estuarine, Coastal and Shelf Science* **48**, 177-191.

Turner, A. & Millward, G. E. 1994 Partitioning of trace metals in a macrotidal estuary. Implication for contaminant transport models. *Marine Chemistry* **39**, 45-58.

Turner, A. & Tyler, A. O. 1997 Modelling adsorption and desorption processes in estuaries. In: *Biogeochemistry of intertidal sediments*. Jickells, T. D. & Rae J. E. (Eds.) Cambridge University Press, Cambridge, 43-58.

Turner, A., Millward, G. E. & Morris, A. W. 1991 Particulate metals in five major North Sea estuaries. *Estuarine, Coastal and Shelf Science* **32**, 325-346.

Turner, A., Millward, G. E., Bale, A. J. & Morris, A. W. 1992a The solid solution partitioning of trace metals in the southern North Sea – *in situ* radiochemical experiments. *Continental Shelf Research* **12**, 1311-1329.

Turner, A., Millward, G. E., Schuchardt, B., Schirmer, M. & Prange, A. 1992b Trace metal distribution coefficients in the Weser Estuary (Germany). *Continental Shelf Research* **12**, 1277-1292.

Turner, A., Millward, G. E., Bale, A. J. & Morris, A. W. 1993 Application of the K_d concept to the study of trace metal removal and desorption during estuarine mixing. *Estuarine, Coastal and Shelf Science* **36**, 1-13.

Turner, A., Nimmo, M. & Thuresson, K. A. 1998 Speciation and sorption behaviour of nickel in an organic-rich estuary (Beaulieu, UK). *Marine Chemistry* **63**, 105-118.

Turner, D. R., Whitfield, M. & Dickson, A. G. 1981 The equilibrium speciation of dissolved components in freshwater and seawater at 25°C at 1 atm pressure. *Geochimica et Cosmochimica Acta* **45**, 855-881.

Turrel, W. R. & Slesser, G. 1992 Annual cycles of physical, chemical and biological parameters in Scottish waters. *Scottish Fisheries Working Paper* No. 5/92.

Tyler, A. O., Rymell, M. C. & Smith, J. P. 1997 Facility-specific models as an essential aid to determining predicted environmental concentrations (PECs) for production water risk analysis. *Society of Petroleum Engineers* **SPE 37868**, 239-246.

Tweed River Purification Board 1992 *Annual Report 1991-1992*, TWPB, 47 pp.

Uncles, R. J. & Stephens, J. A. 1989 Distribution of suspended sediment at high water in a macrotidal estuary. *Journal of Geophysical Research* **94**, 14395-14405.

Uncles, R. J. & Stephens, J. A. 1990 The structure of vertical current profiles in a macrotidal, partially-mixed estuary. *Estuaries* **13**, 349-361.

Uncles, R. J. & Stephens, J. A. 1993 Nature of the turbidity maximum in the Tamar Estuary. *Estuarine, Coastal and Shelf Science* **36**, 413-431.

Uncles, R. J. & Stephens, J. A. 1996a Buoyancy Phenomena in the Tweed Estuary. In: *Buoyancy Effects on Coastal and Estuarine Dynamics, Coastal and Estuarine Studies.* Aubrey, D. G. & Friedrichs, C. T. (Eds.) American Geophysical Union, Washington DC, 175-193.

Uncles, R. J. & Stephens, J. A. 1996b Salt intrusion in the Tweed Estuary. *Estuarine, Coastal and Shelf Science* **43**, 217-293.

Uncles, R. J. & Stephens, J. A. 1997 Dynamics of turbidity in the Tweed Estuary. *Estuarine, Coastal and Shelf Science* **45**, 745-758.

Uncles, R. J., Bale, A. J., Howland, R. J. M., Morris, A. W. & Elliot, R. C. A. 1983 Salinity of surface water in a partially mixed estuary and its dispersion at low run-off. *Oceanologica Acta* **6**, 289-295.

Uncles, R. J., Elliot, R. C. A. & Weston, S. A. 1985 Observed fluxes of water, salt and suspended sediment in a partially mixed estuary. *Estuarine, Coastal and Shelf Science* **20**, 147-167.

Uncles, R. J., Woodrow, T. Y. & Stephens, J. A. 1987 Influence of long-term sediment transport on contaminant dispersal in a turbid estuary. *Continental Shelf Research* **7**, 1489-1493.

Uncles, R. J., Stephens, J. A. & Barton, M. L. 1990 Observations of fine-sediment concentrations and transport in the turbidity maximum region of an estuary. In: *Dynamics and Exchange in Estuaries and the Coastal Zone*. Prandle, D. (Ed.), American Geophysical Union, Washington, 255-276.

Uncles, R. J., Barton, M. L. & Stephens, J. A. 1994 Seasonal variability of fine-sediment concentrations in the turbidity maximum region of the Tamar Estuary. *Estuarine, Coastal and Shelf Science* **38**, 19-39.

Uncles, R. J., Bloomer, N. J., Frickers, P. E., Griffiths, M. L., Harris, C., Howland, R. J. M., Morris, A. W., Plummer, D. H., & Tappin, A. D. 2000 Seasonal variability of salinity, temperature, turbidity and suspended chlorophyll in the Tweed Estuary. *The Science of the Total Environment* **251/252**, 115-124.

Unnikrishnan, A. S. & Shetye, S. R. & Gouveia, A. D. 1997 Tidal propagation in the Mandovi-Zuari Estuarine network, west coast of India: impact of freshwater influx. *Estuarine, Coastal and Shelf Science* **45**, 737-744.

Valiela, I., McClelland, J., Hauxwell, J., Behr, P. J., Hersh, D. & Foreman, K. 1997 Macroalgal blooms in shallow estuaries: controls and ecophysiological and ecosystem consequences. *Limnology and Oceanography* **42**, 1105-1118.

Vazquez, G. F., Sharma, V. K., Magallanes, V. R. & Marmolejo, A. J. 1999 Heavy metals in a coastal lagoon of the Gulf of Mexico. *Marine Pollution Bulletin* **38**, 479-485.

Vojak, P. W. L., Edwards, C. & Jones, M. V. 1985 Evidence for microbial manganese oxidation in the River Tamar Estuary, South West England. *Estuarine, Coastal and Shelf Science* **20**, 661-671.

Vuksanovic, V., de Smedt, F. & van Meerbeeck, S. 1996 Transport of polychlorinated biphenyls (PCB) in the Scheldt Estuary simulated with the water quality model WASP. *Journal of Hydrology* **174**, 1-18.

Walling, D. E., Owens, P. N., Waterfall, B. D., Leeks, G. J. L. & Wass, P. D. 2000 The particle size characteristics of fluvial suspended sediment in the Humber and Tweed catchments, UK. *The Science of the Total Environment* **251/252**, 205-222.

Wallis, S. G. & Brockie, N. J. W. 1997 Modelling the Forth Estuary with MIKE11. In: *Coastal Zone Topics: Process, Ecology and Management. 3. The Estuaries of Central Scotland.* McLusky, D. S. (Ed.). JNCC & ECSA, Edinburgh, UK, 1-10.

Wanninkhof, R., Lewis, E., Feely, R. A. & Millero, F. J. 1999 The optimal carbonate dissociation constants for determining surface water pCO_2 from alkalinity and total inorganic carbon. *Marine Chemistry* **65**, 291-301.

Warren, L. A. & Zimmerman, A. P. 1994 The influence of temperature and NaCl on cadmium, copper and zinc partitioning among suspended particulate and dissolved phases in an urban river. *Water Research* **28**, 1921-1931.

Wass, P. D., Marks, S. D., Finch, J. W., Leeks, G. J. L. & Ingram, J. K. 1997 Monitoring and preliminary interpretation of in-river turbidity and remote sensed imagery for suspended sediment transport studies in the Humber catchment. *The Science of the Total Environment* **194/195**, 263-283.

Wen, L., Santschi, P. H. & Tang, D. 1997 Interactions between radioactively labelled colloids and natural particles: Evidence for colloidal pumping. *Geochimica et Cosmochimica Acta* **61**, 2867-2878.

Whitfield, M., Turner, D. R. 1986 The carbon dioxide system in estuaries – an inorganic perspective. *The Science of the Total Environment* **49**, 235-255.

Whitehead, P. G., Williams, R. J. & Lewis, D. R. 1997 Quality simulation along river systems (QUASAR): model theory and development. *The Science of the Total Environment* **194/195**, 447-456.

Wilmot, R. D. & Collins, M. B. 1981 Contemporary fluvial sediment supply to the Wash. *Special Publication of the International Association of Sedimentologists*, **5**, 99-110.

Windom, H. L., Byrd., J., Smith, R. Jr., Hungspreugs, M., Dharmuanij, S., Thumtrakul, W. & Yeats, P. 1991 Trace metal-nutrient relationship in estuaries. *Marine Chemistry* **32**, 177-194.

Wolanski, E., Huan, N. N., Dao, L. T., Nhan, N. H. & Thuy, N. N. 1996 Fine sediment dynamics in the Mekong River Estuary, Vietnam. *Estuarine, Coastal and Shelf Science* **43**, 565-582.

Wolanski, E., King, B. & Galloway, D. 1997 Salinity intrusion in the Fly River Estuary, Papua New Guinea. *Journal of Coastal Research* **13**, 983-994.

Wong, G. T. F. 1979 Alkalinity and pH in the southern Chesapeake Bay and the James River Estuary. *Limnology and Oceanography* **24**, 970-977.

Wong, K. –C. & Moses-Hall, J. E. 1998 The tidal and subtidal variations in the transverse salinity and current distribution across a coastal plain estuary. *Journal of Marine Research* **56**, 489-517.

Wood, T. M., Baptista, A. M., Kumabara, J. S. & Flegal, A. R. 1995 Diagnostic modelling of trace metal partitioning in south San Francisco Bay. *Limnology and Oceanography* **40**, 345-358.

Yang, M. S. & Sanudo-Wilhelmy, S. A. 1998 Cadmium and manganese distributions in the Hudson River Estuary: interannual and seasonal variability. *Earth and Planetary Science Letters* **160**, 403-418.

Yellow Springs Instruments Incorporated 1993 6000UPG multi-parameter water quality monitor. Instruction Manual. Yellow Springs, USA.

Zwolsman, J. J. G. & van Eck, B. T. M. 1999 Geochemistry of major elements and trace metals in suspended matter of the Scheldt Estuary, southwest Netherlands. *Marine Chemistry* **66**, 91-111.

Zwolsman, J. J. G., van Eck, B. T. M., van der Weijden, C. H. 1997 Geochemistry of dissolved trace metals (cadmium, copper, zinc) in the Scheldt Estuary, southwestern Netherlands: Impact of seasonal variability. *Geochimica et Cosmochimica Acta* **61**, 1635-1652.0